HIGHWAY RESEARCH BOARD
Bulletin 125

Flexible Culverts Under High Fills

National Academy of Sciences—
National Research Council
publication 412

HIGHWAY RESEARCH BOARD

Officers and Members of the Executive Committee
1956

OFFICERS

K. B. WOODS, *Chairman* — REX M. WHITTON, *Vice Chairman*

FRED BURGGRAF, *Director* — ELMER M. WARD, *Assistant Director*

Executive Committee

C. D. CURTISS, *Commissioner, Bureau of Public Roads*

A. E. JOHNSON, *Executive Secretary, American Association of State Highway Officials*

LOUIS JORDAN, *Executive Secretary, Division of Engineering and Industrial Research, National Research Council*

R. H. BALDOCK, *State Highway Engineer, Oregon State Highway Commission*

PYKE JOHNSON, *Consultant, Automotive Safety Foundation*

G. DONALD KENNEDY, *President, Portland Cement Association*

O. L. KIPP, *Consultant, Minnesota Department of Highways*

BURTON W. MARSH, *Director, Safety and Traffic Engineering Department, American Automobile Association*

C. H. SCHOLER, *Head, Applied Mechanics Department, Kansas State College*

REX M. WHITTON, *Chief Engineer, Missouri State Highway Department*

K. B. WOODS, *Head, School of Civil Engineering and Director, Joint Highway Research Project, Purdue University*

Editorial Staff

FRED BURGGRAF — ELMER M. WARD — HERBERT P. ORLAND

2101 Constitution Avenue — Washington 25, D. C.

HIGHWAY RESEARCH BOARD
Bulletin 125

Flexible Culverts Under High Fills

PRESENTED AT THE
Thirty-Fourth Annual Meeting
January 11–14, 1955

1956

Washington, D. C.

Department of Materials and Construction

R. R. Litehiser, Chairman
Engineer of Tests, Testing & Research Laboratories
Ohio Department of Highways

GENERAL MATERIALS DIVISION

J. H. Swanberg, Chairman
Engineer of Materials and Research
Minnesota Department of Highways

COMMITTEE ON CULVERTS AND CULVERT PIPE

M. G. Spangler, Chairman
Professor, Iowa State College

John L. Beaton, Supervising Highway Engineer, Materials and Research Department, California Division of Highways

E. F. Bespalow, Vice President, Choctaw Inc., Memphis

T. F. de Capiteau, Drainage Products Engineer, Sheet and Strip Steel Division, Republic Steel Corporation, Cleveland

John G. Hendrickson, Jr., Research Engineer, American Concrete Pipe Association, Chicago

E. F. Kelley, Chief, Physical Research Branch, Bureau of Public Roads

C. E. Proudley, Chief Materials Engineer, North Carolina State Highway and Public Works Commission

Rockwell Smith, Research Engineer - Roadway, Association of American Railroads, Chicago

Howard White, Armco Drainage and Metal Products Inc., Middletown, Ohio

Contents

Load Study of Flexible Pipes under High Fills

JOHN H. TIMMERS, Research Engineer
Armco Research Laboratories, Middletown, Ohio

Earth load tests were conducted on three 7-foot-diameter corrugated-metal pipes under 137 feet of fill. Each pipe was 512 feet long on a grade of 2.5 percent with 6 inches of parabolic camber at the center. Pipes were filled strutted to 3 percent elliptical cross-section with long axis vertical.

The fill to a height of 3 feet above the pipe was composed of a granular material of 100 percent Proctor density. At a fill height of 10 feet, a 7-foot-wide and 7-foot-deep trench was cut over each pipe and backfilled with loose uncompacted material before proceeding with normal fill operations. The remainder of the fill was placed in 3-foot lifts compacted by sheepsfoot rollers.

Loads were determined using load cells placed between the sills and the struts, and by attaching SR-4 strain gages to the pipe on the neutral axes of the corrugations. Deflection and subsidence measurements were also made.

Strain-gage data revealed that each increment of fill added its load increment in direct proportion. Deflection and subsidence of the pipe were within design limits.

● WITH the vast improvements in earth-moving equipment and the high cost of labor in construction and maintenance of bridge structures, the use of flexible metal pipe under high fills exceeding 100 feet has become competitive with bridges. While sufficient information has been available to apply corrugated metal pipe safely under high fills, it was recognized that field test data would aid in making such installations more effective.

Load tests were conducted on an installation of three parallel, 84-inch-diameter, Multiplate pipes under 137 feet of embankment which carries US 31 across Hurricane Creek in Cullman County, Alabama. The depth and span of the gorge as well as the volume of the flow in the creek ordinarily would have called for a bridge.

CONSTRUCTION

A section through the center pipe and fill is shown in Figure 1.

The pipes are 512 feet long, laid on a grade of 2.5 percent, and spaced 20 feet, center to center. The pipes were parabolically cambered 6 inches higher at the midpoint than a straight line joining the ends. Pipes were field-strutted to an essentially elliptical cross-section using 8-by-8-inch oak struts and 2-by-8-inch pine compression caps (Figure 2). This caused the vertical axis of the cross-section to be 3 percent greater than original diameter. The struts were placed at 3-foot centers in the middle half of the pipe length and at 6-foot centers at the ends. The pipe was fabricated from 1-gage (0.281-in.) plates at the center, stepping down to 3- to 5- to 8-gage (0.172-in.) at the ends.

After diverting the stream the pipe lines were laid on a 2-foot uniform bed of creek-bed sand. Fill material beneath, between, and to a depth of 3 feet over the pipes was selected granular material compacted to a 100-percent Proctor density value. Springs encountered in preparing the bed were handled with 6-inch corrugated-metal underdrains.

Prior to backfilling, the outside of each pipe was sprayed with an asphalt-base protective coating. Bolts were tightened with pneumatic impact wrenches and checked with a torque wrench to insure a screw-up torque of not less than 150 ft.-lb.

In the imperfect trench method of construction, the conduit is first installed as a positive projecting conduit. Then a fill is constructed over it up to an elevation which is 1 to 1½ times the width of the conduit (Figure 3). The fill is well compacted during construction, and then a trench as wide as the conduit width is dug in the compacted fill directly over the conduit down to its top. The trench is then refilled with loose backfill material to the original level and the embankment continued in conventional manner.

The purpose of the imperfect trench method is to allow the interior prism of fill material to settle downward relative to the exterior prisms so that the settlement will

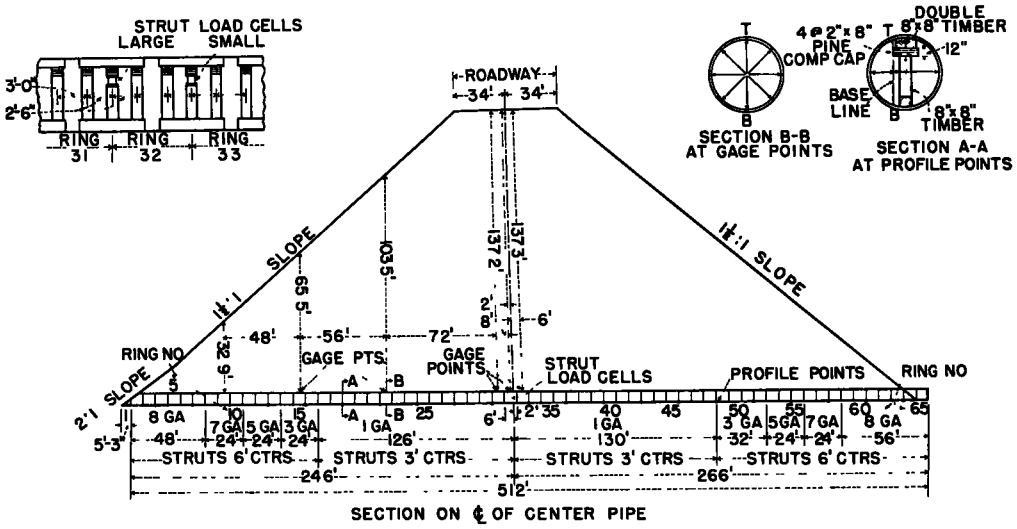

Figure 1. Section through center pipe showing test locations and fill profile.

generate shearing forces which are directed upward, reducing the load that the pipe must support.

In this particular installation at a fill height (above the top of the pipe) of 10 feet, a 7-foot-wide and 7-foot-deep trench was cut over each pipe and backfilled with loose material before proceeding with normal fill operations.

The fill was placed in layers of 3-foot maximum depth. For the first 10-foot depth of cover, rock was kept away from the area directly over the pipes to keep from disturbing the banks when the imperfect trench was excavated.

The fill was mainly a crumbly sandstone and rock for the first 25 feet. Choking was accomplished by alternately placing layers of rock and earth, except for the first 10 feet immediately over the pipes. The lower fill was handled with Euclid wagons over steep haul roads, however as the fill progressed it was largely built using self-loading scrapers. Compaction was accomplished by dual-tandem sheepsfoot rollers.

Upon completion of the fill the slopes were dressed, apron beddings cleared, and the struts pulled from the structure. The aprons and boulder deflector were constructed and the toe of the slopes paved with grouted riprap. The invert of the pipe was paved for a third of the circumference with bituminous concrete.

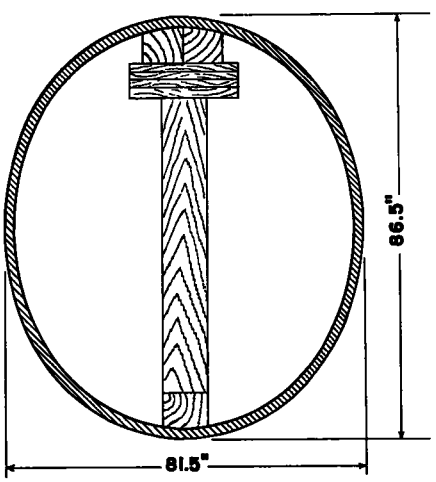

Figure 2. Schematic diagram showing 3% vertical elongation of pipe by use of timber struts.

TEST MEASUREMENTS

Plate stresses, vertical and horizontal deflections, invert elevation and side shift, compression-cap deformation, and strut loads were measured at various intervals during the grading operation. The height of the fill at the time of the test measurements is shown by the fill cross-sections of Figure 4. Location of various test equipment and reference points are shown in Figure 1.

Strain gages were applied on the inside of the pipe at the neutral axis of the corrugation at vertical and horizontal diameters. The gages were located at the center of Rings 31, 32, and 33 under the center of the fill and at the center of Rings 9,

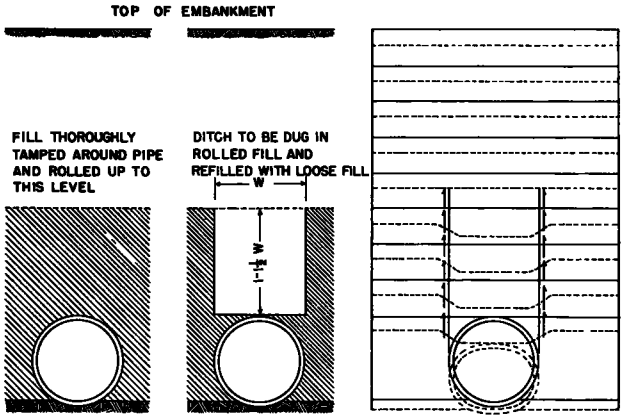

Figure 3. Diagram showing imperfect trench construction and subsequent settlement of interior prism with resulting upward shear forces.

15, and 22, which are 65 feet, 113 feet, and 173 feet from the upstream end of the pipe.

Readings of vertical and horizontal deflection were made at every third plate (24 feet) and at every strain-gage location. Vertical deflections were made on a chord parallel to the vertical diameter 12 inches to one side of the vertical diameter. Vertical, horizontal, and also 45-deg. deflection readings were made at the strain-gage stations.

Invert settlement readings and side-shift readings were made every 24 feet along the complete length of the pipe by means of level measurements.

The deformation of the four 2-by-8-inch pine compression caps was measured to a nail point on the oak strut 4 inches below the top of the strut. A set of these pine compression caps was calibrated under similar loading conditions in a universal testing machine.

Two strut load cells were placed between the struts and compression caps at the center of the pipe under the maximum fill height. These load cells were constructed from 6-inch steel pipe each of a different wall thickness to insure that the load range would be covered by a cell of suitable sensitivity. Wire strain gages were installed on the inside of the load cells before top and bottom bearing plates were assembled. Extreme care was taken to waterproof all strain gage installations. These load dynamometers were calibrated in a universal testing machine.

Test measurements were made at fill heights (above the top of the pipes) of 3 feet, 10 feet, (before and after trenching), 25 feet, 45 feet, 60 feet, 100 feet, and 137 feet (before and after removing struts).

TEST RESULTS

The maximum vertical deflection upon removal of the struts was 1. 84 inches or approximately 2 percent of the original diameter. This occurred at the strain-gage location at Plate 15 (Figure 5). The deflection measurements made on the vertical chords at every third circumferential seam indicate a maximum deflection of about 1. 2 inches at Plate 15 (Figure 6). This point of measurement is located approximately 4 feet from the aforementioned strain-gage location. In no case did the pipe return to its original round shape. The pipe remains from ½ to 2½ percent vertically elongated.

The deflection, in general, followed the pattern that would be expected by examining the fill cross-section, with the exception that, at Plate 15 (about 117 feet from the inlet end), the pipe deflection was slightly greater than the deflection under the full height of the fill. While the reason for this cannot be conclusively established, certain factors which could have contributed to this result can be identified. First, the strut spacing at this point changed from 6 feet to 3 feet, and the plate changed from 3-gage to 1-gage material. Second, this part of the pipe was continually under the haul road, until about 80 feet of fill had been placed. This, of course, meant that the fill and pipe under this ramp were being continually subjected to the

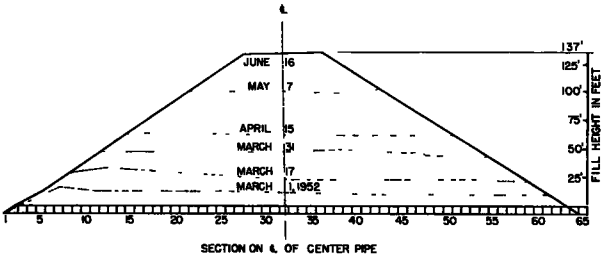

Figure 4. Fill cross-section.

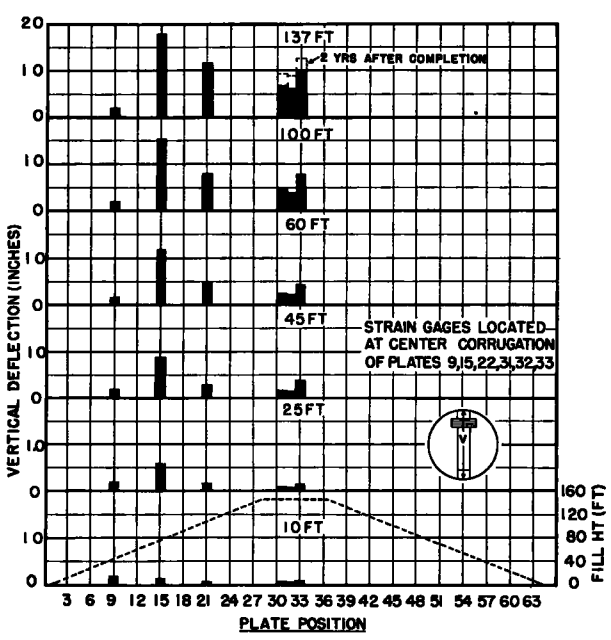

Figure 5. Vertical deflection at strain gage positions.

compaction of heavy construction equipment. Thirdly, since all struts and sills were only approximately the same length, a shorter strut (smaller installation strut load) could have resulted in a greater deflection.

Since the increase in horizontal diameter is practically the same as the decrease in vertical diameter, the graphs of horizontal deflection have been omitted. The average diameter of the pipe appears to remain practically a constant. This illustrates the complementary effect of changes in horizontal and vertical diameters.

The invert settlement, as shown in Figure 7, indicates a maximum settlement of 4.44 inches. As originally installed, the pipe had 6 inches of camber at the center. From the invert settlement curve as shown in Figure 7, the average settlement at the ends was approximately 2 inches. Deducting this from the invert settlement at the center of the pipe, it appears that about $2\frac{1}{2}$ inches of camber were lost (about $3\frac{1}{2}$ inches of camber retained.)

The settlement curve approximates the fill weight distribution. To a certain extent the deflection and invert settlement measurements are complementary. That is, positions that show relatively higher deflections tend to show relatively less invert settlement, and conversely. This probably means that where the invert fill was well compacted greater pipe deflections resulted than where the invert fill was softer. This, of course, assumes that the side fill material was tamped to a similar degree of compaction.

One of the design criteria for corrugated-metal structures is the bolt load at the longitudinal seam. Thrust determinations based on plate loads developed by a unit length of plate lead to evaluation of joint load. For ease of computation, all strut load and plate stress measurements were converted to load per foot of seam.

The strut load per foot of pipe per side is shown in Tables 1 and 2 and Figures 8 and 9. The strut load as obtained by measuring compression of the compression caps is shown in Table 1 and Figure 8. Although the points obtained from readings of the strut load cells at 137 feet were unstable, from the curve in Figure 9, it is evident that the strut load increased proportionately to the fill height up to approximately 60 feet. Above this fill height there is evidence that the strut load increased at a slower rate.

A comparison of the strut load

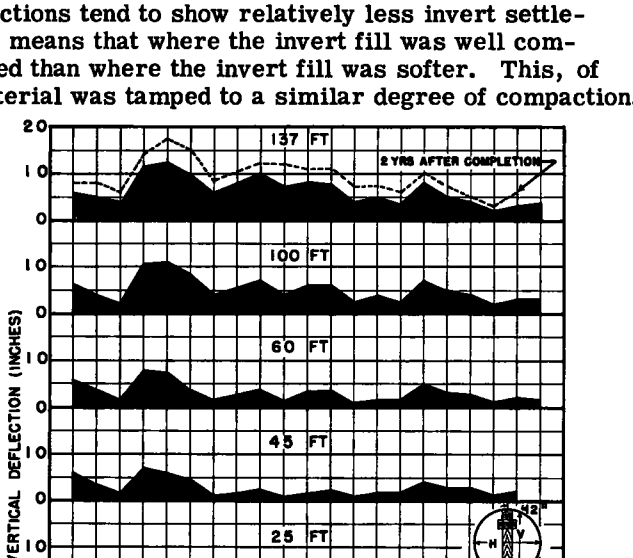

Figure 6. Vertical deflection at every third plate junction (24-ft.).

with the load carried by the plate on the basis of 1 foot of seam length indicates that at low fill heights (low loads) the struts carried an appreciable amount of the total load, while at high fill heights (higher loads) the struts carried a decreasing proportion of the total load (Figure 10), less than 20 percent of total load at final grade.

The plate loads as measured by the strain gages are shown in Table 3. These results were taken from the readings of the gages on the north and south side only. This practice was followed because the bottom gages,

TABLE 1

STRUT LOAD PER FOOT BASED ON STRUT LOAD CELLS

Fill Height ft.	Load		Load per Ft. per Side		
	Large Cell lb.	Small Cell lb.	Large Cell lb.	Small Cell lb.	Ave.
12	7,000	8,000	1,400	1,600	1,500
25	12,000	16,000	2,400	3,200	2,800
45	22,000	27,000	4,400	5,400	4,900
60	30,000	34,000	6,000	6,800	6,400
100	40,000	44,000	8,000	8,800	8,400
137	52,000	39,500	10,400	7,900	9,150

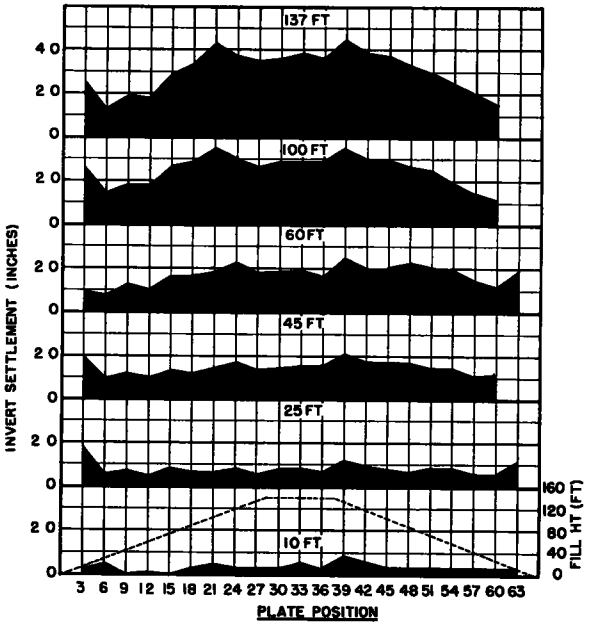

Figure 7. Invert settlement.

which were subjected to water and debris continually after installation, gave inaccurate readings shortly after installation. While the top gages were operative throughout the tests, some high strains were noted, particularly at the higher fills. It is believed that this was due to the fact that local bending of the plate occurred over the top sill.

The total load per foot of seam was computed as the sum of the strut load per foot per side plus the seam load as determined by strain gages (see appendix). The results of these calculations are shown in Figure 11 and Table 4. A comparison of the total load per foot of seam as determined in the test with the theoretical total load per foot of seam appears in Table 4. The theoretical seam load is based on a projected column of earth above the pipe with a density of 118 pcf. as averaged from the dry weight per cubic foot of embankment as determined by the State Highway Department of Alabama.

Figure 12 shows a plot of the total seam load per foot versus fill height based on the test results and on the weight of the projected column of earth. This plot indicates the agreement of the test results with the design calculations and shows that each increment of fill added its load in almost direct proportion to fill height.

The test results are of the same order of magnitude as the theoretical, except in the case of Plate 15 (which was under the haul road) where the

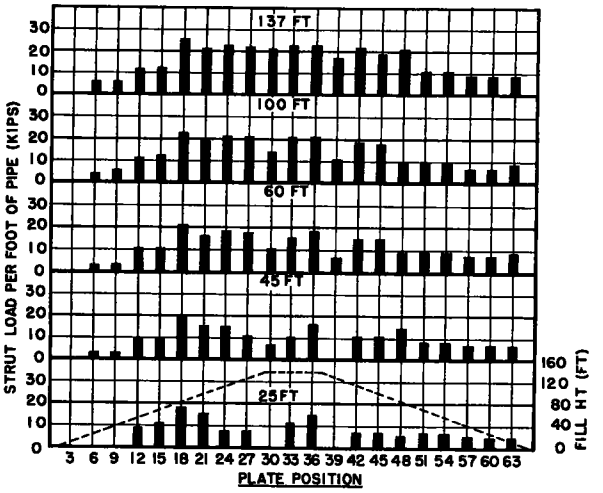

Figure 8. Strut load per foot of pipe.

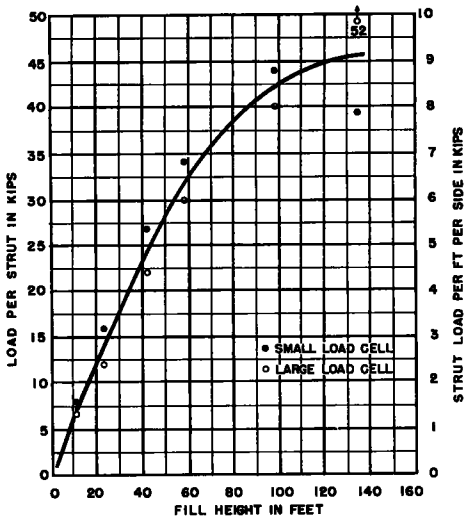

Figure 9. Fill height versus load per strut as measured by strut load cells.

test results appear over 100 percent higher than the theoretical. While this relatively high load cannot be wholly explained, the high deflection and strut load at this location coupled with the low invert settlement partially substantiate the higher load. At Plate 32 the agreement of the test results with the theoretical are satisfactory, having a maximum disagreement of approximately 18 percent, with most values falling within 10 percent.

The pipe showed a maximum horizontal shift of about 0. 8 inch from a base line established when the pipe was covered with 3 feet of fill.

TABLE 2

STRUT LOAD PER FOOT PER SIDE BASED ON COMPRESSION CAP DEFLECTION

Plate Position	25 Feet	45 Feet	60 Feet	100 Feet	137 Feet
3-4	0	0	0	0	0
6-7	0	1667	1667	1667	2917
9-10	0	1667	1667	2917	2917
12-13	4250	5170	5250	5520	5625
15-16	5170	5250	5520	6333	6625
18-19	9000	9666	10500	11833	12500
21-22	7500	7500	7500	9667	10666
24-25	3333	7500	9083	10667	11833
27-28	3333	5833	8500	10333	11250
30-31	0	3333	5833	7500	10333
33-34	5833	5833	7500	10333	11250
36-37	7500	8500	9083	10667	11833
39-40	0	0	3333	5833	8500
42-43	3333	5833	7500	9083	11250
45-46	3333	5833	7500	8500	9667
48-49	2915	7500	4250	4833	10333
51-52	3750	4250	4530	5000	5250
54-55	3750	4250	4530	5000	5250
57-58	2915	3750	3750	3750	4250
60-61	2915	3750	3750	3750	4250
63-64	2915	3750	4250	4530	4530

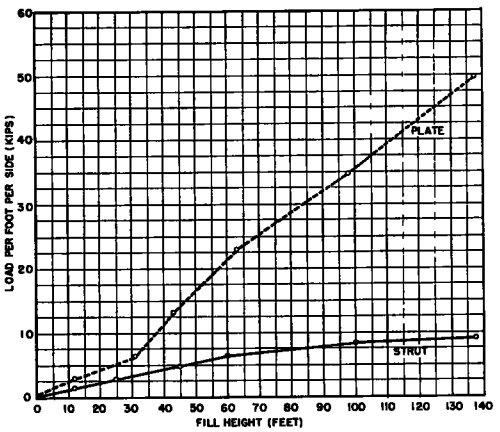

Figure 10. Comparison of strut load and plate load versus fill height for Plate 32 under center of fill.

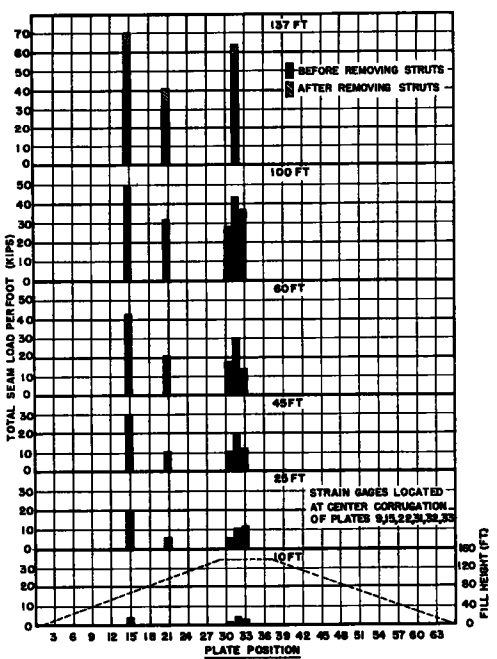

Figure 11. Total load per foot based on strut load plus seam load as determined by strain gages.

The deflection measurements showed little change before and after trenching at the 10-foot level, as did the load measurements. The deflection measurements upon removal of the struts at the completion of the fill showed practically no change, the maximum being 0. 05 inch. The load in the plate, however, did show a considerable increase, as would be expected, since the struts had been carrying part of the load.

Deflection and invert elevation readings

were made two years after completion of the fill. The vertical deflection has increased an average of 0.2 to 0.3 inch, resulting in a maximum deflection of about 2.14 inches as compared with 2.5 inches of original vertical elongation as strutted. The increased invert settlement has been insignificant, generally less than 0.2 inch. The upstream end of the pipe actually indicated a rise of 0.4 to 0.6 inch.

The loads, as determined by the strain gages applied to the plate corrugations, are a direct measure of the load imposed on the plates by the weight of the fill. However, the final plate stresses cannot be determined, because the original tensile stresses due to strutting were not predetermined. Strutting caused the joints and plates to be placed under tension at an unknown tensile stress level. This was the condition of the pipe at the time the strain gages were installed and base readings made.

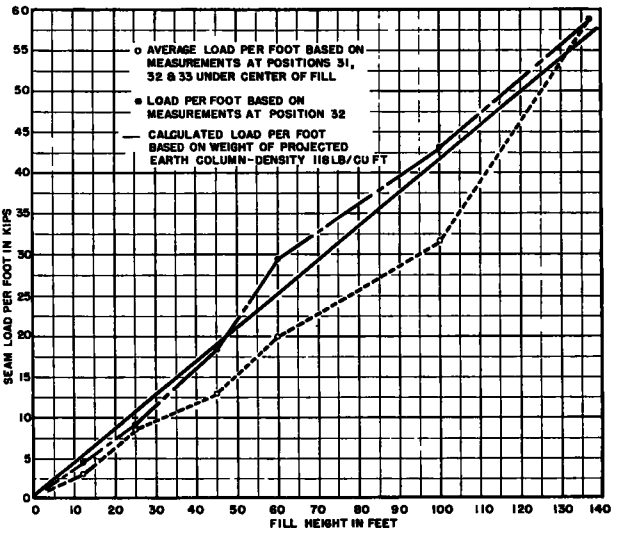

Figure 12. Comparison of measured loads and calculated under center of fill.

TABLE 3

SEAM LOAD PER FOOT BASED ON STRAIN GAGE DATA
AVERAGE OF HORIZONTAL DIA. GAGE POSITIONS

Height ft.	Load in Pounds per Foot at Plant Number				
	No. 15	No. 22	No. 31[b]	No. 32	No. 33
12	+545	+3,040	-3,000	-3,000	-2,400
	-3,790	+2,720	-1,800	-3,000	-3,000
31	-14,350	+900	-6,000	-6,400	-4,800
43	-23,560	-2,390	-6,600	-13,500	-4,800
61	-36,200	-11,960	-11,400	-23,100	-5,700
98	-41,100	-20,960	-19,800	-34,800	-14,400
137	[c] -56,250	-22,750[a]		-49,800	
	[d] -68,750	-39,500[a]		-63,900	

[a] Based on reading of N side only
[b] Based on reading of S side only
[c] Before strut removal
[d] After strut removal

Vertical and horizontal diameter measurements made at every third circumferential seam on the other two pipes in the fill indicate that these pipes also retained some of their original vertical elongation, except at one location in the south pipe where diameters were approximately equal.

TABLE 4

TOTAL LOAD PER FOOT OF SEAM CALCULATED VERSUS MEASURED

Height	Total Load per Foot of Seam in Pounds at Plate Number									
	15		22		31		32		33	
	Calc.	Meas.	Calc.	Meas.	Calc.	Meas.	Calc.	Meas.	Calc.	Meas.
12	-4950	+545[a]	-4950	+3040	-4950	-3000	-4950	-4500	-4950	-2400
		-3790[b]		+2720		-1800		-4500		-3000
25	-10330	-19520	-10330	-4270	10330	-6000	-10330	-9200	-10330	-10633
45	18600	-28810	-18600	-9890	-18600	-9933	-18600	-18400	-18600	-10633
60	24800	-41720	-24800	-19460	-24800	-17233	-24800	-29500	-24800	-13200
100	27150	-47433	-41300	-30627	-41300	-27300	-41300	-43200	-41300	-24733
137	27150	-62875	-43300	-33416	-56600		-56600	-58950	-56600	

[a] Before trenching
[b] After trenching

CONCLUSIONS

1. The vertical load on the pipe, as shown by strain readings, agrees substantially with the weight of the vertical column of fill immediately above the pipe. This is the weight ordinarily used to design culverts under high fills.

2. Lack of knowledge of the stresses imposed by the strutting operation prevented complete measurement of the stress on the pipe.

3. Part of the elongation of the vertical diameter still remained in the structure after completion of the fill and removal of the struts. This shows that the amount of elongation by strutting the strength of the pipe, compaction of the fill and the spacing of the struts had all been given proper consideration in the design.

4. The invert camber of 6 inches above straight grade, as originally established by foundation analysis, proved adequate, as about 3 inches of this camber remained after completion of the fill.

5. Analysis of the observed load distribution on the pipe shows that the methods used to construct a fill can affect the amount of load transmitted to the structure. In the construction of this fill, the material was repeatedly brought in over the pipe at one place. Greater loads were measured at this point than the weight of the vertical column immediately above the structure, because of this "hard spot" in the fill. In constructing such large fills, it would appear desirable to place the material in relatively thin horizontal layers and compact them uniformly so as to transmit the load to the original ground and to the structure in a uniform manner.

6. Data taken on strut cells and pipe wall strain gages at successive stages of fill height show that each increment of fill added its increment of load in almost direct proportion.

7. In this installation the use of the "imperfect-trench method" to reduce the loads on the structure was of only temporary value, as the load transmitted to the pipe substantially equaled the weight of the vertical column immediately above the pipe when the fill was completed.

The many factors involved in the construction of a fill of such proportions make it difficult to draw conclusions of other than a general nature. Such conclusions as are made can be specifically applied only to this test. However, general trends can be predicted. The indications are that flexible pipe under reasonably high fills can have the vertical diameter timber strutted in the field and the backfill around the pipe can be so compacted that little or no change in the pipe diameter will occur during the building and consolidation of the fill.

ACKNOWLEDGMENT

The author wishes to express his appreciation for the able assistance from H. D. Burnum, M. C. Davis, and C. W. Gibson, of the Alabama State Highway Department; G. E. Shafer, B. C. Steed, and H. L. White, of Armco Drainage and Metal Products, Inc.; and G. D. Miller and D. S. Wolford, of the Armco Research Laboratories.

References

1. Spangler, M. G., Soil Engineering, 1951 p. 427-430.
2. Tribble, J. F., Roads and Streets, Volume 95, Number 6, June 1952.

Appendix

Calculations that were used in processing the data appear below:

1. Strut load per foot per side.

$$\text{Strut load per foot per side} = \frac{\text{Strut load}}{\text{Strut spacing x 2}}$$

At Plate 15 for 137-ft. fill height

Compression-cap deformation - $1\frac{5}{16}$ in.
Strut load - 79,500 lb.
Strut spacing - 6-ft.

$$\text{Strut load per foot per side} = \frac{79,500}{6 \text{ x } 2} = 6,625 \text{ lb.}$$

2. Plate load based on strain-gage readings.

Horizontal Gage Position	Strain in Micro-inches
North	365
South	675

Stress for north gage = $30 \times 10^6 \times 365 = 10,950$ psi.
Stress for south gage = $30 \times 10^6 \times 675 = 20,250$ psi.
Cross-sectional area of one foot of plate = Formed length x 1.21 x thickness
Cross-sectional area of one foot of plate = $12 \times 1.21 \times .249 = 3.61$ sq. in.
Average load per foot of plate = Average stress x cross-sectional area

$$= \frac{10,950 + 20,250}{2} \times 3.61 = 56,250 \text{ lb.}$$

3. Total load per foot of seam.

$$\text{Total load per foot} = \frac{\text{Seam load per foot}}{\text{from strain gages}} + \frac{\text{Strut load per}}{\text{foot per side}}$$

Total load per foot of seam for Plate 15 at 137 feet fill $= 56,250 + 6,625 = 62,875$ lb.

4. Load per foot of pipe based on theoretical weight of fill.

(a) $W = W_1 + W_1 + W_S$

where W = load per lineal ft. of pipe
W_1 = load per lineal ft. per side
$\frac{W_S}{2}$ = Strut load per lineal ft. per side

(b) $W = D \times h \times c$

where D = pipe diameter (ft.)
h = fill height (ft.)
c = unit weight of fill (density)

(a) $W = W_1 + W_1 + W_S$
$W = 2W_1 + W_S$

when struts are removed $W_S = 0$

then $W = 2W_1$

(b) $W_1 = \frac{W}{2} = \frac{D \times h \times c}{2}$

$W_1 = \frac{D \times h \times c}{2}$ where $D = 7$ ft.
$h = 65.6$ ft.
$c = 118$ pcf.

$$W_1 = \frac{7 \times 65.5 \times 118}{2}$$

$W_1 = 27,150$ lb. for fill height of 65.6 ft.

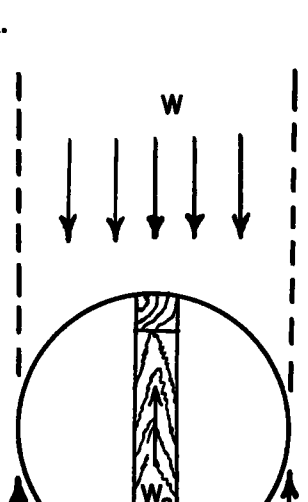

Discussion

M. G. SPANGLER, Department of Civil Engineering, Engineering Experiment Station, Iowa State College — Timmers' paper marks a significant milestone in the advance of our knowledge relative to the loads imposed upon culverts under earth fills. His observations show conclusively that the load on the structure increased with every increment of height of fill up to the maximum of 137 feet which prevailed on this job. This fact is definitely in harmony with the results indicated by Marston's "Theory of Loads on Conduits."

In the experimental research which accompanied the development of Marston's theory, the maximum height of fill employed was about 21 feet. In some concurrent experiments of a similar nature conducted by the University of North Carolina, the maximum height of fill used was about 12 feet. The American Railway Engineering Association, in 1926, published results of some field measurements of loads on pipe culverts under a railway

embankment near Farina, Illinois, in which the height of fill was 35 feet. Still later, in 1947, Wilson V. Binger, of the U. S. Corps of Engineers, described measurements of load on a concrete box culvert in Panama under 51 feet of fill. In all of these load measuring projects, the principle of linear relationship between load and height of fill above the plane of equal settlement was demonstrated.

Furthermore, in the North Carolina project, reported at the 1955 Annual Meeting of the Highway Research Board, by Costes and Proudley, preliminary indications are that this same principle held in the case of a culvert under 168 feet of fill, although final digest of the data on this job is not complete.

These qualitative checks on the validity of the Marston theory are of extreme importance at this time, because the requirements of modern highway transportation will undoubtedly result in the need for much higher fills as the highway program goes forward.

The writer would like to comment relative to Timmers' Conclusions 1 and 7, in which it is stated that the vertical load on the pipe was substantially equal to the weight of the prism of soil directly above the pipe and, therefore, that the imperfect-ditch method of construction was of only temporary value as a procedure for reducing load. If we limit consideration of measured loads to Sections 31, 32, and 33, which were under the roadway portion of the embankment and were not influenced by haul roads or by the side slopes of the embankment, it is seen that the average load on the culvert was only 75 percent of the weight of soil above 100 feet of fill (see Figure 12 and Table 4). The next load measurements were made at 137 feet of fill, when it is noted that no data were obtained for Sections 31 and 33. The only load measurement at this height of fill was on Section 32, which had consistently indicated a load approximately a third greater than the average of these three sections throughout the period of observation. A study of the data given in Figure 12 and Table 4 leads this writer to conclude that the average load on Sections 31, 32, and 33 was about 75 percent of the weight of the prism of soil directly above the pipe. Therefore, it is also concluded that the imperfect-ditch method of construction was effective to a substantial degree in accomplishing a reduction in load on the culvert.

As a further comment, although Timmers' paper does not state specifically, it is the writer's understanding that the backfill material in the imperfect trench consisted of the same crumbly, friable, sandstone soil which was removed during construction of the trench. Although this material was replaced in the trench in a loose state without compaction, from the description of the soil, it is probable that it was not very-compressible material.

Most effective results of the imperfect-ditch method of construction are obtained when the trench backfill is a highly compressible material. As a matter of fact, when Marston invented this method of construction, he recommended that, in some cases, high compressibility of the backfill material might be achieved by filling the trench part way with straw, hay, cornstalks, or brush to obtain the desired result. The writer does not know of an instance where this recommendation has been followed in actual construction, but it serves to emphasize the desirability of exerting special effort to achieve high compressibility of the trench backfill, which will result in greater reduction in load on the structure.

JOHN H. TIMMERS, Closure — Spangler's comment that the author's paper marks a significant milestone in the advance of knowledge relative to loads imposed upon culverts under earth fills is much appreciated. The author would like to thank him for pointing out that the test observations show results in agreeance with Marston's theory.

The marshalling of substantiating evidence from past tests as stated in Spangler's discussion adds considerably to the value of the author's report.

In discussing the comments relative to Conclusions 1 and 7, the author has no wish to refute Spangler's interpretation of the data. He would like, however, to present his reasons for his interpretation of the data. In regard to Conclusion 1 of the report, in which it is stated that vertical load on the pipe was substantially equal to the weight of the prism of the soil directly above the pipe, the author would like to say that this conclusion was drawn largely from the readings taken on Section 32, which had consistently

indicated more reliable action of the strain gages than any of the other sections.

Since this was the initial use of electrical strain gages in an installation subject to inundation of the gages, no precedent existed for waterproofing the gages. Several different methods of waterproofing and protecting against physical damage from waterborne rocks, etc., were made up in sample form and tested in the laboratory. Of these methods, the most promising were selected for use in the test; of these, the gages in Section 32 proved the most reliable. Several of the other gages displayed instability in readings and some became inoperative — among these were the gages of Sections 31 and 33, which had shown sluggish responses as compared to gages of Section 32 and could not be read for the final 137 feet of fill. It should be noted that the test structure had flowed full several times during the construction of the fill.

Hence, from actual close personal contact with the gage readings as the work progressed the author believed the data from Section 32 to be the most reliable and indicative of the loads on the structure. When the weight of the vertical column above the structure was compared to the loads computed from the strain gages of Section 32, the magnitudes were the same and since there was no change in the slope of the curve as the fill height increased the author could see no permanent reduction of load from the imperfect trench construction.

Thus the author arrived at what he considered the best and most-logical interpretation of the data. However, knowing that other interpretations were possible and plausible, the entire data was published.

There could even be argument as to the exact weight of the vertical column of earth above the pipe. The author chose to use the dry density of 118 pcf., as determined from samples taken adjacent to the structure itself. Although the moisture content was 10 percent, it was believed that the dry density of the thin layers well compacted near the structure, most closely approximated the moist weight of the material placed in 3-foot lifts above the structure. Hence, the value of 118 pcf. was used, since no other data was available on the precise weight of the material above the structure.

In concluding the author would like to point out that Spangler's interpretation based on averages of readings is just and plausible and can be as nearly correct as that of the author based on the most-severe readings from the gages considered most reliable. Both interpretations do not differ in magnitude but in detail and both confirm that present design practice is conservative.

Factors Affecting Vertical Loads on Underground Ducts Due to Arching

NICHOLAS C. COSTES, Materials Engineer
North Carolina State Highway and Public Works Commission[1]

A theory of earth pressure on underground conduits is presented. Expressions for the general case of an $s = c + \sigma \tan\phi$ material have been derived. Expressions relating to $s = \sigma \tan\phi$ and $s = c$ soil types appear as special cases of the general case.

It is shown that the pressure on top of both covered-up and mined-in conduits is governed by the same mathematical relations. However, the values of the physical factors appearing in the theoretical expressions depend on the geometry and nature of installation, the physical properties, and the initial state of the materials, as well as on the construction methods and workmanship employed.

Curves for the evaluation of the load on top of covered-up conduits installed under an $s = \sigma \tan\phi$ material have been constructed. Under certain conditions the same curves can also be used for the general case of an $s = c + \sigma \tan\phi$ material.

The load on covered-up conduits becomes a minimum if the conduit side supporting material is thoroughly compacted, the ditch directly above the conduit is made as high as economically feasible, and the ditch is filled with a compressible, loose material.

● THIS paper was intended originally to be the theoretical part of a report on a three-year research project directed by the North Carolina State Highway and Public Works Commission. The project involved the study of the performance of a 66-in. flexible, metal-pipe culvert installed under a 170-ft. earth embankment that was constructed by end-dumping.

Existing earth pressure theories on underground conduits are applicable to low or medium height embankments consisting of perfectly granular material. Because of the unusual fill height and the construction methods employed in this project it was considered desirable to review and extend these theories, and revise them if necessary, in order to make them applicable to the above conditions.

In the process of extending these theories it was noticed that the mathematical expressions that govern the loading action of a fill placed on top of a conduit also govern the loading action of a natural earth deposit on a conduit that has been installed by a tunneling process. The geometrical similarity existing among various types of conduits covered by an earth fill and a conduit installed by a mining process is shown in Figure 1.

All underground conduits are either covered with an earth embankment after they have been assembled in place or are mined-in through a natural earth deposit. Therefore, an earth pressure theory that is applicable to these two main categories is generally applicable to all types of underground conduits.

Because of these considerations the general theoretical treatment is presented here as a separate study. The experimental part of the same project appears as a separate report by the North Carolina State Highway and Public Works Commission (Costes and Proudley, 1955). In the latter report appropriate mathematical expressions were derived from the general theory to make a speculative analysis of the earth pressure existing on top of the particular culvert under study.

Definitions

In this paper, an underground conduit is defined as a hollow prismatic structure that is installed with its longitudinal axis substantially horizontal under either a man-made earthen embankment or a natural earthen deposit.

---

[1] Presently, with Snow, Ice and Permafrost Research Establishment, Corps of Engineers, U. S. Army.

Underground conduits can be used for a multiplicity of purposes; they can be used as aquaducts, drainage structures, sewers, viaducts, runways for conductors or cables, gas mains, etc.

If a conduit is installed first, and then an earth embankment is constucted above it, the conduit is defined as a "covered-up conduit." If the conduit is installed through a natural earthen deposit by means of a mining process, the conduit is defined as a "mined-in conduit."

If judged according to their relative stiffness, underground conduits may be classified as "rigid conduits" or as "flexible conduits." The demarcation line between these two classes is not defined clearly.

Problems Relating to Underground Conduit Design

When designing an underground conduit, the engineer faces a variety of problems whose relative influence on the final design of the conduit depends on the purpose for

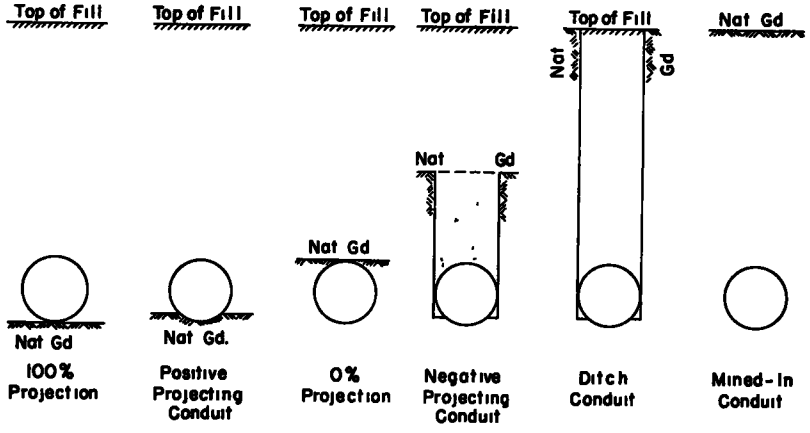

Figure 1. Geometrical relationship among underground conduits.

which the conduit is installed, the desired life expectancy of the conduit, and the size of the earth mass that the conduit will sustain. Some of these problems relate to: (1) durability; (2) hydraulic factors in case the conduit is installed as an aquaduct; (3) traffic considerations in case the conduit is installed as a viaduct; (4) adequate space in case a close inspection of the conduit is desired; and (5) structural capacity.

If the conduit is treated from the structural point of view the designer is mainly concerned with: (1) choosing the right conduit material and employing the right construction methods in order that the load on the conduit will be a minimum; (2) providing for adequate side support so that the conduit will not fail by excessive lateral bulging; (3) selecting the proper bedding material and deciding on the proper camber so that the conduit will not go out of alignment as the foundation settles; and (4) designing properly the thickness and the structural connections of the conduit so that it will withstand the internal stresses that are generated in its structure by the external pressures, namely, the top load, the lateral pressures exerted by the side supporting material, and the bottom reaction from the bedding material.

If the earth mass above the conduit is not too high, then, in addition to the dead load due to the earth mass, the influence of live loads that may exist on the surface of the mass must be considered also.[2] If the earth mass, however, is sufficiently high and pressure waves due to live loads are dissipated before reaching the conduit, the main load on the conduit will be due to the pressure of the earth that it sustains.

Scope of Paper

The purpose of this paper is to (1) present a general, uniplanar, theoretical study of

[2] For such treatment see References, Spangler and Hennessy (1946).

the factors influencing the pressure that is developed on top of both covered-up and mined-in conduits due to the earth mass alone; (2) apply the general study to special cases; (3) examine the physical meaning of the derived mathematical expressions; (4) draw conclusions in connection with the implications that certain installations may have on the conduit load; (5) construct curves from which the load on top of a conduit can be obtained for as many cases as possible; (6) suggest the main principles that should guide the engineer's judgment when designing an underground conduit; and (7) make recommendations relating to future research efforts in connection with this field of engineering.

This study makes no differentiation between "rigid" or "flexible" conduits. The shape of the conduit is also considered not to be a variable.

The mathematical treatment deals with the pressures acting in the plane perpendicular to the longitudinal axis of the conduit. The study of the development of earth pressures above the conduit and in the direction parallel to its longitudinal axis is beyond the scope of this paper.

REVIEW OF PREVIOUS RELATED STUDIES

All earth pressure theories relating to underground conduits have been based on one of the most universal phenomena encountered in soils, both in the laboratory and in the field, the so-called "arching effect." The arching effect as defined by Terzaghi (1943a) is a transfer of pressure from a yielding mass of soil onto adjoining relatively stationary parts. This pressure transfer takes place through a mobilization of the shearing resistance of the material which tends to oppose the relative movement within the soil mass.

Most of the existing theories on arching deal with the pressure of dry sand on yielding horizontal strips. Terzaghi (1943a) divides these theories into three groups:

1. In the first group only the conditions for the equilibrium of the sand immediately above the loaded strip have been considered. No attempt has been made to investigate whether or not the results of the computations have been compatible with the conditions for the equilibrium of the sand at a greater distance from the strip.
2. The theories of the second group have been based on the unjustified assumption that the entire mass of sand located above the yielding strip is in a state of plastic equilibrium.
3. In the third group the assumption has been made that the vertical sections through the outer edges of the yielding strip represent surfaces of sliding and that the pressure on the yielding strip is equal to the difference between the weight of the sand located above the strip and the full frictional resistance along the vertical sections.

No attempt will be made in this paper to describe each one of the above groups in any further detail.[3]

As far as studies of pressures on underground conduits are concerned, one may go as far back as the year 1882 when Forchheimer (1882) studied the development of earth pressures on the roof of a tunnel. This study was related to the studies by Janssen and Airy on the development of pressures observed in bins and grain elevators (Janssen, 1895), (Ketchum, 1913). As a matter of reference, the term, "bin effect," may be found in place of the term, "arching effect," in some publications.

Dean Anson Marston, Professor M. G. Spangler, and their associates of Iowa State College, deserve great credit for advancing the knowledge of loads developed on underground conduits. Under their direction, an extensive program of research, starting in 1908, has been carried out. Their main aim was to develop a rational method for determining the loads on covered-up conduits. The result of their work has been the "Marston Theory of Loads on Underground Conduits." This theory has been applied extensively in this country in the design of covered-up conduits. The theory is applicable

[3] For a comprehensive summary of each theory, see K. Terzaghi, Theoretical Soil Mechanics (New York: John Wiley & Sons, 1943), pp. 69-74. Detailed information on the same subject may be obtained from the following References: Engesser (1882), Kötter (1899), Janssen (1895), Koenen (1896), Bierbaumer (1913), Caquot (1934), Terzaghi (1936), Völlmy (1937) and Ohde (1938).

mainly to embankments constructed of perfectly granular materials (Marston, 1913, 1930), (Spangler, 1950a, 1950b).

In addition to the work conducted by Marston in the Iowa Engineering Experiment Station, several other extensive studies concerning earth pressures on underground conduits have been carried out both in the United States and in other countries.

These studies include the following:

1. Experiments were conducted at the University of North Carolina in 1927 in which the top vertical pressure, radial pressures, and the decrease in the conduit vertical diameter were measured in pipes of various diameters and materials, installed as positive projecting conduits (Braune, Cain and Janda, 1929).
2. Pressure tests were conducted on corrugated metal, concrete, and cast iron pipe culverts by the American Railway Engineering Association at Farina, Illinois, during the period 1923-1926 (Area, 1928).
3. During the construction of liner-plate and shield tunnels installed in the Chicago, Illinois, subway, an extensive research on earth pressures developed in mined-in conduits due to plastic clay, as well as on the deformations of the conduit structures, was conducted and reported by Terzaghi (1942-1943) and Peck (1943).
4. Similar tests on earth pressure on tunnels installed in plastic clay were conducted and reported by Housel (1943) in Detroit, Michigan.
5. Strain gage and load cell pressure measurements, as well as data from deformations and settlements, were obtained by the Alabama State Highway Department and Armco engineers from corrugated metal culvert pipe installations under 137 ft. of embankment (Timmers, 1953).
6. Similar tests were conducted by the North Carolina State Highway and Public Works Commission on a Multi-Plate culvert pipe installed under 170 feet of embankment. An attempt to develop a technique to measure directly the earth pressures exerted on the culvert under study is discussed also (Costes and Proudley, 1955).
7. In the laboratories of the Zurich Technical University, Switzerland, Völlmy (1936, 1937) conducted a series of tests on sand located above a yielding support to prove his assumption that the potential sliding surfaces are oblique planes.
8. Experiments on pipe models by using centrifuges to generate forces similar to these acting on the pipes in ditch conduit installations were conducted in the Moscow Municipal Academy (Pokrowski, 1937).[4]
9. A series of articles on culvert pipe analysis has been published in France by the Hungarian engineer Bela (1937), and by Guerrin (1938).
10. Information of culvert pipe analysis may also be found in the catalogues and publications of pipe manufacturers.[5]

THEORETICAL STUDY

Method of Analysis

The theoretical concepts and the resulting relations of this paper are presented as follows: (1) the basic assumptions are stated and discussed; (2) the fundamental differential equation describing the loading action of an earth mass on top of an underground conduit is derived; (3) the general load equation for an $s = c + \sigma \tan\phi$ material is derived; (4) Case I is defined and discussed; (5) Case II is defined and discussed; (6) factor $u = (2K_e \tan\phi_e)H_e/B_d$ is evaluated and discussed for Case II existing in covered-up and mined-in conduits; (7) the analysis of the general case is applied to an $s = \sigma \tan\phi$ material; (8) the analysis of the general case is applied to an $s = c$ material; and (9) families of curves are constructed for which the load by an $s = \sigma \tan\phi$ material on a covered-up conduit can be obtained. Conditions are stated under which the same curves can be used for the evaluation of the conduit load when the loading agent is an $s = c + \sigma \tan\phi$ material.

---

[4] For a brief summary of the findings and conclusions of the experiments mentioned in items (7) and (8), see D. P. Krynine, "Design of Pipe Lines from Standpoint of Soil Mechanics," Proceedings of the Highway Research Board, XX (1940), 726-727.

[5] see References.

Analysis

Statement of Assumptions. The following basic assumptions are made in the evaluation of the theoretical relations governing the loading action of masses on top of underground conduits:

1. The loading agent is an ideal, homogeneous, isotropic material whose shearing resistance, s, per unit of area can be represented by the empirical equation: $s = c + \sigma \tan\phi$ where σ is a force per unit area, normal on a section through a mass. The symbol c represents the cohesion, which is equal to the shearing resistance per unit area if $\sigma = 0$. The symbol ϕ represents the angle of internal friction of the material.
2. Because of the fact that the foundation, which supports the material directly above the conduit, does not yield the same amount as the foundation, which supports the material adjacent to the middle mass, the former subsides more or less than the adjacent material depending upon the relative yielding of their respective supports. The relative subsidence takes place along vertical plane surfaces extending from the top of the conduit to some horizontal plane above the conduit designated as, "plane of equal settlement." Above the plane of equal settlement no relative subsidence takes place and all parts of the fill material settle the same amount due to the consolidation of the fill. Henceforth, the mass directly above the conduit will be referred to as the "interior prism." During the subsidence of the interior prism, horizontal layers remain horizontal.
3. The side supporting material has not been compressed excessively so as to cause the structure to fail by excessive horizontal bulging.
4. The internal stresses generated in the conduit structure on account of the external pressures have not exceeded the critical buckling load of the structure.
5. The unit weight of the material, γ, is constant throughout the fill height.
6. The angle of internal friction of the material, ϕ, is constant along the potential sliding planes.
7. The cohesion of the material, c, is constant along the potential sliding planes.
8. The ratio of the horizontal principal stress component within an element of the fill material to the vertical principal stress acting on the same element, K_e, is constant along the potential sliding planes. The ratio may be called, therefore, "hydrostatic pressure ratio."

Discussion of Assumptions. Every stress theory is based on the assumption that the material subject to stress is either homogeneous and isotropic or that the departure from these ideal conditions can be described by simple equations. If the material is also assumed strictly to follow Hooke's law, then the term "homogeneity" denotes identical elastic properties at every point of the material in identical directions whereas the term "isotropy" involves identical elastic properties throughout the material and in every direction at any point of it. When the material under study is soil not subject to stratification, then both assumptions may be understood to have a statistical average value.

Assumption 2 that the potential surfaces of sliding are vertical planes, is unlikely to occur in the actual case and it is made only to simplify the mathematical computations. Actually, as Terzaghi (1943a) points out, the real surfaces of sliding are curved and at the top of the fill their spacing is considerably greater than the width of the conduit. From this, it follows that along the assumed vertical, potential sliding surfaces the internal friction of the material will never be fully mobilized and, thus, plastic equilibrium conditions are not realized. The error due to ignoring this fact is on the unsafe side.

Also, during the relative subsidence of the material above the conduit, horizontal layers within the interior prism do not remain horizontal, but they become either concave or convex curved surfaces depending on whether or not the interior prism subsides more or less than the adjacent masses. Therefore, the surfaces of equal, normal pressure are not plane but are curved, like arches.

The existence of the "plane of equal settlement" was discovered on purely mathematical grounds by Marston (1922). The actual existence of such a plane has been demonstrated by laboratory models, and by measurements of the settlements of the soil both over and adjacent to some experimental conduits (Spangler, 1950a, 1950b).

Assumptions 3 and 4 must be fulfilled in order that the analysis made in this paper

has a meaning. The problems of insuring adequate side support to the conduit as well as designing the conduit structure to withstand the internal stresses that are generated due to the external pressures are beyond the scope of this paper.

Assumption 5 requires that an overall average value of the unit weight of the material be used. Actually, everything else remaining constant the unit weight of the material will vary with the fill height with higher values at the bottom of the fill. The method of fill construction and the water content are major factors influencing γ.

Assumptions 6 and 7 pertain to the values of the angle of internal friction and cohesion that are actually mobilized along the potential sliding planes. Because of the reasoning applied in discussing Assumption 2 , both values will generally be smaller than the laboratory values of ϕ and c exhibited by a series of tests from samples of the same material. Therefore, in the subsequent theoretical treatment of the problem the values of ϕ and c that are used will denote the amount of both properties that are actually mobilized. They will be designated as ϕ_e and c_e respectively. These values depend not only on the nature of the soil and its initial state, but also on the rate of stress application, the permeability of the material, the deformation characteristics, and the size of the mass.

The last assumption, that the ratio of the horizontal principal stress to the vertical principal stress acting on an element within the mass of the material is constant along the potential sliding planes, is at great variance with reality. Everything else remaining constant this ratio depends on the nature, initial state, and strain characteristics of the material.

If the material is a solid block, then the ratio is equal to zero. If the material behaves like a liquid then the ratio is equal to one.

For a semiinfinite, sedimentary deposit of cohesionless material, it has been found experimentally that this ratio varies between 0.45 and 0.55 depending on the geologic history of the deposit and it is approximately the same for every point of the mass. In this particular case, the ratio is called the coefficient of earth pressure at rest, or coefficient of natural earth pressure and it is denoted by K_O. The range of values of K_O for clays in their natural state is not yet known.

If a homogeneous, semiinfinite mass bounded by a horizontal plane and extending to infinity downward and in every horizontal direction is given an opportunity for lateral expansion to a very great depth, z, in such a manner that the lateral strain remains constant with depth, then the mass passes from an initial state of elastic equilibrium to an active state of plastic equilibrium. In this condition the internal resistance of the material is fully mobilized and conditions of incipient shear failure exist along two sets of surfaces of sliding that are symmetrical to each other with respect to a vertical axis and inclined at an angle of $45^0-\phi/2$ with the vertical. Under such conditions the lateral intensity of pressure decreases to the smallest value compatible with equilibrium. Such a condition is called an active earth pressure condition. The value of the lateral earth pressure is designated σ_A and the ratio K is equal to

$$K_A = \tan^2 (45^0 - \phi/2) - \frac{2c}{\gamma z} \tan(45^0 - \phi/2) \qquad (1)$$

for an $s = c + \sigma\tan\phi$ material.

For an $s = \sigma\tan\phi$ material

$$K_A = \tan^2 (45^0 - \phi/2). \qquad (2)$$

For a perfectly cohesive material; that is, for an $s = c$ material

$$K_A = 1 - \frac{2c}{\gamma z}. \qquad (3)$$

If the same semiinfinite mass is compressed laterally to a great depth, z, in such a manner that the lateral compressive strain remains constant, then the mass reaches a passive state of plastic equilibrium. In this state the internal resistance of the material is fully mobilized and conditions for incipient shear failure exist along two sets of sliding surfaces, symmetrical to each other with respect to a vertical axis and inclined at an angle equal to $45^0 + \phi/2$ with the vertical. Under such conditions the lateral intensity of pressure increases to the largest value compatible with equilibrium. Such a condition

is called a state of passive earth pressure. The corresponding lateral pressure is designated σ_p and the ratio K is equal to

$$K_P = \tan^2 (45^0 + \phi/2) + \frac{2c}{\gamma z} \tan (45^0 + \phi/2) \quad (4)$$

for an $s = c + \sigma \tan\phi$ material.

For a cohesionless material; that is, for an $s = \sigma \tan\phi$ material

$$K_P = \tan^2 (45^0 + \phi/2). \quad (5)$$

For a perfectly cohesive material; that is, for an s = c material

$$K_P = 1 + \frac{2c}{\gamma z} \cdot \quad (6)$$

In the actual case, the lateral expansion or compression which cohesive soils must

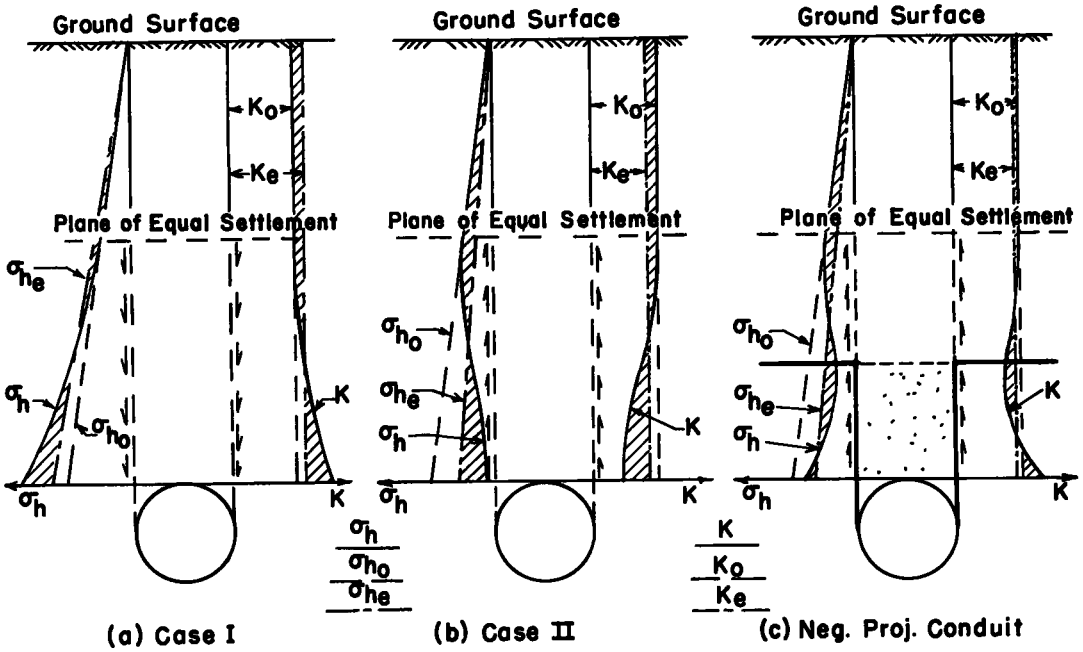

Figure 2. Variation of σ_h and K with fill height.

undergo in order that they reach active or passive states of plastic equilibrium is much greater than any allowable movement within the engineering structures which they bear contact with and, therefore, the ratio K will always lie between the limiting values K_A and K_P.

With cohesionless soils such as dry clean sand, a very small lateral stretching is sufficient to insure active state conditions, whereas a considerable compressive movement must precede passive state conditions.

However, even if the least trace of moisture is present in a cohesionless mass, the material will exhibit a property known as "apparent cohesion" and it will behave like a cohesive material (Terzaghi 1943a). Since in engineering practice water is almost always present in a soil mass, even a granular mass must be stretched laterally a considerable amount before an active state of plastic equilibrium is reached and before K assumes the limiting value K_A.

From Equations 1 and 3 it can be seen that for cohesive materials in an active state of plastic equilibrium K depends mathematically on the fill height and for small values of the fill height it may assume even negative values.

The above discussion on the ratio K was made in reference to constant strain conditions for various materials. If the lateral strain within the mass varies with depth then

K must be expected to vary also.

In the case of an underground conduit, as the middle prism slides along the vertical planes, the lateral strain along these planes may be visualized to vary as follows: Along the vertical extensions of the sliding planes from the top of the embankment to the plane of equal settlement, the lateral strain within the mass is zero because the settlement is uniform at all parts of the mass. Therefore, K may be expected to be constant within this region. If the conduit is mined in a sedimentary deposit of granular material the value of K will be K_o. If the conduit is installed under a man-made granular embankment the value of K will be K_s. K_s will be dependent on the nature and condition of the material, the methods of compaction, the degree of compaction and the height of the fill.

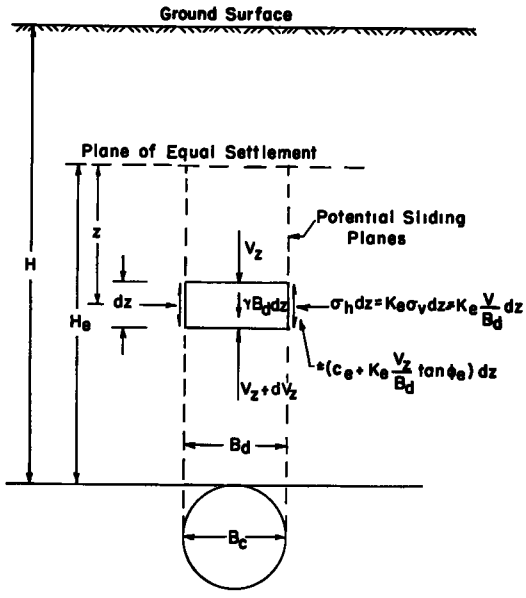

Figure 3. Force diagram for an underground conduit.

In the region between the plane of equal settlement two cases may develop: (1) the adjacent mass may settle more then the interior prism and (2) the interior prism may settle more than the adjacent mass.

In the first case the lateral strain changes from zero at the plane of equal settlement and becomes compressive gradually increasing to a maximum at the top of the conduit. Accordingly, K should be expected to increase from the value K_o or K_s at the plane of equal settlement to a maximum value in the vicinity of the top of the conduit (Figure 2a).

In the second case the lateral strain changes from zero at the plane of equal settlement and becomes tensile gradually increasing to a maximum at the yielding support of the conduit. Accordingly, K should be expected to decrease from the values K_o or K_s at the plane of equal settlement to a smaller value approaching K_A in the vicinity of the yielding support of the middle prism (Figure 2b).

Since the object of the subsequent mathematical treatment is to develop a relation for the load on top of the conduit upon which the integrated influence of K is reflected, the diagram of the variation of K with fill height may be substituted with an equivalent diagram in which K is constant and has a value equal to the mean abscissa, K_e of the diagrams of Figure 2. Thus, the mathematical computations will be simplified appreciably without altering the resulting load expression. Adequate experimentation will give values of K_e for various types of installations and earthen materials.

In Figure 2 the lateral principal stress diagrams σh_o, σh, and σh_e, corresponding to $K = K_o$, $K = K$, and $K = K_e$ respectively, are also shown for the two cases. From these diagrams it can be seen that the ordinates of the equivalent hydrostatic stress diagram, σh_e, are larger or smaller in magnitude than the ordinates of the lateral stress at rest diagram, σh_o, depending on whether the interior prism subsides less or more than the adjacent mass.

Differential Equation Describing the Loading Action of an $s = c + \sigma \tan\phi$ Material on Top of Underground Conduits

Let Figure 3 represent the installation conditions and the force diagram for an underground conduit of external diameter B_c installed under an embankment composed of an $s = c + \sigma \tan\phi$ material.

Let:

H = height of embankment measured from the top of the conduit, ft.

H_e = height of the potential sliding planes from the top of the conduit to the plane of equal settlement. Henceforth, this height will be referred to as "height of arching," ft.

z = distance from the plane of equal settlement down to any horizontal plane, ft.

B_c = width of conduit, ft.

B_d = effective width of the interior prism, ft.

γ = unit weight of the material on top of the conduit, pcf.

ϕ_e = portion of the angle of internal friction of the material that is mobilized along the potential sliding planes.

c_e = portion of the cohesion of the material that is mobilized along the potential sliding planes, psf.

σ_v = vertical principal stress acting on an element of the material along the sliding planes at a distance z from the plane of equal settlement, psf.

σ_h = horizontal principal stress acting on an element of the material along the sliding planes at a distance z below the plane of equal settlement, psf.

$K_e = \frac{\sigma_h}{\sigma_v}$ = equivalent hydrostatic pressure ratio along the sliding planes.

$V_z = \sigma_v B_d$ = resultant vertical pressure acting on a horizontal layer in the interior prism at a distance z from the plane of equal settlement, lb. per lin. ft. of length.

W_c = vertical load on top of the conduit due to overburden material, lb. per lin. ft. of length.

$W = \gamma B_d H$ = weight of the earth column on top of the conduit, lb. per lin. ft. of length.

The weight of the thin slice of the interior prism with a thickness dz at a depth z below the plane of equal settlement is $\gamma B_d dz$ per unit of length perpendicular to the plane of the drawing. The slice is acted upon by the forces indicated in the figure. The condition that the sum of the vertical components that act on the slice must equal to zero can be expressed by the equation

$$\gamma B_d dz + V_z - dV_z - V_z \pm 2\left(c_e + K_e \frac{V_z}{B_d} \tan\phi_e\right) dz = 0, \qquad (7)$$

or

$$-\frac{dV_z}{dz} \pm 2K_e \frac{V_z}{B_d} \tan\phi_e \pm 2c_e + \gamma B_d = 0. \qquad (8)$$

Equation 8 is the fundamental differential equation describing the conditions of equilibrium during the loading action of an $s = c + \sigma \tan\phi$ material acting on top of an underground conduit. The plus or minus signs represent the case in which the interior prism subsides less or more than the adjacent masses respectively.

Evaluation of the General Load Expression for an $s = c + \sigma \tan\phi$ Material

Equation 8 is a linear differential equation of first order.

Integrating and considering the limits

$$V = (H - H_e)\gamma B_d \quad \text{for} \quad z = 0$$

$$V = V_z \quad \text{for} \quad z = z$$

one obtains after rearranging terms

$$V_z = \frac{\gamma B_d^2}{2K_e \tan\phi_e} \left\{ e^{\pm(2K_e \tan\phi_e)\frac{z}{B_d}} \left[(2K_e \tan\phi_e)\left(\frac{H - H_e}{B_d}\right) \pm \left(1 \pm \frac{2c_e}{\gamma B_d}\right) \right] \mp \left(1 \pm \frac{2c_e}{\gamma B_d}\right) \right\}. \qquad (9)$$

When $z = H_e$ $\qquad V_z = W_c$.

Substituting in Equation 9 one obtains

$$W_c = \frac{\gamma B_d^2}{2K_e \tan\phi_e} \left\{ e^{\pm(2K_e \tan\phi_e)\frac{H_e}{B_d}} \left[(2K_e \tan\phi_e)\left(\frac{H - H_e}{B_d}\right) \pm \left(1 \pm \frac{2c_e}{\gamma B_d}\right) \right] \mp \left(1 \pm \frac{2c_e}{\gamma B_d}\right) \right\}. \qquad (10)$$

Equation 10 is the general load expression for an $s = c + \sigma \tan\phi$ material. The plus or minus signs represent respectively the cases in which the interior prism subsides

less or more than the adjacent masses.

Equation 10 may be written also

$$W_c = \gamma B_d(B_d/2K_e\tan\phi_e)C, \tag{11}$$

where

$$C = e^{\pm(2K_e\tan\phi_e)\frac{H_e}{B_d}\left[(2K_e\tan\phi_e)(\frac{H-H_e}{B_d}) \pm (1 \pm \frac{2c_e}{\gamma B_d})\right] \mp (1 \pm \frac{2c_e}{\gamma B_d})}. \tag{12}$$

Henceforth, factor C will be called the "load factor."

Letting

$$(B_d/2K_e\tan\phi_e)C = H_{eff} \tag{13}$$

and substituting in Equation 11 one obtains

$$W_c = \gamma B_d H_{eff}. \tag{14}$$

Factor H_{eff} may be thought of as an effective height along which no relative subsidence occurs between the material directly above the conduit and the adjacent material. In such case neither mass would tend to brace itself against the adjacent one, no sliding surfaces would tend to form, and the load on top of the conduit per unit length would be equal to the full weight of the column of the material directly above it.

By inspection of Equation 12 , and since:

$$C = \left[(2K_e\tan\phi_e)/B_d\right] H = C_o,$$

$$H_{eff} = H,$$

and

$$W_c = \gamma B_d H = W, \tag{15}$$

when

$$H_e = 0,$$

it can be seen that if the interior prism subsides less than the adjacent masses, in which case the shearing resistance of the material mobilized along the sliding planes have the same direction and sense as the weight of any thin slice within the interior prism, the positive signs are used in Equations 7 through 12,

$$C_p = \text{Load factor with positive signs} > C_o,$$

$$H_{eff} > H,$$

and

$$W_c > W.$$

Similarly, if the interior prism subsides more than the adjacent masses, in which case the shearing resistance of the material mobilized along the sliding planes has the same direction but opposite sense than the weight of any thin slice within the interior prism, the negative signs are used in Equations 7 through 12,

$$C_n = \text{load factor with negative signs} < C_o,$$

$$H_{eff} < H,$$

and

$$W_c < W.$$

In the subsequent analysis the above two cases will be studied separately. However, every engineer dealing with underground conduits should direct all his efforts toward creating the proper environmental conditions during the construction of such structures in order that conditions corresponding to the second case will be realized.

Case I. The Interior Prism Subsides Less Than the Adjacent Masses

This case may develop as a result of the following two environmental conditions in the construction of a conduit.

1. In the case of a covered-up conduit, the conduit is installed by means of the so-called "positive projection" method (Spangler 1946). According to this method the conduit is installed with its top projecting some distance above the natural ground surface. Then, the fill material is placed around and on top of the conduit. No special effort is made to compact the side material to a higher degree of compaction than the rest of the fill material (Figure 4).

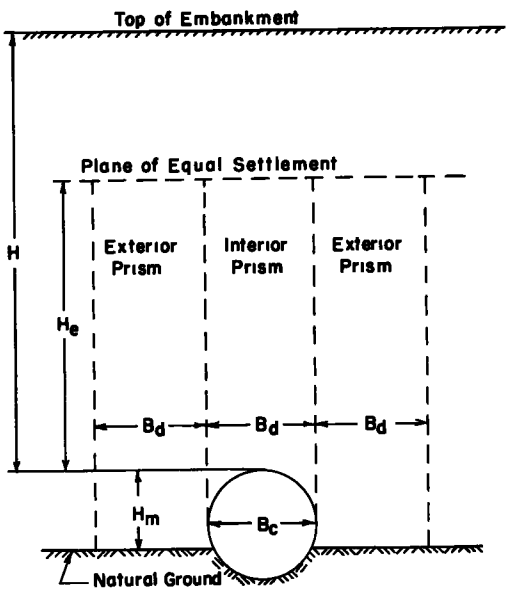

Figure 4. Installation diagram for a positive-projecting conduit.

Assuming that the natural ground surface settles by the same amount everywhere, let us compare the vertical deformation of the interior prism with the deformation of the two adjacent masses extending from the natural ground surface to the plane of equal settlement and having a width equal to the width of the interior prism which in this case is equal to the width of the conduit. Henceforth, these two masses will be called "exterior prisms."

All three prisms are loaded with the same overburden weight equal to $(H-H_e)\gamma B_d$. Therefore, any relative differential deformation existing among them would be a function of the weight of each prism which, accordingly, is a function of its height as well as the characteristics of the material. Hence, if no contact existed among these prisms and each one were allowed to deform freely, the summation of deformations from the bottom upward would normally be at a greater rate in the high prisms than in the lower ones. Since the two exterior prisms are higher than the interior prism by an amount H_m, and since the material within this region is compacted by the same amount as any other part of the fill, the exterior prisms will tend to settle at a greater rate than the interior prism. However, in the actual case all three prisms are in contact with each other and, consequently, the exterior prisms transfer part of their vertical pressures to the interior prism. The result is that, because of this stress transfer, the rate of summation of vertical deformations will be reduced in the exterior prisms and increased in the interior prism. The total summation of deformations in the interior prism will approach that in the exterior prisms, and the height at which the deformations become equal is the height of equal settlement (Marston 1922).

2. In the case of a mined-in conduit, the conduit is installed in a bed of a very soft compressible material, and the conduit is too rigid to "give in" under the influence of the top vertical load. Under such conditions it is conceivable that the material adjacent to the conduit will have the tendency to settle more than the material on top of it. Therefore, as in the case of "positive projecting conduits," the exterior prisms will tend to brace themselves against the interior prism and in doing so they will transfer part of their vertical pressures on to the interior prism.

From the above discussion and for reasons which were discussed, one should use the positive signs in the general load expression when the conditions insuring the existence of Case I have been realized.

Hence, Equation 10 becomes

$$W_c = \frac{\gamma B_d^2}{2K_e\tan\phi_e}\left\{e^{+(2K_e\tan\phi_e)\frac{H_e}{B_d}\left[(2K_e\tan\phi_e)(\frac{H-H_e}{B_d}) + (1+\frac{2c_e}{\gamma B_d})\right]} - (1+\frac{2c_e}{\gamma B_d})\right\}, \quad (16)$$

from which

$$C_p = e^{+(2K_e\tan\phi_e)(\frac{H_e}{B_d})\left[(2K_e\tan\phi_e)(\frac{H-H_e}{B_d}) + (1+\frac{2c_e}{\gamma B_d})\right]} - (1+\frac{2c_e}{\gamma B_d}). \quad (17)$$

A quick inspection of Equations 16 and 17 will show that in this case the shearing resistance of the material on top of the conduit works against the engineer; the more resistant to shear the material is and the larger the portion of its shear components that is mobilized along the sliding planes, the greater will be the load on top of the conduit.

Furthermore, from Figure 2b, it was shown that in Case I the equivalent hydrostatic pressure ratio K_e will generally be larger in magnitude than the coefficients of earth pressure at rest, K_o, or K_s. By inspecting Equations 16 and 17 again, one can also see

that the larger the value of K_e the larger will be the load.

Now let us examine what other serious implications Case I might have on the load expression.

Equations 16 and 17 contain the ascending exponential function e^u, where $u = (2K_e \tan\phi_e) H_e/B_d \geq 0$, multiplied by a positive sum. The ascending exponential function is equal to 1 for u = 0, and increases very rapidly with increasing values of u. For example:

$$\text{if } u = 1,\ e^u \approx 2.7;\ \text{if } u = 2,\ e^u \approx 7.4;$$
$$\text{if } u = 4,\ e^u \approx 54;\ \text{if } u = 8,\ e^u \approx 2980,\ \text{etc.}$$

Therefore, if the over-all height of the material on top of the conduit is in the region of 100 ft. or more, which with modern construction equipment has come within the realm of engineering endeavor, the load on top of the conduit, W_c, will be many times greater than the weight of the column of the material, W. Consequently, even if the side-supporting material is able to mobilize sufficient reactive pressure to equalize the top pressure before the structure bulges out excessively, the ring stresses that are generated in the conduit structure will exceed the critical buckling load of the conduit and the results will be catastrophic.

To illustrate the above, let

$H = 100$ ft.
$B_d = 5.0$ ft.
$K_e = 1.0$
$\phi_e = 10^0$
$c_e = 200$ psf.
$\gamma = 120$ pcf.

The weight of the column of the material above the conduit is, therefore, $W = \gamma B_d H = 60{,}000$ lb. per lin. ft.

Substituting the above data in Equations 16 and 17 and solving for $H_e = 0$, $H_e = 10$ ft., $H_e = 20$ ft., and $H_e = 50$ ft. one obtains respectively:

H_e	C_p	H_{eff}	H_{eff}/H	W_c/W
0	7.1	100	1.0	1.0
10 ft.	14.6	207 ft.	2.1	2.1
20 ft.	28.3	401 ft.	4.0	4.0
50 ft.	176	2495 ft.	25.0	25.0

In other words, if the height of arching is one-half the fill height, the load on a 5.0 ft. diameter conduit due to a 100 ft. fill will be almost twenty-five times the weight of the column of the material on top of it; i.e., $W_c = 1{,}320{,}000$ lb. per lin. ft. No conceivable factor of safety employed in the design of the conduit will provide for such a possibility and stay within reasonable economical limits.

From the above, one may conclude that conditions for Case I are very undesirable from the engineering standpoint and, therefore, every effort should be made to avoid them in the field.

If a conduit is installed by the "positive projection" method, the material immediately adjacent to the conduit should be thoroughly compacted to a much higher degree than the remainder of the fill material. If such a procedure is followed, the stiffness of the mass within the height H_m will be much greater than that of the material within the rest of the exterior prism. Consequently, the effective height of the exterior prism will be decreased to a value approaching the height of the interior prism. Furthermore, if the conduit is sufficiently flexible, the support furnished by the stiffened mass to the shortened exterior prism, will yield much less than the support under the interior prism. Therefore, the reverse action will take place; the interior prism will tend to brace itself against the exterior prisms thereby reducing the load on top of the conduit.

In the case of a mined-in conduit within a bed of soft compressible material, if the conduit is made sufficiently flexible so as to adjust its shape to any external differential pressure, then, even if the top load is originally greater in magnitude than the weight of the column of the material, a subsequent change in the conduit shape will result in a redistribution of the external pressures. Further changes in the conduit shape will result in further redistribution of the external pressures and this process will continue until

all differential moments that are generated within the conduit structure are eliminated and only axial ring stresses will exist. Hence, if the conduit is designed to withstand these stresses, no failure will occur and the conduit will function satisfactorily.

Case II. The Interior Prism Subsides More Than the Adjacent Masses

This case will be discussed in detail, because it is most likely to occur in the field. It may be present even in positive projecting conduits, provided their side supporting material has been compacted very thoroughly. The engineer should always be able to visualize the action which takes place in this case and to know what to expect in terms of load ranges from various construction methods and materials.

The existence of Case II is insured by the following construction methods and conditions:

1. Covered-up conduits are installed by the following three methods:

(a) The Ditch Conduit Method. According to this method (Spangler, 1946) the conduit is placed in a ditch not wider than two or three times its outside width and it is covered up with backfill material that is in a relatively loose condition as compared to the natural ground in which the ditch is dug. (Figure 5a).

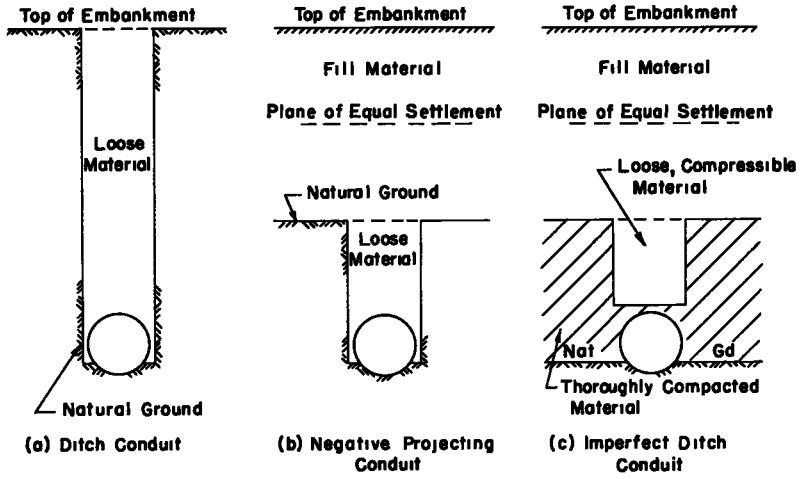

Figure 5. Covered-up conduits.

In a ditch conduit the potential sliding planes will be the walls of the ditch. The backfill material has the tendency to settle downward. In doing so it tends to brace itself against the sides of the ditch transferring part of its weight onto the natural ground. Thus, the load on top of the conduit is reduced by an equal amount.

(b) The Negative Projecting Conduit Method. Conduits falling within this category are placed in shallow ditches of such depths that the top of the conduit is below the adjacent natural ground surface that is covered by an embankment as shown in Figure 5b (Spangler, 1946).

(c) The Imperfect Ditch Conduit Method. In this method of construction the conduit is originally installed as a positive projecting conduit (Spangler, 1946). The soil on both sides and above the conduit for some distance above its top is thoroughly compacted. Then a ditch is dug in this compacted fill by removing the prism of material directly over the conduit. The ditch is refilled with very loose compressible material, after which the embankment is compacted above it (Figure 5c).

In the last two cases the potential sliding planes are assumed to be the vertical extensions of the sides of the ditch on top of the conduit. These planes will extend as far as the plane of equal settlement. In both cases the material on top of the ditch will subside more than the adjacent masses. The loose material in the ditch furnishes a support that yields much more than the adjacent natural ground in the case of a negative projecting conduit or more than the very well compacted material in the case of an imperfect ditch conduit.

2. In the case of a mined-in conduit that is flexible enough so that its roof will give in sufficiently to act as a yielding support to the material above, three cases (Terzaghi, 1942-1943, 1943a, 1943b) are of interest:

(a) The conduit is installed through cohesive material and its lower part is located within an exceptionally stiff layer of clay between soft layers (Figure 6a). The sliding planes will extend through the edges of the bottom of the conduit (Terzaghi, 1942-1943).

(b) If the cohesive material on both sides of the conduit is not exceptionally stiff (Figure 6b), the width of the interior prism is approximately $B_d = B_c + 2H_m$ (Terzaghi, 1942-1943).

(c) The conduit is installed through cohesionless granular material (Figure 6c). In this case, because of the yield of the timbering and the imperfection of the joints on the sides of the conduit, the granular material adjoining these sides subsides to the same extent as the subsiding material on top of the conduit on account of the yield of its roof. This lateral yield may cause the granular mass to come to an active state of plastic equilibrium. In such case the boundaries of the zone of subsidence will rise at the bottom of the conduit at an angle $45^\circ - \phi/2$ with respect to the vertical and gradually the boundaries will become vertical at the plane of equal settlement. The width of the interior prism will, therefore, be equal to:

$$B_c + 2H_1 \tan(45^\circ - \phi/2) = B_d \text{ on top of the conduit}$$

and

$$B'_d \text{ at the plane of equal settlement where } B'_d > B_d.$$

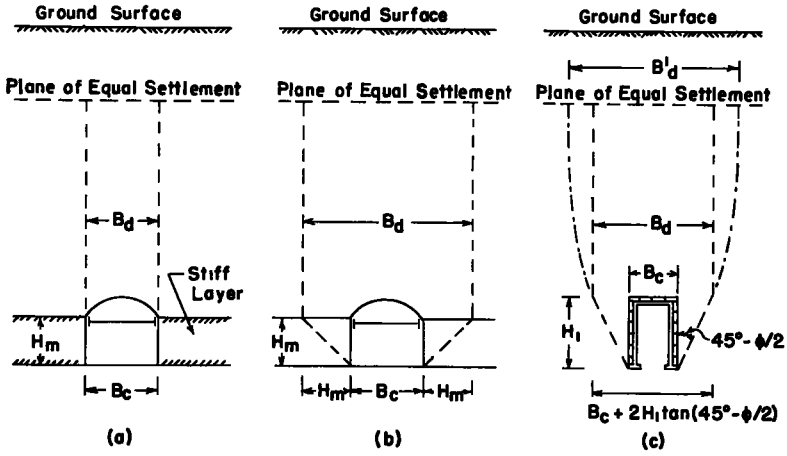

Figure 6. Mined-in conduits.

In order that the mathematical computations be simplified, it is assumed that the effective width of the interior prism is equal to B_d throughout the height from the top of the conduit to the plane of equal settlement (Terzaghi, 1943a).

From the above discussion and for reasons that were discussed previously one should use the negative signs in the general load expression when the conditions insuring the existence of Case II have been realized.

Hence, Equation 10 becomes

$$W_c = \frac{\gamma B_d^2}{2K_e \tan\phi_e} \left\{ e^{-(2K_e \tan\phi_e)\frac{H_e}{B_d}} \left[(2K_e \tan\phi_e)\left(\frac{H - H_e}{B_d}\right) - \left(1 - \frac{2c_e}{\gamma B_d}\right) \right] + \left(1 - \frac{2c_e}{\gamma B_d}\right) \right\}, \quad (18)$$

from which

$$C_n = e^{-(2K_e \tan\phi_e)\frac{H_e}{B_d}} \left[(2K_e \tan\phi_e)\left(\frac{H - H_e}{B_d}\right) - \left(1 - \frac{2c_e}{\gamma B_d}\right) \right] + \left(1 - \frac{2c_e}{\gamma B_d}\right). \quad (19)$$

A quick inspection of Equations 18 and 19 will show that the shearing resistance of the material on top of the conduit works to the engineer's advantage. The more resistant

to shear the material is and the larger the portion of its shear components that is mobilized along the sliding planes, the lower will be the load on top of the conduit.

The above discussion may be expressed in mathematical form as follows:

$$\lim_{\phi_e \to 90^0} W_c = 0, \tag{20}$$

$$\lim_{c_e \to \infty} W_c = -\infty . \tag{21}$$

Equation 21 has mathematical meaning only. Physically, it may mean that for a certain installation, if the material is able to mobilize a sufficient amount of cohesion and if the deformation characteristics within the mass are such that such an amount is mobilized along the sliding planes, the load on top of the conduit will be a minimum approaching zero.

Let us see now what other implications some other conditions may bring on the load expression.

Equations 18 and 19 contain the descending exponential function e^{-u} where $u = (2K_e \tan\phi_e)\, H_e/B_d \geq 0$. This function is equal to 1 for $u = 0$ and decreases very rapidly with increasing positive values of u, and approaches zero. For example:

if $u = 1$, $e^{-u} \approx 0.3679$; if $u = 2$, $e^{-u} \approx 0.1353$;
if $u = 4$, $e^{-u} \approx 0.0183$; and, if $u = 8$, $e^{-u} \approx 0.003$, etc.

From the above it can be seen that if $u \gg 1$ the first part of Equation 19 will become negligible and

$$C_n \approx 1 - \left[2c_e/\gamma B_d \right], \tag{22}$$

from which

$$W_c \approx \frac{\gamma B_d^2}{2K_e \tan\phi_e} \left(1 - \frac{2c_e}{\gamma B_d}\right). \tag{23}$$

Hence, if the material is potentially able to mobilize along the sliding planes an amount of cohesion equal to $c_e = \frac{\gamma B_d}{2}$ the load on top of the conduit will be:

$$W_c \approx 0. \tag{24}$$

The above expression is at variance with reality because the general load expression was evaluated on the assumption that the normal stresses in the interior prism are the same everywhere on a horizontal layer. Actually, the surfaces of equal normal stresses will be curved like arches. If the conduit has a flat roof, then the region within the surface of zero pressure and the roof of the conduit will be in a state of tension. Consequently, the material within this planoconvex region will have the tendency to drop out of the roof. As Terzaghi points out, "in order to prevent such an accident, an unsupported roof in a tunnel through cohesive earth should always be given the shape of an arch."[6]

In the case of either a covered-up or a mined-in conduit whose top is curved, such as in the case of circular, eliptical, or oval shaped conduits, Equation 24 may describe conditions very close to reality if the proper deformation conditions are insured within the mass and if the material is able to mobilize a sufficient amount of cohesion along the sliding planes.

From the above discussion, it was shown that if the factor $u = (2K_e \tan\phi_e)\, H_e/B_d$ is made sufficiently large, the load factor C_n and, accordingly, the load W_c will become minimum on top of the conduit. Therefore, an understanding of the behavior of the factor u for various physical conditions is considered to be an indispensable guide in directing the engineer's judgment when dealing with underground conduit design.

In the following chapter, a study of the factors governing the behavior of u will be made for covered-up as well as for mined-in conduits.

---

[6] K. Terzaghi, Theoretical Soil Mechanics (New York: John Wiley & Sons, 1943), p. 199.

Evaluation of the General Expression Governing the Behavior of Factor $u = (2K_e \tan\phi_e) H_e/B_d$ for Case II

1. Evaluation of u for Covered-Up Conduits. In this treatment a negative projecting conduit represents the general case. An imperfect ditch conduit as well as a ditch conduit can be deduced as special cases.

Let Figure 7 represent a negative ditch conduit installation in which the previous notation is employed with the addition of the following:

H_d = height of ditch above the top of the conduit, ft.

$H' = H - H_d$ = height of fill above the top of the compacted material, ft.

$H'_e = H_e - H_d$ = height of the plane of equal settlement above the surface of the compacted material, ft.

s_f = settlement of the conduit foundation, ft.

d_c = shortening of the vertical dimension of the conduit, ft.

s_d = compression of the loose material in the ditch within the distance H_d, ft.

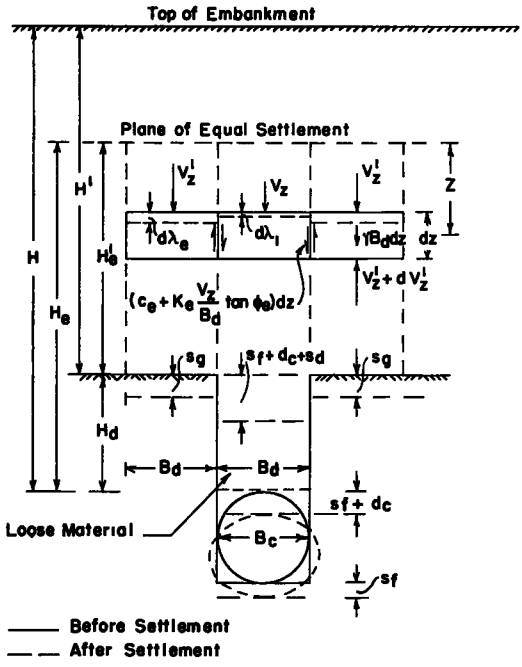

Figure 7. Force diagram for a covered-up conduit.

$s_f + d_c + s_d$ = settlement of the surface of the loose material, ft.

s_g = settlement of the surface of the compacted material, ft.

r_{sd} = settlement ratio = $[s_g - (s_d + d_c + s_f)]/s_d$

V'_z = resultant vertical pressure acting on a horizontal layer of width B_d in the exterior prism at a distance z from the plane of equal settlement, lb. per lin. ft. of length.

λ'_i = compression of the interior prism between the surface of the compacted material and the plane of equal settlement due to the vertical pressure within the fill height H', ft.

λ'_e = compression of the exterior prisms between the surface of the compacted material and the plane of equal settlement due to the vertical pressure within the fill height H', ft.

E_F = modulus of deformation of all fill material except the loose mass in the ditch within the distance H_d, lb. per ft. per ft.

E_L = modulus of deformation of the loose mass in the ditch within the distance H_d, lb. per ft. per ft.

$a' = E_L/E_F$.

The following assumptions must be made in addition to the previously stated basic assumptions:

(a) The average behavior of both the compacted and the loose fill materials is such that these materials may be considered to obey Hooke's law when subjected to compression. Their respective moduli E_F and E_L, therefore, are assumed to be constant within any region of the fill.

(b) The settlement ratio r_{sd} is considered to be constant throughout the life of the conduit.

(c) The internal friction of the fill materials distributes the infinitely small decrements of pressure from shear into the interior prism below the plane of equal settlement in such a manner that the effect on settlement is substantially the same as for uniform vertical pressure (Spangler, 1950a).

(d) The internal friction in the fill materials distributes the infinitely small increments of pressure from shear onto each of the exterior prisms below the plane of equal

settlement in such a manner that the effect on settlement is substantially the same as though the pressure were distributed uniformly over a width of prism equal to the width of the interior prism, B_d (Spangler, 1950a).

(e) With the exception of the moduli of deformation both the compacted and the loose masses exhibit the same physical properties.

Assumptions (a) through (e) are made in order that the subsequent mathematical treatment will be simplified. Their variance with reality depends upon the nature of the materials used, the method of construction, and the magnitude of the quantities involved. The engineer's judgment, based on previous experience, will determine how large the involved error is and what allowances should be made in each individual case.

To evaluate factor u one must consider the deformation characteristics of the interior and exterior prisms.

The over-all settlement of the interior prism at the plane of equal settlement must equal the over-all settlement of the exterior prism at the same plane.

Hence

$$\lambda_i' + s_d + d_c + s_f = \lambda_e' + s_g \tag{25}$$

or

$$\lambda_i' = \lambda_e' + s_g - (s_d + d_c + s_f). \tag{26}$$

Since

$$r_{sd} = \left[s_g - (s_d + d_c + s_g)\right] / s_d,$$

Equation 26 may be written

$$\lambda_i' = \lambda_e' + r_{sd} s_d. \tag{27}$$

Since the material within the interior and exterior prisms is assumed to obey Hooke's law, the vertical compression of a thin horizontal slice of the interior prism with thickness dz at a depth z below the plane of equal settlement must equal

$$d\lambda_i = (V_z / B_d E_F)\, dz. \tag{28}$$

Similarly, the vertical compression of a thin horizontal slice of the exterior prism with thickness dz at a depth z below the plane of equal settlement must equal

$$d\lambda_e = (V_z' / B_d E_F)\, dz. \tag{29}$$

Substituting in Equation 28 the value of V_z from Equation 9, in which the negative signs have been employed, and integrating between the limits

$$\lambda_i = 0 \quad \text{for} \quad z = 0$$

$$\lambda_i = \lambda_i' \quad \text{for} \quad z = H_e'$$

one obtains after rearranging terms

$$\lambda_i' = \frac{\gamma B_d^2}{E_F} \frac{1}{(2K_e \tan\phi_e)^2} \left\{ e^{-(2K_e \tan\phi_e)\frac{H_e'}{B_d}} \left[\left(1 - \frac{2c_e}{\gamma B_d}\right) - 2K_e \tan\phi_e \left(\frac{H' - H_e'}{B_d}\right) \right] + \left[2K_e \tan\phi_e \left(\frac{H' - H_e'}{B_d}\right) + \left(1 - \frac{2c_e}{\gamma B_d}\right) \left((2K_e \tan\phi_e)\left(\frac{H_e'}{B_d}\right) - 1 \right) \right] \right\}. \tag{30}$$

To evaluate V_z' the conditions of static equilibrium are considered for a thin slice of the exterior prism with a thickness dz at a depth z below the plane of equal settlement (Figure 7). The conditions that the sum of the vertical forces that act on the slice must equal zero can be expressed by the equation

$$\gamma B_d dz + \left(c_e + K_e \frac{V_z}{B_d} \tan\phi_e\right) dz + V_z' - V_z' - dV_z' = 0, \tag{31}$$

or

$$dV_z' = \left(\gamma B_d + c_e + K_e \frac{V_z}{B_d} \tan\phi_e\right) dz. \tag{32}$$

Substituting in Equation 32 the value V_z from Equation 9 and integrating between the limits

$$V_z' = (H - H_e)\, \gamma B_d \quad \text{for} \quad z = 0$$

$$V_z' = V_z' \quad \text{for} \quad z = z$$

or, since $H - H_e = H' - H'_e$, between the limits

$$V'_z = (H' - H'_e)\,\gamma B_d \quad \text{for } z = 0$$

$$V'_z = V'_z \quad \text{for } z = z$$

one obtains after rearranging terms

$$V'_z = \frac{\gamma B_d^2}{2K_e\tan\phi_e}\left\{\frac{3}{2}\cdot(2K_e\tan\phi_e)\left(\frac{H' - H'_e}{B_d} + \frac{z}{B_d}\right)\right.$$

$$\left. - \frac{1}{2}\left[e^{-(2K_e\tan\phi_e)\frac{z}{B_d}}\left\{(2K_e\tan\phi_e)\left(\frac{H' - H'_e}{B_d}\right) - \left(1 - \frac{2c_e}{\gamma B_d}\right)\right\} + \left(1 - \frac{2c_e}{\gamma B_d}\right)\right]\right\},$$

or

$$V'_z = \frac{\gamma B_d^2}{2K_e\tan\phi_e}\left[\frac{3}{2}(2K_e\tan\phi_e)\left(\frac{H' - H'_e}{Bd} + \frac{z}{Bd}\right)\right] - \frac{1}{2}V_z. \tag{33}$$

Substituting in Equation 29 the value V_z from Equation 33 one obtains

$$d\lambda_e = \frac{1}{B_d E_F}\cdot\frac{\gamma B_d^2}{2K_e\tan\phi_e}\left[\frac{3}{2}(2K_e\tan\phi_e)\left(\frac{H' - H'_e}{B_d} + \frac{z}{B_d}\right)\right]dz - \frac{1}{2}\frac{V_z}{B_d E_F}\,dz,$$

or, from Equation 28,

$$d\lambda_e = \frac{1}{B_d E_F}\cdot\frac{\gamma B_d^2}{2K_e\tan\phi_e}\left[\frac{3}{2}(2K_e\tan\phi_e)\left(\frac{H' - H'_e}{B_d} + \frac{z}{B_d}\right)\right]dz - \frac{1}{2}\,d\lambda_i. \tag{34}$$

Integrating between the limits

$$\lambda_e = 0 \quad \lambda_i = 0 \quad \text{for } z = 0$$

$$\lambda_e = \lambda'_e \quad \lambda_i = \lambda'_i \quad \text{for } z = H'_e$$

one obtains after rearranging terms (35)

$$\lambda'_e = \frac{\gamma B_d^2}{E_F}\frac{1}{(2K_e\tan\phi_e)^2}\left\{\frac{3}{2}\left[(2K_e\tan\phi_e)\left(\frac{H' - H'_e}{B_d}\right) + \frac{1}{2}(2K_e\tan\phi_e)\frac{H'_e}{B_d}\right]\right\}(2K_e\tan\phi_e)\frac{H'_e}{B_d} - \frac{1}{2}\lambda'_i.$$

Since the loose material in the ditch is considered to obey Hooke's law, the vertical compression of the prism within the distance H_d due to the vertical pressure $V_z = H'_e$ on top of the ditch is

$$s_d = \frac{V_{z = H'e}}{B_d E_L}\cdot H_d. \tag{36}$$

Substituting $z = H'_e$ in Equation 9 and since $H - H_e = H' - H'_e$ one obtains

$$V_{z = H'_e} = \frac{\gamma B_d^2}{2K_e\tan\phi_e}\left\{e^{-(2K_e\tan\phi_e)\frac{H'_e}{B_d}}\left[(2K_e\tan\phi_e)\left(\frac{H' - H'_e}{B_d}\right) - \left(1 - \frac{2c_e}{\gamma B_d}\right)\right] + \left(1 - \frac{2c_e}{\gamma B_d}\right)\right\}. \tag{37}$$

Hence, Equation 36 becomes

$$s_d = \frac{\gamma B_d^2}{E_L B_d}\frac{H_d}{2K_e\tan\phi_e}\left\{e^{-(2K_e\tan\phi_e)\frac{H'_e}{B_d}}\left[(2K_e\tan\phi_e)\left(\frac{H' - H'_e}{B_d}\right) - \left(1 - \frac{2c_e}{\gamma B_d}\right)\right] + \left(1 - \frac{2c_e}{\gamma B_d}\right)\right\},$$

or

$$s_d = \frac{\gamma B_d^2}{a' E_F}\frac{1}{(2K_e\tan\phi_e)^2}\cdot(2K_e\tan\phi_e)\frac{H_d}{B_d}\left\{e^{-(2K_e\tan\phi_e)\frac{H'_e}{B_d}}\left[(2K_e\tan\phi_e)\left(\frac{H' - H'_e}{B_d}\right) - \left(1 - \frac{2c_e}{\gamma B_d}\right)\right]\right.$$

$$\left. + \left(1 - \frac{2c_e}{\gamma B_d}\right)\right\}. \tag{38}$$

Substituting the values of λ'_i, λ'_e, and s_d from Equations 30, 35, and 38 in Equation 27 and letting

$$v' = (2K_e\tan\phi_e)\frac{H'}{B_d}, \tag{39}$$

$$u' = (2K_e\tan\phi_e)\frac{H'_e}{B_d}, \tag{40}$$

$$w' = (2K_e\tan\phi_e)\frac{H_d}{B_d}, \tag{41}$$

one obtains after collecting terms

$$v' = \frac{(\frac{3}{4}u'^2 - \frac{3c_e}{\gamma B_d}u') - (\frac{3}{2} + \frac{r_{sd}w'}{a'})(1 - \frac{2c_e}{\gamma B_d}) + (\frac{3}{2} + \frac{r_{sd}w'}{a'})(u' + 1 - \frac{2c_e}{\gamma B_d})e^{-u'}}{(\frac{3}{2} + \frac{r_{sd}w'}{a'})e^{-u'} + \frac{3}{2}(u' - 1)} \quad . \qquad (42)$$

Equation 42 governs the behavior of u' for a given installation and material. Since $H_e = H_d + H'_e$, it follows that $u = u' + w'$. Therefore, Equation 42 governs the behavior of factor u as well. All other quantities are independent variables in Equation 42.

Factor u' can be obtained from the above equation implicitly. This, however, would be a cumbersome and time consuming operation for design purposes. Since v' is a single valued function of u', one may solve Equation 39 for v' and construct curves from which u' can be obtained in a reverse manner for a given installation and material.

An inspection of Equation 42 will show that if the denominator

$$(\frac{3}{2} + \frac{r_{sd}w'}{a'})e^{-u'} + \frac{3}{2}(u' - 1)$$

approaches zero, v' increases without limit.

The physical significance of the above is that for a given material and conduit width, if the fill is made very high, factor u' and, accordingly, the height of arching, H_e, does not depend on the cohesion and the unit weight of the material.

Hence, no matter what the values of cohesion or the unit weight of the material are, for infinitely high fills, the height of arching is governed by the equation

$$(\frac{3}{2} + \frac{r_{sd}w'}{a'})e^{-u'} + \frac{3}{2}(u' - 1) = 0. \qquad (43)$$

It should be noted that in Equation 42 u' can be larger in magnitude than v' for certain conditions. However, physically, u' is limited in the region $0 \leq u' \leq v'$ because the height of arching, H_e, can vary only in the region $H_d \leq H_e \leq H$.

If u' is mathematically larger than v', the plane of equal settlement becomes imaginary. In such case, a trough-like depression appears at the surface of the embankment directly above the conduit.

If u' is mathematically smaller than v', then the arching effect does not extend along the whole fill height. Consequently, the plane of equal settlement will be below the top of the embankment, and no settlement will be noticeable at the surface.

The above discussion holds for both imperfect ditch and negative projecting conduits because no differentiation was made between the stiffness of the thoroughly compacted material and the stiffness of the natural ground in the above theoretical treatment.

In the case of a ditch conduit:

$$H_d = H_e = H. \qquad (44)$$

Substituting Equation 44 in Equation 18 one obtains as the load expression for a ditch conduit and an $s = c + \sigma \tan\phi$ material

$$W_c = \frac{\gamma B_d^2}{2K_e\tan\phi_e}\left\{e^{-(2K_e\tan\phi_e)\,H/B_d}\left[-(1 - \frac{2c_e}{\gamma B_d})\right] + (1 - \frac{2c_e}{\gamma B_d})\right\},$$

or

$$W_c = \frac{\gamma B_d^2}{2K_e\tan\phi_e}\left\{(1 - \frac{2c_e}{\gamma B_d})(1 - e^{-(2K_e\tan\phi_e)\,H/B_d})\right\}. \qquad (45)$$

If $H \gg 1$

$$W_c \approx \frac{\gamma B_d^2}{2K_e\tan\phi_e}(1 - \frac{2c_e}{\gamma B_d}), \qquad (46)$$

which is identical to Equation 23.

Letting $(2K_e\tan\phi_e)\,H/B_d = v$, and substituting in Equation 45 one obtains

$$W_c = \frac{\gamma B_d^2}{2K_e\tan\phi_e}\left\{(1 - \frac{2c_e}{\gamma B_d})(1 - e^{-v})\right\}, \qquad (47)$$

from which

$$C_n = (1 - \frac{2c_e}{\gamma B_d})(1 - e^{-v}) . \tag{48}$$

The method of utilizing dimensionless factors reduces the number of independent variables in any problem and facilitates the mathematical computations considerably. Therefore, in the subsequent analysis their use will be extensive.

Since $u = w' + u'$ and $H - H_e = H' - H'_e$ in imperfect ditch and negative projecting conduits, by substituting the dimensionless factors of Equations 39, 40, and 41 in Equations 18 and 19 one obtains, respectively

$$W_c = \frac{\gamma B_d^2}{2K_e \tan\phi_e} \left\{ e^{-w'} e^{-u'} \left[(v' - u') - (1 - \frac{2c_e}{\gamma B_d}) \right] + (1 - \frac{2c_e}{\gamma B_d}) \right\} \tag{49}$$

and

$$C_n = e^{-w'} e^{-u'} \left[(v' - u') - (1 - \frac{2c_e}{\gamma B_d}) \right] + (1 - \frac{2c_e}{\gamma B_d}) . \tag{50}$$

As has been discussed previously, if either of the two exponents w' and u' in Equation 50 are large enough, C_n will approach the value $1 - (2c_e/\gamma B_d)$.

Factor u' is governed by Equation 42 in which many independent variables must be determined in order that this factor can be evaluated.

Factor w', however, is an independent variable in Equation 42 and depends only on the properties of the material, the width of the conduit, and the height of the ditch on top of the conduit. Therefore, for a given material and width of conduit, if the height of ditch is made large enough so that $w' \gg 1$ then the load on top of the conduit will be

$$W_c \approx \frac{\gamma B_d^2}{2K_e \tan\phi_e} (1 - \frac{2c_e}{\gamma B_d}) , \tag{51}$$

which is identical to Equations 23 and 46.

Again, if the cohesion of the material that is mobilized along the sliding planes is equal to $c_e = \frac{\gamma B_d}{2}$ theoretically there should be no load on top of the conduit.

Equation 42 may be written also (52)

$$(\frac{3}{2} + \frac{r_{sd} w'}{a'})(1 - e^{-u'}) - \frac{3}{2} u' = \frac{\gamma B_d}{2} \left\{ \frac{(\frac{3}{2} + \frac{r_{sd} w'}{a'}) \left[1 + (v' - u' - 1) e^{-u'} \right] - \frac{3}{4} u'^2 + \frac{3}{2} v' (u' - 1)}{c_e} \right\} .$$

If c_e is allowed to increase without limit, the left hand member of Equation 52 will approach zero. Hence in the limit one obtains

$$(\frac{3}{2} + \frac{r_{sd} w'}{a'})(1 - e^{-u'}) - \frac{3}{2} u' = 0. \tag{53}$$

Equation 53 may also be written

$$e^{-u'} = 1 - \frac{\frac{3}{2} u'}{(\frac{3}{2} + \frac{r_{sd} w'}{a'})} . \tag{54}$$

From Equation 53 or 54 it can be seen that for all real values of the parameter $r_{sd} w'/a'$, the only solution of Equation 54 is $u' = 0$.

One may conclude, therefore, that

$$\lim_{c_e \to \infty} u' = 0 \tag{55}$$

In a similar manner it can be shown that

$$\lim_{\left| \frac{r_{sd} w'}{a'} \right| \to \infty} u' = \infty , \tag{56}$$

and

$$\lim_{\frac{r_{sd} w'}{a'} \to 0} u' = 0 \tag{57}$$

The physical significance of Equations 55, 56, and 57 is as follows:

(a) The higher the amount of cohesion that is mobilized along the sliding planes, the lower will be the height of arching. However, in such case the quantity $1 - (2c_e/\gamma B_d)$ becomes the predominant factor in the general load equation. Therefore, although in the same equation the descending exponential e^{-u} will become maximum for an infinite amount of cohesion, the load on top of the conduit, as it has been discussed in the previous section will vanish.

(b). For a given installation and material, the height of arching H_e varies directly with the settlement ratio r_{sd}, the height of the ditch on top of the conduit, H_d, and the relative stiffness between the compacted fill material and the loose material in the ditch, which is expressed by the ratio $1/a'$. Therefore, the larger the above quantities are, the higher will be the height of arching and, consequently, the lower will be the load on the conduit.

From the above discussion it can be seen that if w' is made large enough, not only will the exponential $e^{-w'}$ decrease, but the exponential $e^{-u'}$ will also decrease.

As it was pointed out previously, from a physical standpoint, u' cannot be larger than v' even if the quantity $r_{sd}w'/a'$ increases without limit. Therefore, for a given installation and material, u' is bounded by the condition u' = v'.

Substituting the above in Equation 42, one obtains for a given installation and materials the maximum fill height for which the material on top of the conduit will brace itself against the adjacent mass along the whole fill height in a similar manner as in a ditch conduit.

Hence, for u' = v'

$$v' = \frac{(\frac{3}{4}v'^2 - \frac{3c_e}{\gamma B_d}v') - (\frac{3}{2} + \frac{r_{sd}w'}{a'})(1 - \frac{2c_e}{\gamma B_d}) + (\frac{3}{2} + \frac{r_{sd}w'}{a'})(v' + 1 - \frac{2c_e}{\gamma B_d})e^{-v'}}{(\frac{3}{2} + \frac{r_{sd}w'}{a'})e^{-v'} + \frac{3}{2}(v' - 1)},$$

or, after collecting terms

$$e^{-v'} = \frac{\frac{3}{4}v'^2 - \frac{3}{2}v'(1 - \frac{2c_e}{\gamma B_d})}{(1 - \frac{2c_e}{\gamma B_d})(\frac{3}{2} + \frac{r_{sd}w'}{a'})} + 1 \qquad (58)$$

from which v' may be obtained by successive trials.

(c) If the ditch material, the conduit, and the conduit foundation have an over-all stiffness that is equal to the stiffness of the adjacent masses, the middle prism will settle the same amount as these masses. Consequently, there will be no arching effect.

Since the material in the ditch behaves like the adjacent masses, no distinction can be made between the two materials; consequently, w' = 0 and u' = u = 0.

Substituting the above in Equation 18 and since $v' - u' = v - u$ and $v = (2K_e\tan\phi_e)H/B_d$ one obtains

$$W_c = \gamma B_d H = W \quad \text{when} \quad r_{sd}w'/a' = 0, \qquad (59)$$

which is identical to Equation 15.

Evaluation of u for Mined-In Conduits

In this treatment case (a) of Figure 6 will be considered to be the general case. Cases (b) and (c) can be treated in a similar manner if the quantities involved in the expressions derived for case (a) are modified accordingly.

Let Figure 8 represent a mined-in conduit installed through cohesive material with its lower part located within an exceptionally stiff layer of clay between soft layers. The same notation is employed as in previous sections with the addition of the following:

H_m = thickness of the stiff layer on either side of the conduit, ft.

λ_i = compression of the interior prism between the top of the conduit and the plane of equal settlement, ft.

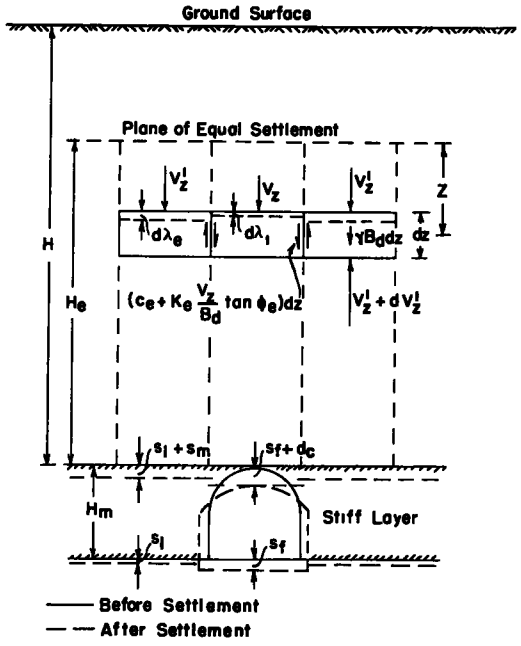

Figure 8. Force diagram for a mined-in conduit.

λ_e = compression of the exterior prism between the top of the conduit and the plane of equal settlement, ft.

s_m = compression of the stiff mass on either side of the conduit within the distance H_m, ft.

s_1 = settlement of the foundation supporting the stiff layer, ft.

$s_m + s_1$ = settlement of the mass supporting the exterior prisms, ft.

$d_c + s_f$ = settlement of the mass supporting the interior prism, ft.

r_{sm} = settlement ratio = $[(s_m + s_1) - (d_c + s_f)]/s_m$.

E_f = modulus of deformation of all other material on top of the conduit except the stiff layer on its sides, lb. per ft. per ft.

E_m = modulus of deformation of the stiff mass within the distance H_m, lb. per ft. per ft.

$a = E_m/E_f$.

The assumptions made in the case of covered-up conduits are modified in order that the subsequent analysis can be made. Thus:

(a) The average behavior of the material surrounding the conduit is such that it may be considered to obey Hooke's law when subjected to compression. Thus, the moduli E_f and E_m are assumed constant within any region occupied by their respective materials.

(b) The settlement ratio r_{sm} is considered constant throughout the life of the conduit.

Assumptions (c), (d), and (e) are the same as in the case of covered-up conduits. Assumption (e), however, should be modified to include the stiff mass on the sides of the conduit instead of the loose mass within the ditch on top of a covered-up conduit.

In addition to the above:

(f) In setting up the expression for s_m, the friction between the sides of the conduit and the stiff layer is neglected to simplify the mathematical computations (Spangler, 1950b).

As in the previous case, for the evaluation of u one considers the relative deformation of the interior and exterior prisms. The over-all settlement of the interior prism at the plane of equal settlement must equal the over-all settlement of the exterior prism at the same plane. Hence

$$\lambda_i + d_c + s_f = \lambda_e + s_m + s_1$$

or

$$\lambda_i = \lambda_e + s_m + s_1 - (d_c + s_f). \tag{60}$$

Since

$$r_{sm} = [(s_m + s_1) - (d_c + s_f)]/s_m,$$

Equation 60 may be written

$$\lambda_i = \lambda_e + r_{sm} \cdot s_m. \tag{61}$$

To evaluate λ_i one substitutes in Equation 28 the value of V_z from Equation 9 employing the negative signs, and integrates between the limits

$$\lambda_1 = 0 \quad \text{for} \quad z = 0,$$

$$\lambda_i = \lambda_i \quad \text{for} \quad z = H_e.$$

Rearranging terms and letting

$$(2K_e \tan\phi_e)\, H/B_d = v, \tag{62}$$

$$(2K_e \tan\phi_e)\, H_e/B_d = u, \tag{63}$$

$$(2K_e\tan\phi_e)\, H_m/B_d = w, \tag{64}$$

one obtains

$$\lambda_i = \frac{\gamma B_d^2}{E_f}\,\frac{1}{(2K_e\tan\phi)^2}\left\{e^{-u}\left[(1-\frac{2c_e}{\gamma B_d}) - (v-u)\right] + \left[(1-\frac{2c_e}{\gamma B_d})(u-1) + (v-u)\right]\right\}. \tag{65}$$

Similarly, by substituting Equation 33 in Equation 29 and integrating between the limits

$$\lambda_e = 0 \quad \lambda_i = 0 \quad \text{for} \quad z = 0$$

$$\lambda_e = \lambda_e \quad \lambda_i = \lambda_i \quad \text{for} \quad z = H_e$$

one obtains in terms of the dimensionless factors v and u defined from Equations 63 and 64,

$$\lambda_e = \frac{\gamma B_d^2}{E_f}\,\frac{1}{(2K_e\tan\phi_e)^2}\left\{\frac{3}{2}(v-\frac{1}{2}u)\,u\right\} - \frac{1}{2}\lambda_i. \tag{66}$$

Since the stiff mass within the distance H_m is considered to obey Hooke's law, the vertical compression of the prism of width B_d and height H_m, due to the vertical pressure $V'_z = H_e$ on top of the stiff layer, is

$$s_m = (V'_z = H_e/B_d E_m)\, H_m. \tag{67}$$

Substituting $z = H_e$ in Equation 33 and since $H' - H'_e = H - H_e$, one obtains in terms of the dimensionless factors v and u

$$V'_z = H_e = \frac{\gamma B_d^2}{2K_e\tan\phi_e}\left\{\frac{3}{2}v - \frac{1}{2}e^{-u}\left\{\left[(v-u) - (1-\frac{2c_e}{\gamma B_d})\right] + (1-\frac{2c_e}{\gamma B_d})\right\}\right\}. \tag{68}$$

Substituting in Equation 67 the value for $V'_{z=H_e}$ from Equation 68 and, since $E_m = \alpha E_f$ and $2K_e\tan\phi_e\,\frac{H_m}{B_d} = w$ one obtains

$$s_m = \frac{\gamma B_d^2}{E_f}\,\frac{1}{(2K_e\tan\phi)^2}\,\frac{w}{\alpha}\left\{\frac{3}{2}v - \frac{1}{2}\left\{e^{-u}\left[(v-u) - (1-\frac{2c_e}{\gamma B_d})\right] + (1-\frac{2c_e}{\gamma B_d})\right\}\right\}. \tag{69}$$

Substituting in Equation 61 the values λ_i, λ_e, and s_m from Equations 65, 66, and 69, respectively, one obtains after rearranging terms

$$v = \frac{(\frac{3}{2}u^2 - \frac{6c_e}{\gamma B_d}u) - (3-\frac{r_{sm}w}{\alpha})(1-\frac{2c_e}{\gamma B_d}) + (3-\frac{r_{sm}w}{\alpha})(u+1-\frac{2c_e}{\gamma B_d})\,e^{-u}}{(3-\frac{r_{sm}w}{\alpha})\,e^{-u} + 3(u-1+\frac{r_{sm}w}{\alpha})}. \tag{70}$$

Equation 70 governs the behavior of u for a given installation and material in the case of a mined-in conduit. The same equation may be used in the case of positive projecting conduits if their side supporting material has been thoroughly compacted.

As in the case of covered-up conduits, u may be obtained from curves that have been constructed by solving Equation 63 for v.

It can be seen for this case that again, for infinitely high fills u does not depend on the cohesion and the unit weight of the material but is governed by the equation

$$(3-\frac{r_{sm}w}{\alpha})\,e^{-u} + 3(u-1+\frac{r_{sm}w}{\alpha}) = 0. \tag{71}$$

By following the same method of approach applied to covered-up conduits, it can be shown also that

$$\lim u = 0 \quad c_e \to \infty \tag{72}$$

$$\lim u = \infty \quad \left|\frac{r_{sm}w}{\alpha}\right| \to \infty \tag{73}$$

$$\lim u = 0 \quad \frac{r_{sm}w}{\alpha} \to 0 \tag{74}$$

Again, physically, u is bounded by the condition u = v.

Substituting u = v in Equation 70 one obtains

$$v = \frac{(\frac{3}{2}v^2 - \frac{6c_e}{\gamma B_d}v) - (3 - \frac{r_{sm}w}{a})(1 - \frac{2c_e}{\gamma B_d}) + (3 - \frac{r_{sm}w}{a})(v + 1 - \frac{2c_e}{\gamma B_d})e^{-v}}{(3 - \frac{r_{sm}w}{a})e^{-v} + 3(v - 1 + \frac{r_{sm}w}{a})},$$

or

$$e^{-v} = \frac{\frac{3}{2}v^2 - 3v\left[(1 - \frac{2c_e}{\gamma B_d}) - \frac{r_{sm}w}{a}\right] + 1.}{(1 - \frac{2c_e}{\gamma B_d})(3 - \frac{r_{sm}w}{a})} \qquad (75)$$

From Equation 75 one may obtain for an $s = c + \sigma \tan\phi$ material, the maximum height of the mass on top of a mined-in conduit for which the arching effect will extend as far as the ground surface thereby causing a trough-like depression to appear at the surface directly above the conduit.

From Relation 74 and Equation 18 one may see that, as in the case of a covered-up conduit, if the over-all stiffness of the body furnishing support to the middle prism equals the stiffness of the mass supporting the exterior prisms above a mined-in conduit, there will be no relative settlement between the interior and exterior prisms and, consequently, there will be no arching effect. Consequently u = 0 and the load on top of the conduit will be

$$W_c = \gamma B_d H = W \quad \text{when} \quad r_{sm}w/a = 0, \qquad (76)$$

which is identical to Equations 59 and 15.

In both cases of covered-up and mined-in conduits the corresponding settlement ratios r_{sd} and r_{sm} are empirical quantities and must be determined by direct measurement. Since in either case the interior prism subsides a greater amount than the exterior prism, both quantities are negative.

A positive settlement ratio would indicate that the reverse action has taken place in the relative subsidence of the masses on the top of the conduit. Under such circumstances, conditions corresponding to Case I would be present, which, as it has been discussed previously, is very undesirable because of its detrimental influence on the conduit. Therefore, every effort must be made in the design and construction of an underground conduit in order that the settlement ratio of the masses above it remains negative at all times.

Both settlement ratios were defined originally by Dean Anson Marston (1922) and Professor Spangler (1950b) of Iowa State College in their theoretical treatment of covered-up positive and negative projecting conduits installed in a granular material. To avoid confusion, the writer has adopted the same definitions in his treatment of the general case. However, he believes that if both ratios had a common denominator, say d_c, which would always be a positive quantity, then the two cases could have been united into one general treatment. Furthermore, if both ratios were defined in such a manner that they would be positive quantities, the mathematical treatment and the resulting expressions for all cases would have been much less complicated.

The employment of the shortening of the vertical dimension of the conduit, d_c, as a denominator in the expressions for settlement ratios would also tie in the height of arching and, consequently, the load expression, with the stiffness of the conduit and the distribution of external pressure on its sides and bottom. Consequently, the resulting load expression would have been also a function of the support which the side material can furnish to the conduit, as well as of the stiffness of the conduit. Such treatment, however, is beyond the scope of this paper.

The Analysis of the General Case as Applied to an $s = \sigma \tan\phi$ Material

The theoretical relations describing the loading action of a perfectly cohesionless material on top of underground conduits can be deduced from the expressions derived for the general case in which the loading agent is an $s = c + \sigma \tan\phi$ material, by taking the limits of these expressions when c_e is allowed to approach zero. Thus:

1. From Equation 10 the general load expression for an $s = \sigma \tan\phi$ material will

become

$$\lim_{c_e \to 0} W_c = \frac{\gamma B_d^2}{2K_e \tan\phi_e} \left\{ e^{\pm (2K_e \tan\phi_e) \frac{H_e}{B_d}} \left[(2K_e \tan\phi_e)\left(\frac{H - H_e}{B_d}\right) \pm 1 \right] \mp 1 \right\}, \tag{77}$$

from which

$$C = e^{\pm (2K_e \tan\phi_e) \frac{H_e}{B_d}} \left[(2K_e \tan\phi_e)\left(\frac{H - H_e}{B_d}\right) \pm 1 \right] \mp 1 .^{7} \tag{78}$$

In terms of the dimensionless factors v and u, the above equations may be written respectively

$$\underset{c_e = 0}{W_c} = \frac{\gamma B_d^2}{2K_e \tan\phi_e} \left\{ e^{\pm u} \left[(v - u) \pm 1 \right] \mp 1 \right\} \tag{79}$$

and

$$C = e^{\pm u} \left[(v - u) \pm 1 \right] \mp 1. \tag{80}$$

In the event that the interior prism subsides less than the exterior prisms, which was defined previously as Case I, the positive signs should be used in Equations 77 through 80. Hence, in terms of the dimensionless factors v and u, one obtains

$$\underset{c_e = 0}{W_c} = \frac{\gamma B_d^2}{2K_e \tan\phi_e} \left\{ e^{+u} (v - u + 1) - 1 \right\} \tag{81}$$

and

$$C_p = e^{+u} (v - u + 1) - 1 . \tag{82}$$

From the above equations one may conclude that Case I will be just as detrimental to an underground conduit installed under an $s = \sigma \tan\phi$ material.

In the event that the interior prism subsides more than the exterior prisms, which case was previously defined as Case II, the negative signs should be used in Equations 79 and 80. Hence, in terms of the dimensionless factors v and u, one obtains, respectively

$$\underset{c_e = 0}{W_c} = \frac{\gamma B_d^2}{2K_e \tan\phi_e} \left[e^{-u} (v - u - 1) + 1 \right] \tag{83}$$

and

$$C_n = e^{-u} (v - u - 1) + 1 . \tag{84}$$

If $u \gg 1$, e^{-u} will become negligible. Hence;

$$C_n \approx 1$$

and

$$\underset{c_e = 0}{W_c} \approx \frac{\gamma B_d^2}{2K_e \tan\phi_e} . \tag{85}$$

Equation 85 is identical to the expression derived by Terzaghi for the pressure on top of deep tunnels through dry sand, i. e., for Case c of Figure 6.[8]

For a ditch conduit, $H_d = H_e = H$. Hence, $u = v$ and Equation 83 becomes

$$\underset{c_e = 0}{W_c} = \frac{\gamma B_d^2}{2K_e \tan\phi_e} (1 - e^{-v}) . \tag{86}$$

As in the case of an $s = c + \sigma \tan\phi$ material, if the height of the fill is large enough so that $v = (2K_e \tan\phi_e) H/B_d \gg 1$, e^{-v} becomes negligible and the load on top of the conduit approaches the value

$$\underset{c_e = 0}{W_c} \approx \frac{\gamma B_d^2}{2K_e \tan\phi_e}$$

given by Equation 85.

For either a negative or an imperfect ditch conduit, since $u = w' + u'$ and $H - H_e = H' - H'_e$

[7] Equations 77 and 78 are identical to Equations 11 and 12 obtained by Spangler. See References, Spangler (1950b), p. 24.

[8] Terzaghi, op. cit., p. 196.

Equations 83 and 84 may be written, respectively, as

$$\underset{c_e=0}{W_c} = \frac{\gamma B_d^2}{2K_e\tan\phi_e}\left\{e^{-w'}e^{-u'}(v' - u' - 1) + 1\right\} \tag{87}$$

and

$$C_n = e^{-w'}e^{-u'}(v' - u' - 1) + 1 . \tag{88}$$

Because of the descending exponential functions $e^{-w'}$ and $e^{-u'}$, if either w' or u' is large enough, C_n will approach one and the load on top of the conduit will be given by Equation 85.

Since $w' = (2K_e\tan\phi_e)\,H_d/B_d$, it follows that for a given material and width of ditch, if the height of ditch is made large enough so that $w' \gg 1$, the conduit load will be

$$\underset{c_e=0}{W_c} \approx \frac{\gamma B_d^2}{2K_e\tan\phi_e} .$$

2. The equation governing the behavior of u' for a covered-up conduit may be obtained by taking the limit of Equation 42 when c_e is allowed to approach zero. Thus

$$\lim_{c_e\to 0} v' = \frac{\frac{3}{4}u'^2 - (\frac{3}{2} + \frac{r_{sd}w'}{a'}) + (\frac{3}{2} + \frac{r_{sd}w'}{a'})(u' + 1)\,e^{-u'}}{(\frac{3}{2} + \frac{r_{sd}w'}{a'})\,e^{-u'} + \frac{3}{2}(u' - 1)} . \tag{89}$$

Similarly, the equation governing the behavior of u in the case of a mined-in conduit may be obtained by taking the limit of Equation 70 when c_e is allowed to approach zero. Thus

$$\lim_{c_e\to 0} v = \frac{\frac{3}{2}u^2 - (3 - \frac{r_{sm}w}{a}) + (3 - \frac{r_{sm}w}{a})(u + 1)\,e^{-u}}{(3 - \frac{r_{sm}w}{a})\,e^{-u} + 3(u - 1 + \frac{r_{sm}w}{a})} .[9] \tag{90}$$

By inspection it can be seen that if the denominator of the right hand member of the above equations approaches zero, factors v' and v will increase without limit.

Hence, for a given material, if the mass on top of a conduit is infinitely high, u' and u will be governed by the equations

$$(\frac{3}{2} + \frac{r_{sd}w'}{a'})\,e^{-u'} + \frac{3}{2}(u' - 1) = 0 \tag{91}$$

and

$$(3 - \frac{r_{sm}w}{a})\,e^{-u} + 3(u - 1 + \frac{r_{sm}w}{a}) = 0 \tag{92}$$

respectively.

Equations 91 and 92 are respectively identical with Equations 43 and 71 which had been derived for infinitely high masses consisting of $s = c + \sigma\tan\phi$ material. One may conclude, therefore, that for very high earth masses on top of either covered-up or mined-in conduits, the influence of the cohesion of the material on the height of arching is negligible and an $s = c + \sigma\tan\phi$ material will behave like a perfectly granular material. Since the general load equation depends primarily on the height of arching it follows that for very high masses consisting of $s = c + \sigma\tan\phi$ material, the conduit load may be computed as for an $s = \sigma\tan\phi$ material. The error due to neglecting the cohesion, besides being on the safe side, will be negligible.

What constitutes a very high earth mass will depend not only on the height, H, but on the factors $2K_e\tan\phi_e$ and B_d as well, because $v = (2K_e\tan\phi_e)\,H/B_d$.

3. As in the general case of an $s = c + \sigma\tan\phi$ material the following relations can be established for an $s = \sigma\tan\phi$ material:

(a)
$$\lim_{\substack{c_e=0 \\ \phi_e\to 90^0}} W_c = 0. \tag{93}$$

[9] Equations 89 and 90 are respectively identical to Equations 18 (Spangler, 1950a, p. 158), and 18 (Spangler, 1950b, p. 28).

(b) In the case of a covered-up conduit:

$$\lim u' = \infty, \quad \left|\frac{r_{sd}w'}{a'}\right| \to \infty \tag{94}$$

$$\lim u' = 0. \quad \frac{r_{sd}w'}{a'} \to 0 \tag{95}$$

(c) In the case of a mined-in conduit:

$$\lim u = \infty, \quad \left|\frac{r_{sm}w}{a}\right| \to \infty \tag{96}$$

$$\lim u = 0. \quad \frac{r_{sm}w}{a} \to 0 \tag{97}$$

As in the general case u' and u are physically bounded by the conditions u' = v', and u = v respectively.

The maximum height of a mass of a perfectly granular material above an underground conduit for which the arching effect will extend as far as the surface of the mass causing a trough-like depression to appear on the surface may be obtained by substituting u' = v' and u = v in Equations 89 and 90 respectively.

Thus, for a covered-up conduit one obtains after rearranging terms

$$e^{-v'} = \frac{\frac{3}{4}v'^2 - \frac{3}{2}v'}{(\frac{3}{2} + \frac{r_{sd}w'}{a'})} + 1. \tag{98}$$

For a mined-in conduit

$$e^{-v} = \frac{\frac{3}{2}v^2 + 3v\left[\frac{r_{sm}w}{a} - 1\right]}{3 - \frac{r_{sm}w}{a}} + 1. \tag{99}$$

From relations 95 and 97 and by applying the same reasoning as in the general case it can be shown also that

$$\lim_{c_e = 0} W_c = \gamma B_d H = W, \quad \frac{r_{sd}w'}{a'} \to 0 \tag{100}$$

$$\lim_{c_e = 0} W_c = \gamma B_d H = W. \quad \frac{r_{sm}w}{a} \to 0 \tag{101}$$

The Analysis of the General Case as Applied to an s = c Material

As in the previous section, the theoretical relations describing the loading action of a perfectly cohesive material on top of underground conduits may be deduced from the general case by taking the limits of the expressions derived from an $s = c + \sigma \tan\phi$ material when ϕ_e is allowed to approach zero. Thus:

1. From Equation 10, the general load expression for an s = c material will become equal to

$$\lim_{\phi_e \to 0} W_c = \gamma B_d^2 \left\{ \left(\frac{H - H_e}{B_d}\right) + \left(1 \pm \frac{2c_e}{\gamma B_d}\right)\frac{H_e}{B_d} \right\}, \tag{102}$$

from which

$$C = \left(\frac{H - He}{B_d}\right) + \left(1 \pm \frac{2c_e}{\gamma B_d}\right)\frac{H_e}{B_d} \quad . \tag{103}$$

Let

$$H/B_d = v_o, \qquad H'/B_d = v'_o,$$
$$He/B_d = u_o, \qquad H'_e/B_d = u'_o,$$
$$H_m/B_d = w_o, \qquad H_d/B_d = w'_o,$$

Substituting in Equations 102 and 103 one obtains

$$\underset{\phi_e = 0}{W_c} = \gamma B_d^2 \left\{(v_o - u_o) + \left(1 \pm \frac{2c_e}{\gamma B_d}\right) u_o \right\}, \tag{104}$$

and

$$C = (v_o - u_o) + \left(1 \pm \frac{2c_e}{\gamma B_d}\right) u_o \tag{105}$$

respectively.

In the above equations the positive signs should be used in the event that the interior prism subsides less than the exterior prisms, and the negative signs in case the reverse action takes place.

Hence, if Case I obtains

$$\underset{\phi_e = 0}{W_c} = \gamma B_d^2 \left\{(v_o - u_o) + \left(1 + \frac{2c_e}{\gamma B_d}\right) u_o \right\} \tag{106}$$

and

$$C_p = \left\{(v_o - u_o) + \left(1 + \frac{2c_e}{\gamma B_d}\right) u_o \right\} . \tag{107}$$

If Case II obtains

$$\underset{\phi_e = 0}{W_c} = \gamma B_d^2 \left\{(v_o - u_o) + \left(1 - \frac{2c_e}{\gamma B_d}\right) u_o \right\} \tag{108}$$

and

$$C_n = \left\{(v_o - u_o) + \left(1 - \frac{2c_e}{\gamma B_d}\right) u_o \right\} . \tag{109}$$

From the above equations, it can be seen that the conditions for Case I are just as undesirable for an s = c material as for an s = c + $\sigma \tan\phi$ or for an s = $\sigma \tan\phi$ material.

For a ditch conduit, since $H_d = H_e = H$,

$$\underset{\phi_e = 0}{W_c} = \gamma B_d^2 \left(1 - \frac{2c_e}{\gamma B_d}\right)\frac{H}{B_d} , \tag{110}$$

or

$$\underset{\phi_e = 0}{W_c} = \gamma B_d^2 \left(1 - \frac{2c_e}{\gamma B_d}\right) v_o . \tag{111}$$

Hence, if $c_e = \frac{\gamma B_d}{2}$,

$$W_c = 0. \tag{112}$$

Equation 112 is similar to Equation 24.

For a negative or an imperfect ditch conduit, since $H_e = H_d + H'e$ and $H - He = H' - H'_e$, Equation 102 may be written

$$\underset{\phi_e = 0}{W_c} = \gamma B_d^2 \left\{\left(\frac{H' - H'e}{B_d}\right) + \left(1 - \frac{2c_e}{\gamma B_d}\right)\left(\frac{H'e + H'd}{B_d}\right) \right\} , \tag{113}$$

or

$$\underset{\phi_e = 0}{W_c} = \gamma B_d^2 \left\{(v'_o - u'_o) + \left(1 - \frac{2c_e}{\gamma B_d}\right)(u'_o + w'_o) \right\} . \tag{114}$$

in terms of the dimensionless factors v'_o, u'_o, and w'_o.

2. The equation governing the behavior of u'_o in the case of a covered-up conduit may be obtained from the general case as follows:

Equation 42 may be written also

$$\frac{H'}{B_d} = v'_o = \frac{1}{2K_e \tan\phi_e} \cdot \frac{(\frac{3}{4}u'^2 - \frac{3c_e}{\gamma B_d}u') - (\frac{3}{2} + \frac{r_{sd}w'}{a'})(1 - \frac{2c_e}{\gamma B_d}) + (\frac{3}{2} + \frac{r_{sd}w'}{a'})(u' + 1 - \frac{2c_e}{\gamma B_d})e^{-u'}}{(\frac{3}{2} + \frac{r_{sd}w'}{a'})e^{-u'} + \frac{3}{2}(u' - 1)} \quad (115)$$

Applying L'Hospital's rule twice on Equation 115 and letting ϕ_e approach zero one obtains

$$\lim_{\phi_e \to 0} v'_o = -\frac{2c_e}{\gamma B_d} \cdot \frac{\frac{3}{4}u'^2_o - \frac{r_{sd}w'_o}{a'}u'_o}{\frac{r_{sd}w'_o}{a'}} \quad (116)$$

from which

$$u'_o = \frac{2}{3}\frac{r_{sd}w'_o}{a'}\left\{1 \pm \sqrt{1 - \frac{3v'_o}{\frac{r_{sd}w'_o}{a'} \cdot \frac{2c_e}{\gamma B_d}}}\right\}. \quad (117)$$

Similarly the equation governing the behavior of u_o in the case of a mined-in conduit if Equation 70 is written in the form

$$\frac{H}{B_d} = v_o = \frac{1}{2K_e \tan\phi_e} \cdot \frac{(\frac{3}{2}u^2 - \frac{6c_e}{\gamma B_d}u) - (3 - \frac{r_{sm}w}{a})(1 - \frac{2c_e}{\gamma B_d}) + (3 - \frac{r_{sm}w}{a})(u + 1 - \frac{2ce}{\gamma B_d})e^{-u}}{(3 - \frac{r_{sm}w}{a})e^{-u} + 3(u - 1 + \frac{r_{sm}w}{a})} \quad (118)$$

If L'Hospital's rule is applied twice on Equation 118 and ϕ_e is allowed to approach zero one obtains

$$\lim_{\phi_e \to 0} v_o = -\frac{2c_e}{\gamma B_d} \cdot \frac{\frac{3}{4}u_o^2 + \frac{1}{2}\frac{r_{sm}w_o}{a}u_o}{\frac{r_{sm}w_o}{a}} \quad (119)$$

from which

$$u_o = \frac{1}{3}\frac{r_{sm}w_o}{a}\left\{-1 \pm \sqrt{1 - \frac{12v_o}{\frac{r_{sm}w_o}{a} \cdot \frac{2c_e}{\gamma B_d}}}\right\}. \quad (120)$$

By inspection of Equations 117 and 120 and by noting that r_{sd} and r_{sm} are negative quantities the physical meaning of these equations can be interpreted if written as follows:

$$u'_o = \frac{2}{3}\frac{r_{sd}w'_o}{a'}\left\{1 - \sqrt{1 - \frac{3v'_o}{\frac{r_{sd}w'_o}{a'} \cdot \frac{2ce}{\gamma B_d}}}\right\} \quad (121)$$

for all values of $\dfrac{3v'_o}{\frac{r_{sd}w'_o}{a'} \cdot \frac{2c_e}{\gamma B_d}}$.

$$u_o = -\frac{1}{3}\frac{r_{sm}w_o}{a}\left\{1 + \sqrt{1 - \frac{12\,v_o}{\frac{r_{sm}w_o}{a} \cdot \frac{2ce}{\gamma B_d}}}\right\} \quad (122)$$

for $\left|\dfrac{12v_o}{\frac{r_{sm}w_o}{a}\frac{2c_e}{\gamma B_d}}\right| \neq 0$,

and

$$u_o = 0 \quad (123)$$

for $\dfrac{12v_o}{\frac{r_{sm}w_o}{a}\frac{2c_e}{\gamma B_d}} = 0.$

3. From the above equations the following relations can be established for an s = c material:

(a) $\lim_{\substack{\phi_e = 0 \\ c_e \to \infty}} W_c = -\infty$. (124)

(b) In the case of a covered-up conduit:

$$\lim_{c_e \to \infty} u'_o = 0, \tag{125}$$

$$\lim_{\left|\frac{r_{sd} w'_o}{a'}\right| \to \infty} u'_o = \infty, \tag{126}$$

$$\lim_{\frac{r_{sd} w'_o}{a'} \to 0} u'_o = 0. \tag{127}$$

(c) In the case of a mined-in conduit:

$$\lim_{c_e \to \infty} u_o = 0, \tag{128}$$

$$\lim_{\left|\frac{r_{sm} w_o}{a}\right| \to \infty} u_o = \infty, \tag{129}$$

$$\lim_{\frac{r_{sm} w_o}{a} \to 0} u_o = 0. \tag{130}$$

As in the cases of $s = c + \sigma \tan\phi$ material and $s = \sigma \tan\phi$ material, u'_o and u_o are bounded by the conditions $u'_o = v'_o$ and $u_o = v_o$, respectively.

The maximum height of a mass of s = c material above an underground conduit for which the arching effect will extend as far as the surface of the mass causing a trough-like depression to appear on the surface may be obtained by substituting $u'_o = v'_o$ and $u_o = v_o$ in Equations 116 and 119, respectively.

Thus for a covered-up conduit one obtains after rearranging terms:

$$v'_{o_{max}} = -\frac{2}{3} \frac{\gamma B_d}{c_e} \frac{r_{sd} w'_o}{a} \left(1 - \frac{2c_e}{\gamma B_d}\right). \tag{131}$$

If

$$c_e = \frac{\gamma B_d}{2}, \qquad v'_{o_{max}} = 0. \tag{132}$$

For a mined-in conduit:

$$v_{o_{max}} = -\frac{2}{3} \frac{\gamma B_d}{c_e} \frac{r_{sm} w_o}{a} \left(1 + \frac{c_e}{\gamma B_d}\right). \tag{133}$$

From Relations 127 and 130 and by applying the same reasoning as in the general case, it can be shown also that

$$\lim_{\substack{\phi_e = 0 \\ \frac{r_{sd} w'_o}{a'} \to 0}} W_c = \gamma B_d H = W, \tag{134}$$

$$\lim_{\substack{\phi_e = 0 \\ \frac{r_{sm} w_o}{a} \to 0}} W_c = \gamma B_d H = W. \tag{135}$$

From Equations 102, 117, and 120, it can be seen that the load on top of underground conduits installed under a purely cohesive material is independent of the pressure ratio K.

Construction of Load Curves for a Covered-Up Conduit Installed Under an $s = \sigma \tan\phi$ Material

The purpose of the construction of the following families of curves is to facilitate the computation of load on top of covered-up conduits if the loading agent is an $s = \sigma \tan\phi$ material. Curves to estimate the earth load on top of mined-in conduits can be constructed in a similar manner.

The presentation of these curves will follow the same sequence as the order in which they would be used by a designer to make a load estimate for a given installation and material.

1. Factor $K\tan\phi$ has been plotted against the angle of internal friction ϕ for various values of the equivalent hydrostatic pressure ratio $K = K_e$. (Table A and Figure A in the Appendix).

The upper boundary of this family of curves is the curve $K_p\tan\phi$ which is obtained if K assumes the upper limiting value, $K_p = \tan^2(45^0 + \phi/2)$ for a passive state of plastic equilibrium.

The lower boundary of the same family of curves is the curve $K_A\tan\phi$ which is obtained if K assumes the lower limiting value, $K_A = \tan^2(45^0 - \phi/2)$ for an active state of plastic equilibrium.

K_e can be obtained by constructing an equivalent pressure ratio diagram similar to Figure 1a. The value ϕ_e may be considered to be a fraction of the maximum value of the angle of internal friction of the material. This fraction will depend on the desired factor of safety for the particular project.

2. By solving Equation 89 for v', curves were prepared showing the relation v' versus u' for various values of $r_{sd}w'/a'$. From these curves, which are not presented in this paper, u' was plotted against $r_{sd}w'/a'$ for various values of v'. (Table B and Figure B in the Appendix).

The upper boundary of this family of curves is the curve for which u' = v' and it is obtained by solving Equation 98.

The lower boundary of the same family of curves is the curve for which $v' = \infty$, and it is obtained by solving Equations 43 or 91.

From the given data of the project and the value $K_e\tan\phi_e$ obtained in Step 1, the values $v' = (2K_e\tan\phi_e)\, H'/B_d$ and $w' = (2K_e\tan\phi_e)\, H_d/B_d$ can be computed.

From available records of previous installations, the settlement ratio r_{sd} as well as the stiffness ratio $a' = E_L/E_F$ can be estimated for a given installation and material. Hence, the quantity $r_{sd}\, w'/a'$ can be computed. Accordingly, u' can be obtained from the above family of curves.

By substituting the obtained values of v', u', w' and $2K_e\tan\phi_e$, in Equation 87, the load W_c can be computed.

From the above curves it can be seen that for a given finite value of $r_{sd}w'/a'$, as v' increases, u' decreases from a maximum value $u' = v'_{max}$ to a lower limiting finite value $u'_{v'=\infty}$. For values of v' less than v'_{max}, u' is larger than v' in magnitude and, therefore, it becomes imaginary from a physical standpoint.

From the above, the nature and extent of arching for a given material and ditch width can be visualized as follows:

If the yield of the loose mass in the ditch induces a constant relative movement within the fill material above the top of the ditch, the shearing resistance of the material will be mobilized along the whole fill height and will oppose this movement. This action is called the "arching effect." During this action a visible, trough-like depression will exist on the surface of the fill directly above the conduit.

If the fill height exceeds a maximum value H_{max}, the arching effect will extend upward to the surface below the top of the fill which is called, "the plane of equal settlement." Above this plane no relative movement exists within the soil mass, therefore, no depression will appear on the surface of the fill directly above the conduit.

If the fill height increases without limit, the height of arching will approach a lower limiting finite value.

3. To facilitate the computational part of the above described procedure, two other families of curves have been plotted as follows:

The load factor C_n may be written also:

$$C_n = 1 + e^{-w'} C_m \tag{136}$$

where

$$C_m = e^{-u'}(v' - u' - 1). \tag{137}$$

By substituting in Equation 137 the values for v' and u' from the family of curves presented in Step 2, C_m has been plotted versus v' for different values of $r_{sd}w'/a'$ (Table C and Figures C and C1 in the Appendix).

The above family of curves makes possible the evaluation of the conduit load W_c without computing u' first.

The upper boundary of these curves is the curve for which $r_{sd}w'/a' = 0$. From Relation 95 and the discussion involved in evaluating the general expression governing the behavior of factor u, it was shown that under such conditions, $u' = 0$ and $w' = 0$. Hence, $v' = v$ and the upper boundary will be the curve

$$C_m = v' - 1 = v - 1. \tag{138}$$

Since u' is physically bounded by the condition $u' = v'$ the above curves will be bounded by the same condition.

Letting $u' = v'$ in Equation 137 one obtains

$$C_m = -e^{-v'} \tag{139}$$

which, as it can be seen from Equation 86 is the corresponding C_m factor for a ditch conduit. Hence, the locus of the lower points of the above curves, is the C_m curve obtained for a ditch conduit.

Since Equations 137 and 139 have obviously the same derivative with respect to v' at the point $v' = u'$, it follows that the ditch conduit C_m curve is tangent to each one of the curves of the above family. Hence, at their respective $v' = u'$ points, each one of these curves merges with the ditch conduit curve.

From the above it follows that the process of arching as visualized in Step 3 is also mathematically continuous.

It can be shown also that for a fixed value of $r_{sd}w'/a'$

$$\lim_{v' \to \infty} C_m = \infty, \tag{140}$$

whereas

$$\lim_{\left|\frac{r_{sd}w'}{a'}\right| \to \infty \atop v' \to \infty} C_m = 0. \tag{141}$$

4. By solving Equation 136, C_n has been plotted versus C_m for different values of w' (Table D and Figure D).

The upper boundary of this family of curves is the curve obtained for $w' = 0$. As it was previously shown, under such conditions

$$\frac{r_{sd}w'}{a'} = 0 \qquad \text{and} \qquad u' = 0.$$

Therefore,

$$C_m = v - 1 \qquad \text{and} \qquad C_n = v.$$

Since

$$v = (2K_e \tan\phi_e)\, H/B_d,$$

$$W_c = \frac{\gamma B_d^2}{2K_e \tan\phi_e} \cdot (2K_e \tan\phi_e)\, H/B_d = \gamma B_d H = W.$$

The lower boundary of the same family of curves is the curve for which $w' = \infty$. Under such conditions the second member of Equation 136 vanishes, C_m becomes equal to one, and the load assumes the value

$$W_c = \frac{\gamma B_d^2}{2K_e \tan\phi_e}.$$

From the last family of curves one can see that the load on top of the conduit is greatly influenced by the factor $w' = (2K_e\tan\phi_e)\, H_d/B_d$.

Recapitulating, one can compute the load on top of covered-up underground conduits installed under a cohesionless material as follows:

Given the material and the dimensions H, H_d, and B_d:

(a) Estimate K_e, ϕ_e, γ, r_{sd}, and a'.

(b) From Table A or Figure A obtain the value $2K_e\tan\phi_e$.

(c) Compute factors, $v' = (2K_e\tan\phi_e)\, H'/B_d$, $w' = (2K_e\tan\phi_e)\, H_d/B_d$, and $r_{sd}w'/a'$.

(d) From Table C or Figures C or C1 determine the value of C_m corresponding to v' and $r_{sd}w'/a'$ computed in Step c.

(e) From Table D or Figure D determine the value of C_n corresponding to the values of C_m obtained in Step d, and w' computed in Step c.

(f) Substitute the value of C_n and $2K_e\tan\phi_e$ in the equation $W_c = \frac{\gamma B_d^2}{2K_e\tan\phi_e}\, C_n$ and compute the load.

Although the above procedure utilizes three different charts for the load evaluation instead of one utilized in other publications, it has the over-all advantage over the latter in that the same charts can be used for any kind of covered-up conduit installation. Load factor charts in other publications can be used for only one value of the quantities $K\tan\phi$, and H_d/B_d.

In previous sections it was shown that if factor $v' = (2K_e\tan\phi_e)\, H'/B_d$ increases without limit, $u' = (2K_e\tan\phi_e)\, H'_e/B_d$ is governed by Equations 43 or 91,

$$(\frac{3}{2} + \frac{r_{sd}w'}{a'})\, e^{-u'} + \frac{3}{2}(u' - 1) = 0,$$

regardless of whether the material is an $s = c + \sigma\tan\phi$ type or an $s = \sigma\tan\phi$ material. Hence, if factor $2K_e\tan\phi_e$ is made large enough by proper construction methods and if the ratio H/B_d of the fill height to the width of the ditch is also large enough, the use of Equation 43 instead of Equation 42, for determining factor u' for an $s = c + \sigma\tan\phi$ material, will not result in a serious error.

Under the above conditions, one may solve the load Equation 49 for an $s = c + \sigma\tan\phi$ material, by substituting the value of u' obtained from Equation 43.

It can also be shown by numerical examples that under the same conditions, for the values of cohesion c_e up to $c_e = \gamma B_d/2$, an $s = c + \sigma\tan\phi$ material may be assumed to be cohesionless and the error, besides being on the safe side, will not be appreciable enough to affect economy. Therefore, in such cases the above constructed charts may be used also for evaluating the conduit load for an $s = c + \sigma\tan\phi$ material.

If the construction of a high ditch with very loose material on top of the conduit is economically feasible, then factor $w' = (2K_e\tan\phi_e)H_d/B_d$ will be large enough and, consequently, the exponential function e^{-u} will approach zero and the first part of the load factor C_n will become negligible. Hence, under these conditions the load becomes independent of factor u' and it may be obtained either from Equation 23 or from Equation 85. However, if the construction conditions are such that w' is not large enough to make the first part of the load factor C_n negligible, the load must be computed by means of the appropriate equations.

SUMMARY AND CONCLUSIONS

I. From the construction point of view, underground conduits may be classified into two main categories:

A. Covered-Up Conduits.
Conduits belonging in this category are installed under artificial earth embankments that are constructed after the conduits have been assembled in place.

B. Mined-In Conduits.
Conduits of this category are installed by a mining process through natural earthen deposits.

II. Mathematical relations have been derived, describing the loading action on top of an underground conduit of a material whose shearing resistance can be represented by the general Coulomb equation $s = c + \sigma\tan\phi$.

III. Theoretical relations governing the loading action of a perfectly cohesionless or a perfectly cohesive material have been obtained by taking the limits of the expressions derived for the general case when c or ϕ are allowed to approach zero, respectively.

IV. From the mathematical standpoint the earth load on top of either covered-up or mined-in conduits can be evaluated by means of the same general expression

$$W_c = \gamma B_d H_{eff}$$

where:

W_c = vertical load on top of conduit, lb. per lin. ft.
γ = unit weight of the material, pcf.
B_d = effective width of the earth column above the conduit, ft.
H_{eff} = effective height of the earth column above the conduit, ft.

V. The effective height H_{eff} is a fictitious quantity and is a measure of the arching effect that takes place within the earth mass above the conduit. Generally:

A. If the mass directly above the conduit subsides less than the adjacent masses, the effective height, H_{eff}, is greater in magnitude than the actual height of the mass, H. Accordingly, the conduit load will be greater than the weight of the earth column directly above the conduit. This possibility has been defined as Case I.

B. If the reverse action takes place, H_{eff} is smaller in magnitude than H, and, consequently, the conduit load will be less than the weight of the earth column above the conduit. This possibility has been defined as Case II.

C. If no relative movement takes place within the earth mass above the conduit, H_{eff} will equal H and, consequantly, the weight on top of the conduit will be equal to the weight of the earth column directly above it.

VI. Case I has been shown to have detrimental effects on underground conduits regardless of the type of overlying soil. Therefore, this condition should always be avoided by proper methods of design and construction.

Case II with possibility C as a limiting condition is very advantageous and, consequently, the conditions for this case must always be sought by proper methods of design and construction. The theoretical analysis presented in this paper has dealt mainly with the factors influencing the conduit load when the conditions insuring the existence of Case II have been realized.

VII. From the analysis for Case II one may conclude that the effective height is the product of the effective width of the column of earth directly above the conduit multiplied by a function of dimensionless factors that depend:

A. Directly:

1. On the geometry of the installation.
2. On the initial state and physical properties of the loading agent.
3. On the height of arching, H_e.

B. Indirectly:

1. On the relative movement that takes place within the soil mass directly above the conduit.
2. On the relative stiffness between the body supporting the soil prism directly above the conduit defined as the "interior prism," and the body supporting the soil prisms adjacent to the interior prism, defined as "exterior prisms."
3. On the construction methods and workmanship employed.

VIII. Elaborating on Item VII, the following may be deduced from the mathematical analysis for Case II:

A. The higher the factor $v = (2K_e \tan\phi_e)\, H/B_d$, the higher will be the effective height.

B. The higher the factors $2K_e \tan\phi_e$, $2c_e/\gamma B_d$ and $u = (2K_e \tan\phi_e)\, H_e/B_d$, the lower will be the effective height.

C. For given values of v and $2c_e/\gamma B_d$, factor u varies directly with:

1. Factor $r_{sd}w'/a' = r_{sd}(E_F/E_L)(2K_e\tan\phi_e)\ H_d/B_d$ for covered-up conduits.

2. Factor $r_{sm}w/a = r_{sm}(E_f/E_m)(2K_e\tan\phi_e)\ H_m/B_d$ for mined-in conduits, or positive projecting conduits with their side supporting material compacted very thoroughly.

Factors $r_{sd}w'/a'$ or $r_{sm}w/a$ are measures of the relative yielding and the relative stiffness between the supports of the interior and the exterior prisms in covered-up or mined-in conduits respectively. Therefore, the larger in magnitude of these quantities, the higher will be the factor u, or, for a given installation, the higher will be the height of arching, H_e.

D. For fixed values of $2c_e/\gamma B_d$, and given values of $r_{sd}w'/a'$ or $r_{sm}w/a$, if v' or v are allowed to increase without limit, u' or u decrease respectively from maximum values $u' = v'_{max}$ or $u = v_{max}$ to limiting finite values $u' = u'_{v'=\infty}$ or $u = u_{v=\infty}$, that are independent of the cohesion c_e.

For values of v' or v smaller in magnitude than v'_{max} or v_{max}, factors u' or u are respectively greater in magnitude than v' or v and, therefore, they do not have a physical meaning dimensionwise.

E. For given values of v' and $r_{sd}w'/a'$, or v and $r_{sm}w/a$, if $2c_e/\gamma B_d$ is allowed to increase without limit, u' or u will approach zero. Under the same conditions the effective height will approach the value $-\infty$. However, physically, the above height can approach only the value zero. Consequently, the load on top of the conduit will vanish.

IX. From a knowledge of the behavior of the physical factors that are involved in the aforementioned mathematical analysis, the following conclusions may be drawn relative to the development of earth pressure on top of underground conduits:

A. The unit weight γ, the angle of internal friction ϕ and the cohesion c of the loading agent are understood to have a statistical average value meaning. Local deviations from this value depend:

1. In the case of covered-up conduits on the type of earthen material, the method of fill construction, and the water content of the fill material.
2. In the case of mined-in conduits on the geologic history, the initial state, and the water content of the overlying natural earth deposit.

B. Inasmuch as the potential sliding surfaces are not vertical planes but are in reality curved surfaces whose spacing is considerably greater at the top of the mass than it is at the top of the conduit, the shearing resistance of the soil is only partially mobilized along the assumed vertical planes in order to oppose any relative movement within the soil mass above the conduit. Consequently:

1. Only a portion of the maximum value of the angle of internal friction of the soil is mobilized along the vertical planes.
2. Only a portion of the maximum value of the cohesion of the material is mobilized along the vertical planes.
3. The earth pressure ratio, K, will never assume the extreme values K_A and K_P that are realized respectively for active and passive states of plastic equilibrium, but it will vary between these two limiting values.

To simplify the theoretical treatment of the problem, the above factors are assumed constant along the vertical planes and equal to ϕ_e, c_e, and K_e, respectively.

C. The values of ϕ_e, c_e, and K_e depend on the type, the initial state, the permeability, and the strain characteristics of the soil as well as on the size of the mass and the rate of application of stress to it.

From the foregoing it may be concluded that for a given installation and soil type, the construction methods and the workmanship employed, as well as time are major factors influencing ϕ_e, c_e, and K_e.

D. The strain characteristics of the material as well as the stress application mentioned in Item C, depend on the settlement ratio defined as r_{sd} for covered-up conduits, and r_{sm} for mined-in conduits. This ratio, which is a measure of the relative yield between the support of the interior prism and the support of the exterior prisms, depends on time and varies directly with the relative stiffness between supports.

E. For a given installation and soil type, the greater the magnitude of the settlement ratio, the higher will be the height of arching, H_e.

Physically, H_e can be only as high as the height of the mass above the conduit, H. If numerically, H_e is greater in magnitude than H, a trough-like depression will appear at the top of the mass directly above the conduit. This indicates that the soil mass along the sliding planes is being subjected to a greater amount of strain.

If the above conditions are realized, the effective values ϕ_e and c_e that are mobilized along the vertical planes will approach the limiting values of ϕ and c and K will approach the limiting value K_A at the top of the mass.

F. The maximum fill height up to which the surface of the fill may be expected to settle directly above an installed conduit can be obtained from Equation 58.

G. Everything else remaining the same, as the fill height increases the height of arching decreases and a greater portion of the mass acts directly on the conduit.

H. For very high fills the influence of the cohesion of the material becomes negligible and the material acts as if it were perfectly granular.

X. From the discussion of Item IX one may conclude that:

A. In a Covered-Up Conduit:

1. The better the gradation of the fill material and the more uniformly it is compacted, the greater will be the values, γ, ϕ, and c.
2. The greater the relative stiffness between the support of the interior prism and the support of the exterior prisms, the greater will be the relative movement within the soil above the conduit. Consequently, the greater will be the amount of ϕ and c that is mobilized along the vertical planes. If such conditions are realized, a greater portion of the load will be sustained by the shearing resistance of the material; hence, the pressure on top of the conduit will be reduced.
3. Since in the discussion of Item 2 it was indicated that the governing factor in the development of pressure on top of the conduit is the relative stiffness between the supports of the interior and exterior prisms and not the individual stiffness of each constituent part of these supports, it follows that the more rigid the conduit is:
   a. The stiffer should be the side supporting material.
   b. The looser and the more compressible should be the material in the ditch directly above the conduit.
   c. The more yielding should be the foundation.
4. The higher the ditch and the more compressible the material in it, the higher will be the equivalent earth pressure ratio K_e.

Since the shortening of the vertical diameter of the conduit is very small as compared with the compression of the material in the ditch, it follows that as this material is compacted due to the weight of the fill it subjects the side masses to compression. Consequently, K increases gradually from the minimum value it attains at the top of the ditch, to a maximum value at the top of the conduit. Thus, the value of the equivalent hydrostatic pressure ratio, K_e is increased also (Figure 2c).

5. From the mathematical analysis and the discussion of Item 4 it follows that the higher the ditch above the conduit and the more compressible the material in it, the greater will be the factor $w' = (2K_e \tan\phi_e)\, H_d/B_d$ and, consequently, the lower will be the conduit load.
6. The effective width B_d may be considered to be equal to the mean width of the

ditch above the conduit.

7. The settlement ratio r_{sd} can be determined by measuring directly the subsidence of the parts constituting the supports of the interior and exterior prisms.

8. It may be concluded that:

a. The side supporting material of a covered-up conduit should consist of thoroughly compacted, well- graded, granular material.

b. The ditch material should be of a compressible type and it should be placed in such a way that it will be in the loosest possible state.

c. The ditch should be made as high as economically feasible. In order that a sheeting and bracing operation be avoided during the construction of a high ditch, the following method may be adopted:

The heavy equipment, which is compacting the material adjacent to the ditch, may follow a course perpendicular to the longitudinal axis of the conduit. Each pass should end at lines pre-staked along the conduit axis and on both sides of the ditch. When the ditch sides become sufficiently high, the compressible material may be end-dumped from the heavy equipment into the ditch.

By the above method the ditch can be filled up with compressible material at the same time it is constructed. Therefore, it can reach any desirable height with its sides remaining vertical.

d. If Items a, b and c are fulfilled and should other considerations indicate that they will be more economical to use than flexible conduits, rigid conduits may also be installed safely under high fills.

B. In a Mined-In Conduit:

1. The values ϕ and c of a natural earth deposit will generally be greater than the same values of an identical material that has been remolded and used as a fill material on top of a covered-up conduit.

2. The greater the relative stiffness between the supports of the interior and exterior prisms, the greater will be the corresponding settlement ratio; accordingly, the greater will be the height of arching and the portions of ϕ and c that are mobilized along the sliding planes. Consequently, the load will be lower.

The softer the layer of the soil adjacent to the conduit, the more flexible should the conduit be made so that it will adjust its shape and thereby minimize the development of nonuniform external pressures.

3. The effective width of the earth column on top of the conduit, B_d, depends on the relative stiffness between the material adjacent to the conduit and the remainder of the mass above it.

4. The load on top of mined-in conduits that are installed under a deep natural earth deposit consisting of as $s = c + \sigma \tan \phi$ material becomes independent of the cohesion and may be evaluated by means of Equation 85.

5. The maximum height of the mass up to which the surface of the mass should be expected to settle assuming a trough-like shape directly above an installed conduit can be obtained from Equation 75.

6. In mined-in conduits the settlement ratio r_{sm} can be determined only indirectly. In positive projecting conduits, however, it can be obtained by direct measurements.

C. Generally:

A good knowledge of the physical properties of the soils that are involved in a project is always necessary. Therefore, a good soil exploration of the site where the conduit is to be installed is imperative.

The factor of safety can be applied to the values ϕ_e, and c_e that are considered to be the developed fractions of the maximum values of the angle of internal friction and cohesion of the material.

The value K_e will vary with the method of installation and with the soil type. Tentatively, it is suggested that for small depths of overburden its value be chosen between 0.5 and K_A; for high depths its value be chosen between 0.5 and 1.0

The relative stiffness between the supports of the interior and exterior prisms should be made as high as possible.

XII. Families of curves have been constructed from which the conduit load due to an $s = \sigma \tan\phi$ material can be computed. Under certain conditions these curves can be used to evaluate the conduit load due to an $s = c + \sigma \tan\phi$ soil type.

XIII. In this investigation consideration has been given to pressures that act in the plane of a right, cross-section of the conduit with no allowance for variations caused by arching along the longitudinal axis of the conduit nor to tangential forces that act along this axis.

Since an underground conduit has the tendency to settle more in the middle than at its ends, the earth mass, which is above its middle portion, will tend to brace itself against the end masses thereby increasing the normal pressure and the longitudinal strains at the ends and decreasing the pressure at the middle. The effects of such arching action will be especially significant in the case of long conduits installed under high fills.

RECOMMENDATIONS FOR FUTURE STUDY

In order to obtain a better understanding of earth pressures on underground conduits, the author believes that future efforts should be concerned mainly with the development of techniques by means of which the earth pressure exerted around the circumference of an underground conduit can be measured directly. From such information one will be able to gather substantial information to:

I. Evaluate the values ϕ_e, c_e, and K_e for given installation conditions.

II. Determine the magnitude of the lateral pressure that a precompacted side supporting material is potentially able to mobilize per unit of lateral bulging of the conduit.

III. Determine by rational means the type, the size, and the degree of precompaction of the side supporting material in order that a given conduit may not bulge excessively.

IV. Develop a theory expressing the vertical load on top of the conduit as a function of the lateral pressures exerted by the side supporting material as well as the bottom reaction of the bedding material.

V. Understand the arching effect on the earth mass above and along the conduit axis.

VI. Obtain information on settlement ratios especially for mined-in conduits.

VII. Permit the use of a substantially smaller factor of safety and thereby achieve a more economical design.

In conjunction with the above discussion the reader is referred to a report prepared by the research department of the North Carolina State Highway and Public Works Commission (Costes and Proudley, 1955) in which an attempt to develop a technique for the direct measurement of the lateral earth pressures acting on a flexible culvert pipe installed under a high fill is outlined.

ACKNOWLEDGEMENTS

The author wishes to express his deepest appreciation to Dr. Ralph E. Fadum and Dr. John W. Cell, both of North Carolina State College for their valuable assistance in the preparation of this paper.

The author is also grateful to Charles E. Proudley, Chief Material Engineer, and A. Duke Morgan, Materials Research Engineer, as well as to other members of the Division of Materials, of the North Carolina State Highway and Public Works Commission, for their constant aid, advice, and support during the research activities that led to the preparation of this paper.

To Adele Covington and Janet Brown the author is particularly indebted for their indispensable aid in the preparation of the manuscript.

References

1. American Railway Engineering Association. 1926. Report of the committee on roadbed. 27: 794.

2. American Railway Engineering Association. 1928. Report of the committee on roadbed. 29: 527.

3. American Concrete Pipe Association. 1955. Loads on underground conduits. Concrete Pipe News, 7 Nos. 1-4.

4. Armco Drainage and Metal Products, Inc. 1950. Handbook of culvert and drainage practice. R. R. Donnelly and Sons Co., Chicago, Illinois.
5. Bela, E. 1937. Contribution pour le calcul des conduites circulaires. Travaux, August, 1937.
6. Bela, E. 1938. Contribution pour le calcul des conduites circulaires. Travaux, April, 1938.
7. Bierbaumer, A. 1913. Die Dimensionierung des Tunnelmauerwerkes, W. Engelmann, Liepzig.
8. Braune, G. M.; Cain, W.; and Janda, H. F. 1929. Earth pressure experiments on culvert pipe. Public Roads, Wash. 10: 153-176.
9. Cain, W. 1916. Earth pressure, retaining walls and bins. John Wiley and Sons, Inc., New York.
10. Cain, W. 1912. Experiments on retaining walls and pressure on tunnels. Trans. Am. Soc. Civ. Engrs. 72: 403-474.
11. Caquot, A. 1934. Equilibre des massifs a frottement interne. Gautier-Villard, Paris.
12. Concrete Culverts and Conduits. 1940. Portland Cement Association, Chicago, Illinois.
13. Costes, N. C. and Proudley, C. E. 1955. Performance study of multi-plate corrugated-metal-pipe culvert under embankment. Highway Research Board Bulletin 125.
14. Engesser, F. 1880. Geometrische Erddruck theorie. Z. Bauwesen, 30: 189.
15. Federal Works Agency. 1939. Tables of the exponential function e^x. Report of Official Project No. 765-97-3-10. Work Projects Administration for the City of New York, National Bureau of Standards, New York.
16. Forchheimer, P. 1882. Ueber Sanddruck etc. Zeitschr. oest. Ing. und Arch. Vereins.
17. Guerrin, M. A. 1938. Le calcul des conduites circulaires enterees. Travaux, January, 1938.
18. Handbook of Water Control. 1936. New England Metal Culvert Co., Palmer, Massachusetts.
19. Housel, W. S. 1943. Earth pressure on tunnels. Proc. Amer. Soc. Civ. Engrs. 69: 1037-1058.
20. Janssen, H. A. 1895. Versuche über Getreidedruck in Silozellen. Z. Ver dent. Ing. 39: 1045.
21. Kells, L. M. 1947. Elementary differential equations. McGraw Hill Book Company, Inc., New York and London.
22. Ketchum, M. S. 1911. Walls, bins, and grain elevators. McGraw Hill Book Company, Inc., New York.
23. Koenen, M. 1896. Berechnung des Seiten und Bodendrucks in Silozellen. Centrbl. Bauverwaltung, 16: 446-447.
24. Kotter, F. 1888. Über das Problem der Erddruck bestimmung. Verhandl. Physik. Ges. Berlin, 7: 1-8.
25. Krynine, O. P. 1940. Design of pipe culverts from standpoint of soil mechanics. Proc. Highw. Res. Bd., Wash. 20: 722-729.
26. Loving, M. W. 1942. Concrete pipe lines. American Concrete Pipe Association, Chicago, Illinois.
27. Marston, A. and Anderson, A. O. 1913. The theory of loads on pipes in ditches and tests of cement and clay drain tile and sewer pipe. Iowa State College, Engr. Exp. Sta. Bull. No. 31.
28. Marston, A. 1922. Second progress report to the joint concrete culvert pipe committee (Mimeograph). Iowa State College, Engr. Exp. Sta., Ames, Iowa.
29. Marston, A. 1930. The theory of external loads on closed conduits in the light of the latest experiments. Proc. Highw. Res. Bd., Wash. 9: 138-170.
30. Merriman, T. and Wiggin, T. H. 1943. American civil engineer's handbook. John Wiley and Sons, Inc., New York.
31. Peck. O. K. and Peck, R. B. 1948. Earth pressure against underground constructions. Experience with flexible culverts through railroad embankments. Proc.

Intern. Conf. Soil Mechanics, 2: 95-98.
32. Peck, R. B. 1943. Earth-pressure measurements in open cuts, Chicago (Ill.) subway. Proc. Amer. Soc. Civ. Engrs. 69: 1008-1036.
33. Peckworth, H. F. 1951. Concrete pipe handbook. American Concrete Pipe Association, Chicago, Illinois.
34. Pokrowski, G. I. and Kouptzoff, J. G. 1937. Determination of pressure on pipes in trenches (in Russian). Official publication, Moscow.
35. Reddick, H. W. and Miller, F. H. 1938. Advanced mathematics for engineers. John Wiley and Sons, Inc., New York.
36. Schlick, W. J. 1932. Loads on pipes in wide ditches. Iowa State College, Engr. Exp. Sta. Bull. No. 108.
37. Schlick, W. J. 1952. Loads on negative projecting conduits. Proc. Highw. Res. Bd., Wash. 31: 308-319.
38. Smith, W. A.; Kent, F. L.; and Stratton, G. B. 1952. World list of scientific periodicals published in the years 1900-1950. Third edition. New York Academic Press, Inc., New York.
39. Spangler, M. G. 1937. The structural design of flexible pipe culverts. Proc. Highw. Res. Bd., Wash. 17 part I: 235-237.
40. Spangler, M. G. 1946. Analysis of loads and supporting strengths and principles of design for highway culverts. Proc. Highw. Res. Bd., Wash. 26: 189-212. Discussion pp. 213-214.
41. Spangler, M. G. and Hennessy, R. L. 1946. A method of computing live loads transmitted to underground conduits. Proc. Highw. Res. Bd., Wash. 26: 179-184.
42. Spangler, M. G. 1948. Stresses and deflections in flexible pipe culverts. Proc. Highw. Res. Bd., Wash. 28: 249-257.
43. Spangler, M. G. 1950a. A theory on loads on negative projecting conduits. Proc. Highw. Res. Bd., Wash. 30: 153-161.
44. Spangler, M. G. 1950b. Field measurements of the settlement ratios of various highway culverts. Iowa State College, Engr. Exp. Sta. Bull. No. 170.
45. Spangler, M. G. 1951. Soil engineering. International Textbook Co., Scranton, Pennsylvania.
46. Spangler, M. G. 1951-1952. Protective casings for pipe lines. Iowa State College, Engr. Exp. Sta. Engineering Report No. 11.
47. Spangler, M. G. 1954. Subsidence under earth embankments. Unpublished discussion presented before the Geology Section of the Iowa Engineering Society, Des Moines, Iowa.
48. Taylor, D. W. 1948. Fundamentals of soil mechanics. John Wiley and Sons, Inc., New York.
49. Terzaghi, K. 1936a. Stress distribution in dry and in saturated sand above a yielding trap-door. Proc. Intern. Conf. Soil Mechanics, 1: 307-311.
50. Terzaghi, K. 1936b. A fundamental fallacy in earth pressure computations. J. Boston Soc. Civ. Engrs. 23: 71-88.
51. Terzaghi, K. 1941. General wedge theory of earth pressure. Trans. Amer. Soc. Civ. Engrs. 106: 68-97.
52. Terzaghi, K. 1942-1943. Shield tunnels of the Chicago subway. Harvard University, Graduate School of Engineering. Soil Mechanics Series No. 19.
53. Terzaghi, K. 1943a. Theoretical soil mechanics. John Wiley and Sons, Inc. New York.
54. Terzaghi, K. 1943b. Liner-plate tunnels on the Chicago (Ill.) subway. Proc. Amer. Soc. Civ. Engrs. 69: part 2: 970-1007.
55. Terzaghi, K. and Peck, R. B. 1948. Soil mechanics in engineering practice. John Wiley and Sons, Inc., New York.
56. Timmers, J. H. 1953. Multi-plate compression measurements at Cullman, Alabama installation. Research Report. Armco Drainage and Metal Products, Inc., Middletown, Ohio.
57. Tschebotarioff, G. P. 1949. Large scale model earth pressure tests on flexible bulkheads. Trans. Amer. Soc. Civ. Engrs. 114: 415-454.
58. Völlmy, A. 1937. Eingebettete Röhre. Mitt. Institut fur Baustatik, Eidgen.

Tech. Hochschule, Zurich, Mitteilung No. 9.
59. Völlmy, A. 1938. Erddruck auf elastisch eingebettete Röhre. International Association for Bridge and Structural Engineering, Vol. 4.

Appendix

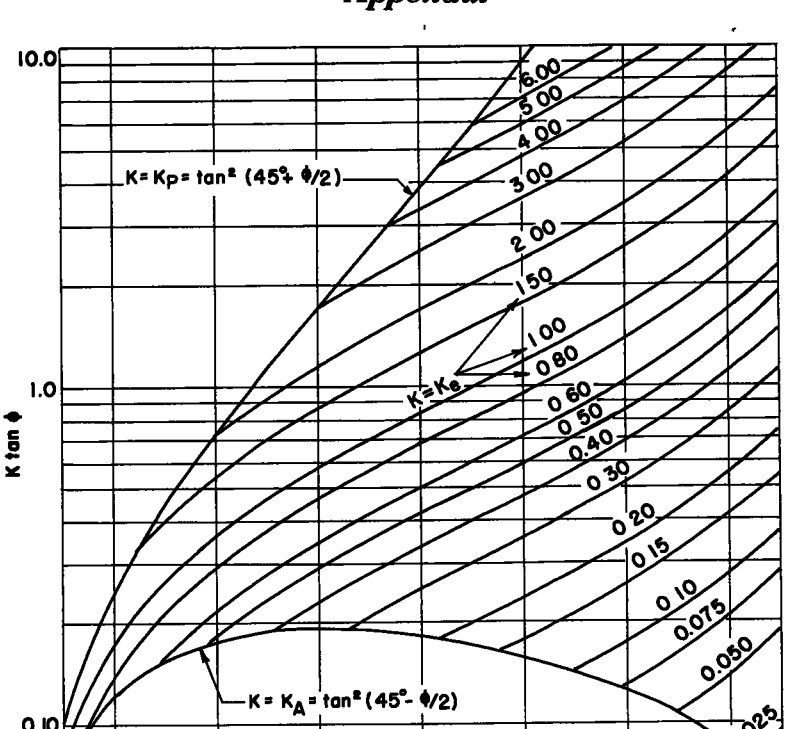

Figure A.

TABLE A

VALUES OF Ktanϕ FOR GIVEN VALUES OF K AND ϕ

K	5°	10°	15°	20°	25°	30°	35°	40°	45°	50°	55°	60°	65°	70°	75°
K_A	0 073	0 125	0 158	0 178	0 189	0 192	0 190	0.182	0 171	0.159	0 141	0 125	0.105	0.085	0 063
0 025															0.093
0 050													0 107	0.137	0.187
0 075												0.130	0.161	0.206	0.280
0 100											0.143	0 173	0 215	0 275	0.373
0 150										0 179	0.214	0.260	0 322	0.412	0 560
0.200									0 200	0.238	0 286	0 346	0.429	0 550	0 746
0 300							0 210	0 252	0 300	0.358	0.428	0 520	0 644	0 824	1.120
0 400						0 231	0 280	0 336	0 400	0 477	0.571	0.693	0.858	1 099	1 493
0 500				0 182	0.233	0 289	0 350	0.420	0 500	0.596	0 714	0.866	1 073	1 374	1 866
0 600			0 161	0 218	0 280	0 346	0 420	0.503	0 600	0.715	0.857	1.039	1 287	1 649	2.239
0 800		0 142	0 214	0 291	0.373	0 462	0 560	0 671	0 800	0 954	1 142	1 386	1 716	2 198	2 986
1 000	0 087	0 177	0 268	0 364	0 466	0 577	0 700	0 839	1 000	1 192	1 428	1 732	2 145	2 748	3 732
1 500			0 402	0 546	0 699	0 866	1 050	1.259	1 500	1 788	2 142	2 598	3 218	4 122	5 598
2 000				0 728	0 932	1 154	1 400	1.678	2 000	2 384	2 856	3 464	4 290	5 496	7 464
3 000						1 731	2 100	2 517	3 000	3 576	4 284	5 196	6 435	8 244	11 196[a]
4 000								3 356	4 000	4 768	5 712	6 928	8 580	10 992[a]	14 928[a]
5 000									5 000	5 960	7 140	8.660	10 725[a]	13 740[a]	18 660[a]
6 000										7.152	8 568	10.392[a]	12 870[a]	16.482[a]	22.392[a]
K_P	0 104	0 252	0 455	0 742	1 147	1 731	2 583	3.860	5 827	8 995	14.369[a]	24 123[a]	43 649[a]	88 378[a]	215 333[a]

[a] Values of Ktanϕ beyond plotting range of Figure A

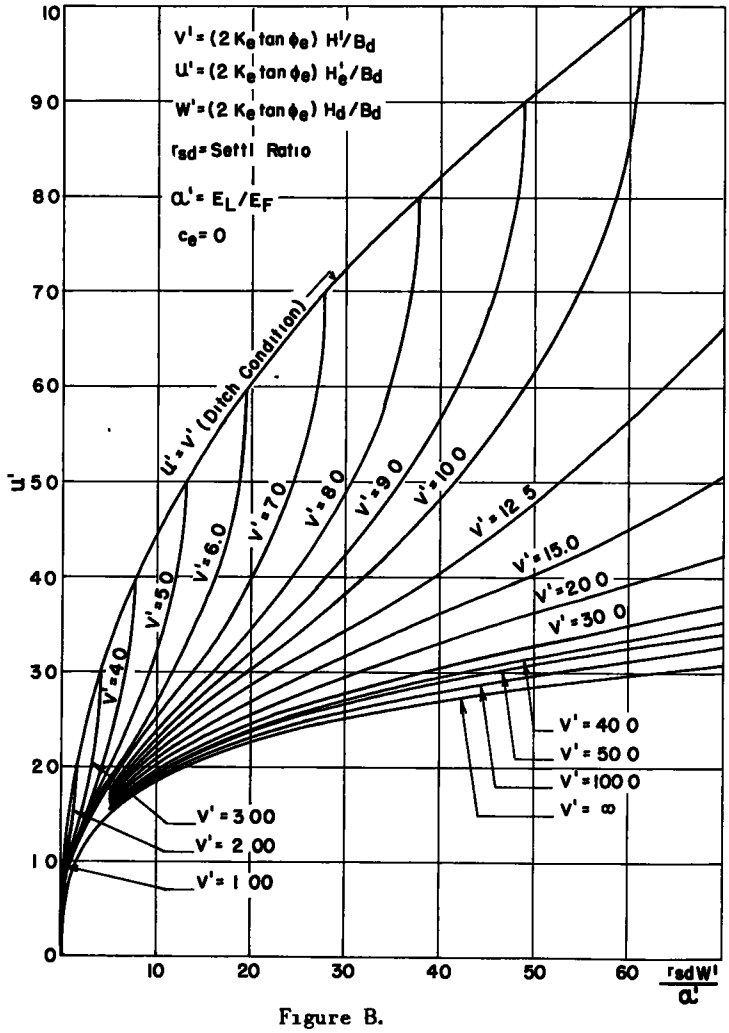

Figure B.

TABLE B

VALUES OF u' FOR GIVEN VALUES OF v' AND $r_{sd}w'/\alpha'$

v'	0.0	-0.5	-1.0	-1.5	-2.0	-3.0	-4.0	-5.0	-7.5	-10	-20	-30	-40	-50	-60	-70
						$\frac{r_{sd}w'}{\alpha'}$										
0.0	0.000	0.000	0.000	0.000	0.000	0.000	0.000	0.000	0.000	0.000	0.000	0.000	0.000	0.000	0.000	0.000
v' = u'	0.000	1.234	1.680	2.000	2.260	2.693	3.043	3.343	3.975	4.495	6.058	7.243	8.200	9.100	9.888	10.595
1.0	0.000	-[a]	-	-	-	-	-	-	-	-	-	-	-	-	-	-
2.0	0.000	0.794	1.210	2.000	-	-	-	-	-	-	-	-	-	-	-	-
3.0	0.000	0.732	1.025	1.270	1.495	2.000	-	-	-	-	-	-	-	-	-	-
4.0	0.000	0.708	0.970	1.170	1.347	1.658	1.960	2.265	3.625	-	-	-	-	-	-	-
5.0	0.000	0.695	0.941	1.125	1.281	1.546	1.775	1.990	2.575	3.19	-	-	-	-	-	-
6.0	0.000	0.687	0.925	1.100	1.245	1.483	1.688	1.875	2.280	2.69	-	-	-	-	-	-
7.0	0.000	0.682	0.915	1.085	1.222	1.445	1.637	1.799	2.163	2.49	3.95	-	-	-	-	-
8.0	0.000	0.677	0.907	1.070	1.205	1.420	1.598	1.745	2.077	2.37	3.45	4.90	-	-	-	-
9.0	0.000	0.674	0.900	1.063	1.193	1.401	1.572	1.720	2.040	2.29	3.21	4.21	5.70	-	-	-
10.0	0.000	0.672	0.897	1.056	1.185	1.389	1.550	1.680	1.978	2.23	3.04	3.85	4.80	6.19	8.50	-
12.5	0.000	0.668	0.889	1.044	1.168	1.362	1.518	1.649	1.920	2.18	2.81	3.40	3.95	4.62	5.38	6.22
15.0	0.000	0.666	0.883	1.035	1.158	1.348	1.493	1.625	1.875	2.08	2.69	3.18	3.62	4.04	4.51	5.07
20.0	0.000	0.663	0.877	1.026	1.145	1.327	1.475	1.589	1.831	2.03	2.56	2.96	3.30	3.62	3.93	4.24
30.0	0.000	0.660	0.870	1.016	1.133	1.309	1.456	1.565	1.778	1.97	2.45	2.78	3.05	3.29	3.51	3.71
40.0	0.000	0.658	0.867	1.012	1.128	1.301	1.441	1.545	1.765	1.94	2.40	2.71	2.95	3.16	3.34	3.51
50.0	0.000	0.657	0.866	1.010	1.124	1.298	1.437	1.535	1.750	1.93	2.37	2.66	2.90	3.09	3.26	3.41
100.0	0.000	0.655	0.861	1.005	1.117	1.283	1.419	1.525	1.728	1.92	2.32	2.59	2.79	2.96	3.11	3.25
∞	0.000	0.653	0.859	1.000	1.110	1.278	1.408	1.514	1.718	1.872	2.271	2.524	2.701	2.845	2.980	3.065

[a] For these values of v' and $r_{sd}w'/\alpha'$, u' is equal to v' physically

TABLE C

VALUES OF C_m FOR GIVEN VALUES OF v' AND $r_{sdw'}/a'$

$r_{sdw'}/a'$ \ v'	0.0	1.0	2.0	3.0	4.0	5.0	6 0	7.0	8.0	9.0	10
0.00	-1.000	0.000	1.000	2.000	3.000	4.000	5.000	6.000	7 000	8.000	9.000
0.01	-1.000	-0.110	0.799	1.700	2.580	3.480	4.390	5.280	6.14	7.04	7.90
0.05	-1.000	-0.200	0.586	1.370	2.180	2.950	3.720	4.500	5.30	6.11	6.90
0.10	-1.000	-0.265	0.464	1.175	1.910	2.620	3.340	4.050	4.77	5.51	6.25
0.20	-1.000	-0.325	0.314	0.959	1.600	2.230	2.850	3.490	4.13	4.77	5.40
0.40	-1.000	-0.368[a]	0.155	0.704	1.230	1.800	2.350	2.900	3.45	4.00	4.48
0.60	-1.000	-0.368	0.054	0.548	1.020	1.550	2.040	2.520	3.02	3.52	4.00
0.80	-1.000	-0.368	-0.010	0.440	0.880	1.350	1.800	2.250	2.68	3.13	3.58
1.00	-1.000	-0.368	-0.059	0.352	0.777	1.190	1.610	2.020	2.43	2.85	3.26
1.50	-1.000	-0.368	-0.132	0.211	0.572	0.932	1.300	1.680	2.04	2.40	2.75
2.00	-1.000	-0.368	-0.135[a]	0.119	0.440	0.760	1.070	1.400	1.76	2.05	2.40
3.00	-1.000	-0.368	-0.135	0.000	0.262	0.530	0.800	1.080	1.37	1.62	1.90
4.00	-1.000	-0.368	-0.135	-0.049	0.150	0.380	0.617	0.858	1.13	1.35	1.59
5.00	-1.000	-0.368	-0.135	-0.050[a]	0.078	0.280	0.488	0.701	0.93	1.13	1.35
6.00	-1.000	-0.368	-0.135	-0.050	0.028	0.201	0.386	0.580	0.80	0.98	1.17
8.00	-1.000	-0.368	-0.135	-0.050	-0.017	0.100	0.249	0.410	0.59	0.75	0.92
10.00	-1.000	-0.368	-0.135	-0.050	-0.018[a]	0.035	0.155	0.293	0.44	0.58	0.73
15.00	-1.000	-0.368	-0.135	-0.050	-0.018	-0.007[a]	0.034	0.123	0.23	0.33	0.45
20.00	-1.000	-0.368	-0.135	-0.050	-0.018	-0.007	-0.003[a]	0.035	0.11	0.20	0.29
∞	0.000	0.000	0.000	0.000	0.000	0.000	0.000	0.000	0.000	0.000	0.000

[a] For values of v' and $r_{sdw'}/a'$ below marked horizontal lines, u' is equal to v' physically and $C_m = -e^{-v'}$ (Ditch Condition).

$r_{sdw'}/a'$ \ v'	15	20	30	40	50	60	70	80	90	100	∞
0.00	14.000	19.000	29.000	39.000	49.000	59.000	69.000	79.000	89.000	99.000	∞
0.01	12.4	16.8	25.8	34.7	43.8	52.5	61.0	70.8	80.0	88.5	∞
0.05	10.8	14.7	22.6	30.5	38.5	46.3	54.2	62.1	70.5	78.0	∞
0.10	9.85	13.4	20.5	27.9	35.2	42.6	49.8	57.0	64.0	71.5	∞
0.20	8.62	11.8	18.2	24.6	31.0	37.5	44.0	50.2	57.0	63.0	∞
0.40	7.35	10.1	15.6	21.0	26.5	32.1	37.5	43.1	48.9	54.0	∞
0.60	6.48	8.95	13.8	18.8	23.8	28.7	33.6	38.7	43.8	48.6	∞
0.80	5.87	8.10	12.7	17.3	21.9	26.5	31.0	35.5	40.3	44.8	∞
1.00	5.40	7.50	11.7	16.0	20.2	24.5	28.7	33.0	37.3	41.5	∞
1.50	4.59	6.40	10.1	13.8	17.5	21.1	24.8	28.4	32.0	35.9	∞
2.00	4.04	5.66	8.98	12.3	15.6	18.8	22.1	25.3	28.7	32.0	∞
3.00	3.28	4.65	7.48	10.2	13.0	15.7	18.5	21.4	24.2	27.0	∞
4.00	2.78	4.00	6.45	8.90	11.3	13.8	16.2	18.7	21.2	23.5	∞
5.00	2.46	3.56	5.75	8.00	10.2	12.4	14.6	16.8	19.0	21.2	∞
6.00	2.18	3.17	5.20	7.20	9.20	11.2	13.3	15.3	17.4	19.4	∞
8.00	1.75	2.61	4.35	6.10	7.82	9.59	11.3	13.1	14.8	16.5	∞
10.00	1.50	2.24	3.75	4.09	6.85	8.39	9.90	11.5	13.0	14.5	∞
15.00	1.02	1.64	2.86	4.04	5.30	6.50	7.75	9.00	10.2	11.5	∞
20.00	0.77	1.27	2.28	3.30	4.30	5.35	6.40	7.43	8.50	9.55	∞
∞	0.000	0.000	0.000	0.000	0.000	0.000	0.000	0.000	0.000	0.000	0

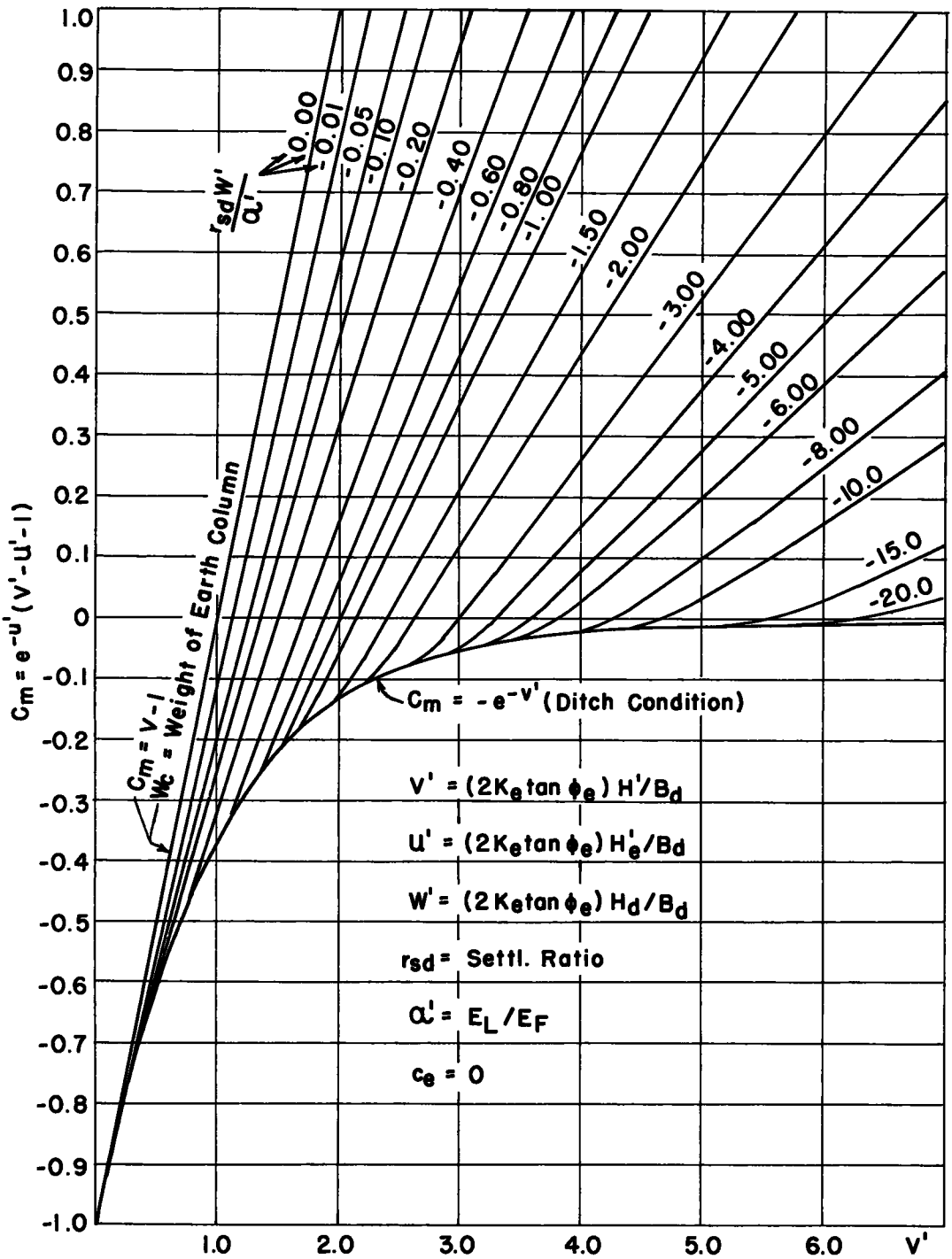
$C_m = e^{-u'}(v'-u'-1)$
$C_m = v-1$
W_c = Weight of Earth Column
$\frac{r_{sd}W'}{\alpha'}$
0.00
-0.01
-0.05
-0.10
-0.20
-0.40
-0.60
-0.80
-1.00
-1.50
-2.00
-3.00
-4.00
-5.00
-6.00
-8.00
-10.0
-15.0
-20.0
$C_m = -e^{-v'}$ (Ditch Condition)
$V' = (2K_e \tan \phi_e) H'/B_d$
$U' = (2K_e \tan \phi_e) H'_e/B_d$
$W' = (2K_e \tan \phi_e) H_d/B_d$
r_{sd} = Settl. Ratio
$\alpha' = E_L/E_F$
$c_e = 0$
1.0
0.9
0.8
0.7
0.6
0.5
0.4
0.3
0.2
0.1
0
-0.1
-0.2
-0.3
-0.4
-0.5
-0.6
-0.7
-0.8
-0.9
-1.0
1.0
2.0
3.0
4.0
5.0
6.0
V'

Figure C.

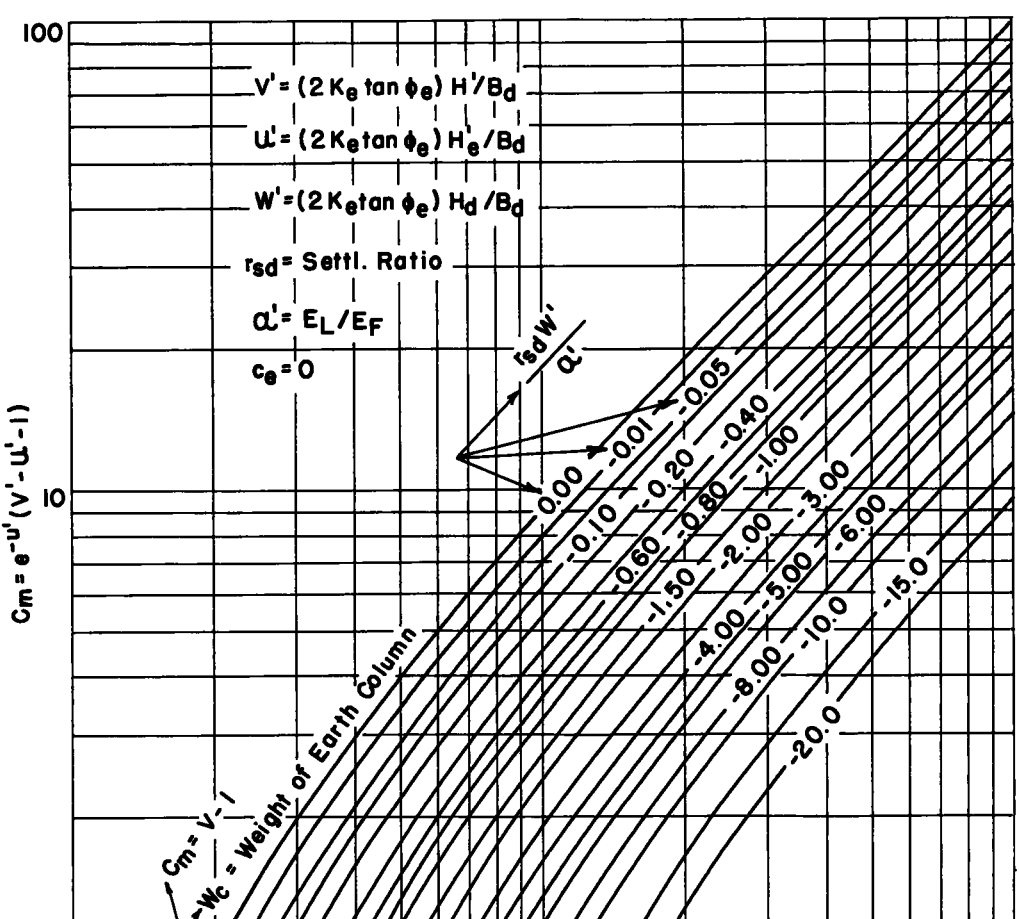

Figure C1.

TABLE D

VALUES OF C_n FOR GIVEN VALUES OF C_m AND w'

C_m	w' 0 0	0 5	1 0	1.5	2 0	2.5	3.0	3.5	4.0	4.5	5.0	6 0	7.0	8.0	∞
0 1	1.10	1.06	1.04	1 02	1.01	1 01	1.00	1.00	1.00	1.00	1 00	1 00	1.00	1 00	1.00
0.2	1 20	1.12	1.07	1 04	1.03	1.02	1 01	1 01	1.00	1 00	1.00	1 00	1.00	1 00	1.00
0.4	1 40	1.24	1.11	1.09	1 05	1.03	1.02	1 01	1.01	1.00	1.00	1 00	1.00	1.00	1.00
0.5	1.50	1.30	1.18	1.11	1 07	1.04	1 02	1.02	1.01	1.01	1.00	1 00	1.00	1.00	1.00
0.6	1.60	1.36	1.22	1.13	1.08	1 05	1.03	1.02	1.01	1.01	1.00	1 00	1.00	1.00	1.00
0 8	1.80	1 49	1.29	1.18	1.11	1.07	1.04	1 02	1.01	1.01	1.01	1.00	1.00	1.00	1.00
1 0	2.00	1.61	1 37	1 22	1.14	1.08	1 05	1 03	1 02	1.01	1 01	1 00	1.00	1.00	1.00
2.0	3.00	2 21	1.74	1.45	1 27	1.16	1.11	1.06	1.04	1.02	1 01	1 00	1.00	1.00	1.00
4.0	5.00	3.43	2 47	1.89	1.54	1.33	1 20	1.12	1.07	1 04	1.03	1 01	1.00	1.00	1.00
5.0	6.00	4 03	2 84	2 12	1.68	1.41	1.25	1 15	1.09	1.06	1.03	1 01	1.00	1.00	1.00
6 0	7.00	4.64	3.21	2 34	1.81	1.49	1.30	1 18	1 11	1.07	1.04	1 01	1.00	1 00	1.00
8.0	9.00	5.85	3.94	2.79	2.08	1.66	1.40	1 24	1.15	1.09	1.05	1.02	1.00	1 00	1.00
10.0	11.00	7.07	4 68	3.23	2.35	1 82	1.50	1.30	1 18	1.11	1.07	1 02	1.01	1.00	1.00
20.0	21 00	13.13	8.36	5 46	3.71	2.64	2.00	1 60	1.37	1 22	1.13	1 05	1.02	1 01	1.00
40.0	41.00	25.26	15.72	9.93	6.41	4.28	2.99	2.21	1.73	1.44	1.27	1.10	1.04	1.01	1.00
50.0	51 00	31.33	19.39	12 16	7.77	5.11	3.49	2.51	1 92	1.56	1 34	1.12	1.05	1 02	1.00
60 0	61.00	37 39	23.07	14 39	9.12	5.93	3 99	2.81	2.10	1 67	1.40	1 15	1.05	1 02	1.00
80.0	81 00	49.52	30.43	18.85	11.83	7.57	4.98	3.42	2 47	1.89	1.54	1 20	1 07	1 03	1.00
100.0	101 00	61.65	37.79	23.31	14.53	9.21	5.98	4 02	2.83	2.11	1.67	1 25	1.09	1.03	1.00
∞	∞	∞	∞	∞	∞	∞	∞	∞	∞	∞	∞	∞	∞	∞	1.00

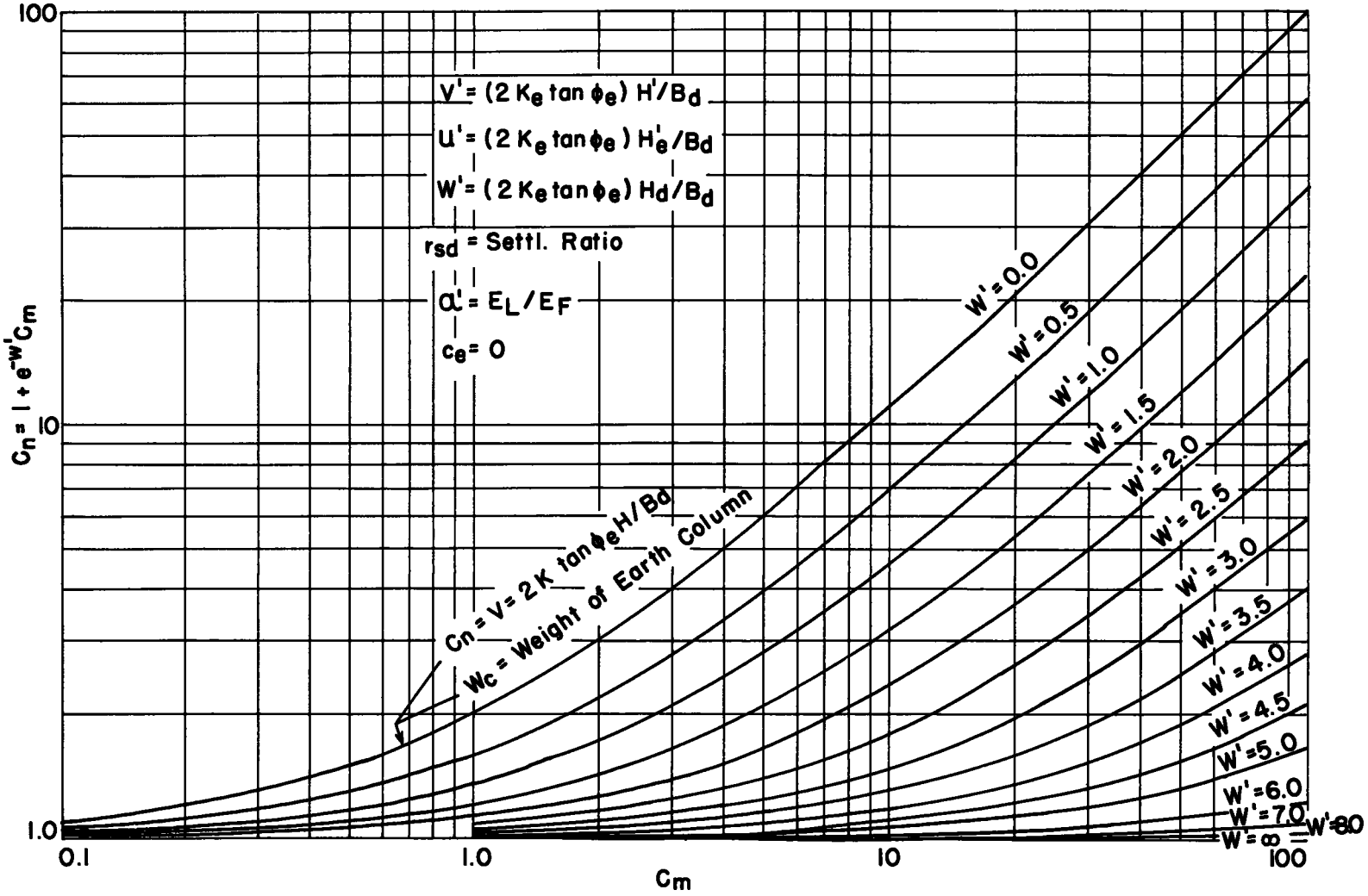
100
10
1.0
0.1
1.0
10
100
$C_n = 1 + e^{-W'C_m}$
C_m
$V' = (2 K_e \tan \phi_e) H'/B_d$
$U' = (2 K_e \tan \phi_e) H'_e/B_d$
$W' = (2 K_e \tan \phi_e) H_d/B_d$
r_{sd} = Settl. Ratio
$\alpha' = E_L/E_F$
$c_e = 0$
$C_n = V = 2K \tan \phi_e H/B_d$
W_c = Weight of Earth Column
W' = 0.0
W' = 0.5
W' = 1.0
W' = 1.5
W' = 2.0
W' = 2.5
W' = 3.0
W' = 3.5
W' = 4.0
W' = 4.5
W' = 5.0
W' = 6.0
W' = 7.0
W' = ∞ = W' = 8.0

Figure D.

Performance Study of Multi-Plate Corrugated-Metal-Pipe Culvert under Embankment - North Carolina

NICHOLAS C. COSTES, Materials Engineer, and
CHARLES E. PROUDLEY, Chief Materials Engineer
North Carolina State Highway and Public Works Commission

● THIS paper consists of a performance study of one of the major drainage structures of North Carolina Project 8521. The project comprises the relocation of a section of US 70 in the western part of North Carolina. It starts at a point on US 70 in Ridgecrest, Buncombe County, N. C. and, following the eastern slope of the Blue Ridge Mountains, extends eastward for a distance of approximately 6. 15 miles to a point on US 70 in Old Fort, McDowell County, N. C. (Figure 1).

The North Carolina State Highway and Public Works Commission deemed the above relocation necessary for the alleviation of a serious bottleneck existing in the main east-west artery between North Carolina and Tennessee through the Smokies. This bottleneck resulted from the 30-year old, obsolete, two-lane section that had accumulated a bad accident record.

The old road was 8 miles long, consisted of 98 curves including many "hairpins," and rose vertically approximately a quarter-mile between the two terminal towns. The new route consists of 19 easy, spiraled curves. It has a continuous climb of 1,326 feet, in 5. 32 miles with a steady grade varying between 1. 905 percent and 6. 000 percent with no adverse grades, to the summit near Ridgecrest.

The location of the new section was the result of many months of field and office work. Reconnaissance surveys were made, soundings with 25 feet maximum depth of penetration were taken, topographical and air maps were studied, and the best alignment was selected among several proposed routes. The new location has a four-lane pavement; it ramps down along the southern slope of Young's Ridge, and cuts cross-drainage all the way. Consequently, the grading pattern is one of filling deep up-valley ravines and cutting down steep intervening knolls or shoulders. Some cuts are over 150 feet deep and some fills are over 200 feet high (Figure 2).

The location cuts through geological formations which are considerably decomposed. The rock formation is rather complex and structurally folded and faulted. However, there is a thin layer of highly weathered igneous material on top with some semi-weathered pockets on the bottom. Chlorite schist, slate, weathered sandstone, and clay minerals are scattered through the area.

The main factors that decided upon the selected location were safe line and grade, distance between terminal towns, and cost. The principal cost factor was considered to be excavation. About 3,000,000 cu. yd. of unclassified excavation was required to complete the project with fills consisting of as much as 800,000 cu. yd. of earthen material, and cuts to match involving as much as 330,000 cu. yd. of excavation. The contract was awarded to W. E. Graham and Sons of Cleveland, N. C. on September 21, 1951 with a bid of $2,301,000 including 2,787,500 cu. yd. of unclassified excavation at 70 cents per cubic yard.

The project was financed entirely by state funds and did not have to conform with Federal-aid standards. This fact enabled the State Highway Commission to insert in the special provisions of the contract the clause that no rolling of fills would be required. End-dumping or other methods of construction requiring different types of machinery could be used. It was believed that on account of the above provision, a considerable saving in the cost of fill construction would result. Furthermore, it was believed that the nature of soils and rock encountered in this project would not impose serious consolidation or slope stability problems. At any rate it was held that the cost of maintenance and repair of fills in the event of slides, non-uniform settlement, and similar problems, would have been less than the extra cost resulting from a layered and rolled fill construction that would compel the contractor to deliver material

by scraper and other equipment down steep haul roads each time. The soundness of this judgment still remains to be proved but at the present time (after two years) appears to be justified.

The construction of earth fills instead of bridges in order to bridge the valleys encountered was favored by financial considerations. With the exception of a reinforced concrete bridge over Mill Creek at Old Fort, and a pedestrian underpass near Ridgecrest, all structures were earth fills whose drainage was provided by corrugated metal culvert pipe. The pipes ranged in sizes from 6-inch diameter for subdrainage through 54-inch diameter and Multi-Plate pipes 60 inches and 66 inches in diameter.

All pipes up to 54 inches in diameter were riveted and bituminous coated in their lower half portion. Pipes between 48 inches and 54 inches in diameter that were installed under high fills were elongated vertically five percent by the manufacturer. To perform this operation, ½-inch rods were factory mounted along the horizontal pipe diameters. Each set of rods was provided with turnbuckles in order that the initial vertical elongation could be released gradually after construction of the fill. Upon completion of the construction of the fills these rods were removed.

Larger culvert sizes up to 66-inch maximums were of field-bolted Multi-Plate type. The installation procedures for such pipes will be discussed in detail in subsequent sections of this paper.

Provisions for Construction of Special Pipe Lines

The special provisions of the contract called for a special installation procedure on ten of the culvert lines through the highest fills (see, typical cross section at Ring 31, Figure 46). The specified pipes were to be installed in trenches cut in the natural ground to the required section, wherever practical, before any fill was placed. When rock, or other conditions made this impractical, excavation was to be larger than the required trench section, the fill placed and thoroughly compacted up to at least two feet above elevation before installation of the pipe; then the trench was cut through the compacted fill and the pipe was installed in the trench. The sides of the trench were to be as nearly vertical as possible and its maximum permissible width was to be 2.5 feet from the sides of the pipe on the larger structural plate pipes and less on smaller size, riveted pipes. The depth of trench was specified to be two feet below the pipe invert unless otherwise specified.

Where pipes were located on fill sections, any unsuitable material found beneath the pipe location was to be removed for a minimum width of one diameter of the pipe on each side of the pipe before the pipe was placed.

Selected backfill material consisting of crusher-run stone ranging in size from 3 inches down was specified to be used for bedding beneath each pipe, and for backfill in the trench around the pipe up to the top of the trench. The foundation material was to be of as nearly uniform density as possible throughout the length of each pipe.

The material for a depth of two feet below the pipe, and upward to a height of about three quarters of the pipe diameter, was specified to be brought up uniformly in layers not to exceed 6 inches in depth, and each layer to be compacted thoroughly by pneumatic tampers.

The material between the top of the compacted section and the top of the trench was to be placed as loosely as possible. Above the top of the trench, the fill material was to be placed and compacted in accordance with the general specification with the exception that no large rocks should be placed above the pipes for a height equal to two diameters of each pipe.

At the upstream end of the fills, adequate provisions were made to prevent water from entering the bedding and backfill material around the pipe. Headwalls were to be constructed as soon as practical after the fills had been brought up to a reasonable height above the top of the headwall elevation.

The foundation for each culvert was graded with a minimum camber of ¼ percent of the pipe length to provide for differential settlement on account of the fill overburden.

Research Project of Station 298+33

The Research Section of the Division of Materials of the North Carolina State High-

Figu

way Commission considered project 8521 one of those infrequent opportunities to secure some valuable data from the performance of flexible culvert pipes installed under high fills. The unorthodox method of fill construction by end dumping was an additional feature which would be of much interest to such investigation. This method had never been attempted before under similar conditions and, therefore, its effect upon the performance of the structures would be worth studying.

To decide upon and plan the procedures and apparatus to be used in connection with this investigation two meetings were held under the sponsorship of the Division of Materials. In both meetings, representatives of N. C. State Highway and Public Works Commission, N. C. State College, the Bureau of Public Roads, and representatives of metal and concrete pipe manufacturers were present to discuss the various research techniques to be followed in connection with this investigation. M. G. Spangler of Iowa State College was retained by the N. C. State Highway and Public Works Commission as consultant for the general research procedures and installations, and Committee D-4 on Culverts and Culvert Pipe of the Highway Research Board sponsored the presentation and publishing the results of the investigation in the form of research papers.

During the first meeting, held in Washington, D. C., January 1952, it was decided that only the performance of the 66-inch Multi-Plate culvert installed at Station 298+33 under approximately 170 feet of earth fill would be studied in detail (Figure 3). It was

1.

also decided that two methods of trenching would be used above and below the center line of the roadway in order that the loading effect and the performance of two separate culvert installations could be investigated and compared.

During the second meeting, held in Asheville, N. C. March 1952, the general outline of methods and apparatus discussed in the first meeting were put into a specific and detailed form.[1] Also, to save in man-hours and equipment, it was decided that only one type of trenching would be used and this would be the "imperfect ditch" method (Spangler, 1946) since the culvert was located on fill section.

During these meetings the importance of placing the fill symmetrically around and over the pipes during construction was stressed several times. All recommendations regarding construction procedures to be followed for the culvert under study and, generally, for all culverts under high fills were made with the understanding that the fill material would be placed above the culverts in approximately horizontal layers in such a manner that the weight of the fill material would be transmitted to the pipes in a vertical direction at all times.[2]

---

[1] See, Culvert Investigation.

[2] In a memorandum submitted to the State Highway Engineer at a later date, the Chief Materials Engineer urged again the adoption of layered fill construction for at least the

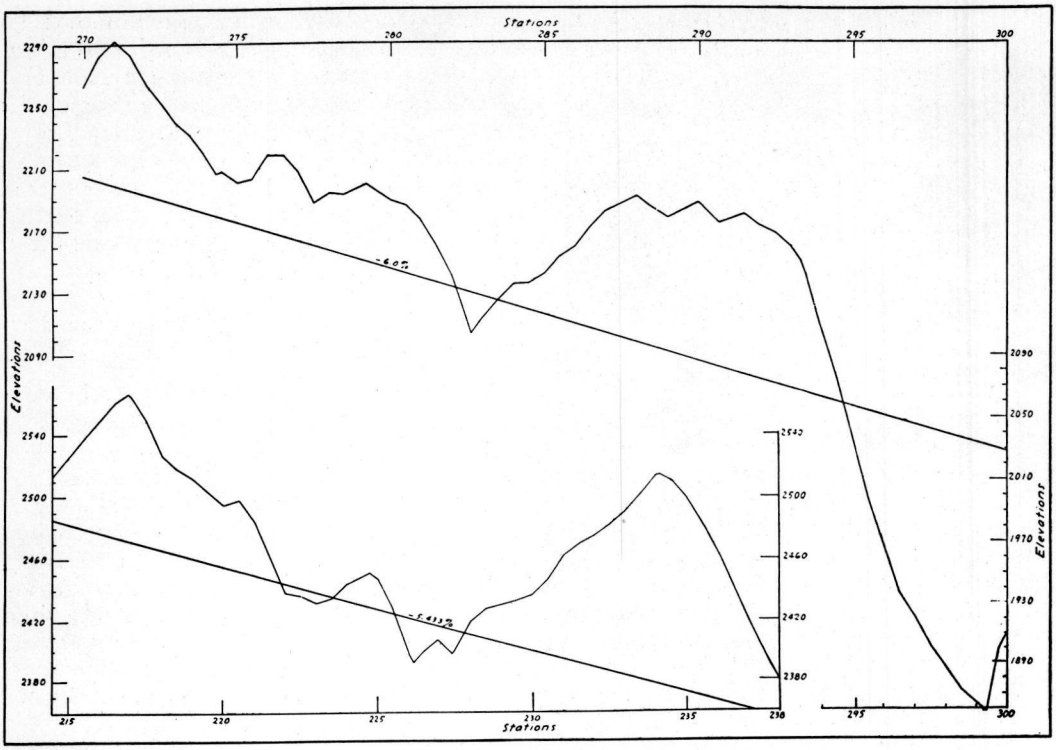

★ Profile at one of largest cuts and deepest fills

Figure 2.

The importance of measuring the external earth pressures around the pipe by direct methods was also stressed at the above meetings. However, no definite method to obtain such information was adopted.[3] Instead, it was decided to evaluate these loads by means of "Marston Theory on Loads on Underground Conduits," and from strain measurements obtained at various points of the pipe structure by means of SR-4 Baldwin strain gages. Such technique, as discussed later in this paper, proved to be very unsatisfactory for this installation.[4]

In addition to the above recommendations, the State Highway Engineer suggested repeatedly that the soil conditions beneath the bedding material of the pipe

Figure 3. Completed fill covering culvert pipe used for experiment.

culvert under study. He recommended as minimum requirements for securing reliable test data, layered and rolled fill construction for a width of at least 50 feet on each side of the pipe center line until the elevation above the pipe line was at least 100 feet. However, the fill was finally constructed by unbalanced end-dumping as described in this paper.

[3] In this paper a testing procedure is proposed for the direct measurement of the pressures exerted by the side supporting material on the sides of the conduit. See, Recommendations.

[4] See, Analysis of Data.

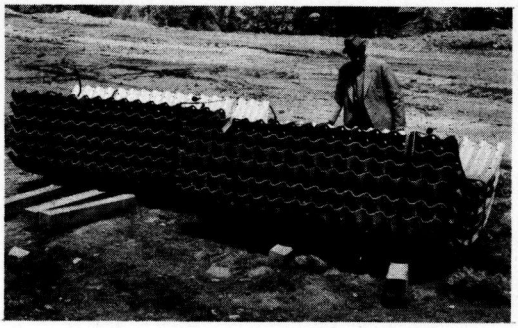

Figure 4. Special bundling of plates on which SR-4 strain gages are attached.

should be identified by whatever method seemed to be most approximate, and if any unsuitable material were found it should be removed immediately and be replaced according to the specifications. Lack of such information together with the adoption of unbalanced end-dumping as the fill construction method, resulted in an earth slide which created a very embarrassing and hazardous situation on the project.[5]

Pipe Installation and Fill Construction at Station 298+33

Earth Slide. The location of the culvert at Station 298+33 with respect to the stream bed that it crosses is shown on Figure 20. The pipe follows a north-south direction; it slopes down from the inlet with a 4.5 percent grade. The fill over the pipe at the center line of the roadway including the temporary bituminous surface-treated gravel surface is approximately 170 feet high.

The culvert is a 66-inch Multi-Plate pipe with 6- by 2-inch corrugations, and consists of 72 rings each 8 feet long having an overall length of 576 feet. It is made of structural steel plate of variable gage. Thusly, 248 feet are made of No. 1 gage, 128 feet of No. 3 gage, and 210 feet of No. 8 gage metal. The No. 1 gage plates have 6 bolts per foot of longitudinal joint, whereas the rest are bolted by the standard 4 bolts per foot of longitudinal joint. No bituminous coating has been applied on the inner surface of the structure because no serious corrosion problems were anticipated on account of the purity of the surrounding water basin.

The pipe plates, stacked and strapped in bundles were shipped by train from Middletown, Ohio to Old Fort, North Carolina. There, they were picked up by trucks and were carried to the job to be assembled according to Armco standard procedures (see Figures 4 through 6).

The pipe after assembly was elongated vertically three percent by field strutting. The struts were 6-inch by 4-foot oak posts set vertical on 3-foot centers for about 345 feet of the central part of the pipe and increasing to 6-foot centers near each end. To distribute the strut load and to minimize any "barn roof" stresses in the structure, 6- by 6-inch oak sills, extending along the whole length of the culvert were placed between the struts and the pipe inner surface: two at the top, and one at the bottom. Furthermore, between the struts and the top sills, 6- by 6- by 18-inch compressible pine caps were placed with their side grain in compression and at right angles to the sills (Figures 7 and 46).

The unit price of pipe including cost of shipment, assembly, vertical elongation by field strutting, placing and compacting of bedding material, tamping of side supporting material, and construction of the imperfect ditch was set as follows:

$58.00 per lin. ft. for No. 1 gage metal.
$55.00 per lin. ft. for No. 3 gage metal.
$45.00 per lin. ft. for No. 8 gage metal.

Despite all previous recommendations, the method of fill construction that was followed after the assembly of the pipe, was very unorthodox although it was not in violation of the special provisions of the contract. Therefore, a detailed description of the various phases of this construction is considered important in order that the reader may appreciate adequately the data from the performance of this culvert, and explain certain deviations from the anticipated results which, otherwise, might have been considered entirely absurd.

The trenching operations for the installation of the pipe and the subsequent backfilling complied with the special provisions of the contract. The pipe was to be installed

[5] See, Earth Slide.

on a fill section. Accordingly, as a first operation, the contractor, by means of a bulldozer, excavated a 12-foot trench along the proposed culvert site and 2 feet below the invert elevation of the pipe as shown in the plans. No borings were taken to investigate the nature of the natural ground underneath to determine whether it would be necessary to remove any unsuitable foundation material as recommended by the special provisions and later by the State Highway Engineer. The trench was refilled with selected backfill bedding material consisting of local soil which came from trenching op-

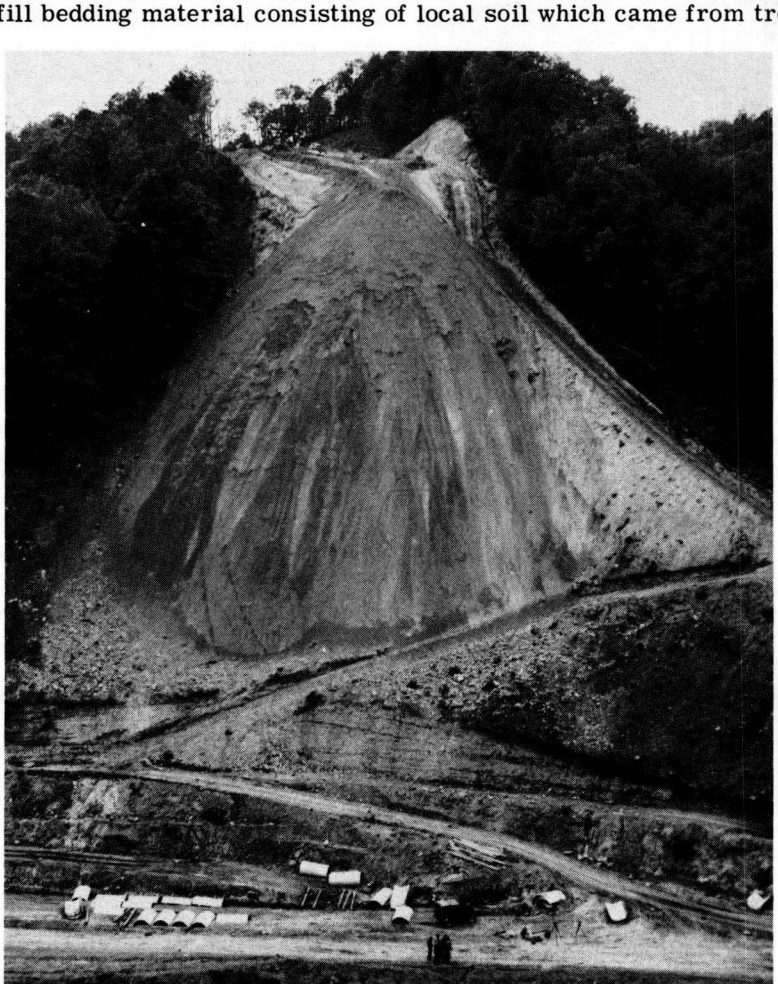

Figure 5. Plate stacking at culvert site. End-dumping operations on western slope are shown in background.

erations on the western mountain slope adjacent and parallel to the pipe line. This material appeared to be clayey in nature, fairly consistent throughout the trench length, and free from 6-inch or larger rock fragments. It was placed and compacted by means of a D-8 bulldozer in layers not exceeding one foot in depth.

As soon as the trench was refilled, a fill was constructed in a like manner and with material from the same source. This fill was brought up 7 feet above the elevation for the pipe invert and extended about 30 feet on each side of the center line of the pipe. Henceforth, the above fill will be referred to as the "initial fill."

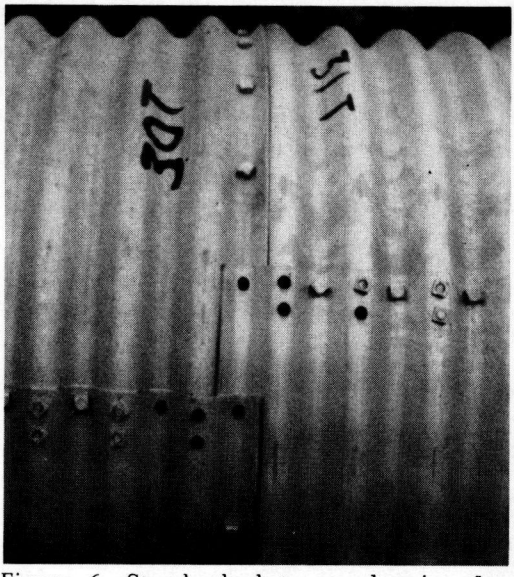

Figure 6. Standard plate overlapping for Multi-Plate culvert pipe.

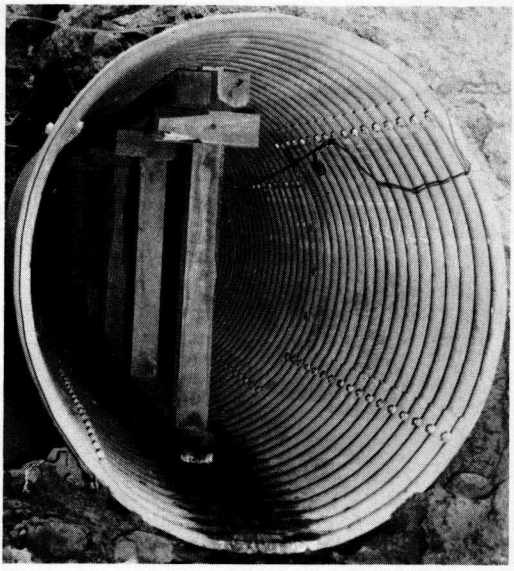

Figure 7. Pipe strutting. Electric line shown is for illuminating pipe interior.

Figure 8. End-dumped material. Toe of western slope.

Upon the completion of the initial fill, a trench was cut according to the specifications, and the contractor started assembling the pipe plates on May 28, 1952. In the meantime, he began to push and end-dump dirt from the western mountain slope using 12-yard pans as soon as operating room was available (Figure 8). This operation, however, caused a load concentration along the slipping planes of an old geological slide. As a result of this load concentration the whole deposit of natural and end-dumped material on the western slope started moving down toward the unfinished pipeline (Figure 9). On or about June 18, 1952, this movement became noticeable from ruptures and cracks formed on each side of the embankment. However, end-dumping on the western slope continued without any balancing operation on the eastern side of the culvert, contrary to all recommendations made in the Asheville meeting and thereafter. Consequently the load on the western slope increased resulting in acceleration of the slide. By that time (June 18) it was noticed that the pipe, which had already been assembled, was slowly raising upward and away from the slide along Rings 36-56 the maximum distortion being at Ring 48 (see Figure 45 Lateral Profile of Pipe Axis. Also, Figures 10-12).

Investigations and tests began immediately to determine the scope and the speed of the movement. Soundings and borings taken immediately adjacent and 50 feet away from the pipe revealed a very wet and unstable condition existing underneath the initial fill between the culvert line and the western slope along the path of the slide. A blue-gray plastic clayey material classified as an A-7-6 material in the Highway Commission's soils laboratory was found predominant in that area. It was decided that this area should be excavated, drained, and backfilled with suitable material, and an appropriate drainage system should be installed with which to intercept the underground water.

The backfill material was brought from the slope where it had caused the slide and was placed in comparatively thin layers by means of tractors and pans. No extra compacting equipment was used. The backfilling operation continued until the elevations

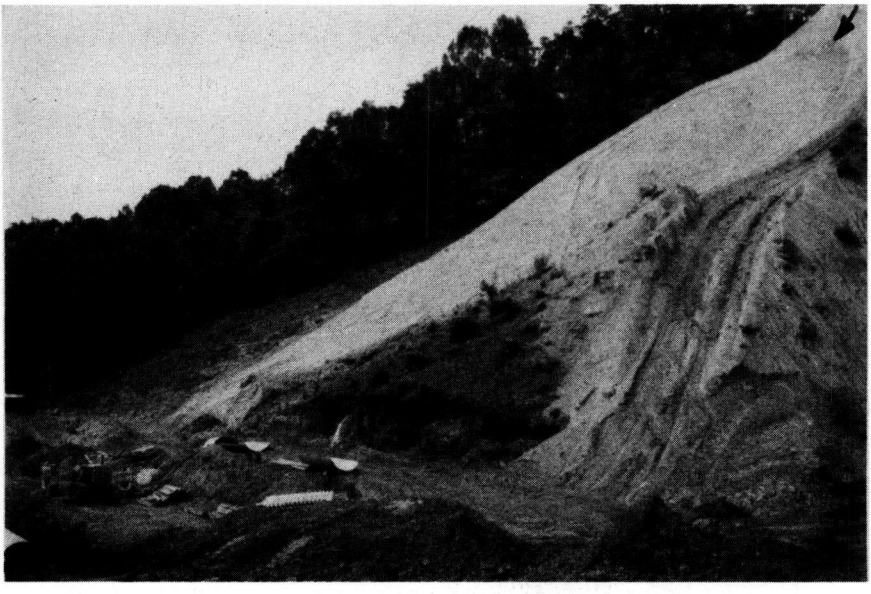

Figure 9. Beginning of slide. Arrow points at trace of failure surface shown clearly on picture.

of the initial fill were reached again and the embankment was as close to the pipe as feasible without interfering with the compaction operations of the side supporting material.

Two 6-inch perforated, corrugated metal pipe drains, extending from Rings 35 through 72, were installed to intercept the underground water and to prevent the backfill material from being saturated. One was placed adjacent to the pipe, and the other 6 feet below the pipe invert elevation and 40 feet west of the pipe center line. These drains were covered with 8-inch to 12-inch concrete sand before backfilling and functioned as planned.

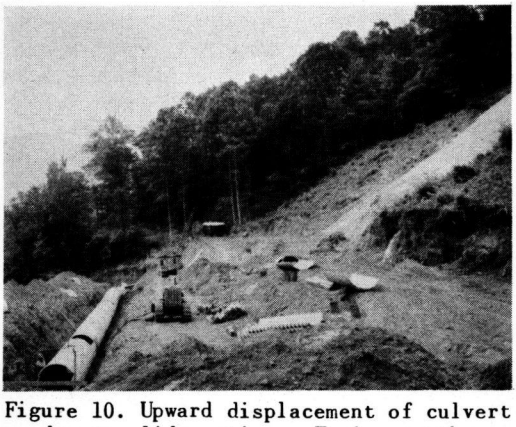

Figure 10. Upward displacement of culvert due to slide action. Facing south.

The material that was removed from the western slope in order to relieve it of the excessive surcharge was deposited on the opposite side of the pipe (Figure 13). By this means the initial fill was widened on the eastern side of the pipe and sufficient resistance was built up to counteract the action of the slide. The pipe itself was

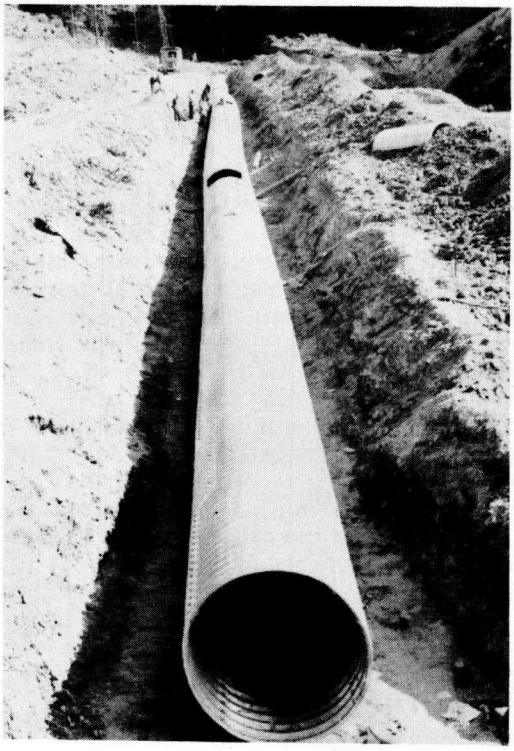

Figure 11. Lateral displacement of culvert due to slide action. Facing north.

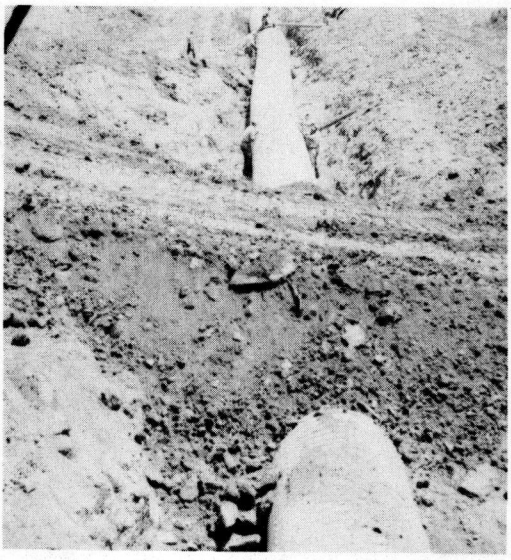

Figure 12. Measuring extent of culvert distortion due to slide action. Facing north.

brought to its original horizontal alignment by means of hydraulic jacks (Figure 14).

The space between the sides of the pipe and the initial fill was backfilled with selected material compacted in 6-inch layers by pneumatic tamping up to a height equal

Figure 13. Removing slide material from immediate vicinity of culvert. Facing north.

to ¾ of the pipe diameter. From this point up to 2-foot elevation above the pipe backfilling was done by means of a motor grader blade running parallel to the center line of the pipe and depositing material from the western slope in a rather loose condition. The remaining part of the trench was backfilled with pans and tractors depositing material in 1-foot lifts. (See Typical Cross Section, Figure 46). The fill was then brought up uniformly to about 8 feet above the top of structure.

Figure 14. Culvert realignment after removal of slide material.

The next operation was to cut the "imperfect ditch" section above the top of the pipe. This was performed by means of a dragline moving along the center line of the pipe and depositing the excavated material on the sides of the ditch (Figure 15). No ditched section was dug between Rings 60 and 72. After the settlement cells were installed, (see Apparatus and Experimental Procedure), the imperfect ditch was backfilled by means of a dragline bucket dragging the excavated material slowly and loosely back into the ditch until it was completely filled (Figure 16). This method was followed along Rings 29 through 49. Other sections of the imperfect ditch were backfilled immediately after the ditch was dug by redepositing the excavated material as loosely as possible. Upon completion of the "imperfect ditch," the whole fill area was dressed by means of a No. 12 motor grader care being taken not to compact the area immediately over the pipe (see Figure 45, Fill Profiles 7-11-54).

Concurrently with the above mentioned operations the contractor continued end-dumping fill material from the western slope concentrating his efforts away from

Figure 15. Cutting the imperfect ditch section on top of pipe. Facing north.

the slide area and toward the upstream sections of the pipe. He also began to deposit fill material from the east with the intention of building a ramp over the pipe so that he would not have to reverse the hauling equipment after dumping (Figure 17). The construction of a ramp would also result in a more balanced distribution of the load on the pipe because the end-dumped material would not be deposited on the sides of the pipe but along a direction parallel to the pipe axis. Therefore, the resultant force on top of the pipe would also lie on a plane parallel to the pipe axis and even if it were not vertical it would not throw the culvert out of alignment as previously happened with the slide.

The first lift of 18 feet was brought in from the east between Rings 15 and 37 and

extending over and 30 feet beyond the culvert line. This operation was completed by August 1, 1952. In the meantime another 12-foot lift began and advanced from the east and in the approximate path of the previous lift. This lift was carried over to Station 297+90 (43 feet beyond the pipe line) and extended from Rings 14 through 16 (see Figure 45, Fill Profiles, 8-7-52).

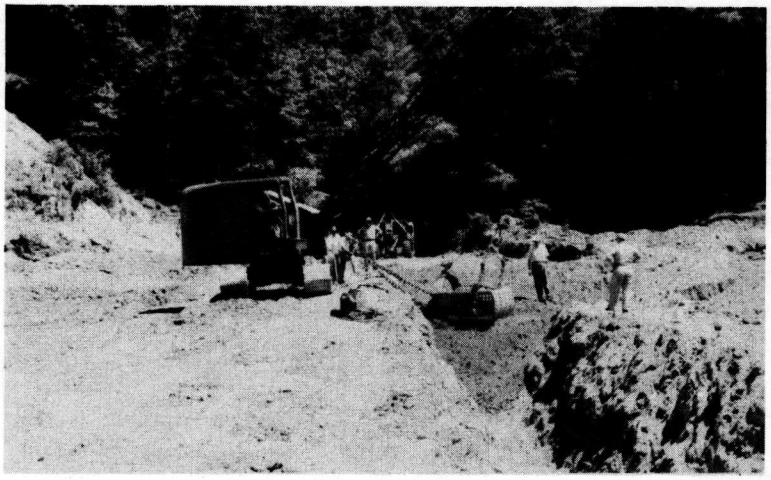

Figure 16. Refilling the imperfect ditch section with loose material. Facing north.

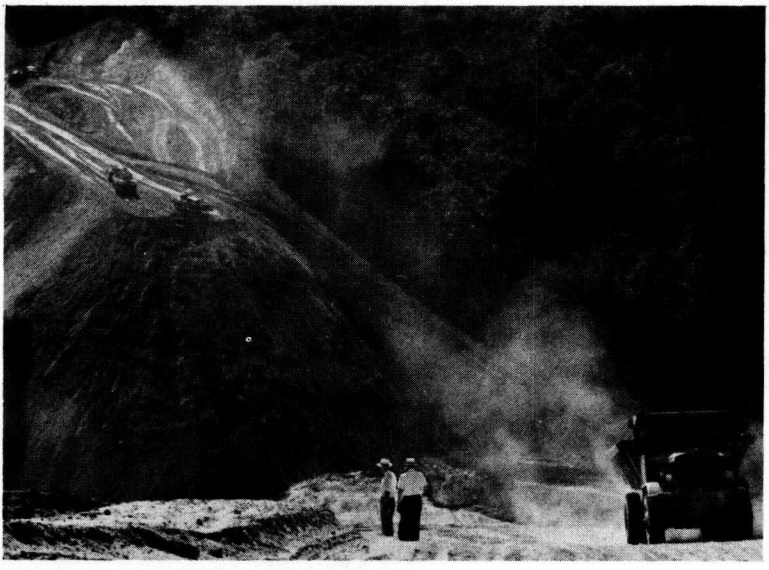

Figure 17. Construction of ramp by end-dumping from both eastern and western slopes. Facing west.

After the second lift had reached a height of approximately 50 feet above the top of the structure between Rings 12 and 32, bulldozers were used to push and end-dump material from this newly constructed embankment on to the western slope until the ramp between the eastern and western slopes was completed (see Figure 45, Fill Profiles, 8-14-52). At this point it was decided that the load on the pipe was again being unevenly distributed because in the construction of the ramp, the first half of the culvert was supporting approximately 50 feet of dirt whereas the second half had only the original

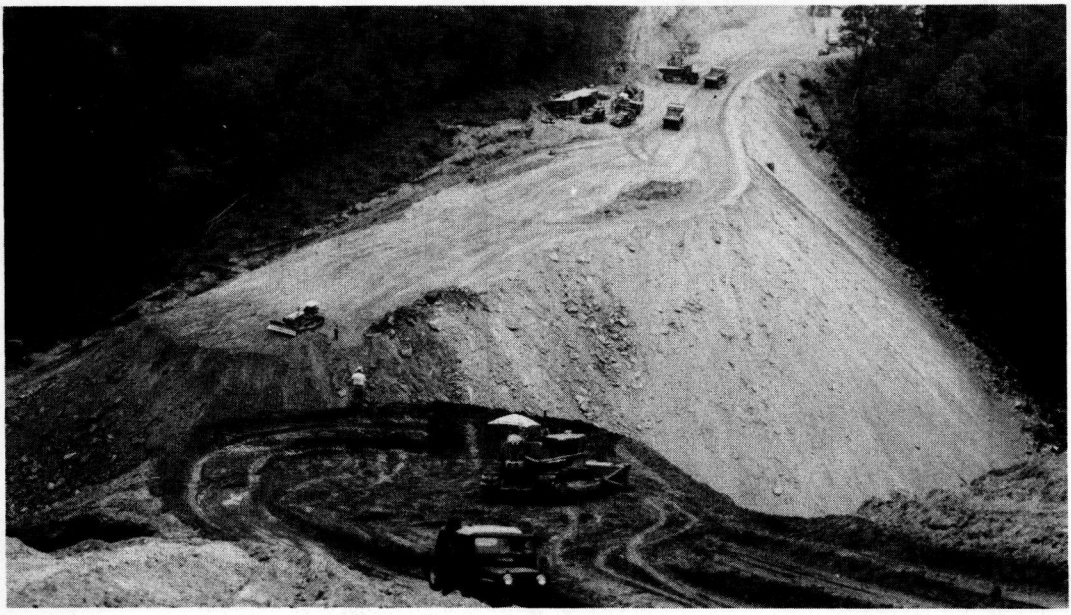

Figure 18. Approaching completion of second ramp. Material is being end-dumped from all sides of fill. Facing east.

8 feet of embankment that was deposited during the construction of the imperfect ditch. Therefore, a 21-foot lift approximately 60 feet wide was next centered over the pipe beginning at Ring 32 and end-dumping from the sides of the ramp and at a direction parallel to the pipe axis as far as Ring 64. Gradually, the western toe of this lift and the toe of the end-dumped embankment at the western slope met and overlapped each other in successions until the southern slope of the ramp was approached.

The above operation was completed about August 24, 1952. In the meantime a 25-foot lift had already begun from the east and was well under way when the 8-28-52 data were taken (see Figure 45, Fill Profiles). As soon as this section was completed so as to allow two-way traffic, a new 22-foot lift was started, extending from roadway Stations 298+00 to 298+60 over Rings 12 to 60 (see Figure 45, Fill Profiles, 9-16-52). The material for this section came from cuts on both ends of the fill. At this stage of construction the method of load application was considered not to have any serious effect on the culvert structure. However, one more lift forming a sort of new ramp was brought from the west (Figure 18, see also Figure 45, Fill Profiles, 10-21-52).

From the above point until the completion of the fill, material was deposited on top of the fill and, subsequently, was being end-dumped over the fill sides in whatever manner was considered most appropriate to facilitate the work (Figure 19). Most of this fill material came from the west by means of 18 cu. yd. Euclids or side dump trucks, and it was pushed over into place by bulldozers and gravity.

The fill reached its highest portion during the latter part of March, 1953. On April 10, 1953 the struts were removed by means of a wire rope looped around a group of struts each time and then pulling the rope with a bulldozer equipped with a winch. The pipe did not deform appreci-

Figure 19. Final stages of end-dumped fill construction. Dressing of fill slopes. Facing west.

ably upon the removal of struts (see Obtained Data, Figures 53-57).

CULVERT INVESTIGATION

Object of Investigation

The experimental procedure adopted at the Asheville, N. C. meeting sought the following objectives:

A. To study the performance of the culvert from a structural capacity point of view. To achieve this purpose three main categories of data were to be collected, namely:

1. Data from the environmental conditions under which the pipe was installed. These conditions included the nature and compaction of the earthen material employed and the methods of pipe installation and fill construction.

2. Data from the settlement and deformations of the bolted structure. Such data would be collected along directions parallel and perpendicular to the longitudinal axis of the pipe as well as in a radial manner.

3. Data from the external pressures generated around the pipe structure during and after the construction of the fill.

B. To ascertain the validity of "Marston Theory on Loads on Underground Conduits," as well as Spangler's "Iowa Formula" for lateral deflection of flexible culvert pipes if applied on high fill installations and under conditions similar to those encountered on Project 8521.

C. To draw conclusions relative to the adequacy and economy of the design of the culvert under study, and to make recommendations for future installations under similar conditions.

D. To make recommendations for future research procedures aiming to further the present knowledge on underground conduits.

Apparatus and Experimental Procedure

To obtain the objective outlined under Object of Investigation, it was decided that in general:

Data from the nature and condition of the soil surrounding the pipe would be obtained from as many points as necessary to form a clear overall picture of the encountered earth mass.

Measurements from the settlement and deformations of the pipe would be taken at the center of every fourth ring, or every 32 feet.

Strain measurements would be obtained by means of strain gages at Rings 31, 37 and 55 (Figures 20 and 21). The first two rings are located under and on either side of the centerline of the roadway, which is above Ring 34, and, consequently, they are situated under the heaviest portion of the fill. Ring 54 is about midway from the roadway centerline to the downstream toe of the fill and under approximately 84 feet of fill.

Settlement cells to measure the relative settlement of the loose to the compacted mass above the pipe would be installed on both sides of the roadway centerline, i. e., at Rings 30, 31, 32 and 36, 37, 38 (Figures 20 and 21).

In order that the various measurements could be obtained, the pipe interior was illuminated by electric lights strung on an electric line run along the whole length of the pipe. Telephone communication was also established by a similar telephone line. The power was provided by a gasoline driven portable generator placed outside the pipe.

To obtain data from the environmental conditions under which the pipe was installed, the following operations were performed:

1. Four permanent bench marks were set on the longitudinal centerline, extended, of the culvert; one 10 feet and another 150 feet upstream from the inlet and the same downstream from the outlet. The monuments at 10 feet were set with their tops at about the elevation of the flow line of the pipe extended. These monuments were made of concrete posts 6-inch by 6-inch at the top and 8-inch by 8-inch at the bottom. They were tied in both laterally and vertically with other bench marks and reference points located a considerable distance from the toe of the slope. The distances between the monuments were accurately measured after the culvert trench was excavated and before the pipe was erected.

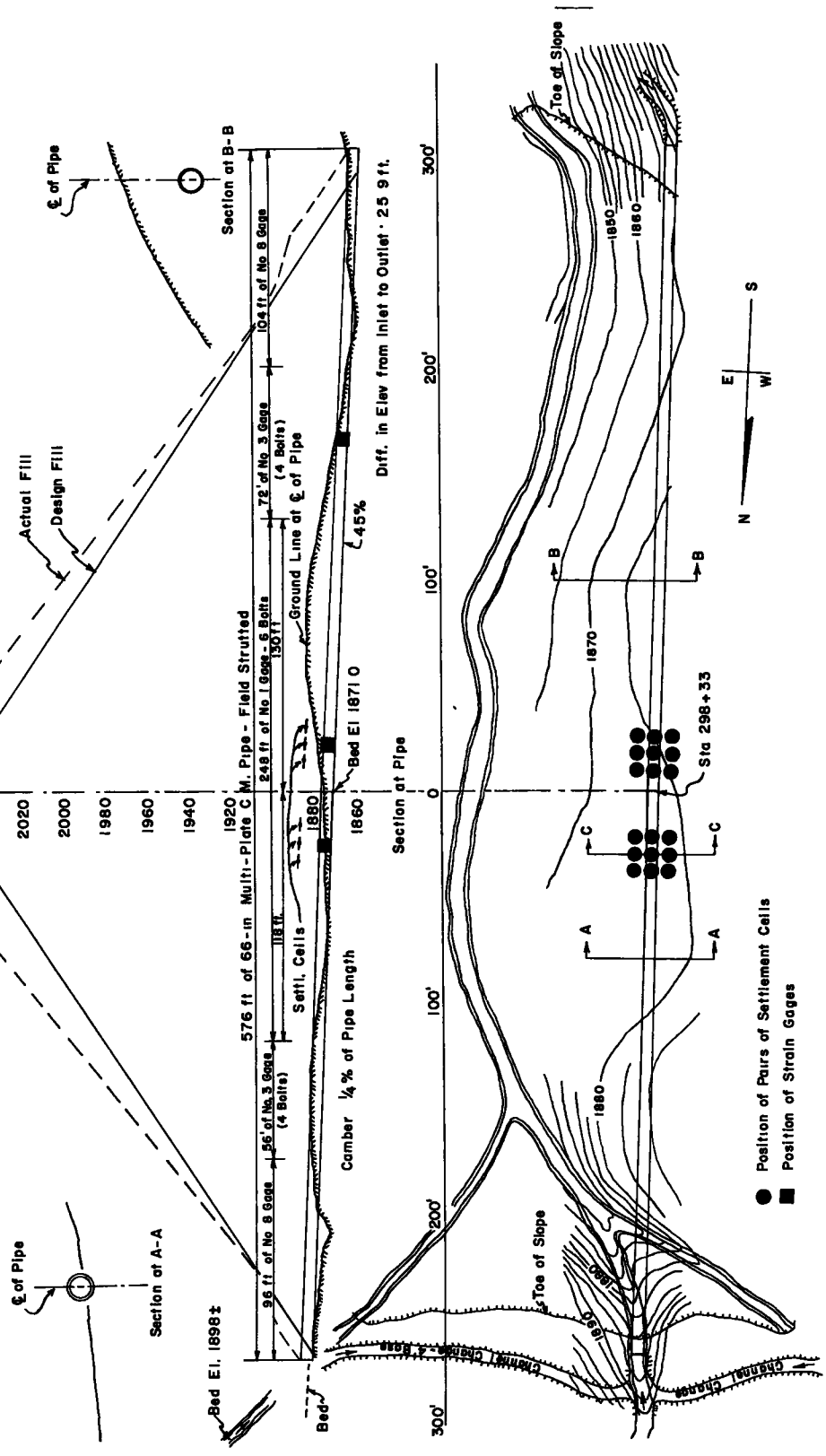

Figure 20. Fill-culvert site and installation.

2. Longitudinal profile was run along the centerline of the culvert on the natural ground before any excavation began. Transverse cross sections were taken from the profile line and were extended about 50 feet on each side. These sections were taken at the ends of the culvert and at the center of Rings 30, 31, 32 and 36, 37, 38 where settlement observations were to be made. Additional profiles and cross sections were obtained at the same stations after benching of the side hill, placement of the initial fill, excavation of the culvert trench, after refilling of the bedding material, at intervals during the construction of the fill, before and after removal of struts, and at time intervals increasing geometrically thereafter.

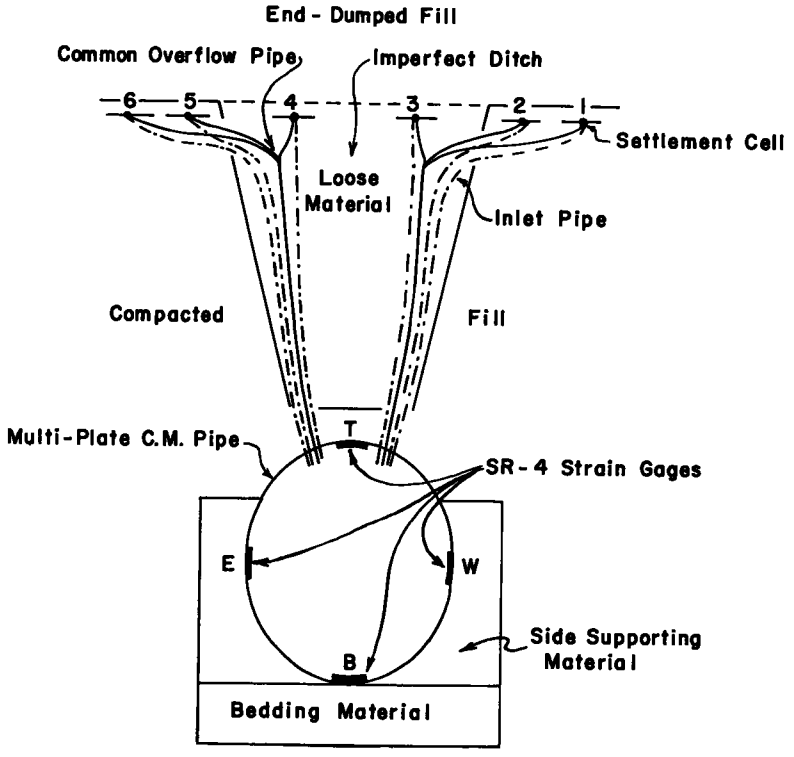

Figure 21. Schematic diagram through Section C-C of Figure 3 showing settlement cell and strain gage installation after the removal of struts.

3. A complete photographic record of all phases of the project was made. Two 16mm color films have been made also by the Photographic Section of the Division of Materials. The first film gives an account of the pipe installation, the fill construction, and the various testing procedures with the apparatus used. The second film shows the complete operation of obtaining soil samples from the material furnishing side support to the pipe a year and a half after the completion of the fill.

4. Copious notes were kept of any unusual developments. As it was not possible to anticipate what might happen, field parties made frequent inspections of the pipe to observe any phenomena as soon after they occurred as possible.

5. Soil identification and density tests were made of the soil bedding material, the initial fill material, the loose material placed in the "imperfect ditch" and the pneumatically tamped material on each side of the pipe (see Data, Figure 47). A standard field density apparatus was used employing the "balloon" method of volume determination. No density tests were made of the fill material, therefore its unit weight for the subsequent computations had to be guessed from previous experience and from the general nature of the material encountered.

6. Data from the present condition of the side supporting material. A year and a

Figure 22. Forcing the sampling device into the side supporting material by means of a mechanical jack.

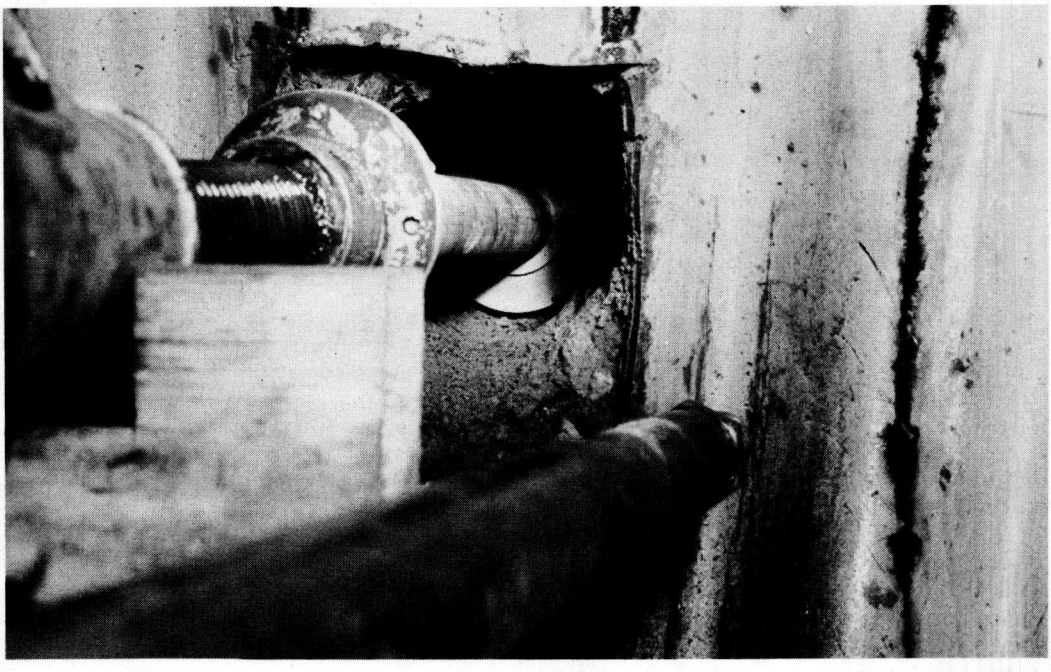

Figure 23. The sampling device forced into the side supporting material to obtain the second soil sample from this opening.

half after the completion of the fill the Research Section of the Division of Materials decided to conduct a new series of tests on the pipe which had not been discussed at the Asheville meeting. The purpose of these tests was to ascertain the current condition and physical properties of the side supporting material. For this purpose 8- by 8-inch square sections were removed from the inner surface of the structure at alternate sides of Rings 8, 16, 24, 34, 44, 45, 56 and 64 (see Data, Figure 48). To remove these sections, an electrically driven drill and a power saw were used. Through these openings, a sampling device specially designed in the research laboratories of

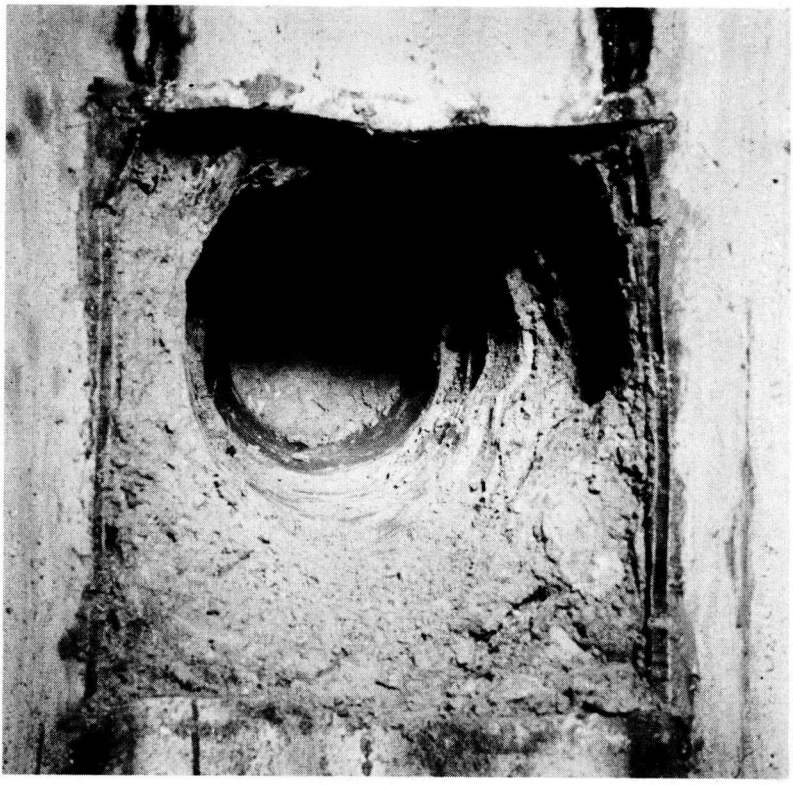

Figure 24. Space left upon the removal of second sample. At a later date these spaces were filled with soil and grout. Opening in pipe was made by an electric drill and a power saw.

the N. C. State Highway Commission, was forced into the soil mass abutting the pipe by means of a mechanical jack (see Experimental Setup, Figures 22-24). The sampling device consisted of three steel cylindrical compartments threaded onto each other: the cutting part, the main chamber, and the tail compartment (Figure 25). The device was designed in such a way that each time it was forced into the soil mass an undisturbed[6] sample with dimensions identical to those of a standard Proctor mold was secured. To obtain a sample the device was forced carefully into the soil mass until the in-coming soil core was well inside the tail compartment. The device was then pulled back, the cutting and the tail parts removed from the main chamber and the protruding parts of the soil core were trimmed down to the edges of the main chamber by means of a wire saw and a spatula (Figures 26 and 27). Thus, the soil sample in the main chamber assumed the dimensions of a standard Proctor mold. The samples were weighed in situ, their wet density in pcf. was determined and after copious notes were recorded pertaining to their general appearance, they were placed in containers and carried to the soil laboratories of the State Highway Commission where they were

[6]The term "undisturbed" here denotes undisturbed from the in situ conditions.

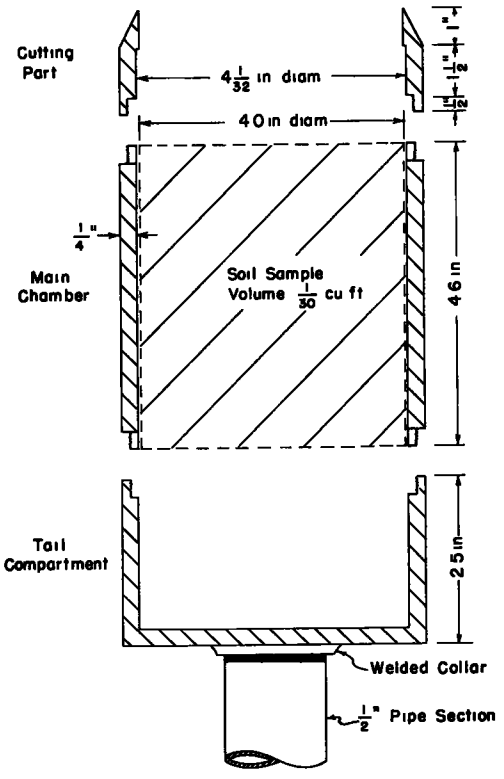

Figure 25. Sampling device.

analyzed and classified (see Data, Table 4). By obtaining as many samples as possible from each position, the variations in density, moisture, and physical properties of the side supporting material were obtained along directions perpendicular to the longitudinal axis of the pipe. Samples were obtained from positions extending as far as 5 feet from either side of the structure (see Data, Figure 48). These tests were run for later correlation with another series of tests designed by the Research Section to ascertain the existing lateral pressures mobilized against the pipe by the side supporting material. The latter tests have not been run yet but the proposed procedure and apparatus are presented below in this paper (see Recommendations).

To collect data from the settlements and deformation of the bolted-plate structure, the following operations were performed:

1. Settlement of the pipe invert was measured by running flow line profiles at periodic intervals (see Data, Figure 28, also Figure 52). In order that these readings be made before the removal of struts, a short rod with goose neck offset at bottom and equipped with leveling rods and a target was used. Readings were made to 0.01 foot.

2. Changes in the pipe diameter were measured by means of an extensometer (Figure 29). This apparatus consists of a calibrated cylindrical steel rod with conical shaped ends; its length was adjustable in a telescopic manner. Measurements of diameters were taken at prespecified intervals at the middle of each selected ring (see Data, Figure 53). To measure the vertical diameters, the extensometer was mounted

TABLE 1

MECHANICAL ANALYSIS AND PHYSICAL CHARACTERISTICS OF MATERIAL PASSING NO. 40 SIEVE OF BEDDING, BACKFILL, AND "IMPERFECT DITCH" MATERIAL

Position	Ring No Indicating Locations Represented in Composite Sample from Respective Position	Particles larger than 2 0mm Ret. #10	Particles less than 2mm (percent by wt) Soil Mortar - 100% Coarse Sand 2.0 to 0.25mm Ret #60	Fine Sand 0.25 to 0.05mm Ret. #270	Silt 0.05 to 0.005mm	Clay Smaller than 0.005mm Passing #270	Passing No 200 Sieve	Passing No 40 Sieve	LL	PI	O M C %	γ_{Pr} pcf	s_s	Soil Classification
1	8, 12, 24, 32	8	22	18	31	29	65	85	39	13	16 1	113.0	2 63	A-6(7)
	16, 20, 28, 31	9	23	20	29	28	63	84	36	10	15 7	114 0	2 63	A-4(6)
	36, 38, 48, 52	1	25	20	29	28	61	84	38	9	16 6	112 0	2 64	A-4(5)
2	24, 28, 31, 36, 38, 48, 52	0	24	23	31	22	59	85	28	N P	14 8	115 0	-	A-4(5)
1 & 2	20, 32, 33, 55	1	23	20	29	28	61	85	38	13	12.5	117 3	-	A-6(6)
	37, 40	3	29	20	27	24	57	78	36	9	13 6	113 6	-	A-4(4)
	56, 60, 68	3	26	21	30	23	59	82	39	10	15 4	111 8	-	A-4(5)
	56, 60, 64, 68	4	25	20	28	27	60	84	37	9	16 6	112 2	2 64	A-4(5)
3	8, 12, 16	2	23	17	32	28	64	84	42	14	15 5	113 7	-	A-7-6(8)
	20, 24, 28, 30, 32	3	23	17	31	29	64	84	40	15			-	A-6(8)
	36, 37, 38, 40, 44	4	21	16	33	30	67	85	41	15	15 2	111 4	-	A-7-6(9)
	48, 52, 55, 56, 60, 64, 68	3	21	16	31	32	67	85	46	17	110 4	17 4	-	A-7-6(10)
	58	2	27	16	30	27	61	81	39	12	-	-	-	A-6(6)
4	24, 28, 30, 31	2	25	22	28	25	59	83	26	N P			-	A-4(5)
	32, 36, 37, 38	2	26	26	30	18	54	83	30	N P			-	A-4(4)
	40, 44, 48, 52, 60	3	25	24	33	18	56	84	28	N P			-	A-4(4)
5	24, 28, 30, 31, 32	4	24	23	30	23	59	85	28	N P			-	A-4(5)
	36, 37, 38, 40, 56	2	24	27	31	18	54	86	28	N P	15 3	110 7	-	A-4(4)
	44, 48, 52, 55, 60	5	26	25	30	19	55	86	29	N P			-	A-4(4)
6	30, 31, 32, 36, 37	4	26	26	29	19	53	84	29	N P			-	A-4(4)
	20, 38, 44, 48, 55	5	28	24	28	20	53	82	28	N P			-	A-4(4)
7	30, 31, 32, 36, 37, 38	5	26	22	31	21	47	83	36	7			-	A-4(2)

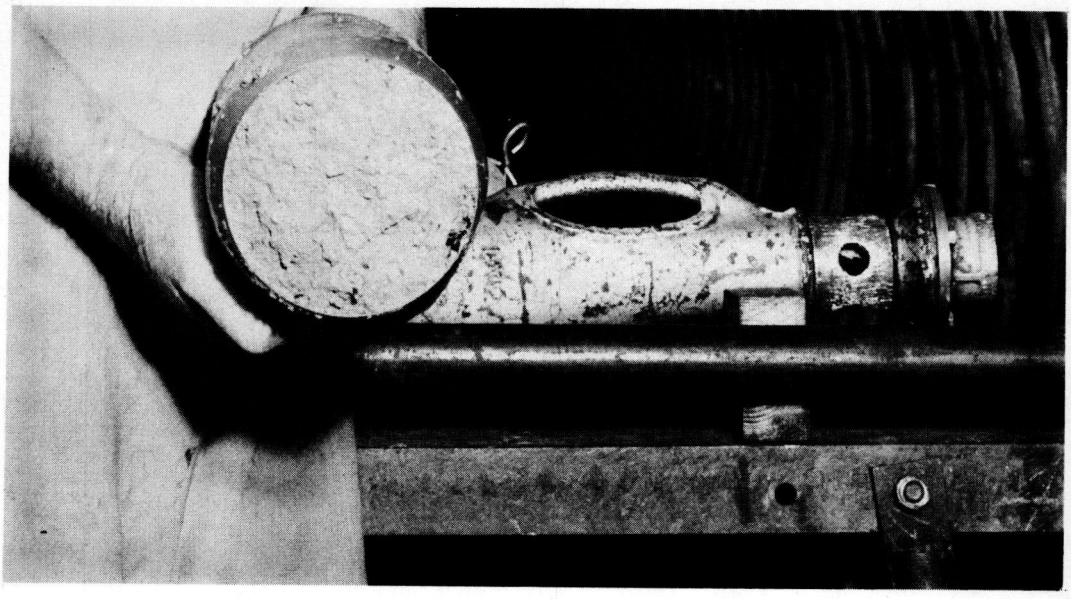

Figure 26. Sampling device with soil sample just removed from jacking apparatus.

TABLE 2

COMPACTION CHARACTERISTICS OF BEDDING, BACKFILL, AND IMPERFECT DITCH MATERIAL DURING CULVERT INSTALLATION

Ring No.	Position 1							Position 2							Position 3						
	Ym pcf.	w %	Yo pcf.	O. M. C. %	YPr. pcf.	% Compact.	e	Ym pcf.	w %	Yo pcf.	O. M. C. %	YPr. pcf.	% Compact.	e	Ym pcf.	w %	Yo pcf.	O. M. C %	YPr. pcf.	% Compact.	e
8	139.2	11.7	124.6	12.5	117.3	106.2	0.320								109.8	17.16	93.72	15.5	113.7	82.4	0.755
12	132.7	14.6	115.8	12.5	117.3	98.7	0.421								122.8	16.95	105.0	15.5	113.7	93.2	0.567
16	139.5	10.4	126.4	12.5	117.3	107.8	0.301								123.4	17.0	105.5	15.5	113.7	92.8	0.559
20	141.5	14.0	124.1	14.8	115.0	107.9	0.326	130.3	13.75	114.5	12.5	117.3	97.6	0.437	121.2	16.2	104.3	15.5	113.7	91.7	0.577
24	137.5	14.8	119.8	14.8	115.0	104.2	0.373	129.5	13.2	114.4	14.8	115.0	99.5	0.438	128.0	17.15	109.3	15.5	113.7	96.1	0.505
28	130.6	13.95	114.6	14.8	115.0	99.7	0.435	125.1	11.8	111.9	14.8	115.0	97.3	0.470	125.8	15.05	109.3	15.5	113.7	96.1	0.505
30	-	-	-	-	-	-	-	-	-	-	-	-	-	-	120.3	17.40	102.5	15.5	113.7	90.1	0.605
31	132.0	13.7	116.1	12.5	117.3	99.0	0.417	129.8	-	-	14.8	115.0	-	-	-	-	-	-	-	-	-
32	124.8	15.95	107.6	12.5	117.3	91.7	0.529	134.7	13.7	118.5	12.5	117.3	101.0	0.388	123.9	16.8	106.1	15.5	113.7	93.3	0.550
33	119.2	14.6	104.0	12.5	117.3	88.7	0.581	124.4	15.4	107.8	12.5	117.3	91.9	0.525	-	-	-	-	-	-	-
36	125.7	-	-	14.8	115.0	-	-	121.8	12.1	108.7	14.8	115.0	94.5	0.513	138.1	16.2	118.8	15.2	111.4	106.6	0.385
37	128.4	14.7	111.9	14.8	115.0	97.3	0.470	125.3	12.7	111.2	14.8	115.0	96.7	0.479	115.6	18.3	97.72	15.2	111.4	87.7	0.683
38	131.4	12.75	116.5	16.6	112.2	103.8	0.412	114.7	12.7	101.8	14.8	115.0	88.5	0.616	102.2	17.70	86.83	15.2	111.4	77.9	0.895
40	133.3	15.0	115.9	16.6	112.2	103.3	0.419	126.8	17.0	108.4	16.6	112.2	96.6	0.518	107.1	17.15	91.42	15.2	111.4	82.1	0.799
44	125.0	15.5	108.2	-	-	-	-	127.1	16.6	109.0	16.6	112.2	97.1	0.509	121.1	18.8	101.9	15.2	111.4	91.5	0.614
48	127.4	13.3	112.4	16.6	112.2	100.2	0.464	122.4	-	-	14.8	115.0	-	-	120.4	19.0	101.2	17.4	110.4	91.7	0.625
52	131.5	12.4	117.0	14.8	115.0	101.7	0.406	115.2	-	-	14.8	115.0	-	-	123.2	19.4	103.2	17.4	110.4	93.5	0.593
55	126.8	14.5	110.7	12.5	117.3	94.4	0.486	115.8	13.3	102.2	12.5	117.3	87.1	0.610	109.6	20.0	91.33	17.4	110.4	82.7	0.801
56	130.0	15.0	113.0	16.6	112.2	100.7	0.456	120.8	16.9	103.3	16.6	112.2	92.1	0.592	117.5	19.3	98.49	17.4	110.4	89.2	0.670
60	133.8	15.3	116.0	16.6	112.2	103.4	0.418	(159.0)	14.5	(138.9)	16.6	112.2	(123.8)	(0.184)	121.0	18.35	102.2	17.4	110.4	92.6	0.610
64	127.5	15.2	110.7	16.6	112.2	98.7	0.486	125.2	16.9	107.1	16.6	112.2	95.5	0.536	117.8	17.05	100.6	17.4	110.4	91.1	0.635
68	122.3	15.9	105.5	16.6	112.2	94.0	0.559	113.8	19.3	95.39	16.6	112.2	85.0	0.724	116.0	17.55	98.68	17.4	110.4	89.4	0.667

Ring No.	Position 4 (s_s = 2.636)							Position 5				
	Ym pcf.	w %	Yo pcf.	O. M. C. %	YPr. pcf.	% Compact.	e	Ym pcf.	w %	Yo pcf.	O. M. C. %	YPr. pcf.	% Compact.	e
24	97.4	10.7	87.99	15.3	110.7	79.5	0.870	113.5	11.15	102.1	15.3	110.7	92.2	0.611
28	116.3	13.4	102.6			92.7	0.603	109.7	13.65	96.52			87.2	0.704
30	113.2	12.0	101.1			91.3	0.627	109.4	11.8	97.85			88.4	0.681
31	104.1	10.55	94.17			85.1	0.747	104.1	10.2	94.46			85.3	0.741
32	111.3	10.1	101.1			91.3	0.627	102.9	11.15	92.58			83.6	0.777
36	110.4	10.75	99.68			90.0	0.650	107.5	11.75	96.20			86.9	0.710
37	108.1	13.85	94.95			85.8	0.732	117.9	11.45	105.8			95.6	0.555
38	114.8	11.2	103.2			93.2	0.594	111.5	11.4	100.1			90.4	0.643
40	110.4	12.15	98.44			88.9	0.671	110.8	11.05	99.77			90.1	0.649
44	111.4	11.75	99.69			90.1	0.650	118.0	12.30	105.1			94.9	0.565
48	93.4	13.55	82.25			74.3	0.997	97.0	12.0	86.61			78.2	0.899
52	108.8	13.2	96.11			86.8	0.712	99.6	12.70	88.38			79.8	0.861
55	-	-	-			-	-	102.8	11.15	92.49			83.6	0.779
56	-	-	-			-	-	117.3	12.65	104.1			94.0	0.580
60	87.3	12.15	77.84			70.3	1.11	119.9	12.80	106.3			96.0	0.548
	Sample No. 6							Sample No. 7						
20	105.0	15.30	91.07	15.3	110.7	82.3	0.806				15.3	110.7		
30	100.0	10.25	90.70			81.9	0.814	89.4	11.95	79.86			72.1	1.06
31	91.3	11.05	82.22			74.3	1.00	74.3	12.15	66.25			59.8	1.48
32	101.3	11.90	90.53			81.8	0.817	86.1	11.60	77.15			69.7	1.13
36	104.3	9.90	94.90			85.7	0.733	84.4	11.95	75.39			68.1	1.18
37	112.5	10.5	101.8			92.0	0.616	59.4	12.55	52.78			47.7	2.12
38	89.9	11.4	80.70			72.9	1.04	72.1	13.25	63.66			57.5	1.58
44	109.4	11.35	98.25			88.8	0.674							
48	112.4	11.5	100.8			91.1	0.632							
55	110.8	12.65	98.36			88.9	0.672							

Note: $s_s = 2.636$

$$\gamma_o = \frac{\gamma_m}{1+w}$$

$$e = \frac{\gamma_w s_s}{\gamma_o} - 1$$

Where: s_s = Specific gravity of solids.
γ_m = Wet unit weight in lb. per cu. ft.
γ_o = Dry unit weight in lb. per cu. ft.
γ_w = Unit weight of water = 62.4 lb. per cu. ft.
$\gamma_{Pr.}$ = Max. dry unit weight, obtained from Standard Proctor Compaction Test.

w = Water Content, %
O. M. C. = Optimum Moisture Content
e = Void Ratio

TABLE 3

MECHANICAL ANALYSIS OF SIDE-SUPPORTING BACKFILL MATERIAL

Ring No.	Side	Depth in.	Total Passing 1 in. %	Total Passing ½ in. %	Total Passing No. 4 %	Total Passing No. 10 %	Total Passing No. 40 %	Total Passing No. 200 %	Soil Mortar - 100% Coarse Sand Ret. #60	Fine Sand Ret. #270	Silt Passing No. 270	Clay Passing No. 270
		6			100	97	84	60	23	21	32	24
8	E	15			100	94	86	62	21	21	33	25
		24			100	93	82	60	24	21	32	23
		6			100	83	84	59	22	23	34	21
16	W	15			100	86	84	60	23	22	34	21
		24			100	96	82	58	25	23	34	18
		9	100	96	91	86	72	55	23	16	36	25
		15	100	98	93	79.5	68	53	21	17	37	25
		21	100	97	93	88	74	58	21	17	35	27
24	E	28	100	99	95	88	77	58.5	19	19	38	24
		34	100	99	96	84	72	54	21	20	32	27
		42	100	99.5	97.5	89	75	57	24	17	34	25
		50	100	97	94	86	71	54	22	18	33	27
		Overall				100	84	64				
		9			100	88	70	45	30	23	32	15
		15			100	89	74	47	26	26	33	15
		21			100	87	71	47	27	25	32	16
		28			100	81	66	44	27	22	35	16
34	W	34			100	84	69	48	26	21	35	18
		41			100	88	74	49	25	25	35	15
		48			100	89	71	47	29	24	31	16
		56			100	92	77	50	26	23	34	17
		62			100	89	76	49	24	25	35	16
44	E	9	100	99	96	94	75	50	28	25	31	16
		18										
		6	100	96	94	90	77	52	23	23	37	17
45	W	15	100	94	88	82	69	46	25	23	35	17
		24		100	97	92	75	51	27	22	34	17
56	E	9		100	96	90	72	49	26	24	33	17
		15		100	96	88	67	43	30	26	28	16
		9		100	96	90	76	54	23	22	35	20
64	W	18	100	97	95	89	76	52	23	23	35	19
		27		100	97	92	72	48	30	21	32	17
		Overall				100	83	58	25	22	36	17

Figure 27. Trimming ends of soil sample trapped inside the main chamber of the sampling device. Shown on the left side of picutre: scales for density determination of samples, soil core extracting apparatus, and moisture cans by means of which samples were taken to the N.C. State Highway Laboratories to be analyzed.

Figure 28. Obtaining profile of culvert flow line. Instrument man was able to communicate with rodman through a two-way telephone line.

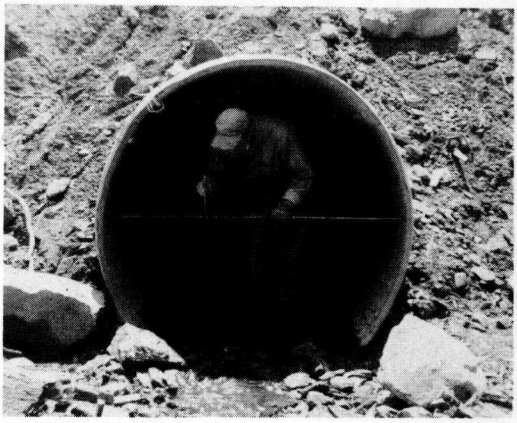

Figure 29. Measuring horizontal diameter of culvert with an extensometer.

on Phillips head screws attached at the crest of the corrugation of the inner surface of the pipe. These screws made the measurements possible under water. The ends of the horizontal diameters were marked by punch-marks in the inner surface of the pipe structure. All subsequent measurements were made at these points which marked the initial vertical and horizontal diameters of each ring; therefore, in the event that the structure rotated about its longitudinal axis, these readings would be called erroneously "the vertical" and "horizontal" diameters of the pipe respectively. Readings were made to 0.001 foot but due to the adverse conditions under which these read-

TABLE 4

COMPACTION CHARACTERISTICS AND PHYSICAL PROPERTIES OF SIDE SUPPORTING MATERIAL TWO YEARS AFTER CULVERT INSTALLATION

Ring No.	Side	Depth in.	γ_m pcf.	w %	γ_o pcf.	O. M. C. %	$\gamma_{Pr.}$ pcf.	% Comp.	s_s	e	LL	PI	Soil Classif.
		6	120.2	23.2	97.56			87.7	2.63	0.682	34	7	A-4(5)
8	E	15	123.8	22.1	101.4	15.1	111.2	91.2	2.63	0.618	33	7	A-4(5)
		24	125.4	21.3	103.4			93.0	2.64	0.593	35	9	A-4(5)
		6	130.0	16.8	111.3			99.5	2.64	0.480	33	6	A-4(5)
16	W	15	125.6	20.7	104.1	15.1	111.9	93.0	2.63	0.576	34	6	A-4(5)
		24	(114.0)[a]	22.1	(93.37)			(83.4)	2.64	(0.764)	34	5	A-4(5)
		9	130.0	18.0	110.2			98.4	2.63	0.489	36	14	A-6(7)
		15	131.0	18.9	110.2			98.4	2.62	0.484	37	13	A-6(7)
		21	132.2	18.4	111.7			99.7	2.63	0.469	34	10	A-4(6)
24	E	28	128.2	17.5	109.1	16.8	112.0	97.4	2.64	0.510	35	11	A-6(7)
		34	129.4	19.6	108.2			96.6	2.62	0.511	38	13	A-6(7)
		42	131.2	19.7	109.6			97.9	2.62	0.492	41	17	A-7-6(9)
		50	128.7	18.7	108.4			96.8	2.62	0.508	39	13	A-6(7)
		Overall				15.6	111.9		2.65		39	15	A-6(8)
		9	126.7	19.0	106.5			95.6	2.64	0.547	29	N. P.	A-4(3)
		15	125.1	21.0	103.4			92.8	2.65	0.599	28	N. P.	A-4(4)
		21	123.6	21.0	102.1			91.7	2.65	0.620	28	N. P.	A-4(4)
		28	124.8	20.7	103.4			92.8	2.65	0.599	29	N. P.	A-4(4)
34	W	34	126.5	18.6	106.7	15.0	111.4	95.8	2.64	0.544	28	N. P.	A-4(4)
		41	127.3	20.0	106.1			95.2	2.65	0.559	29	N. P.	A-4(4)
		48	125.6	19.5	105.1			94.3	2.65	0.573	29	N. P.	A-4(4)
		56	126.3	21.7	103.8			93.2	2.64	0.587	30	N. P.	A-4(4)
		62	123.2	22.9	100.2			89.9	2.64	0.644	31	N. P.	A-4(4)
44	E	9	126.1	17.3	107.5	12.2	114.5	93.9	2.60	0.509	32	7	A-4(4)
		18	126.9	19.8	105.9			92.5		0.532			
		6	-[b]	16.7	-			-	2.63	-	34	6	A-4(5)
45	W	15	128.2	18.3	108.4	13.4	114.8	94.4	2.64	0.520	35	7	A-4(4)
		24	125.1	18.9	105.2			91.6	2.64	0.566	36	9	A-4(4)
56	E	9	125.5	20.2	104.4	15.2	110.3	94.7	2.63	0.572	34	6	A-4(4)
		15	(126.8)[a]	17.1	(108.2)			(98.1)	2.64	(0.523)	34	7	A-4(3)
		9	123.6	21.2	102.0			90.6	2.64	0.615	37	8	A-4(5)
64	W	18	125.1	23.0	101.7	15.5	112.6	90.3	2.62	0.608	35	7	A-4(5)
		27	123.7	23.7	100.0			88.8	2.64	0.647	36	7	A-4(4)
		Overall				15.9	110.2		2.65		37	9	A-4(5)

[a] Sample was sheared in the main chamber of the sampling device and reassembled. Value of w reliable.
[b] Modified density apparatus was used unsuccessfully to obtain γ_m. Only w value reliable.

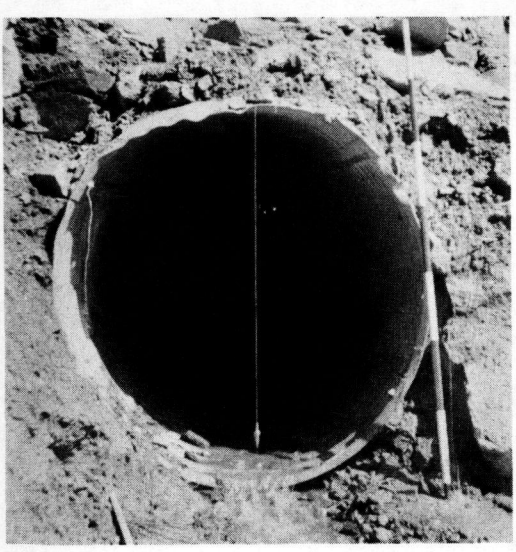

Figure 30. Plumb bob, dropped from top of pipe to ascertain whether structure has rotated about its horizontal axis.

ings were obtained, one is not justified to carry them closer than 0.01 foot. These adverse conditions were caused by: (a) inadequate and poor illumination of the pipe interior (because of burnt-out or grounded light bulbs), (b) inadequate working space because of the presence of struts, pine caps, top and bottom sills, etc. Furthermore, the field personnel had to be constantly in a bending position because of the pipe opening.

3. To ascertain any rotation of the structure about its horizontal axis, a plumb-bob was dropped from the Phillips screw head at the top part of the vertical diameter of the pipe (see Provisions for Construction of Special Pipe Lines), and the distance from the plumb-bob to the original invert of the pipe (bottom Phillips screw head) was measured in inches (Figure 30). The direction was recorded as "E" or "W" (east or west respectively) and, looking upstream, it indicated respectively a clockwise or a counter-clockwise rotation of the pipe. The readings were carried to 0.1 inch but for reasons stated in Provisions for Construction of Special Pipe Lines plus the fact that the bob was never still due to continuous draft and the water flow through the pipe, these readings should be carried only to the nearest 0.05 foot (Table 5).

4. To detect any movement of the centerline of the pipe, lateral profiles (Figure 54) were run as follows: The initial centerline, considered to be the datum line, had been established by means of the two permanent monuments installed 10 feet from the upstream and downstream ends of the pipe. From this line, horizontal deviations of the middle of the horizontal diameters of the centers of the prespecified rings were obtained by: (a) setting a level at the upstream monument and sighting at the downstream monument, and (b) attaching the extensometer at the horizontal diameter marks of each corresponding ring and measuring the distance between the middle of the horizontal diameter and the point where the line of sight intersected the extensometer.

5. Radial deformations of the pipe circumference at the middle of Rings 31, 37 and 55 were measured by means of a device called the pipe protractor. This device consists of a circular steel plate about one foot in diameter and scribed every 10 degrees around the circumference (Figure 31).

The protractor was rigidly mounted at the top and bottom Phillips screws of the corresponding rings. A movable arm of known length, which could be clamped at any angle of the protractor, was mounted at the center. By setting the arm at 10 degree angle intervals, the top of the vertical diameter being the zero reading, and measuring the distance from the end of the arm to the pipe wall, a record of the pipe shape was made.

The center of the protractor was always kept at a constant distance from the bottom Phillips head screw. Consequently, the position of the protractor center relative to the pipe circumference was not kept fixed as it depended on the relative movement of the bottom point. Therefore, the readings on subsequent dates did not yield the actual radial deflection of each initial point of the circumference from this center. Nevertheless, one could plot the overall shape of the ring on a given date regardless of its relative position to previous dates.

The distance between the arm and the pipe wall was measured by an ordinary ruler and the reading was carried to the nearest 0.001 foot. However, because of the already mentioned adverse environmental conditions encountered on this project, plus the fact that overlapping of the plate sections at four points on the circumference do not

TABLE 5

PIPE ROTATION DATA[a]

Ring No.	July 9, 1952 East	July 9, 1952 West	Aug 8, 1952 East	Aug 8, 1952 West	Aug 14, 1952 East	Aug 14, 1952 West	Aug. 28, 1952 East	Aug. 28, 1952 West	Sep. 17, 1952 East	Sep. 17, 1952 West	Oct 21, 1952 East	Oct 21, 1952 West	Nov 13, 1952 East	Nov 13, 1952 West	Dec 8, 1952 East	Dec 8, 1952 West	Jan. 6, 1953 East	Jan. 6, 1953 West
1		0 5		0 5		1.5		1 5		2 0		1.5		1 5		1.5		1 5
4		0 8		0.8		1 2		1 0		1 0		1.0		1 0		1.0		1 0
8		0 5		0.5		1 5		1 5		1 5		2 0		1 5		1 5		1 5
12		0 3		0 5		1 8		2 0		1 5		1 5		1 0		1 5		1 5
16		1 5		1 5		3 5		3.4		3 0		3 5		3 0		2.5		2.5
20		0.3		0 5		1 5		1 5		1 0		1.0		0 5		0.5		0 5
24	0	0	0	0		0.5		1.0	0	0	0	0	0	0	0.5		0.5	
28		1.0		1.0		0 5		0 5	0	0	0	0	0	0	0	0	0	0
30		0.8		1.0		0 5		0 5	0	0	0	0	0	0	0	0	0	0
31		1 0		1 0		0.5	0	0	0	0	0	0	0.5		1 0		1 0	
32		1 2		1.0		1.5		1 5		0 5		1.0		1 0		0.5		0 5
36		1 2		1 5		1.5		1 5		0 5		0.5		0 5	0	0	0	0
37		0.5		0.5	0	0	0 3		1.0		1 0		1.0		1 0		1 0	
38		0 6		0.6	0	0	0	0	0 5		1.0		1 5		1.5		1 5	
40		1 1		1.0		0 5	0 5		0 5		1 5		1 5		1 5		1.5	
44	0	0	0	0		0 4	0 5		1 0		1 0		1.5		2.0		2.0	
48		1 0		1 0		1 0		0 5	0	0	1.0		0	0	0	0	0 5	
52		1 0		1 0		1.0		1 0	0	0	1 0		0.5		0 5		1.0	
55		0.8		1.0		1.2		0 5	0	0	0.5		0.5		1 0		1 0	
56		2 0		1 8		2 0		1 0		0 5	0	0	0	0	0	0	0	0
60		0 8		0.8		1 3		0 5	0	0	0	0	0	0	0	0	0	0
64		0 7		0.7		1 5		1 0		1 0		0.5		0.5		0.5		1.0
68		0.9		0.9		1.5		1 5		1 5		0.5		0.5		0.5		0 5
72		1 0		1 0		1.5		1 5		1 0		1.0		1.0		1 0		0 5

Ring No.	Jan 26, 1953 East	Jan 26, 1953 West	Feb. 25, 1953 East	Feb. 25, 1953 West	Mar 8, 1953 East	Mar 8, 1953 West	Mar. 14, 1953 East	Mar. 14, 1953 West	May 26, 1953 East	May 26, 1953 West	June 16, 1953 East	June 16, 1953 West	Aug 5, 1953 East	Aug 5, 1953 West	Nov 24, 1953 East	Nov 24, 1953 West	Mar 29, 1954 East	Mar 29, 1954 West
1	-[b]	-	-	-	-	-	-	-	-	-	-	-	-	-	-	-	-	-
4		1.0		1.0		1.0		1 0		1 0		1.0		1 0		1.0		1.0
8		1 5		1.5		1.5		1 5		1 5		1.5		1.5		1.5		1 5
12		1 5		1.5		1 5		1 5		1.5		1.5		1.5		1.5		1 5
16		2 5		2.5		2.5		2 5		2 5		2.5		2 5		2 5		2.5
20		0.5		0 5		0.5		0 5		0 5		0 5		0 5		0.5		0.5
24	0.5		0 5		0.5		0 5		0.5		0 5		0.5		0 5		0 5	
28	0	0	0	0	0	0	0	0	0	0	0	0	0	0	0	0	0	0
30	0	0	0	0	0	0	0	0	0	0	0	0	0	0	0	0	0	0
31	1 0		1 0		1.0		1 0		1.0		1 0		1 0		1 0		1.0	
32		0.5		0 5		0.5		0 5		0 5		0 5		0 5		0 5		0.5
36	0	0	0	0	0	0	0	0	0	0	0	0	0	0	0	0	0	0
37	1 0		1 0		1 0		1 0		1.0		1 0		1.0		1.0		1.0	
38	1 5		1 5		1 5		1 5		1 5		1 5		1.5		1 5		1 5	
40	1.5		1.5		1 5		1 5		1 5		1 5		1 5		1 5		1 5	
44	2 0		2 0		2 0		2 0		2 0		2 0		2 0		2 0		2 0	
48	0 5		0 5		0 5		0 5		0 5		0 5		0.5		0 5		0.5	
52	0 5		0 5		0 5		0 5		0.5		0 5		0.5		0 5		0 5	
55	1 0		1 0		1 0		1.0		1.0		1.0		1 0		1 0		1 0	
56	0	0	0	0	0	0	0	0	0	0	0	0	0	0	0	0	0	0
60	0	0	0	0	0	0	0	0	0	0	0	0	0	0	0	0	0	0
64		0 5		0.5		0.5		0 5		0 5		0.5		0 5		0 5		0 5
68		0.5		0 5		0 5		0 5		0 5		0.5		0 5		0.5		0.5
72		0.5		0 5		0.5		0 5		0 5		0 5		0 5		0 5		0.5

[a] Distance measured in inches, measured from the tip of a plumb bob hanging from the top of pipe to the original pipe invert
[b] Ring deformed excessively by fallen boulder

permit securing a truly representative picture of the pipe circumference, it is felt that the experimental error involved cannot be less than ±0.025 foot.

To determine the external pressures generated against the pipe structure, no direct measurements were proposed at the Asheville meeting. Instead, either the total deformation or the strain at various points of the structure was measured by various means and conclusions concerning the loads which caused those deformations were drawn by using suitable load-deformation or stress-strain diagrams. Such data were collected by:

Strain Gages. Thirty-six type A-1 SR-4 strain gages were installed on Rings 31, 37, and 55 by the Armco Research Laboratories (Figure 32, also see Figures 20 and 21). Special care was taken to waterproof these gages and to provide them with mechanical as well as chemical protection (Figures 33-37). The method of insulation was similar to the one followed at another Multi-Plate pipe installation in Cullman, Alabama (Timmers, 1953).

Gages were installed on each of the above mentioned rings. One group was installed

on the vertical plane of the corrugation immediately downstream from the inside crest at the center of the ring. The other two groups were placed two feet on each side of the center group. Each group consists of four gages placed at the top, bottom, east, and west sides of the pipe circumference and as close to the geometrical neutral axis of the corrugated pipe surface as the laboratory facilities rendered possible. The lead wires from the top and bottom gages were protected in pipe conduits attached to the corrugated plates in inside valleys to points 6 inches from the edge of the plates.

Strain measurements were recorded in micro-inches per inch by means of a Bald-

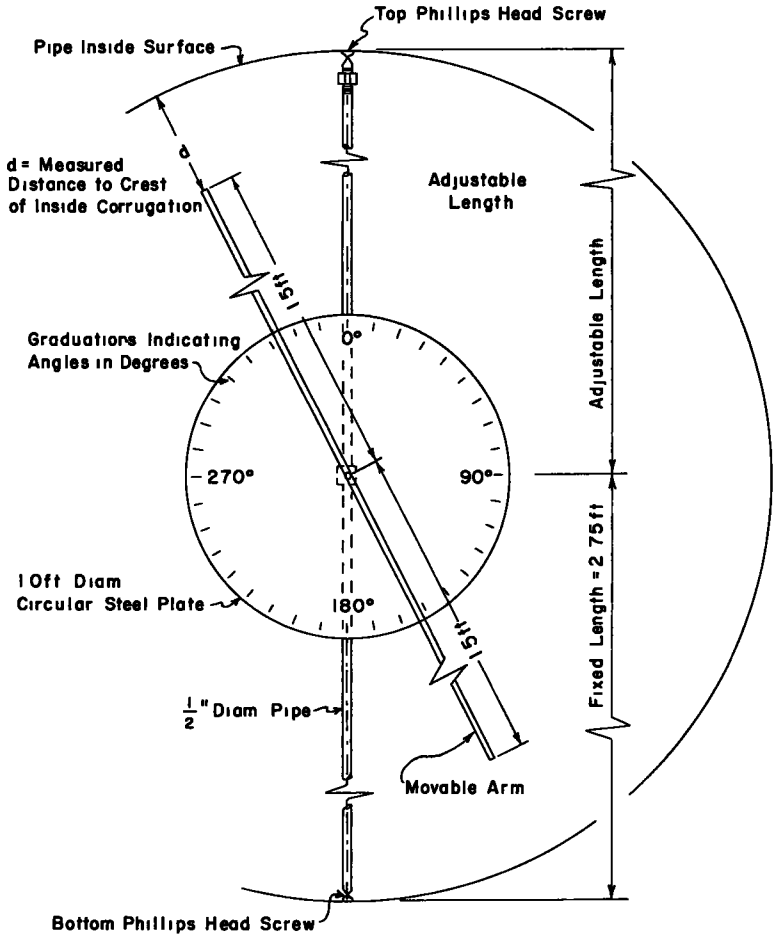

Figure 31. Pipe Protractor.

win Type L portable strain indicator (Figure 38). The measured strain was converted to stress by means of a stress-strain diagram obtained from a series of conventional tensile tests performed at the Armco Research Laboratories on standard ½ inch wide parallel section by 2-inch gage length sheet tensile samples with a type A-1 SR-4 strain gage centered in the parallel section (see Appendix). The thrust per foot of longitudinal seam was computed by multiplying the stress by the cross sectional area of the corrugated surface per foot of longitudinal seam.

Strut Load Cells. Their purpose was to measure the strain and accordingly the load carried by the struts supporting the pipe. From these data, and the strut spacing, the load per lineal foot of pipe carried by the struts alone could be computed for the ring. Strut load cells were placed on two struts at Ring 31 between the oak strut and the pine compression cap. These cells were designed also by the Armco Research Laboratories and they had been used previously in the Cullman, Alabama installation (Timmers,

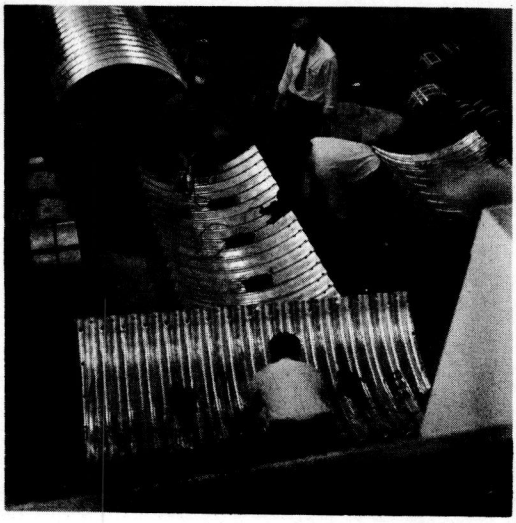

Figure 32. Installation of A-1 SR-4 strain gages on culvert plates (Ring 55, bottom) at the Armco Research Laboratories .

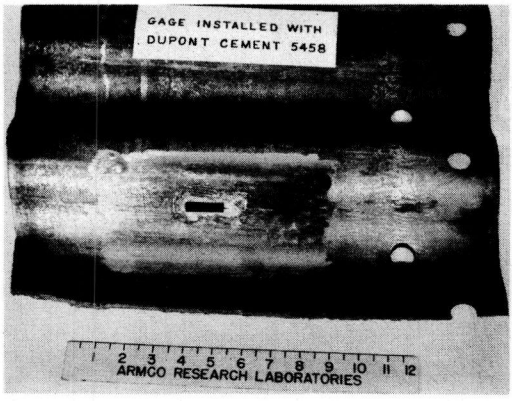

Figure 33.

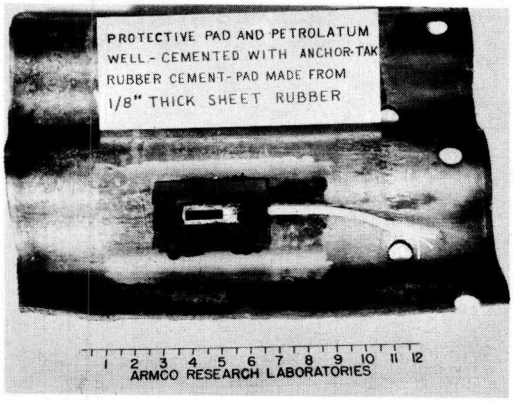

Figure 34.

Figure 35.

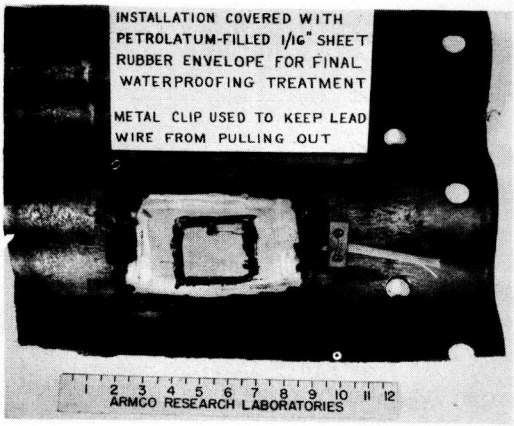

Figure 36.

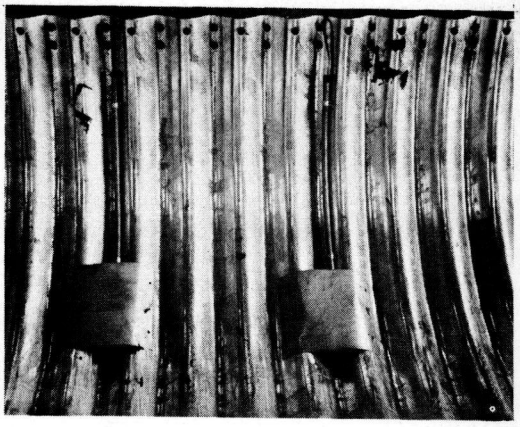

Figure 37. Gages installed on culvert plate (Ring 31, Bottom) and covered with metal plate for mechanical protection.

1953). They were constructed from 6-inch steel pipe, 7 inches high with a 1-by-8-inch steel plate on each end (Figures 39 and 40). They contain nine permanently installed AX-5 type SR-4 strain gages

and a temperature compensator. Readings were made with the same type L portable strain indicator used in recording the strain from the strain gages of item (a). The strain was converted to load in pounds by means of load-strain calibration diagrams. These diagrams were prepared at the research laboratories of N. C. State Highway and Public Works Commission from series of compressive tests run on each cell by using a Baldwin-Southwark Testing Machine with loads up to 200,000 lb., at 20,000 lb. increments (see Appendix).

Measuring the Vertical Deflection of the Pine Caps. A tack was driven into the oak strut at a point one foot from the pine cap. At later dates the distance between the tack and the top of the pine cap was again recorded and subtracted from the initial reading. Thus, the compression in the pine cap was obtained. The readings were carried to the nearest 0.01 foot. The loads which caused these deflections were determined by

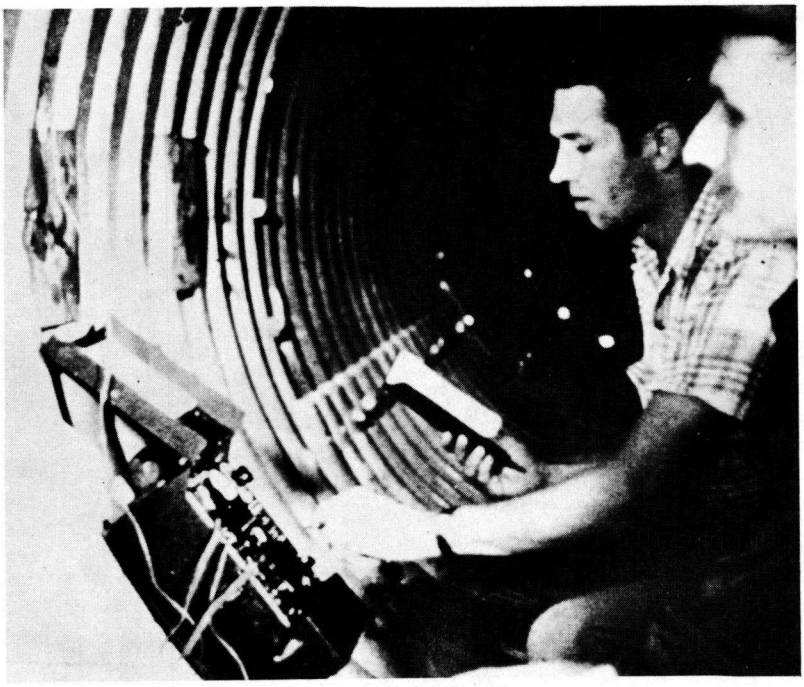

Figure 38. Recording strains on culvert inside surface by means of a Baldwin Type L portable strain indicator.

using a load-deflection diagram constructed in the State Highway Laboratories from a series of nine tests run on similar oak - pine specimens and under conditions simulating those encountered in the field (see Appendix). From the above data and the strut spacing the load per lineal foot that was carried by the struts alone could be computed along the whole pipe.

To estimate the vertical load on top of the conduit by means of the Marston-Spangler theory, the following data must be secured: (1) height of fill, H, in feet; (2) conduit diameter, B_c, in feet; (3) height of imperfect ditch, H_d, in feet; (4) effective width of imperfect ditch, B_d, in feet; (5) average unit weight of fill mate-

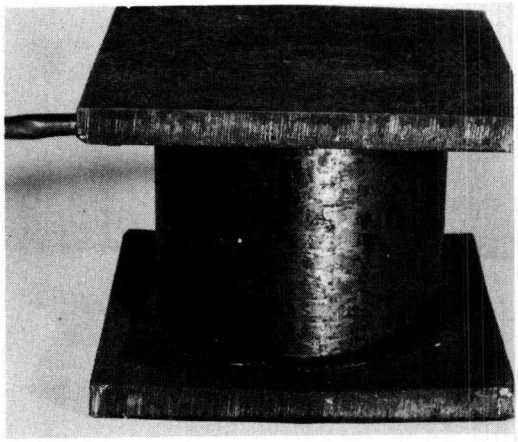

Figure 39. Strut load cell.

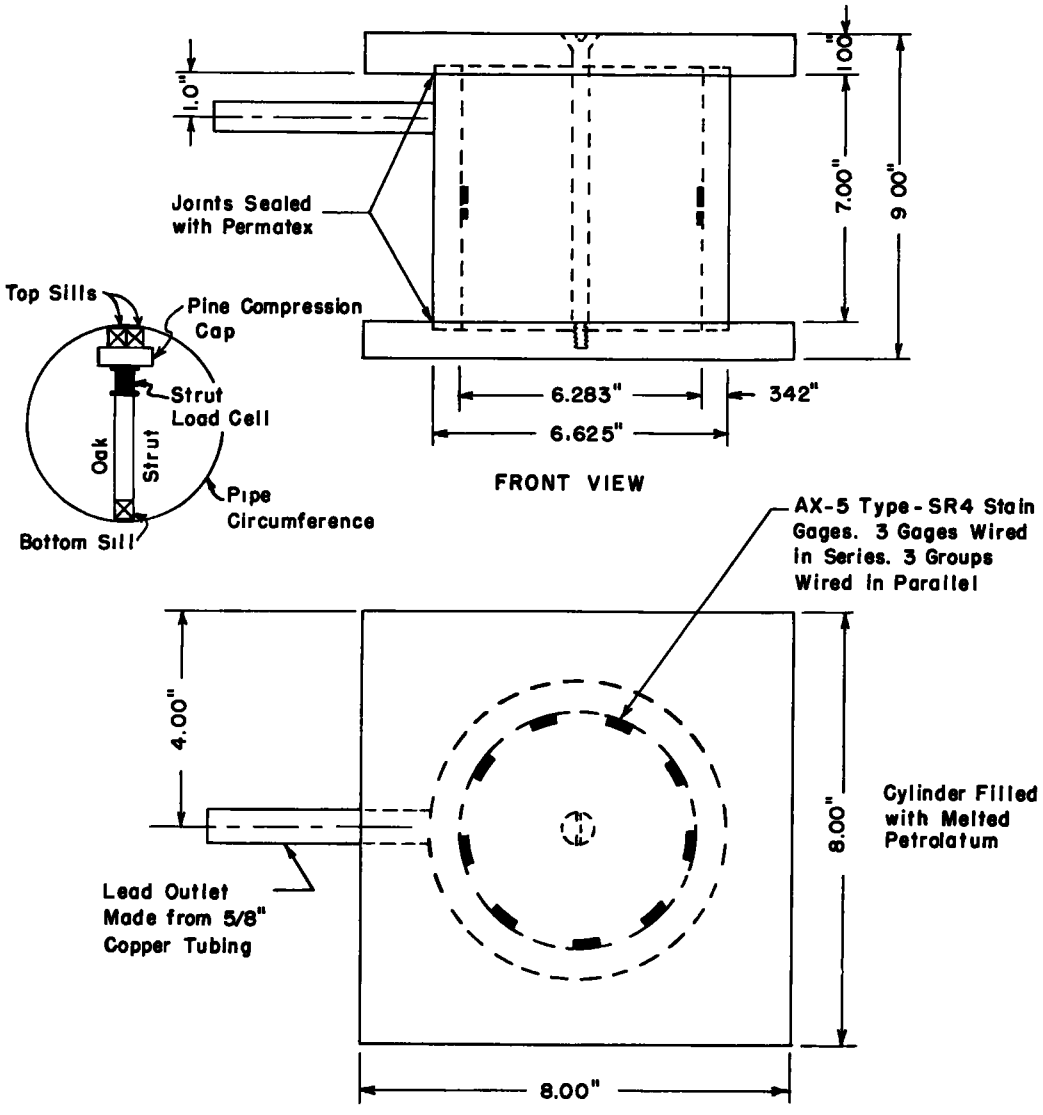

Figure 40. Strut Load Cell.

rial, γ, in pcf.; (6) effective angle of internal friction of fill material, ϕ_e; (7) equivalent "hydrostatic earth pressure ratio," K_e.[7] This ratio is assumed to be identically equal to the coefficient of active earth pressure, K_A.[8] (8) Moduli ratio, α; (9) settlement ratio, r_{sd}.

Items (1)-(4) are measured quantities. Values for items (5)-(8) are estimated from the nature of fill material and the methods of fill construction. The cohesion in the above theory is either neglected or accounted for by an equivalent angle of internal friction (see Analysis of Data).

The settlement ratio, r_{sd}, for an imperfect ditch installation (Spangler, 1946) is

---

[7] See, References, Costes, 1955, p. 22.

[8] $K_A = \tan^2(45^\circ - \phi/2) \equiv \dfrac{\sqrt{\mu^2+1} - \mu}{\sqrt{\mu^2+1} + \mu}$, where $\mu = \tan\phi$. (Spangler, 1951, p. 411)

defined as:

$$r_{sd} = s_c - (s_d + d_c + s_f) / s_d = (s_c - s_l) / s_d$$

where: $s_l = s_d + d_c + s_f$ = Settlement of the surface of the loose material, placed in the imperfect ditch, feet.

s_c = Settlement of the compacted material, placed adjacent to the imperfect ditch, feet.

s_d = Compression of the loose material in the imperfect ditch within the ditch height H_d, feet.

d_c = Shortening of the vertical diameter of the conduit, feet, obtained by means of the extensometer (see Apparatus).

s_f = Settlement of the conduit foundation, measured by running flow line profiles as described previously.

Figure 41. Installation of Ames settlement cells on the compacted fill mass adjacent to the top of the imperfect ditch.

To measure the settlements of the loose and the compacted soil masses directly above and adjacent to the pipe, 36 Ames Settlement Cells were installed under the direct supervision of M. G. Spangler on positions approximately 8 feet above the pipe and over the centers of Rings 30, 31, 32 and 36, 37, 38 (Figure 41). These cells were installed in groups of six and they were assigned identification numbers 1 - 6. Cells 1, 2, 5 and 6 were placed upon compacted fill; cells 3 and 4 were placed at the top of the imperfect ditch section which was refilled with loose material (Figures 20 and 21).

The principle of the Ames Settlement Cell is shown on the diagram of Figure 42. Readings were made by means of a mercury manometer specially designed by Spangler (Figures 43 and 44). To obtain a reading the following procedure was followed:

1. The manometer board was fastened securely at the top and bottom Phillips head screws, which marked the vertical diameter of the corresponding ring, by tightening the nut against the end of the supporting pipe.
2. With mercury in manometer, the upper leg was filled with water through the pinch clamp and the air was worked out of the manometer.
3. The inlet pipe of the settlement cell was connected.
4. The force pump was connected and with valve (a) open, water was pumped slowly into the settlement cell. When inlet pipe and cell were full, water spilled out of the outlet or overflow pipe.
5. While gradually pumping water into cell without surge, valve (a) was closed and the water column was allowed to come to rest.

6. The vertical distance from meniscus (e) to meniscus (f) multiplied by 13.6 (the specific gravity of mercury) represented the vertical distance from point (e) to the overflow orifice in the settlement cell. This distance was added to the measured length (c) - (e), to obtain the vertical distance from the invert of the pipe to the settlement cell. Having obtained the elevation of the pipe invert from the flow line profiles the elevation of the settlement cell could thus be determined also. In addition to the general adverse conditions encountered in the pipe interior the very nature of this experimental setup carries inherent sources of experimental error. These sources will be discussed in detail in the chapter Analysis of Data.

To make a prediction as to what the horizontal diameter of the conduit would be under various fill heights, the following items are employed in Spangler's "Iowa Formula."[9]

1. Vertical load on top of pipe, W_c, in lb. per lin. in., estimated by means of the Marston-Spangler theory.
2. Bedding angle of pipe installation, α, estimated from cross-sections along the culvert line.
3. Mean radius of pipe, r, in inches.
4. The product of modulus of elasticity times the moment of inertia of field-bolted

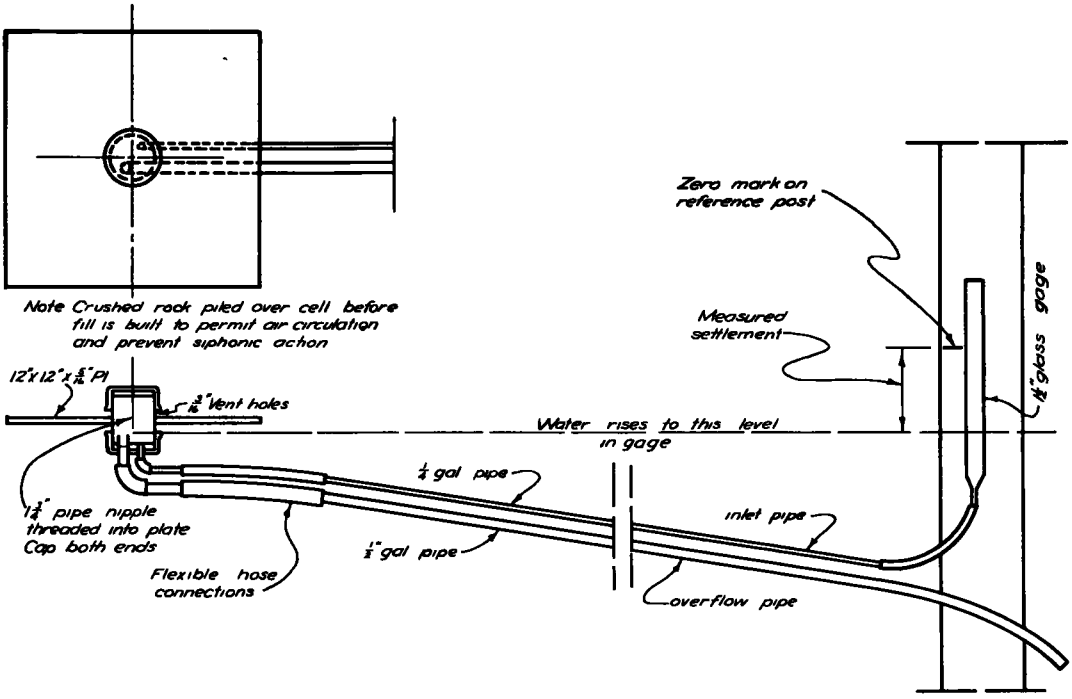

Figure 42. Diagram showing principle of Ames Settlement Cell (after M.G. Spangler).

Multi-Plate ring, EI, in lb. -in.^{2} per inch.

5. The modulus of passive resistance of side supporting material, e, in psi. per in. e is assumed to be a constant quantity depending on the conduit installation and the nature of the side supporting material.
6. The deflection "lag factor," D_e.

For a strutted pipe the following quantities are employed in addition to those mentioned above:

7. Effective length of strut, L_S, in inches.
8. Cross sectional area of strut, A_S, in in.^{2}.

[9]See Analysis of Data. Also, References, Spangler, 1946, 1955.

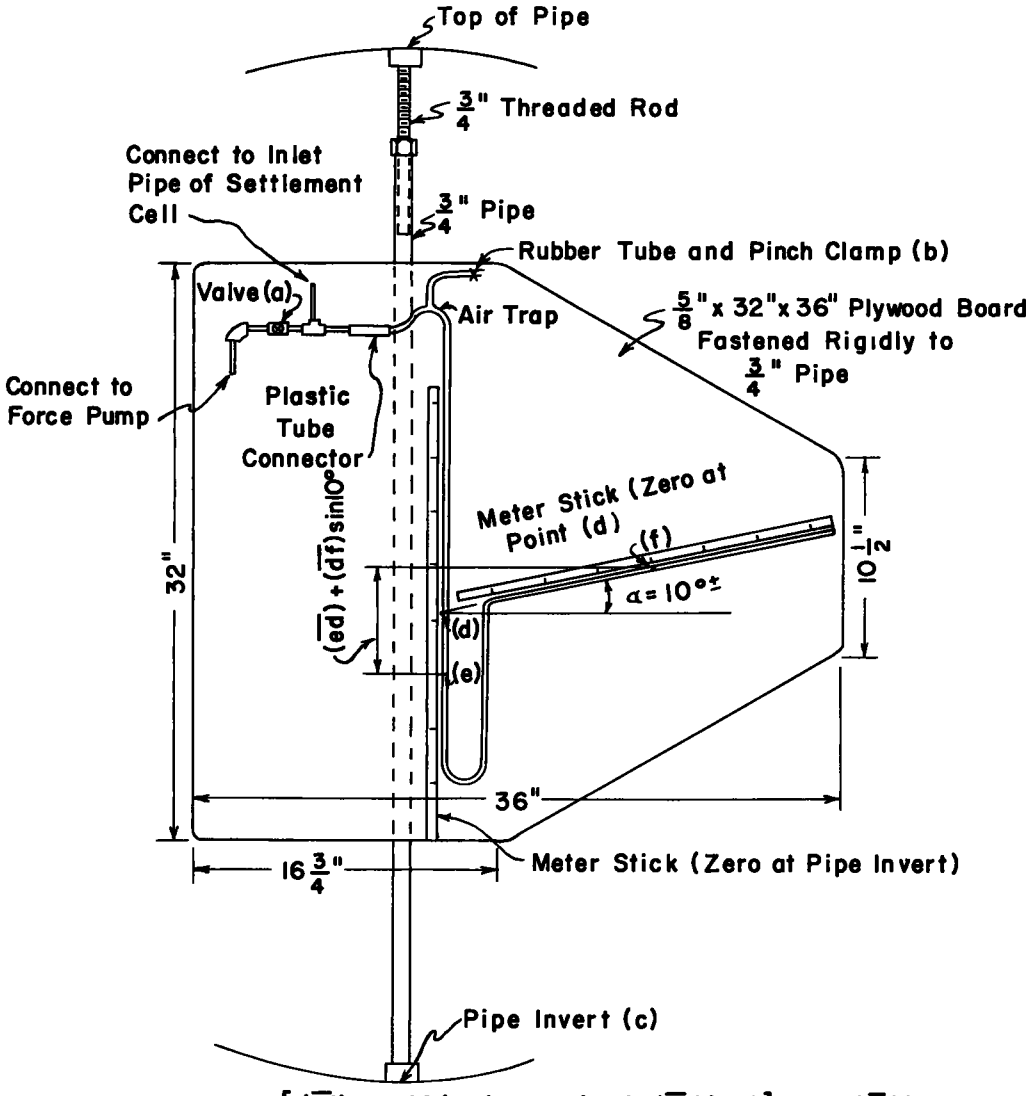

$$\text{Elev. of Cell (ft)} = \frac{[(\overline{df})\sin 10°\,(\text{cm}) + 76.7\,(\text{cm}) - (\overline{ed})(\text{cm})]\,13.6 + (\overline{ce})(\text{cm})}{30.48\ \text{cm/ft}} +$$

Elev. of Invert (ft).

Figure 43. Diagram showing details of mercury manometer device by means of which elevations of settlement cells were obtained. (After M.G. Spangler.)

9. Longitudinal spacing of struts, S_S.
10. Equivalent modulus of compression of the strut, E_S, in psi.

To determine item (4) two different test rings of No. 12 gage metal were used, one of which had been annealed, the other as received. The rings were loaded on diametrically opposed edges. Horizontal and vertical deflection measurements were read on four corrugations for load increments. Load-deflection curves were plotted and load-deflection values taken from the slope of the straight line portion of the curves. These values were substituted in formulas for computing deflections in circular rings and the EI product was evaluated (see Appendix). These results show the effective EI product to be approximately 60 percent of the theoretical value for Multi-Plate rings with-

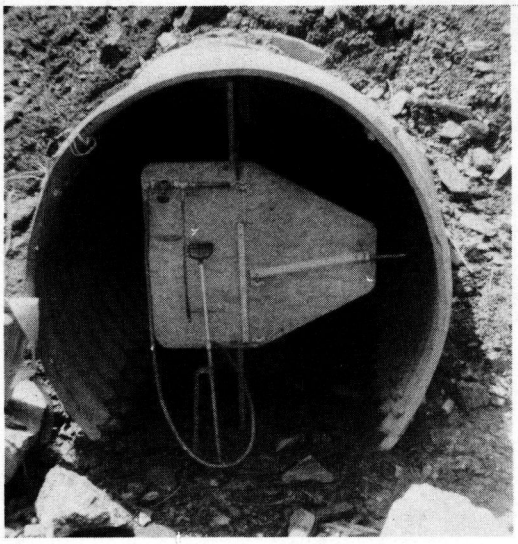

Figure 44. Manometer board with mercury manometer by means of which settlement readings were obtained.

out bolted joints. This difference is considered to be mainly on account of a hinge action at the bolted seams.

To obtain direct information regarding the nature of the modulus of passive resistance and the magnitude of the deflection lag factor for this installation, an experimental procedure is outlined in later sections of this paper (see Recommendations).

In order that the equivalent modulus of compression of the strut be estimated, it was suggested that the entire deflection of the strut system be assumed to occur in the pine compression cap. The load per strut versus fill height could be plotted from the pine compression measurements and the strut load cell readings recorded at various stages of the fill height (see Data, Figure 59). The effective strut length and cross sectional area could be determined by direct measurements. Accordingly, approximate values of E_S could be estimated for various fill heights and a curve of E_S versus fill height, H, could be constructed. Objections to such prodecure appear in the section, Analysis of Data of this paper.

OBTAINED DATA

Data from the Environmental Conditions of Pipe Installation

Figure 45 shows a cross-sectional view of the fill on top of the pipe line. On the same figure the various stages of construction, as well as the final settlement of the flow line, as indicated by the shaded portion, have been plotted from profile data.

The "imperfect ditch" method that was employed in the installation of the culvert is shown in Figure 46. This figure is a typical cross-sectional view of the pipe that was obtained at Ring 31.

In Figure 47, the marked positions (1) - (7) indicate the locations along the pipe line where density tests were performed.

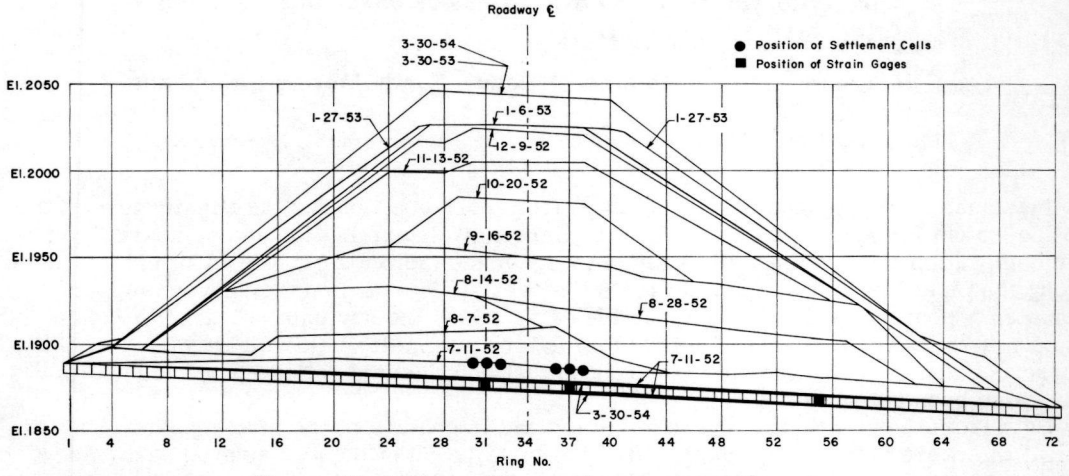

Figure 45. Fill profiles and culvert settlement.

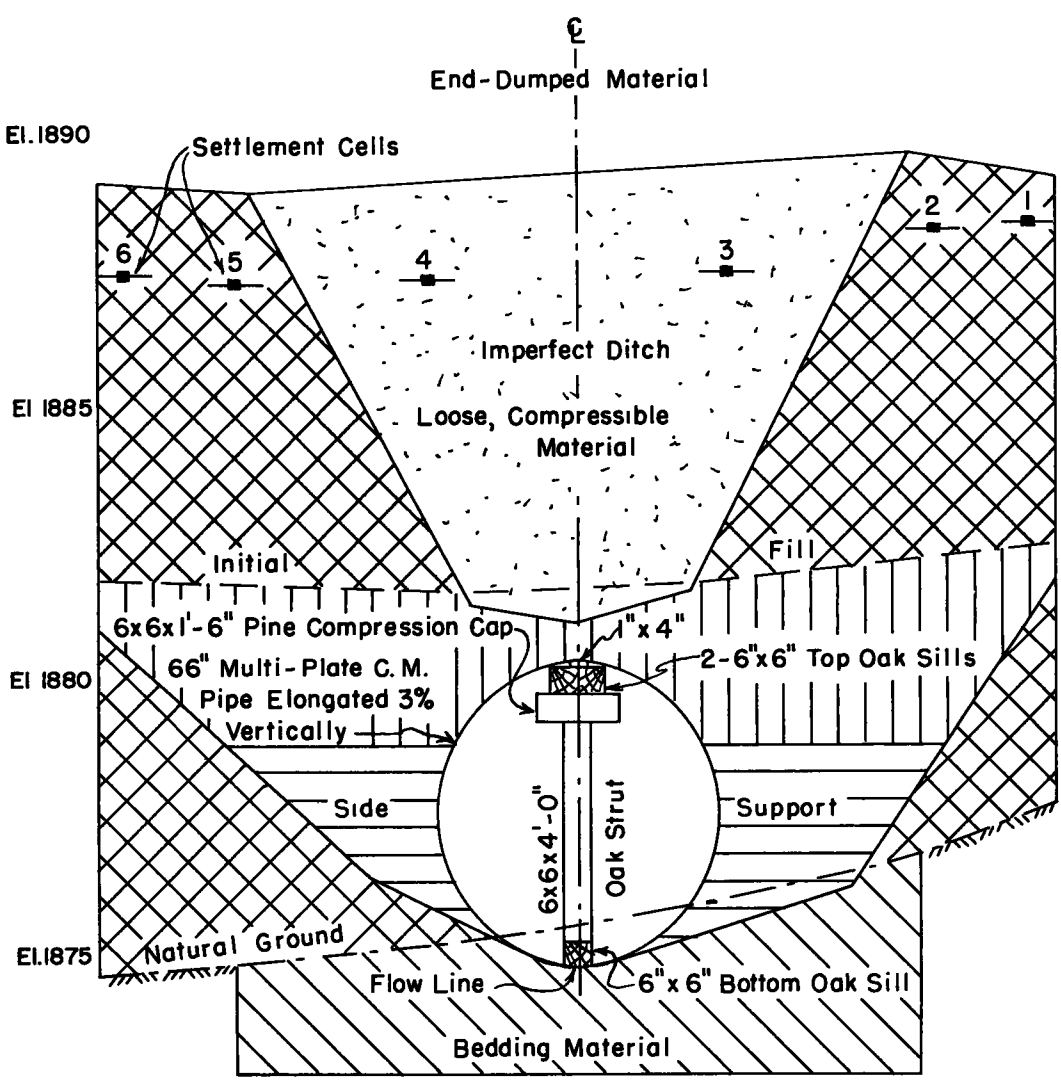

Figure 46. Typical cross section showing culvert installation. Obtained at Ring 31. Looking downstream.

Inasmuch as the amount of soil obtained from each position for the density tests was not sufficient for grain size analysis, Atterberg limit determination and standard Proctor compaction tests, composite samples were made from material of identical positions along the pipe line. The results of tests that were performed on the above composite samples appear in Tables 1 and 2. In the same tables the dry unit weight of the material, γ_0, the percent compaction based on the maximum dry unit weight, $\gamma_{pr.}$, of the corresponding standard Proctor compaction test and the void ratio, e, of each position have also been calculated.

Data from the compaction characteristics and the nature of the side supporting material that were obtained two years after the installation of the pipe (see Apparatus and Experimental Procedure) appear in Tables 3 and 4. The variation of the dry unit weight,

γ_o, water content, w, and void ratio, e, with lateral depth for each position is shown graphically in Figure 48. From visual and manual inspection, the side supporting material was described generally as: Tanish-gray, highly micaceous, non-plastic, clayey-sandy-silt with a fair percentage of weathered rock fragments of coarse sand particle size. Occasionally, a few stones of gravel size and small pockets of low plasticity clay are present. Parent rock was generally gneiss or schist. The moisture content was generally above optimum.

Results from "quick consolidated" triaxial tests performed on the same samples appear in Figures 49 and 50 (also see Appendix).

The initial values of the dry unit weight, γ_o, of the side supporting material, as well as those obtained two years later have been plotted against the respective ring number in Figure 51. The mean initial values of γ_o have also been plotted in the same figure giving a picture of the average initial compaction conditions of the side supporting material.

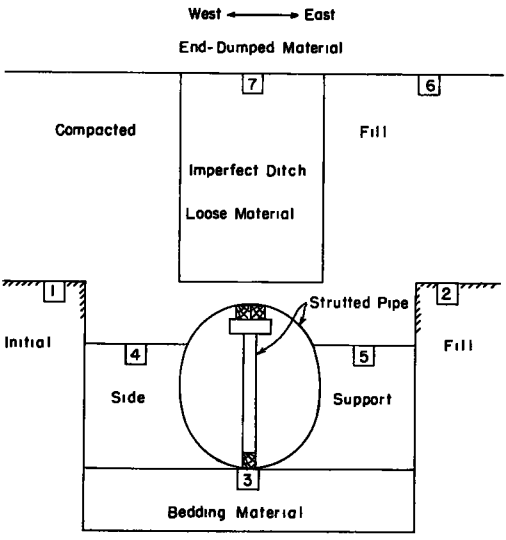

Figure 47. Schematic diagram of pipe installation indicating density test positions.

Data from Settlements and Deformations of Bolted-Plate Structure

Settlement profiles of the pipe invert for various heights are shown in Figure 52. The datum line of these curves is the initial profile of the pipe invert, obtained July 9, 1952. The settlement of the flow line on a given date was calculated by subtracting the elevations obtained at that date from the corresponding initial elevations of the datum line.

Curves showing the shortening of the vertical diameters and the elongation of the horizontal diameter of the pipe for various fill heights have been plotted in Figure 53. Each set of the above two families of curves is referred to the corresponding initial set of readings, obtained July 9, 1952.

Data from the rotation of the pipe structure, as obtained from the plumb-bob measurements, are presented in Table 5.

Lateral profiles of the pipe center line for various fill heights have been plotted in Figure 54. The base line of those profiles is the initial culvert alignment established by the pavement bench marks (see Experimental Procedure).

Figures 55, 56, and 57 show schematic diagrams of the pipe cross section at Rings 31, 37, and 55. These diagrams have been plotted from the Pipe Protractor data. The scale of deviations from the 66-in. diameter circular circumference that serves as the datum line has been increased five times that of the circumference. Thus, an exaggerated but, nevertheless, a clear picture of the load effect on the pipe shape is given.

Data Evaluated from Recorded Strains and Deformations of the Pipe Structure

Graphs showing the magnitude of vertical pressures at Rings 31, 37, and 55, evaluated from strain gage readings at various stages of the fill construction are shown in Figure 58.

The load carried by the strut at Ring 31, as determined from the large load cell readings, has been plotted versus fill height in Figure 59. For comparison purposes the same load, as obtained from the pine cap compression measurements on Ring 31, has been plotted also on the same figure. See Appendix, for load cell calibration curve. No data have been used from the small cell as it was inoperative from the beginning.

In Figure 60, the strut load along the pipe length evaluated from the pine cap com-

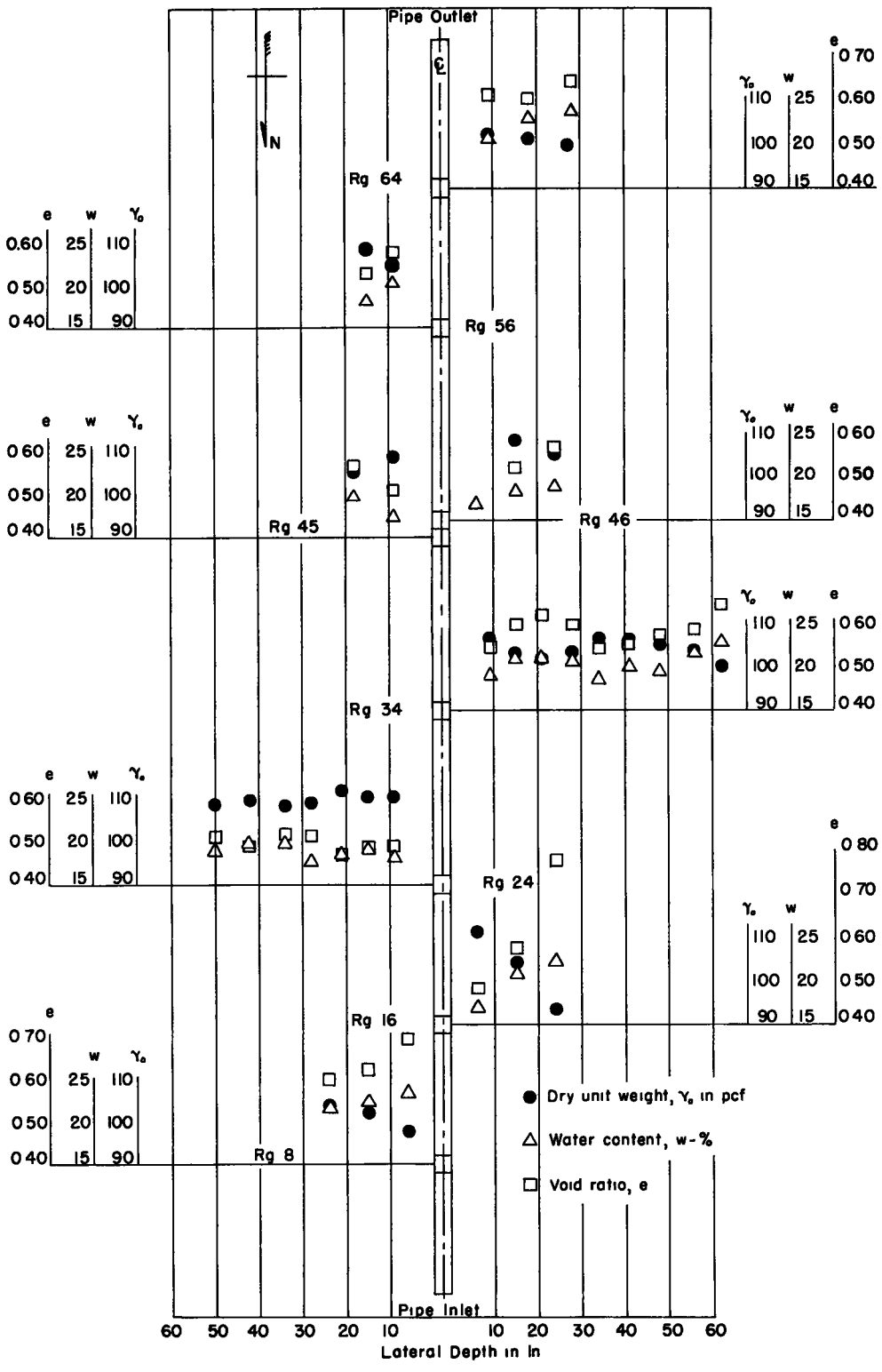

Figure 48. Data from physical properties of side supporting material. Obtained August, 1954, two years after the installation of the culvert.

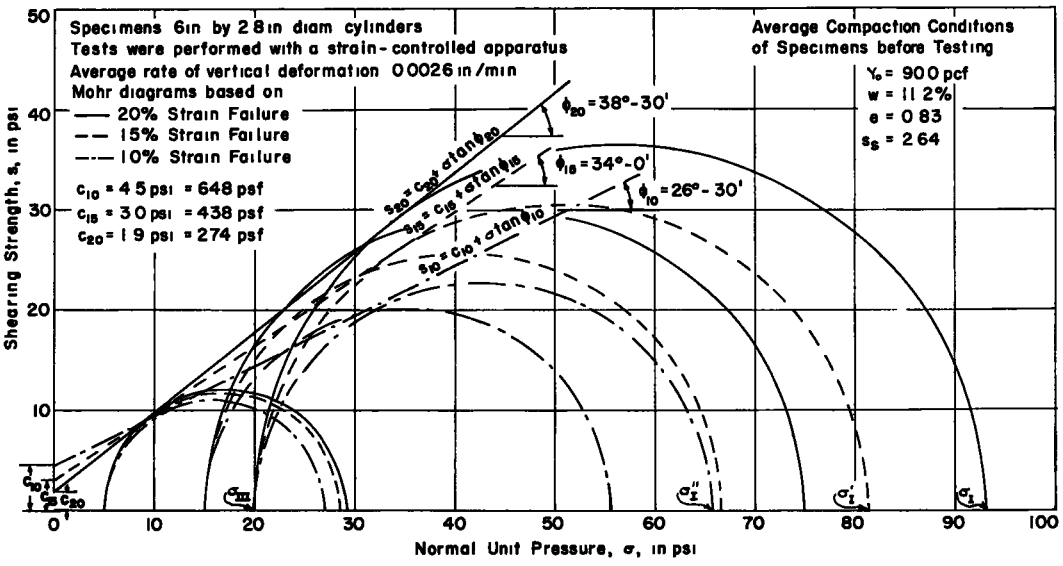

Figure 49. Results from quick consolidated triaxial tests on samples from side supporting material. Representative low compaction conditions during pipe installation.

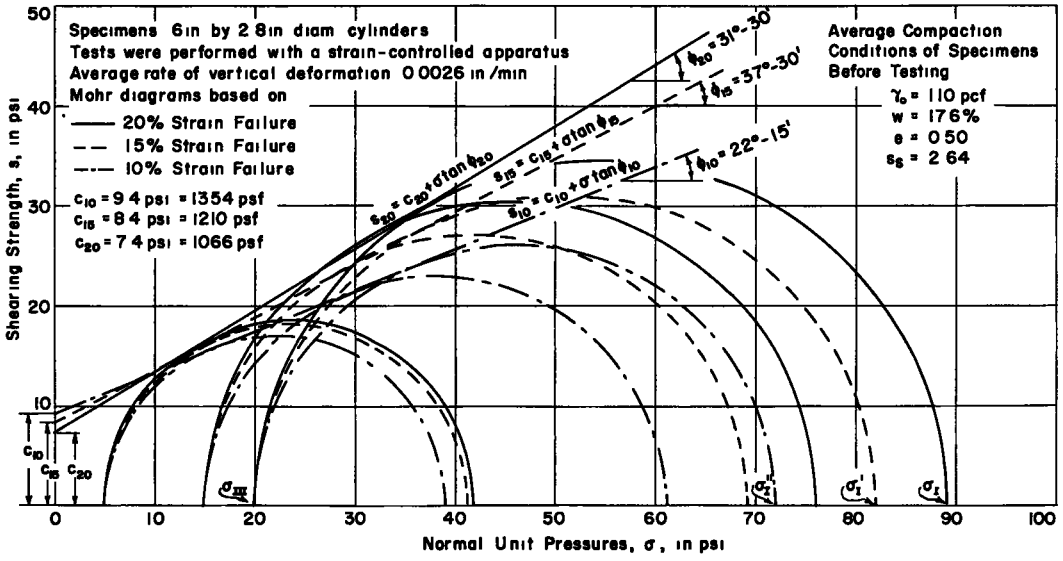

Figure 50. Results from quick consolidated triaxial tests on samples from side supporting material. Representative high compaction conditions two years after pipe installation.

pression measurements has been plotted for various fill heights. From these plottings a qualitative picture of the load distribution along the conduit length may be drawn. However, as will be discussed in the Analysis of Data, no conclusions with respect to the actual magnitudes of these loads may be drawn from the above data because of non-elastic conditions and the time element involved in the pine cap compression measurements. The load-deflection curve that was used to determine the above loads appears in Appendix.

All the above mentioned data have been employed to compute the vertical and lateral external loads in order that one may be able to evaluate the overall significance of such measurements. The results of these calculations appear in Table 6 and in Figures 61,

62, and 63. For comparison purposes, the overburden pressure, i.e., the weight per lineal foot of the earth column on top of the conduit, has also been plotted versus time on the same figures. Again, from the discussion appearing in the Analysis of Data, it will be seen that only qualitative conclusions may, possibly, be drawn from all these measurements.

Data Obtained from Settlement Cells

Figures 64 to 69, inclusive, contain settlement data computed from settlement cell readings. To compute these settlements the initial set of readings obtained on July 9, 1952 as soon as the cells had been installed, was used as the zero settlement.

The experimental error involved in these readings has not been determined as there was only one reading obtained from each cell each time. Nevertheless, to give an idea of the magnitude of deviation that can be expected in each manometer-operated cell reading from the same reading obtained by Wye level, Table 7 is prepared showing the initial cell elevations obtained by both the manometer procedure and by the level.

ANALYSIS OF DATA

Differences Between Construction Projects and Research Setups

To organize and carry out a research project, one is confronted with the following problems: (1) how to plan a program for obtaining data so that reliable conclusions can be made from the data so obtained; (2) how to analyze the data obtained; (3) what valid conclusions can be drawn properly from the data; (4) to what extent are the conclusions reliable; (5) what lessons can be learned from the experience of the present project so that proper recommendations for improvements on future installations can be made.

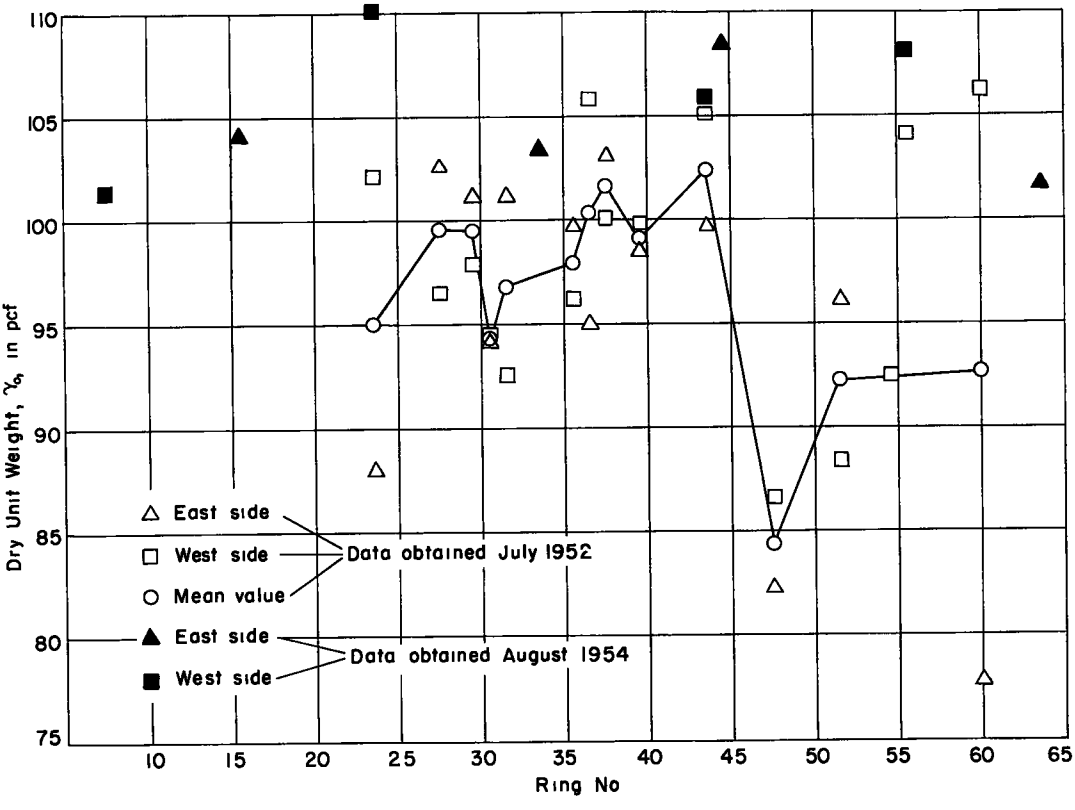

Figure 51. Compaction data from the side supporting material in the immediate vicinity of the culvert.

TABLE 6

EVALUATION OF VERTICAL LOAD, W_V IN LB. PER LIN. FT OF FORMED LENGTH OF PIPE FROM STRAIN GAGE AND STRUT LOAD CELL READINGS - RING 31

Date	East Str. Gages 1	2	3	Mean Rdg in. x 10^{-6}/in.	Stress psi.	W_E lb /ft	West Str. Gages 1	2	3	Mean Rdg in. x 10^{-6}/in.	Stress psi.	W_W lb. /ft.	Strut Load Cell Rdg in. x 10^{-6}/in	W_S lb /ft.	$W_V = W_E + W_W + W_S$ lb. /ft
7- 9-1952	+ 80	+ 75	+ 55	+ 70	+ 2,100	+ 8,610	+ 60	+ 65	+ 50	+ 58	+ 1,800	+ 7,380	10,635	1,167	+ 17,157
8- 5-1952	+ 180	+ 190	+ 155	+ 175	+ 5,500	+ 22,500	+ 150	+ 135	+ 120	+ 135	+ 4,300	+ 17,630	10,635	1,167	+ 41,347
8-14-1952	+ 200	+ 230	+ 135	+ 188	+ 5,900	+ 24,190	+ 195	+ 170	+ 140	+ 168	+ 5,300	+ 21,730	10,610	2,833	+ 48,753
8-28-1952	+ 280	+ 385	+ 90	+ 252	+ 7,900	+ 32,390	+ 270	+ 205	+ 165	+ 213	+ 6,700	+ 27,470	10,630	1,500	+ 61,360
9-16-1952	+ 875	+ 1000	+ 590	+ 822	+24,700	+101,270	+ 605	+ 555	+ 470	+ 543	+20,100	+ 82,410	10,600	3,500	+187,180
10-21-1952	+1875	+ 2440	+ 1545	+1953	+33,300	+136,530	+ 870	+ 800	+ 650	+ 773	+23,500	+ 96,350	10,570	5,300	+238,180
11-13-1952	+2790	+ 3690	+ 2565	+3015	+34,800	+142,680	+1120	+ 975	+ 750	+ 948	+28,500	+116,850	10,540	7,833	+267,363
12- 8-1952	+3260	+ 4320	+ 3375	+3652	+35,300	+144,730	+1300	+ 1105	+ 795	+1067	+28,700	+117,670	10,535	8,167	+270,567
1- 6-1953	+3895	+ 4935	+ 4085	+4305	+35,500	+145,550	+1500	+ 1275	+ 900	+1225	+30,200	+123,820	10,400	17,667	+287,037
1-29-1953	+4190	+ 5420	+ 4725	+4778	+35,700	+146,370	+1705	+ 1415	+ 1085	+1402	+31,400	+128,740	10,335	22,167	+297,277
2-24-1953	+4390	+ 5185	+ 4605	+4727	+35,600	+146,165	+1650	+ 1415	+ 1010	+1358	+31. 100	+127,510	10,490	11,333	+285,008
4- 8-1953[c]	+4815	+ 5460	+ 5515	+5263	+35,900	+147,190	+1885	+ 1615	+ 1220	+1573	+32,200	+132,020	10,695	0	+279,210
4-14-1953[d]	+4855	+ 6030	+ 5485	+5457	+35,900	+147,190	+2220	+ 1875	+ 1485	+1860	+33,100	+135,710	-	0	+282,900
5-26-1953	+3305	+ 3940	+ 4395	+3880	+35,400	+145,140	+1495	+ 1315	+ 1010	+1273	+30,600	+125,460	-	0	+270,600
6-16-1953	+2070	+ 3620	+ 3875	+3188	+35,000	+143,500	+1080	+ 2635[a]	+ 1585	+1767	+32, 800	+134,480	-	0	+277,980
8- 3-1953	+1355	+ 20[a]	+ 745	+1050	+28,400	+116,440	- 940	- 2115[a]	- 3160	-2115	-33,500	-137,350	-	0	Not Determined
11-23-1953	-5810	- 5375[a]	-[b]	-5593	-35,900	-147,190	-3165	- 5985[a]	- 6660	-5270	-35,800	-146,780	-	0	Not Determined
3-29-1954	-9905	-18050[a]	-[b]	-9905	Beyond Range	-	-3800	- 9445[a]	-10190	-7812	Beyond Range	-	-	0	Not Determined

EVALUATION OF LATERAL LOAD, W_L IN LB. PER LIN FT. OF FORMED LENGTH OF PIPE FROM STRAIN GAGE READINGS - RING 31

Date	Top Str. Gages 1	2	3	Mean Rdg in x 10^{-6}/in	Stress psi	W_{top} lb. /ft.	Bottom Str. Gages 1	2	3	Mean Rdg. in. x 10^{-6}/in.	Stress psi.	W_{bot} lb. /ft.	$W_L = W_T + W_B$ lb /ft
7- 9-1952	+ 80	+ 65	+ 95	+ 80	+ 2,500	+ 10,250	- 50	+ 50	+ 35	+ 43	+ 1,300	+ 5,330	+ 15,580
8- 5-1952	+ 135	+ 110	+ 145	+ 130	+ 4,100	+ 16,810	-6480[a]	+ 125	+ 160[a]	+ 143	+ 4,600	+ 18,860	+ 35,670
8-14-1952	+ 115	+ 85	+ 110	+ 103	+ 3,200	+ 13,120	-[b]	+ 220[a]	+ 160[a]	+ 192	+ 6,100	+ 25,010	+ 38,130
8-28-1952	+ 65	+ 150	+ 175	+ 163	+ 5,200	+ 21,320	-	+ 890[a]	+ 360[a]	+ 360	+11,500	+ 47,150	+ 68,470
9-16-1952	+ 280	+ 435	+ 470	+ 395	+12,500	+ 51,250	-	+ 520[a]	+ 570[a]	+ 545	+17,200	+ 70,520	+121,770
10-21-1952	+ 385	+ 680	+ 690	+ 585	+18,400	+ 75,440	-	+ 985[a]	+1060[a]	+1023	+28,100	+115,210	+190,650
11-13-1952	+ 505	+ 765	+ 760	+ 676	+21,100	+ 86,510	-	+1560[a]	+1485[a]	+1523	+32,000	+131,200	+217,710
12- 8-1952	+ 585	+ 815	+ 800	+ 733	+22,500	+ 92,250	-	+1510[a]	+1955[a]	+1733	+32,000	+131,200	+223,450
1- 6-1953	+ 690	+ 875	+ 1020	+ 862	+25,500	+104,550	-	+1420[a]	+2365[a]	+1893	+33,200	+136,120	+240,670
1-29-1953	+ 810	+ 930	+ 1140	+ 960	+27,200	+111,520	-	+1360[a]	+2655[a]	+2008	+33,400	+136,940	+248,460
2-24-1953	+ 775	+ 955	+ 950	+ 893	+25,100	+102,910	-	+1520[a]	+2810[a]	+2165	+33,600	+137,760	+240,670
4- 8-1953[c]	+ 990	+ 1160	+ 1150	+ 1100	+29,100	+119,310	-	+2065[a]	+3090[a]	+2578	+34,300	+140,630	+259,940
4-14-1953	+1285	+ 1305	+ 1370	+ 1320	+30,900	+126,690	-	+1900[a]	+3250[a]	+2575	+34,300	+140,630	+267,320
5-26-1953	+ 825	+ 1085	+ 1135	+ 1015	+27,900	+114,390	-	+2200[a]	+3570[a]	+2885	+34,700	+142,270	+256,660
6-16-1953	+ 430	+ 1085	+ 520	+ 678	+21,200	+ 86,920	-	+1870[a]	+8250[a]	Unreliable	-	-	Not Determined
8- 3-1953	-2525[a]	+ 115[a]	- 1195[a]	- 1202[a]	-30,000	-123,000	-	- 775[a]	+4435[a]	Unreliable	-	-	
11-23-1953	-7950[a]	- 7965[a]	-10550[a]	- 8821[a]	-37,000	-151,700	-	+2360[a]	+9200[a]	Unreliable	-	-	
3-29-1954	-8675[a]	- 8640[a]	-16560[a]	-11291[a]	-37,500	-153,750	-	+4420[a]	+5420[a]	Unreliable	-	-	

(Continued on next page)

TABLE 6 (Continued)

EVALUATION OF VERTICAL LOAD, W_V IN LB. PER LIN. FT. OF FORMED LENGTH OF PIPE FROM STRAIN GAGE READINGS AND PINE CAP COMPRESSION MEASUREMENTS - RING 37

Date	East Str. Gages 1	2	3	Mean Rdg. in. x 10^{-6}/in.	Stress psi.	W_E lb./ft.	West Str. Gages 1	2	3	Mean Rdg. in. x 10^{-6}/in.	Stress psi.	W_W lb./ft.	Pine Cap Compres. in.	W_S lb./ft.	$W_V = W_E + W_W + W_S$ lb./ft.
7- 9-1952	+ 50	+ 70	+ 35	+ 52	+ 1,500	+ 6,150	+ 50	+ 45	+ 45	+ 47	+ 1,400	+ 5,740	0	(1167)	+(13,067)
8- 5-1952	+ 160	+ 175	+ 135	+ 157	+ 5,000	+ 20,500	+ 190	+ 185	+ 155	+ 177	+ 5,500	+ 22,550	0	(1167)	+(44,217)
8-14-1952	+ 195	+ 160	+ 75	+ 178	+ 5,600	+ 22,960	+ 175	+ 165	+ 150	+ 163	+ 5,200	+ 21,320	0	(2833)	+(47,113)
8-28-1952	+ 340	+ 305	+ 55	+ 323	+10,500	+ 43,050	+ 300	+ 280	+ 255	+ 278	+ 8,900	+ 36,490	0	(1500)	+(81,040)
9-16-1952	+ 775	+ 685	+ 205	+ 555	+17,300	+ 70,930	+ 675	+ 670	+ 565	+ 643	+20,300	+ 83,230	0.12	4533	+158,693
10-21-1952	+1255	+ 1040	+ 365	+1147	+28,500	+116,850	+ 985	+ 945	+ 630	+ 853	+25,200	+103,320	0.36	7133	+227,303
11-13-1952	+2020	+ 1750	+ 1105	+1625	+32,400	+132,840	+1415	+ 1425	+ 1010	+1283	+30,600	+125,460	0.36	7133	+265,433
12- 8-1952	+2430	+ 2280	+ 1845	+2185	+33,700	+138,170	+1705	+ 1685	+ 1360	+1583	+32,200	+132,020	0.48	7933	+278,123
1- 6-1953	+3085	+ 2910	+ 2400	+2798	+34,600	+141,860	+1760	+ 2045	+ 1610	+1805	+32,900	+134,890	0.48	7933	+284,683
1-29-1953	+3365	+ 3260	+ 2685	+3103	+34,900	+143,090	+1855	+ 2300	+ 1830	+1995	+33,400	+136,940	0.60	8532	+288,562
2-24-1953	+3715	+ 3810	+ 3170	+3565	+35,300	+144,730	+2860	+ 2405	+ 2170	+2478	+34,200	+140,220	0.60	8532	+293,482
4- 8-1953[c]	+3470	+ 4000	+ 3325	+3598	+35,300	+144,730	+3100	+ 2770	+ 2555	+2808	+34,600	+141,860	0.72	8999	+295,589
4-14-1953[d]	+4620	+ 3055	+ 3525	+3733	+35,300	+144,730	+3320	+3315	+ 2840	+3158	+35,000	+143,500	-	0	+288,230
5-26-1953	+4440	+ 3590	+ 1735	+3255	+35,100	+143,910	+3290	+2745	+ 2155	+2730	+34,500	+141,450	-	0	+285,360
6-16-1953	+4390	+ 3410	+ 7055[a]	+3900	+35,400	+145,140	+3200	+2380	+ 1505	+2362	+34,000	+139,400	-	0	+284,540
8- 3-1953	+2670	+ 3590	- 4200[a]				+2700	- 335	- 435				-	0	Not Determined
11-23-1953	+3470	+ 660	-[b]				+ 560	-8470	- 7070				-	0	Not Determined
3-29-1954	+2975[a]	- 8660	- 4325[a]				- 960	-[b]	- 4105				-	0	Not Determined

EVALUATION OF LATERAL LOAD, W_L IN LB. PER LIN. FT. OF FORMED LENGTH OF PIPE FROM STRAIN GAGE READINGS - RING 37

Date	Top Str. Gages 1	2	3	Mean Rdg. m. x 10^{-6}/in.	Stress psi.	W_{top} lb./ft.	Bottom Str. Gages 1	2	3	Mean Rdg. in. x 10^{-6}/in.	Stress psi	$W_{bot.}$ lb./ft.	$W_L = W_T + W_B$ lb./ft.
7- 9-1952	+1050[a]	+ 30	+ 50	+ 40	+ 1,200	+ 4,920	+ 140[a]	0	0	0	0	0	+ 4,920[a]
8- 5-1952	+1125[a]	+ 95	+ 130	+ 113	+ 3,500	+ 14,350	+ 30	+ 220	- 140[a]	+ 125	+ 3,900	+ 15,990	+ 30,340
8-14-1952	+1115[a]	+ 100	+ 135	+ 118	+ 3,600	+ 14,760	+ 165	+ 170[a]	+ 225[a]	+ 168	+ 5,300	+ 21,730	+ 36,490
8-28-1952	+1240[a]	+ 155	+ 200	+ 178	+ 5,600	+ 27,060	+ 260	+ 690[a]	-1000[a]	+ 260	+ 8,200	+ 33,620	+ 60,680
9-16-1952	+1510[a]	+ 400	+ 460	+ 430	+13,600	+ 55,760	+ 585	+1430[a]	- 250[a]	+ 585	+18,400	+ 75,440	+131,200
10-21-1952	+1700[a]	+ 560	+ 600	+ 580	+18,200	+ 74,620	+ 600	+2110	- 185[a]	+ 600	+18,900	+ 77,490	+152,110
11-13-1952	+1850[a]	+ 700	+ 680	+ 690	+21,500	+ 88,150	- 310[a]	+2520[a]	- 285[a]	Not Reliable	-	-	-
12- 8-1952	+1950[a]	+ 780	+ 720	+ 750	+23,300	+ 95,530	+ 780[a]	+3345[a]	+ 35[a]	+ 780	+23,800	+ 97,580	+193,110
1- 6-1953	+1975[a]	+ 890	+ 770	+ 830	+24,900	+102,090	+1000[a]	+3550[a]	+ 355[a]	+1000	+27,800	+113,980	+216,070
1-29-1953	+2005[a]	+ 1025	+ 825	+ 925	+26,600	+109,060	+1175[a]	+3730[a]	+ 550[a]	+1175	+29,800	+122,180	+231,240
2-24-1953	+2180[a]	+ 1080	+ 940	+ 1010	+27,900	+114,390	+1300[a]	+3770[a]	+1555[a]	+1428	+31,500	+129,150	+243,540
4- 8-1953[c]	+2480[a]	+ 1160	+ 1070	+ 1115	+29,200	+119,720	+1280[a]	+4040[a]	+1680[a]	+1430	+31,500	+129,150	+248,870
4-14-1953[d]	+2420[a]	+ 820	+ 1220	+ 1020	+28,200	+115,620	+1520[a]	-[b]	+1585[a]	+1553	+32,100	+131,610	+247,230
5-26-1953	+2375[a]	- 1480[a]	+ 990	+ 990[a]	+27,500	+112,750	+1260[a]	-[b]	+1520[a]	+1390	+29,300	+120,130	+232,880
6-16-1953	+2250[a]	- 2695[a]	+ 770	+ 770[a]	+23,500	+ 96,350	+1260[a]	-[b]	+2110[a]	+1685	+32,600	+133,660	+230,010
8- 3-1953	+2120[a]	-15870[a]	- 910	- 910[a]	-26,300	-107,830	+1260[a]	-[b]	+1820[a]	+1540	+32,000	+131,200	Not Determined
11-23-1953	-[b]	-[b]	- 4020	- 4020[a]	-35,400	-145,140	+1120[a]	-[b]	+4220[a]	+2670	+34,400	+141,040	Not Determined
3-29-1954	-[b]	-[b]	- 4320	- 4320[a]	-35,600	-145,960	+ 930[a]	-[b]	+4475[a]	+2703	+35,500	+145,550	Not Determined

TABLE 6 (continued)

EVALUATION OF VERTICAL LOAD, W_V IN LB. PER LIN. FT. OF FORMED LENGTH OF PIPE FROM STRAIN GAGE READINGS AND PINE CAP COMPRESSION MEASUREMENTS - RING 55

Date	East Str. Gages 1	2	3	Mean Rdg. in. x 10^{-6}/in.	Stress psi.	W_E lb./ft.	West Str Gages 1	2	3	Mean Rdg. in. x 10^{-6}/in.	Stress psi.	W_W lb./ft.	Pine Cap Compres. in.	W_S lb./ft	$W_V = W_E + W_W + W_S$ lb./ft.
7- 9-1952	+ 60	+ 15	+ 45	+ 40	+ 1,100	+ 4,380	+ 40	+ 55	+ 30	+ 42	+ 1,150	+ 5,110	0	(1167)	+(10,657)
8- 5-1952	+ 15	+ 20	+ 35	+ 23	+ 700	+ 2,550	+ 40	+ 50	+ 40	+ 43	+ 1,200	+ 4,380	0	(1167)	+ (8,097)
8-14-1952	0	+ 20	+ 20	+ 20	+ 600	+ 2,190	+ 30	+ 45	+ 35	+ 37	+ 1,000	+ 3,650	0	(1167)	+ (7,007)
8-28-1952	+ 175	+ 205	+ 175	+ 185	+ 5,800	+ 21,170	+ 90	+ 175	+ 135	+ 133	+ 4,200	+ 15,330	0. 24	6267	+ 42,767
9-16-1952	+ 325	+ 485	+ 485	+ 432	+14,100	+ 51,465	+ 320	+ 425	+ 480	+ 408	+13,300	+ 48,545	0. 36	7133	+107,143
10-21-1952	+ 440	+ 635	+ 625	+ 567	+18,500	+ 67,525	+ 340	+ 540	+ 490	+ 457	+14,700	+ 53,655	0. 36	7133	+128,313
11-13-1952	+ 540	+ 805	+ 805	+ 717	+23,200	+ 84,680	+ 490	+ 715	+ 630	+ 612	+19,900	+ 72,635	0. 60	8532	+165,847
12- 8-1952	+ 580	+ 875	+ 920	+ 792	+25,700	+ 93,805	+ 580	+ 805	+ 800	+ 728	+24,700	+ 90,155	0 72	9000	+192,960
1- 6-1953	+ 675	+ 980	+ 1120	+ 925	+29,300	+106,945	+ 710	+ 900	+ 765	+ 792	+25,700	+ 93,805	0. 72	9000	+209,750
1-29-1953	+ 760	+ 1030	+ 1100	+ 963	+30,300	+110,595	+ 810	+ 995	+ 805	+ 870	+27,900	+101,835	0. 84	9500	+221,930
2-24-1953	+1105	+ 1600	+ 1875	+1527	+38,600	+140,890	+1310	+ 1105	+ 1140	+1185	+34,400	+125,560	0. 96	9833	+276,283
4- 8-1953[c]	+1275	+ 1765	+ 2045	+1695	+39,800	+145,270	+2250	- 275	+ 1250	+1750	+40,100	+146,365	0. 96	9833	+301,468
4-14-1953[d]	+ 405	+ 2070	+ 2385	+1620	+39,300	+143,445	+1550	- 1075	+ 1240	+1395	+37,300	+136,145	-	0	+279,590
5-26-1953	+1375	+ 2200	+ 1715	+1763	+40,200	+146,730	+1480	- 785	+ 1135	+1308	+36,100	+131,765	-	0	+278,495
6-16-1953	+1500	+ 2010	+ 825	+1445	+37,800	+137,970	-1065	- 1745	+ 890	-	-	-	-	0	Not Determined
8- 3-1953	+1355[a]	- 5160	- 2565	-	-	-	-2440	- 4550	- 8350	-	-	-	-	0	Not Determined
11-23-1953	+1010	-13145[a]	- 5295[a]	-	-	-	-8470[a]	-21090[a]	-14455[a]	-	-	-	-	0	Not Determined
3-29-1954	-1450[a]	-15895[a]	-11935[a]	-	-	-	-[b]	-23115[a]	-[b]	-	-	-	-	0	Not Determined

EVALUATION OF LATERAL LOAD, W_L IN LB. PER LIN. FT. OF FORMED LENGTH OF PIPE FROM STRAIN GAGE READINGS - RING 55

Date	Top Str. Gages 1	2	3	Mean Rdg in. x 10^{-6}/in.	Stress psi.	W_{top} lb./ft.	Bottom Str. Gages 1	2	3	Mean Rdg. in. x 10^{-6}/in.	Stress psi.	$W_{bot.}$ lb./ft.	$W_L = W_T + W_B$ lb./ft
7- 9-1952	+ 10	+ 30	+ 25	+ 21	+ 600	+ 2,190	0	+ 5	- 10	+ 5	+ 100	+ 365	+ 2,555
8- 5-1952	+ 30	+ 30	+ 15	+ 25	+ 700	+ 2,555	0	+ 5	- 10	+ 5	+ 100	+ 365	+ 2,920
8-14-1952	- 5	- 5	- 30	+ 13	+ 300	+ 1,095	- 35	+ 35	- 30	+ 35	+ 900	+ 3,285	+ 4,380
8-28-1952	+ 20	- 35	+ 15	+ 17	+ 400	+ 1,460	+ 95	+ 405[a]	+ 330[a]	+ 95	+ 3,000	+10,950	+ 12,410
9-16-1952	+ 195	+ 135	+ 280	+ 203	+ 6,400	+23,360	+ 280	+ 575[a]	+ 650[a]	+ 280	+ 9,000	+32,850	+ 56,210
10-21-1952	+ 260	+ 75	+ 365	+ 233	+ 7,400	+27,010	+ 320	+ 915[a]	+ 950[a]	+ 320	+10,300	+37,595	+ 64,605
11-13-1952	+ 355	+ 110	+ 445	+ 303	+ 9,700	+35,405	+ 310	+1530[a]	+2015[a]	+ 310	+10,100	+36,865	+ 72,270
12- 8-1952	+ 390	+ 105	+ 465	+ 320	+10,300	+37,595	+ 245	+4855[a]	+1070[a]	+ 245	+ 7,800	+28,470	+ 66,065
1- 6-1953	+ 435	+ 115	+ 505	+ 352	+11,400	+41,610	+ 205	+1265[a]	+2410[a]	+ 205	+ 6,500	+23,725	+ 65,335
1-29-1953	+ 470	+ 125	+ 540	+ 378	+12,100	+44,165	+ 175	+2520[a]	+2770[a]	+ 175	+ 5,500	+20,075	+ 64,240
2-24-1953	+ 630	+ 335	+ 755	+ 573	+19,700	+71,905	+ 425	+1185[a]	+1550[a]	+ 425	+13,700	+50,005	+121,910
4- 8-1953[c]	+ 690	+ 355	+ 825	+ 623	+20,300	+74,095	+ 325	+1080[a]	- 275[a]	+ 325	+10,300	+37,595	+111,690
4-14-1953[d]	+ 730	+ 310	+ 860	+ 633	+20,700	+75,555	+ 270	+1055[a]	+2885[a]	+ 270	+ 8,700	+31,755	+107,310
5-26-1953	+ 220	- 225	+ 855	+ 283	+ 9,200	+33,580	- 245	+1125[a]	+3180[a]	- 245	- 7,700	-28,105	Not Determined
6-16-1953	+ 520	- 815	+ 645	+ 117	+ 3,500	+12,775	- 705	+1035[a]	+4590[a]	- 705	-22,900	-83,585	Not Determined
8- 3-1953	-1000	- 5165	- 1750	- 1375	-37,000	-135,050	-1125[a]	-4305[a]	-9835[a]	-1125[a]	-33,400	-121,910	Not Determined
11-23-1953	-6545	-12805	- 4215	- 5380	-45,600	-166,440	+ 715[a]	+4305[a]	-4040[a]	Not Reliable	-	-	Not Determined
3-29-1954	-7880	-13685	- 4175	- 8579	Beyond Range	-	-1465[a]	-7775[a]	-4430[a]	Not Reliable	-	-	Not Determined

[a] Grounded
[b] Inoperative
[c] Before Removal of Struts
[d] After Removal of Struts

+ Sign denotes compression
- Sign denotes tension
Length per foot of formed length: 1 24 ft /ft of formed length
Thickness: 0.2451 in.
Area per ft of formed length: 3.65 in^2/ft. of formed length

These comments are especially true in the case of projects whose frequency of occurrence is very low because of their nature, magnitude, and cost involved, such as North Carolina Highway Project 8521.

To tackle the above problems successfully, in addition to having adequate engineering and physical knowledge of the structures and the materials involved, a statistical outlook must govern the planning of the various experimental procedures and setups.

It is unfortunate to note that in many research projects experimenters tend to con-

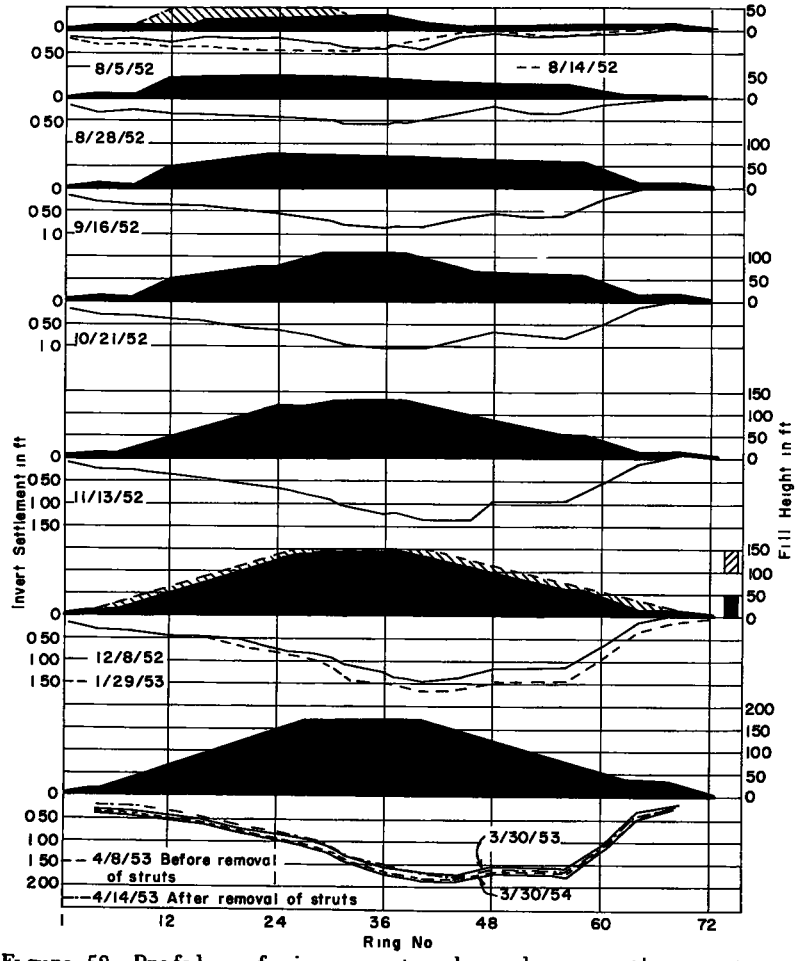

Figure 52. Profiles of pipe invert and overlying earth mass at various stages of fill construction. Datum profiles obtained July 9, 1952.

fuse the two general types of engineering endeavor: (1) projects which are designed primarily to serve an engineering purpose and (2) projects which are set up for research purposes.

In the first type of projects, the main emphasis is given to the overall satisfactory performance and cost of the designed structure. Only that amount of care that can be justified economically is exercised to identify the environmental conditions under which the particular structure will be constructed. To compensate for any uncertainties with respect to the true nature of these conditions, and to account for any future contingencies that are humanly impossible to predict, a factor of safety is always employed in the design of these structures.

The above procedure although necessary for design and safety purposes, renders the task of isolating and controlling various factors influencing the behavior of these struc-

TABLE 7

COMPARISON BETWEEN LEVEL AND MANOMETER - OBTAINED ELEVATION READINGS OF SETTLEMENT CELLS

Ring No.	Cell No.	Elevation by Level - ft.	Elevation by Manometer - ft.	Difference ft.
	1	1888.61	1888.58	+0.03
	2	1888.62	1888.66	-0.04
30	3	1887.75	1887.51	+0.24
	4	1887.14	1886.81	+0.33
	5	1887.81	1887.51	+0.30
	6	1888.08	1887.52	+0.56
	1	1888.29	1887.23	+1.06
	2	1888.15	1888.18	-0.03
31	3	1887.42	1888.22	-0.80
	4	1887.24	1886.90	+0.34
	5	1887.17	1887.09	+0.08
	6	1887.33	1887.18	+0.15
	1	1888.25	1886.61	+1.64
	2	1888.17	1888.68	-0.51
32	3	1887.11	1888.53	-1.42
	4	1886.83	1886.65	+0.18
	5	1886.90	1887.02	-0.12
	6	1887.13	1887.29	-0.16
	1	1886.20	1886.48	-0.28
	2	1886.10	1886.71	-0.61
36	3	1885.58	1886.11	-0.53
	4	1885.75	1885.88	-0.13
	5	1886.11	1886.12	-0.01
	6	1886.17	-[a]	-
	1	1886.29	1886.18	+0.11
	2	1886.09	1886.22	-0.13
37	3	1885.84	1885.80	+0.04
	4	1886.01	1885.86	+0.15
	5	1886.29	1886.24	+0.05
	6	1886.48	1886.38	+0.10
	1	1886.20	1886.25	-0.05
	2	1886.17	1886.25	-0.08
38	3	1886.16	1885.98	+0.18
	4	1885.83	1885.74	+0.09
	5	1886.17	1886.20	-0.03
	6	1886.21	1886.15	+0.06

[a] Cell inoperative.

tures extremely complicated, if not impossible. Furthermore, the introduction of a factor of safety sometimes results in altering the original nature of the environmental conditions thus making the research problem even more complicated. Consequently, in such types of projects, only general conclusions may be drawn regarding the factors influencing the performance of the various structures.

In the second type of projects, no factor of safety is employed in the structural design. Instead, extreme care is taken to isolate, control and study all possible factors that are believed to exercise a decisive influence on the behavior of the structure in question. Particular efforts are made to determine the conditions of ultimate failure.

With such setups one can draw definite conclusions regarding the effect of various

factors upon the performance of a given structure. Furthermore, if a multitude of projects of this type are set up under identical conditions, one may be able to use statistical methods to ascertain:

1. Whether the behavior of an actual material under given conditions may be predicted by mathematical equations that are based on the laws of pure mechanics and that describe the behavior of ideal materials.
2. Whether the physical properties of the materials involved may be accounted for

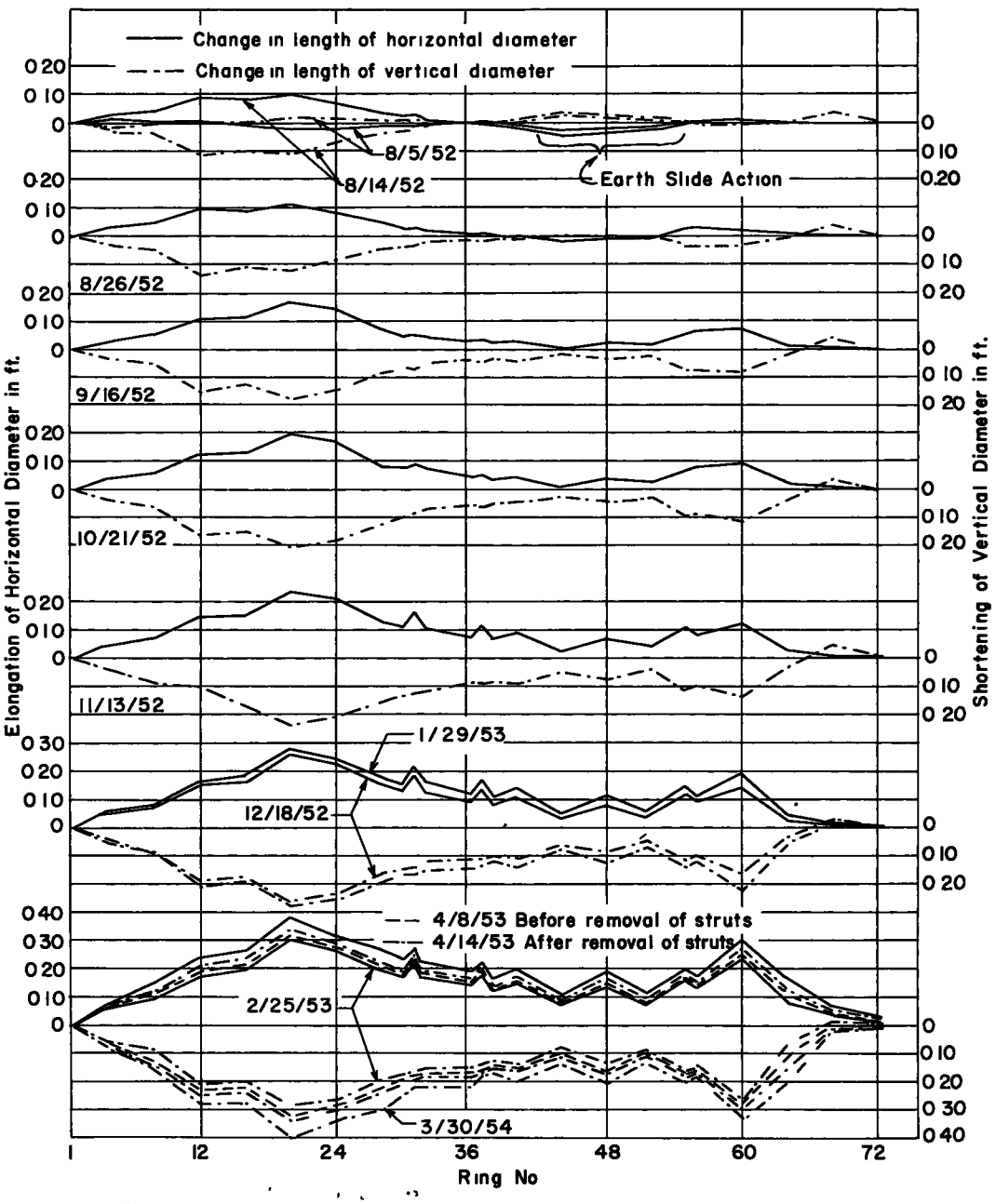

Figure 53. Elongation and shortening of horizontal and vertical pipe diameters at various stages of fill construction. Datum: readings obtained July 9, 1952.

in the above equations by assuming equivalent physical constants as working hypotheses.

3. The ranges of the equivalent physical constants that may be expected for given materials and installation conditions.

Only under the above conditions can a set of mathematical equations be considered to

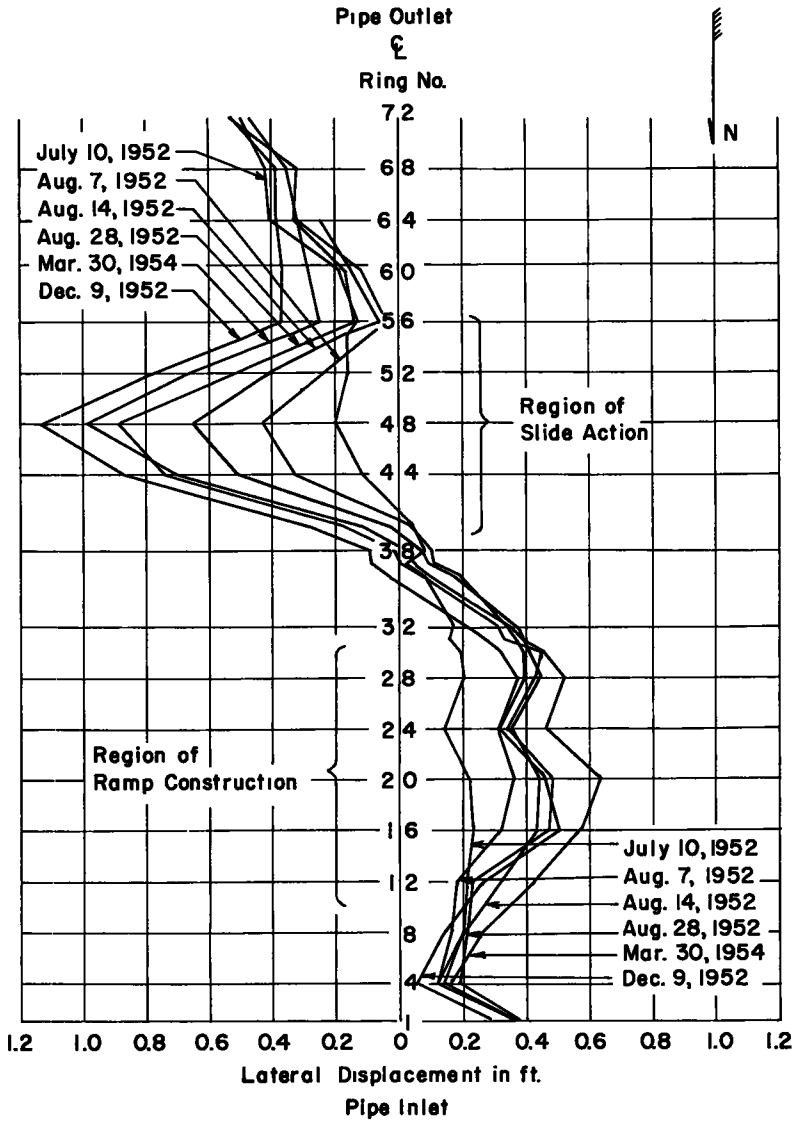

Figure 54. Lateral profiles of pipe center line at various stages of fill construction. Datum original center line, established by surveying equipment.

constitute the "theory" of a corresponding cause-effect proposition.

Unfortunately, as mentioned previously, some theorists confuse the nature of the setup that may actually exist in a given project. In doing so, they may obtain certain entirely uncontrolled, raw data from an installation that is not primarily set up for research purposes, substitute these data into their mathematical equations that have been derived for ideal conditions, and by adjusting conveniently the physical constants of these equations, they may arrive at results agreeing with the ones that their theories predict. Thus, they develop a false sense of satisfaction. The above comments are particularly true in problems dealing with the behavior of soil masses.

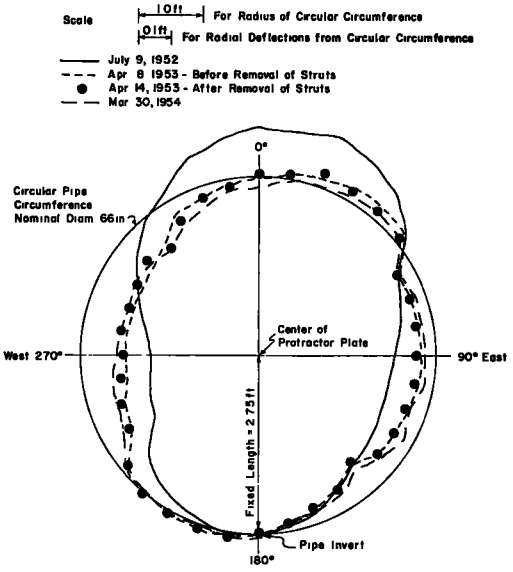

Figure 55. Schematic diagram of pipe cross section at Ring 31. Obtained by pipe protractor measurements. Looking upstream.

North Carolina Project 8521 belongs to the first of the above described cases. The culvert with the overlying fill was primarily designed to serve an engineering purpose, i.e., to bridge a valley so that a highway could pass through. Nevertheless, it was later called upon to serve as an experimental setup for the study of a two-fold problem, the phases of which are closely interrelated: (1) the behavior of a high earth fill supported by a foundation, a strip of which (the culvert installation) yields more than the adjacent parts and (2) the behavior of a flexible conduit under the action of external pressures exerted by the surrounding earth mass.

Therefore, in the light of the previous discussion, before any conclusions are drawn from the experimental findings and before any generalizations are made relative to other projects of similar nature, the conditions under which this investigation was carried out must be examined closely. Accordingly, the following facts should be emphasized once again before any attempt is made to analyze the obtained data item for item:

1. The earth fill was constructed with some of the most unorthodox procedures. Not only was the fill material end-dumped, a procedure which by itself defies good construction practice, but it was deposited on top of the pipe in an unbalanced and almost haphazard way. The best that can be said for such procedure from a construction point of view is that all chances of reasonable analysis and rational expectations are minimized and the future of the culvert structure is thrown on the capricious mercy of sheer luck.[10]

2. The fill material ranged from rock fragments with largest dimension of about 6 feet to highly micaceous sandy-clayey-silty fines. This material was not placed in layers but was compacted by the pass-

[10] On account of the same construction methods, another Multi-Plate, corrugated metal pipe of the same project, 568 feet long, 60 inches in diameter, installed at Station 245+69 under 136 feet of fill, deformed appreciably on one side indicating that the resultant force from the fill overburden had been transmitted to the structure at an angle of about 30 to 40 degrees with the vertical. Although the culvert did not collapse and still functions satisfactorily, shear ruptures 3 inches long and open about ⅛ inch appeared at the bolted connections along Rings 21-27. The situation was alleviated by interrupting the one-sided, unbalanced, end-dumping operation and by placing 6-inch by 6-inch timber struts diagonally on the shortest diameter of the deformed pipe at approximately 2 foot centers and wedged as tight as possible along Rings 21-28.

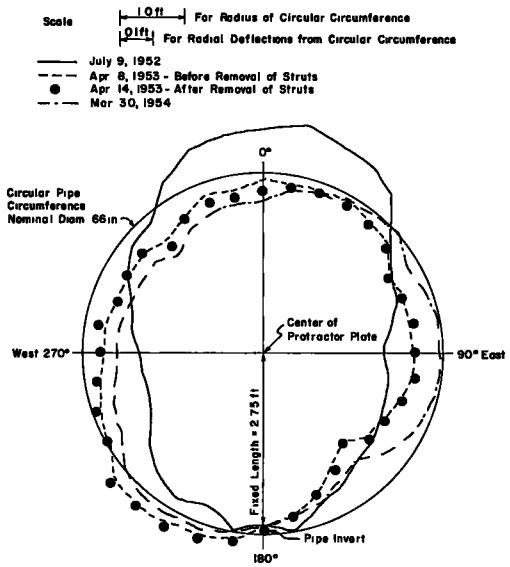

Figure 56. Schematic diagram of pipe cross section at Ring 37. Obtained by pipe protractor measurements. Looking upstream.

age of end-dumping equipment, and by its own weight. As is expected from such methods of compaction, normal segregation processes caused the coarser fragments of this material to pile up toward the edges of the fill leaving the core with more or less finer parts. Therefore, it can hardly be said that the fill constitutes an overall homogeneous earth mass with statistical average physical properties such as unit weight, internal friction, cohesion, etc.

3. The pipe was designed with a factor of safety of 4 which is a standard flexible pipe design. Such design made the supposedly yielding foundation of the fill overburden four times as rigid as required for the anticipated vertical load. As the load is a function of the rigidity of the conduit it can be expected to alter also. Furthermore, the stiffness of the conduit varied along its length. In the middle section, the structural plates were made of No. 1 gage metal, they were bolted by 6 bolts per foot of longitudinal joint, and they were further stiffened by struts spaced at 3 foot centers. Toward the ends, the gage of the plate was reduced to No. 8, the bolt spacing was 4 bolts per foot of longitudinal joint and strut spacing was increased to 6 foot centers. Therefore, if the conduit structure deformed a greater amount at some points one cannot ascertain whether the excessive deformations were caused by a greater amount of external earth pressure or from a lack of inherent resistance to deformation of the conduit structure at the respective points.

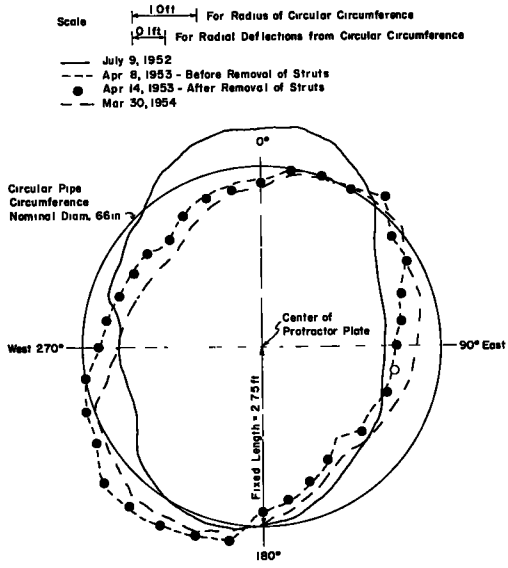

Figure 57. Schematic diagram of pipe cross section at Ring 55. Obtained by pipe protractor measurements. Looking upstream.

4. To add to the confused conditions, an earth slide occurred during the installation of the culvert throwing the pipe out of alignment and introducing a multitude of additional stresses of diversified nature in the structure. The action of the slide continued well beyond the date on which the pipe was realigned. Therefore, it would be rather absurd for one to attempt a stress analysis on this structure from the deformations and strains obtained.

From the above discussion it is evident that only general conclusions may be drawn from the data obtained. The best way for one to utilize these data is to attempt to account for all possible factors that may have influenced the performance of the conduit without trying to pin down the amount of influence exercised by each individual factor. Generalizations cannot be drawn from such installation. Only recommendations can be made with the hope that in the future, job construction procedures unfavorable to research, such as the one followed in this installation, will not be repeated.

Analysis of Data from the Deformations of the Culvert

In the light of the discussion in the previous section one intuitively develops a sense of the degree of refinement that he is justified to use in analyzing the experimental data collected from this project. Accordingly, as a first comment concerning the performance of the pipe line one may quote a humorous remark made by a member of the engineering personnel of the N. C. State Highway and Public Works Commission: "As long as I can still see through the pipe and as long as water still gets through it, the pipe holds good!"

Probably the above comments are the only factual conclusions that one is justified to draw regarding the performance of the culvert under study. However; as a second thought one may ask himself: "Well, what makes it hold 'good'? And what makes it maintain an almost cylindrical shape as shown in Figure 70?" Then he begins to specu-

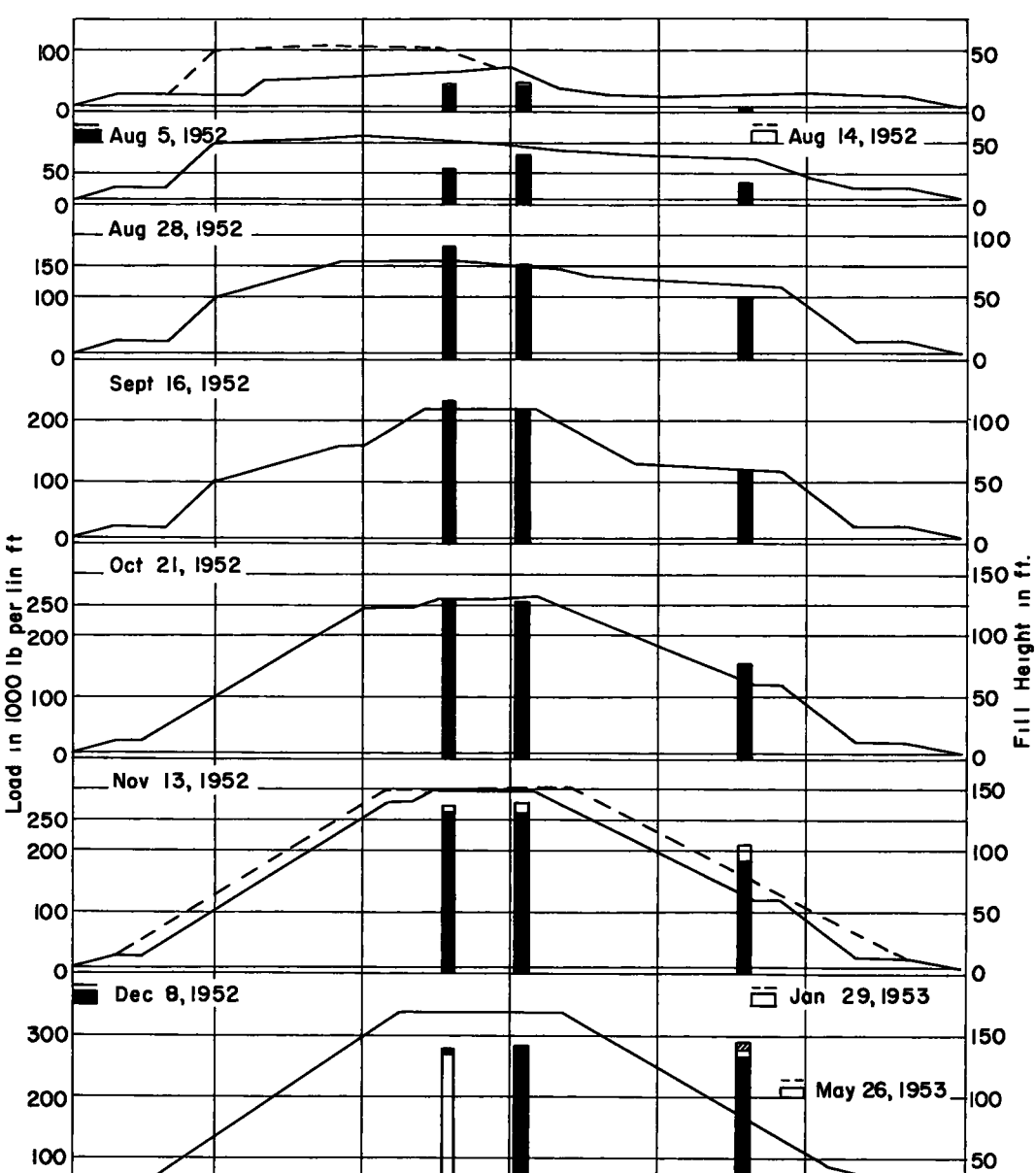

Figure 58. Vertical load in lb. per lin. ft. at various stages of fill construction. Obtained from strain gage measurements.

late and feel a certain sense of mechanical equilibrium that must exist between the pipe structure and the surrounding earth mass in order that the pipe may still maintain its shape. If the distribution of external pressures around the pipe structure were not substantially uniform, the pipe, whose rigidity is negligible when related to the overburden pressures exerted by a 170 foot high earth mass, would have collapsed by excessive deformation under differential pressures of appreciable amount.

Furthermore, if the external pressures had induced circumferential stresses exceeding the critical buckling load of the structure or the shearing strength of the bolts by means of which the corrugated plates are connected, the pipe would have failed either by local buckling or by shearing of the plates. No such indication has been observed in the numerous inspections made of the job. Therefore, the following two speculative conclusions may be drawn with regard to the external pressures generated against the pipe structure:

1. The external pressures around the culvert must be substantially uniform.
2. The magnitude of these pressures is such that the circumferential stresses induced in the pipe structure have not exceeded the critical bulking load of the culvert nor

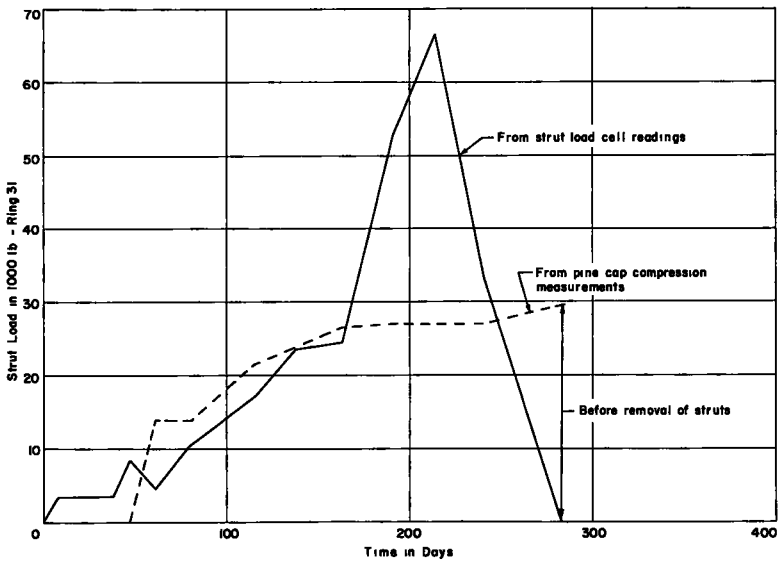

Figure 59. Strut load in 1000 lb. vs. time in days at Ring 31.

the shearing strength of the seam bolts.

As a second step in the process of examining the data obtained, one would be interested in gathering some information regarding the effect of the various phases of the fill construction on the settlements of the masses surrounding the pipe as well as on the deformations that the pipe itself underwent. Data giving such information have been gathered by level, extensometer, plumb bob and pipe protractor. The degree of accuracy of such information depends on the instruments themselves, their precision, and also on the conditions under which the technician was obtaining the data. Nevertheless, these data represent actual direct measurements and, therefore, the picture given by them should be considered factual. One, therefore, may make the following comments regarding these data.

From the invert profile curves of Figure 52 it can be seen that:

1. The flow line of the culvert settled in such a manner that its profile was almost a reflection of the image of the cross section of the overlying fill at every stage of the fill construction.
2. For every fill increment there was a settlement increment.
3. The settlement of the flow line for all practical purposes ceased upon the completion of the fill, increasing only a minute amount in the following year.
4. The maximum measured differential settlement was 1.59 feet. The pipe was installed with a camber of ¼ percent of the pipe length, i.e., the maximum ordinate from the straight line base, was 1.44 feet. Therefore, it seems that the actual differential settlement exceeded the anticipated one by 0.15 foot.
5. The influence of the slide on the pipe flow line may be seen in the data of August 14, 1952 in which an upward movement is indicated along Rings 37-48.

The data from the measurements of the vertical and horizontal diameter of the culvert (Figure 53) indicate that:

1. For every fill increment there was a corresponding change in the length of the vertical and horizontal diameter of the pipe.
2. The pipe bulged out laterally an amount equal to its vertical shortening. The corresponding curves are the image of each other.

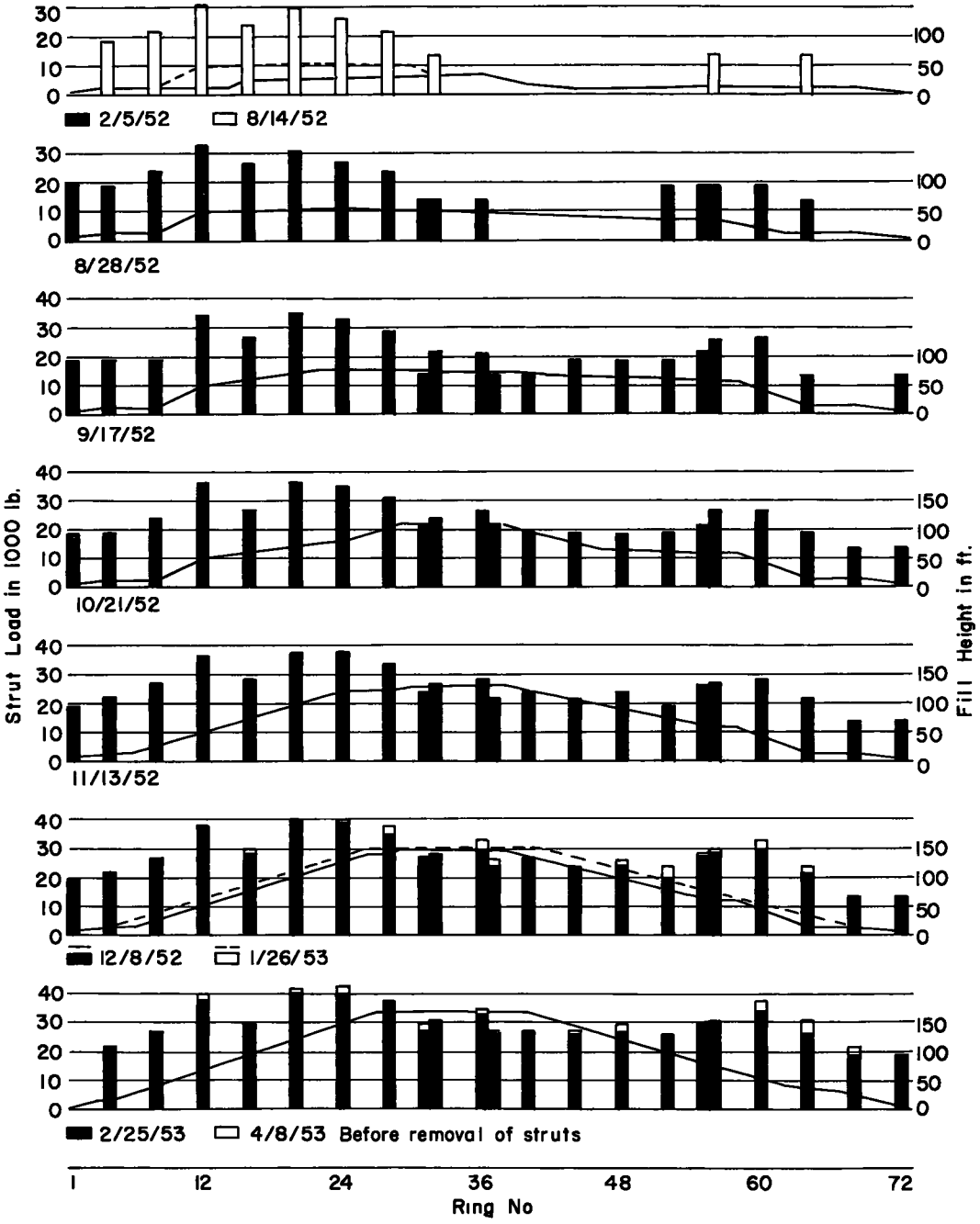

Figure 60. Strut load at various stages of fill construction. Obtained from pine compression cap measurements.

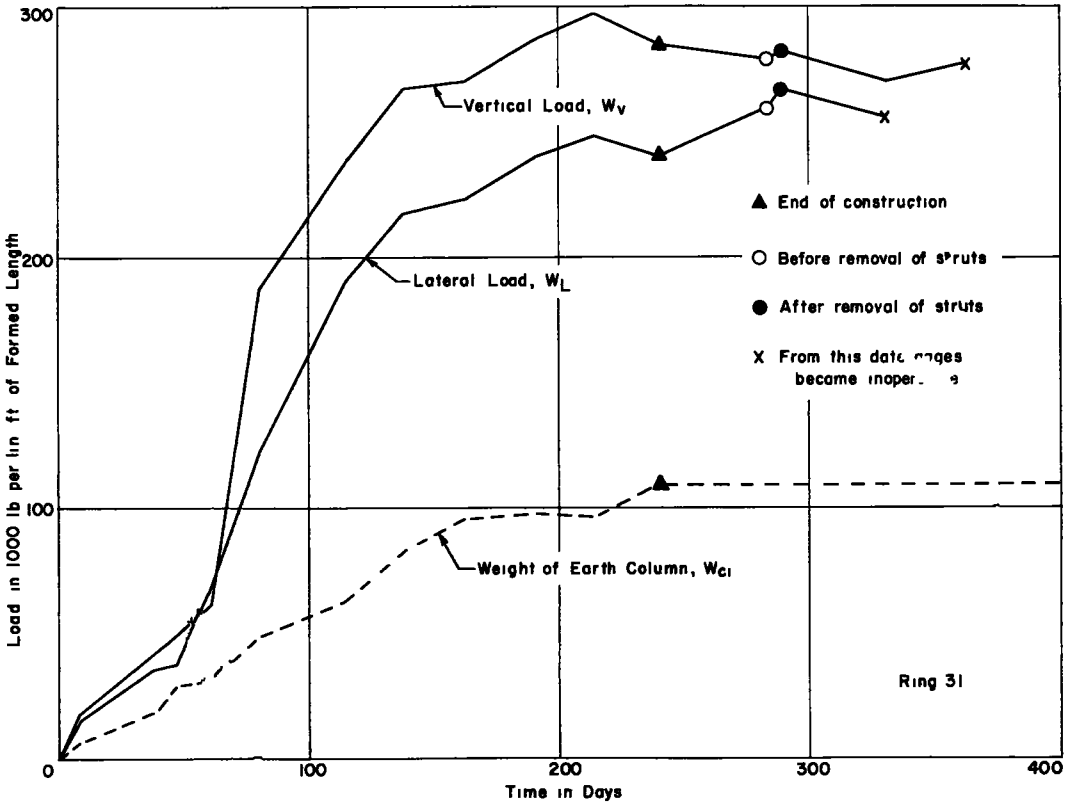

Figure 61. Vertical and lateral conduit earth loads vs. time, evaluated from strain gage, strut load cell, and pine compression cap measurements. Ring 31.

3. At the point of maximum deformation, i. e., at Ring 20, the pipe deformed 1. 4 times the amount recorded on the date the fill was completed. This indicates a maximum deflection lag factor of 1. 4.

4. The maximum measured shortening of the vertical diameter occurred at Ring 20 and it was found to be 0. 40 foot. At the same point the initial vertical diameter was 5. 58 feet, i. e., the pipe had been elongated vertically 1. 45 percent by field strutting. Therefore, the overall vertical shortening, based on the nominal circular pipe diameter of 5. 5 feet, was 5. 82 percent. This is well below the 20 percent deflection considered to be a failure condition by the design specifications. However, considering the fact that a factor of safety of 4 has been used in the design of the structural plates, the actual deflection exceeded by 0. 82 percent the one that was anticipated with the assumed loading conditions.

5. The pipe deflected more at the quarter points than at the middle section. This could be due to the following reasons: (a) load transfer from the middle section of the fill toward the quarter points as a result of arching action in the soil mass occurring in a longitudinal direction;[11] (b) the fact that the side supporting material at these sections had not been precompacted as much as at the middle section. Although no information exists from the first nineteen rings, the data from the initial compaction of the side supporting material indicate that, generally, this material had been compacted to a higher degree at the middle section of the pipe line than at the quarter points or the end sections (Figure 51). (c) The structural plates at the quarter points and the end sections of the pipe line were made of No. 3 and 8 gages, whereas the plates of the middle section

[11] See References, Costes, 1955, p. 100.

were made of No. 1 gage metal. Therefore, the conduit exhibited a lower inherent resistance to deformation at the quarter points and the end sections than at the middle section. (d) A greater strut spacing at the quarter points and at the end sections of the pipe line provided less resistance to vertical deflection than at the middle section of the conduit. (e) A combination of the above reasons discussed in parts (a) - (d).

6. The influence of the slide can be seen by the first two sets of data of Figure 53. Under the pressure exerted by the sliding material in the region between Rings 36 and 56, the sides of the pipe were squeezed-in while the structure bulged out vertically, despite the fact that the initial compaction of the side supporting material at the same region and especially in the vicinity of Ring 48 (Figure 51) was considerably lower. At later dates, however, when sufficient overburden had been accumulated on top of the pipe the structure started deforming as anticipated.

7. The influence of the removal of the struts is shown by the data of April 14, 1953 in which sudden jumps can be detected in the vertical and lateral deformations of the pipe (Figure 53). Such behavior indicates that the material surrounding the pipe is highly elastic as was expected from its description and its physical characteristics (Tables 1-4).

The data from the lateral profile of the pipe axis indicate (Figure 54) that the action induced by the sliding material did not stop after the pipe was realigned. Instead, it continued being active until the fill had been raised to approximately 150 feet in the middle section as shown in the data of December 9, 1952. From then on, however, no appreciable deformation occurred and the last set of data obtained about two years and four months later indicate slight movement in a reverse manner.

The above lateral profiles indicate also that the construction of the fill ramp on top

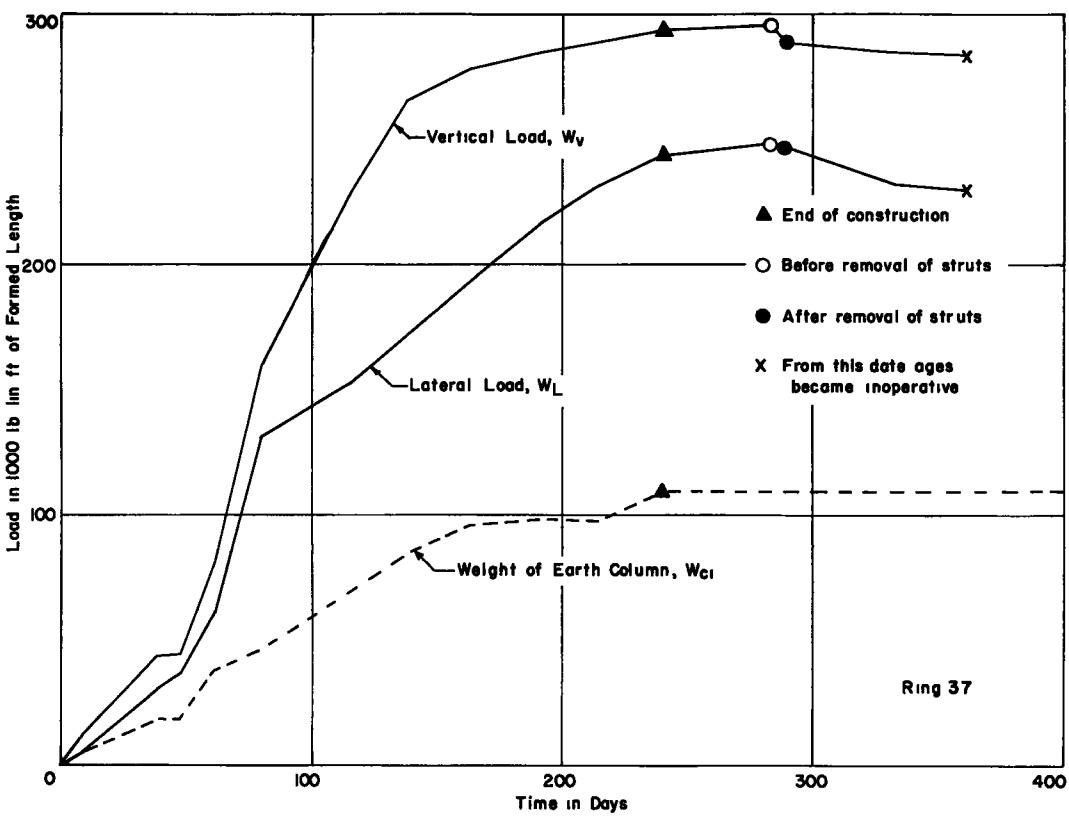

Figure 62. Vertical and lateral conduit earth loads vs. time, evaluated from strain gage, strut load cell, and pine compression cap measurements. Ring 37.

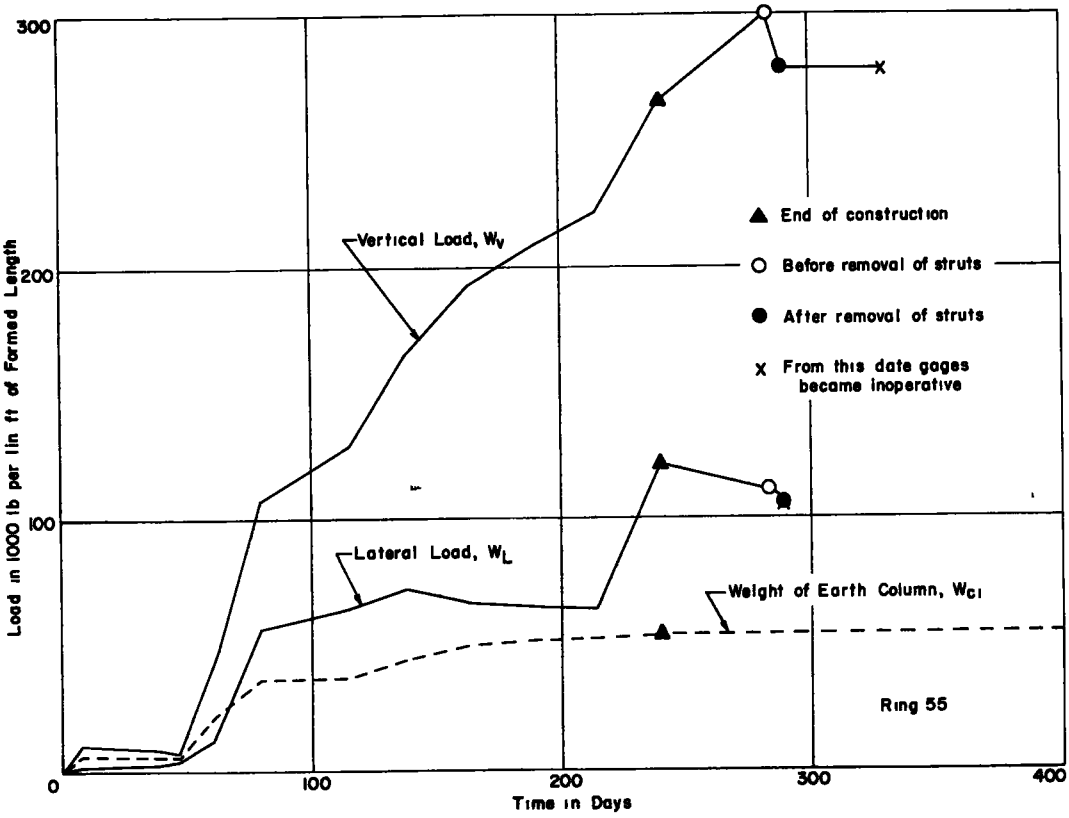

Figure 63. Vertical and lateral conduit earth loads, evaluated from strain gage, strut load cell, and pine compression cap measurements. Ring 55.

of the culvert[12] had a considerable influence on the pipe line. As the ramp material was hauled and end-dumped from the east it caused the pipe to be displaced westwardly along the region where the ramp was constructed (Figure 54).

From the above discussion one may speculate on the two main lateral movements observed in the pipe line and arrive at the conclusion that bending stresses have been induced on the sides of the culvert in addition to any other existing stresses. These stresses must attain maximum values at or about Rings 20 and 48, whereas they must tend to vanish toward the middle section of the pipe line. The latter section, therefore, could be considered to be, after a fashion, a point or a region of contraflexure where no lateral bending stresses exist and the curvature of the analogous pipe-beam reverses its sign.

The diagrams of the pipe cross sections plotted in Figures 55, 56, and 57 from the pipe protractor data indicate that:

1. In the middle section of the pipe line where Rings 31 and 37 are located, the load was more or less vertical causing the pipe to bulge out laterally with a corresponding shortening of its vertical diameter. However, at Ring 55 there is a strong indication that the load came at an angle and from the west. This confirms the indication of previously mentioned data that the action of the slide continued in a latent manner a long time after the pipe had been relatively realigned and the sliding material immediately adjacent to the culvert had been removed.

2. The removal of the struts, for all practical purposes, did not affect the shape of the pipe structure. Only small deformations have been recorded giving further indication that the material surrounding the pipe reacted in an elastic manner following the strut removal.

[12] See Construction Procedure.

3. The pipe for all practical purposes ceased to deform upon the completion of the fill. However, data obtained at intermediate stages of the fill construction that have not been plotted on Figures 55, 56, and 57 indicate that for every fill increment there was a corresponding change in the shape of the pipe which, no matter how small in magnitude, was detected by the apparatus employed.

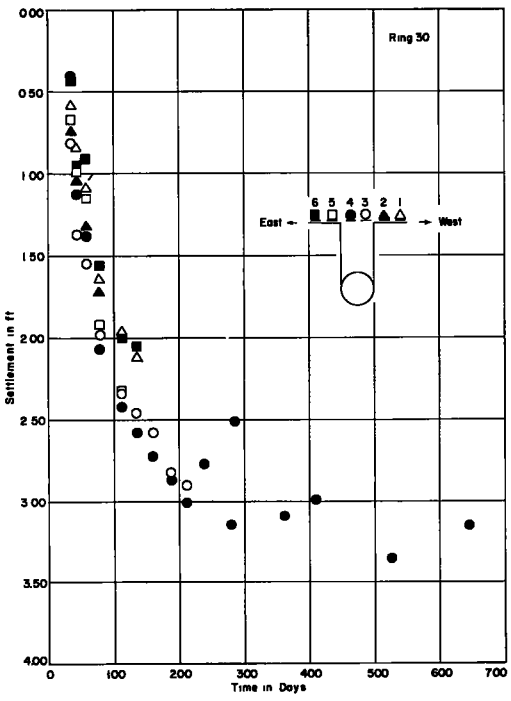

Figure 64. Settlement cell data at Ring 30. Looking downstream.

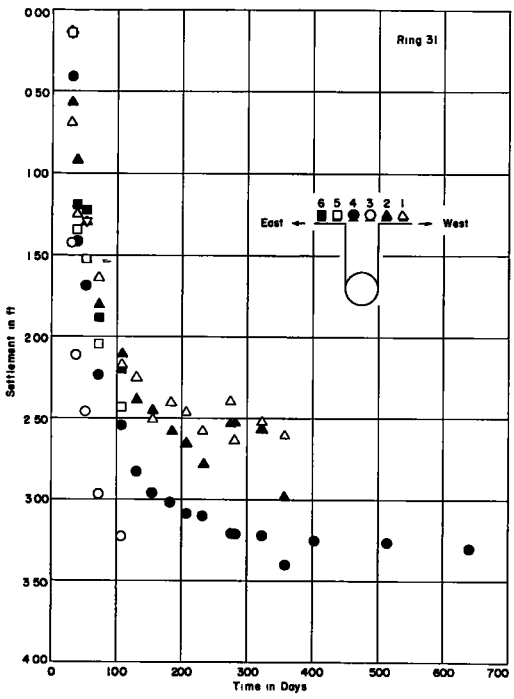

Figure 65. Settlement cell data at Ring 31. Looking downstream.

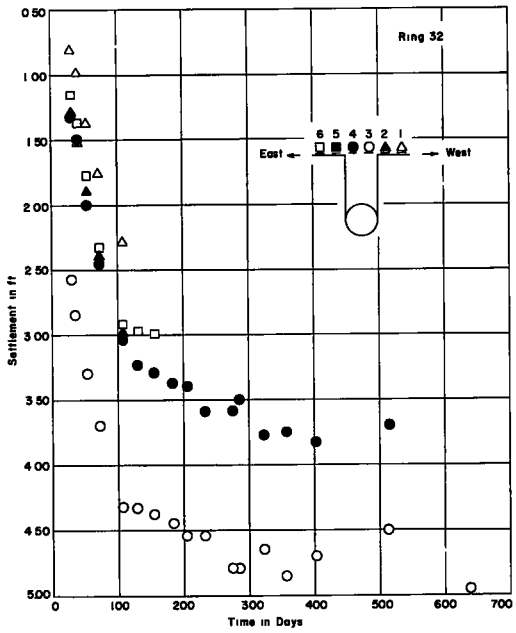

Figure 66. Settlement cell data at Ring 32. Looking downstream.

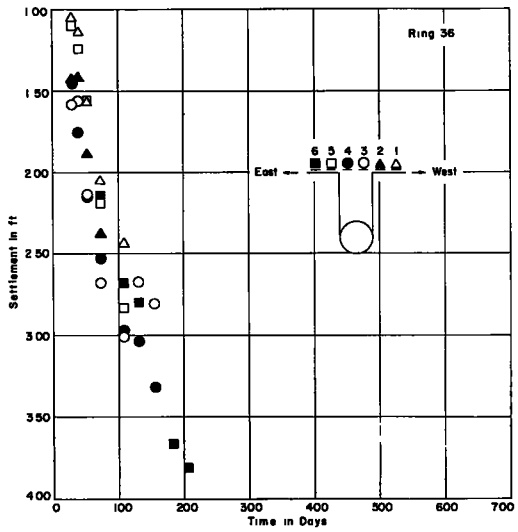

Figure 67. Settlement cell data at Ring 36. Looking downstream.

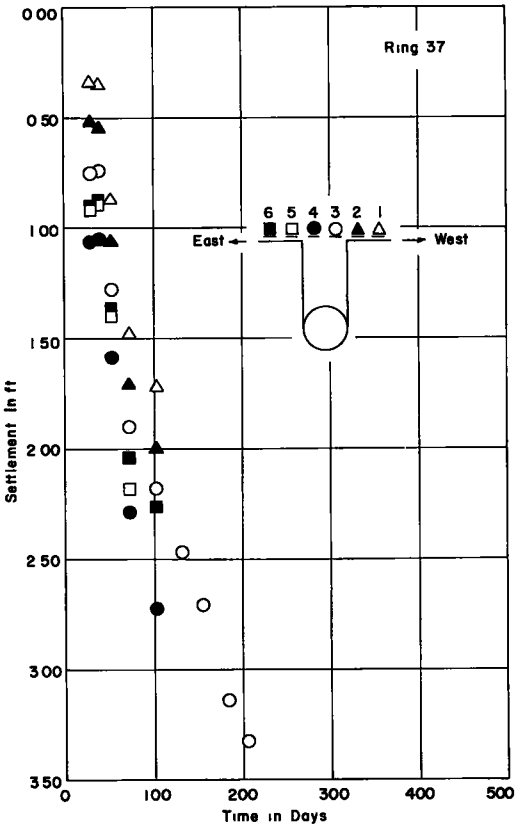

Figure 68. Settlement cell data at Ring 37. Looking downstream.

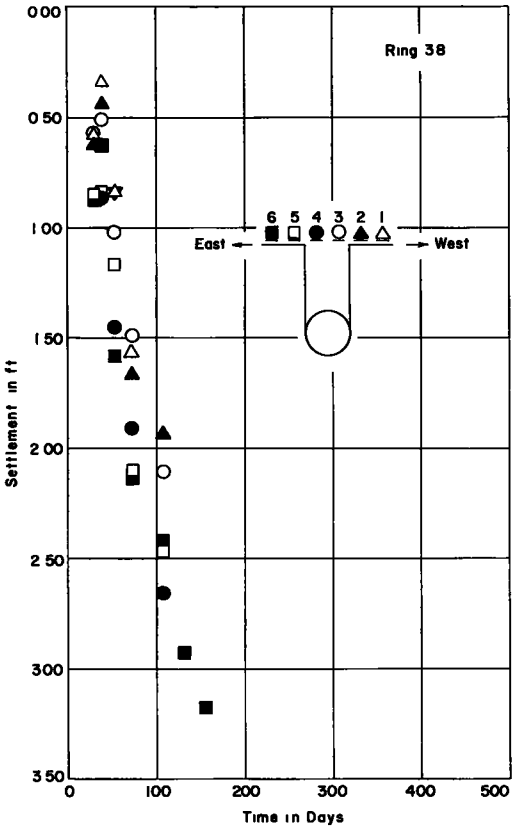

Figure 69. Settlement cell data at Ring 38. Looking downstream.

4. The pipe rotated a small amount about its flow line toward the east at Rings 31 and 55. Such action is expected to have introduced tangential circumferencial stresses in the pipe structure.

5. No further refinement of the analysis of the above data is justified. However, if the deformations of the pipe circumference were measured as radial deflections from a reference center that could always be kept fixed with respect to the initial shape of the circumference, one could utilize the principles of strain energy and Castigliano's theorem to make an extensive analysis of the data, and to determine the distribution of the external pressures that caused these deformations.

If the pipe deformations were measured from a fixed center, then, a rough estimate could be drawn with respect to the distribution of bending moments around the pipe circumference. In such case the initial shape of the ring could be considered as a funicular curve for the external pressure and the areas enclosed by the initial shape and the deflected shape could be considered to be bending moment diagrams drawn to some scale (Timoshenko, 1936).

Discussion of the Behavior and Data Obtained from the Side Supporting Material of the Culvert

Since the early stages of the fill construction, the authors of this paper have been deeply concerned with the physical properties and the behavior of the material that was placed by pneumatic tamping to furnish side support to the culvert under study. It was realized that side supporting materials in general play a very important role in the structural behavior of underground conduits. If these materials are properly selected and compacted, they mobilize and exert against the conduit sides lateral pressures that tend to balance the loading action of the overburden pressures existing on top of the

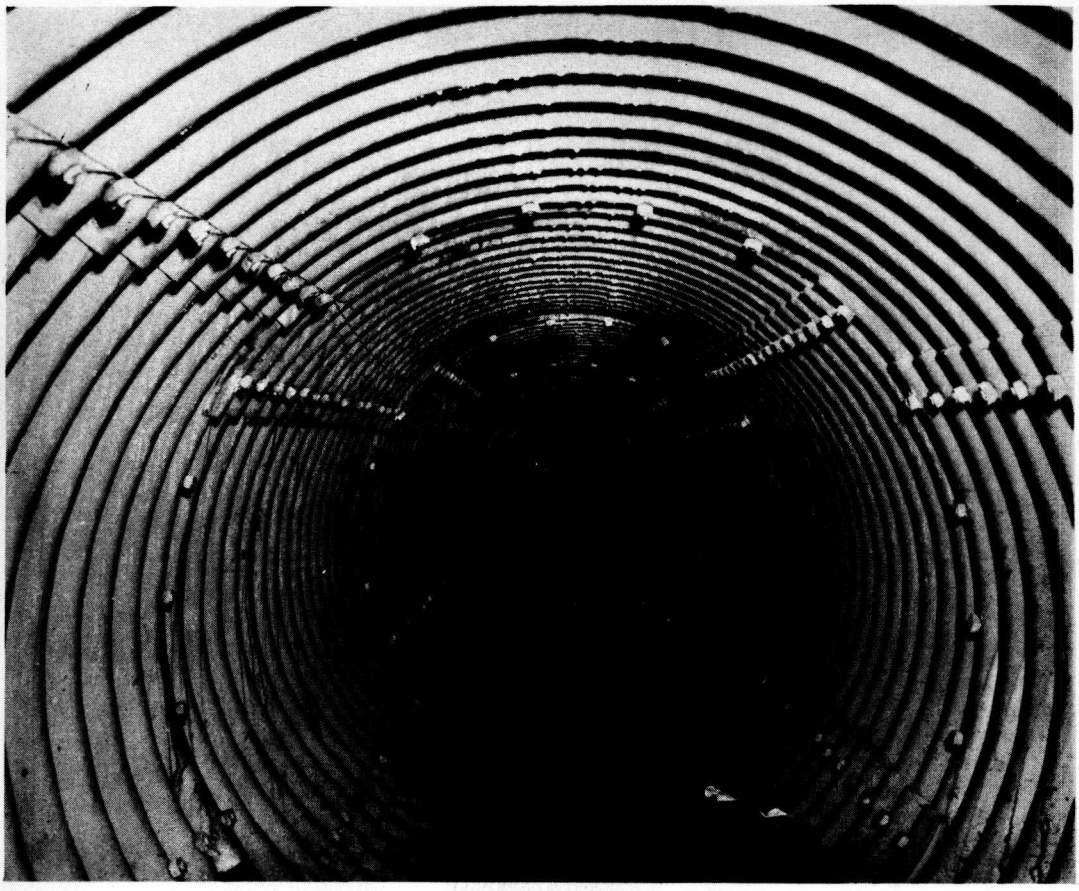

Figure 70. Pipe interior two years after installation.

conduits. Through this action a mechanical equilibrium is established in the conduit-earth mass systems and the conduit structures cease to deform under the pressure of the top earth loads. It follows then that through side supporting materials underground conduits gain additional structural strength on account of which even conduits of low inherent rigidity are able to sustain relatively enormous overburden pressures and to function satisfactorily without failing either in shear, or by excessive deformation, or in buckling.

From a general knowledge of the behavior of earth masses, one realizes that the sides of a conduit are subjected to lateral earth pressures of a two-fold nature: (1) lateral pressures that are mobilized by the side supporting material as a result of lateral bulging of the conduit that subjects the earth mass to compression, and (2) lateral pressures that are exerted by the side supporting material on account of its own weight and that of the portion of the effective fill surcharge that it sustains.

The first type of lateral pressures depends on the nature, size and compaction of the side supporting material, the area of contact between the conduit side surface and the side supporting material, the shape of the conduit, the permeability of the side supporting material, the rate of stress application, and the total amount of lateral movement taking place on account of the lateral bulging of the conduit. Spangler assumes that the above pressures have a parabolic distribution and that they are directly proportional to the lateral deflection of the conduit. The constant of proportionality, e, is termed "modulus of passive resistance;" it is expressed in psi. per in. of lateral pipe deflection, and it is assumed to be a constant physical property of the side supporting material depending on the nature and the compaction characteristics of this material (Spangler 1937, 1946, 1948, 1951-1952).

The second type of lateral pressures depend on the nature, extent and compaction of the side supporting material as well as on the vertical pressures generated within the side earth mass due to the weight of the mass and the surcharge that it sustains. For a homogeneous earthen material that has been compacted uniformly the above lateral pressures have a more or less hydrostatic distribution being directly proportional to the corresponding vertical pressure existing in the same earth mass. The constant of proportionality is generally designated by the symbol "K." Under the above conditions, and if no deformations take place in the side supporting material, K varies between the limits zero, in which case the side supporting material would exhibit properties of an infinitely stiff, rigid block, and unity, in which case the same material would behave like a liquid.[13] From the above it follows that K depends on the nature and compaction of the side supporting material and on the surcharge that this material sustains. Generally, the higher the compaction of the side supporting material and the higher the magnitude of the vertical pressure within this material,[14] the higher will be K and, accordingly, the higher will be the lateral pressures exerted against the sides of the conduit.

Conduit theories have neglected so far the presence of this latter kind of lateral earth pressures. These theories assume that the only lateral pressures existing at the sides of a conduit are those mobilized by the compressive action of the conduit bulging (Spangler, 1937, 1946, 1948, 1952). Such assumption is on the safe side and sufficient to calculate conduit deflections for low or medium height fills. However, when an earth fill is made as high as the one under study one cannot neglect the second type of lateral earth pressures without being at considerable variance with reality.

To illustrate the above consider the following example:

Effective fill height including effect of arching stresses, H_{eff} = 170 ft.
Average unit weight of fill material, γ = 120 pcf.
Coefficient of hydrostatic earth pressure, K = 0.5.

Then, the intensity of the hydrostatic lateral earth pressures, p_h, exerted by the side supporting material against the conduit sides will be:

$$p_h = K \gamma H = (0.5)\ (120)\ (170) = 10,200 \text{ psf.} \qquad (1)$$

Now assume that the maximum lateral deformation of the conduit is 2 inches on each side and that the modulus of passive resistance, e, is 30 psi. per inch of deformation. This value represents an average value for normal compaction efforts.

Then, the maximum intensity of the reactive lateral pressures, p_{r1}, mobilized by the side supporting material against the sides of the conduit will be:

$$p_{r1} = \frac{\Delta x.\ e}{2} = (2)\ (30) = 60 \text{ psi.} = 8,640 \text{ psf.} \qquad (2)$$

If e were equal to 40 psi. per in. of lateral deflection, then the corresponding p_{r2} would have been:

$$p_{r2} = (2)\cdot(40) = 80 \text{ psi.} = 11,520 \text{ psf.} \qquad (3)$$

Compare the last two values of p_r with the above value of p_h (Equation 1) to see the relative magnitude of the two kinds of lateral pressure components. If the overall lateral pressure, $p_{lat.}$, were measured directly, one would have obtained respectively:

$$p_{lat.\,1} = p_{r1} + p_h = 18,840 \text{ psf.} \qquad (4)$$

and

$$p_{lat.\,2} = p_{r2} + p_h = 21,720 \text{ psf.} \qquad (5)$$

---

[13] For natural granular earth deposits, K has been found experimentally to vary between 0.45 and 0.55. In such cases it is called, "coefficient of earth pressure at rest" and it is designated as K_o. The value of K_o for cohesive materials is not known yet.

[14] Vertical pressures within the side supporting material are induced by the weight of the material, by the fill surcharge that it sustains, and by stresses due to arching phenomenon that will be discussed in detail in the next part of this section. The latter stresses may be thought of as an additional surcharge on top of the side supporting material.

Accordingly, if the above overall lateral pressures were assumed to be purely reactive pressures, p_r, mobilized by the side supporting material on account of the overall 4-inch lateral deformation of the conduit, the corresponding equivalent values of e for the above earth mass would have been respectively:

$$e_{Eq.\ 1} = \frac{18,840}{2 \times 144} = 65 \text{ psi. per inch of lateral deflection,} \quad (6)$$

and

$$e_{Eq.\ 2} = \frac{21,720}{2 \times 144} = 72 \text{ psi. per inch of lateral deflection.} \quad (7)$$

In other words the equivalent values of e would have been approximately twice as high as the actual values of e of the same side supporting material.

The above discussion may give some clues for certain unusually high values of e reported from conduit installations under high fills (Spangler and Phillips, 1955). It is suspected that one of the main reasons for such high values is the fact that these quantities have been computed on the assumption that only reactive lateral pressures have been mobilized against the sides of these conduits whereas the presence of hydrostatic lateral pressures due to the fill surcharge on top of the side supporting material and the arching stresses has been entirely neglected.

By considering the above hydrostatic lateral pressures one may also explain rationally the reason for the successful installation and satisfactory performance of rigid conduits under high fills. It would seem impossible for these structures to deform laterally an amount sufficient to mobilize reactive lateral pressures balancing the tremendous overburden loads without cracking seriously. Therefore, had it not been for hydrostatic lateral pressures built gradually on the sides of these conduits for each fill increment, the above structures would have collapsed by shear failure on account of large unbalanced differential pressures concentrated at their top and bottom sections.

From the above discussion it follows that the less compressible is a side supporting material and the higher the degree of its initial compaction, the greater will be: (1) the magnitude of the lateral reactive earth pressures mobilized by the side supporting material on account of the lateral bulging of the conduit; and (2) the magnitude of the lateral pressures exerted by the side supporting material on account of its own weight, and the vertical pressures induced in its mass by the effective surcharge that it sustains.

From the analytical evaluation of the earth load on top of the conduit (see page 127) it will also be seen that the stiffer is the side supporting material, the greater will be the tendency of the soil mass directly above the conduit to arch over the adjacent bodies, thus relieving the top of the structure from part of its overburden pressure and increasing the lateral pressures on its sides through the surcharge action of the arching stresses.

As a result of the above discussion one can see clearly that there is a definite need, especially for high fill conduit installations for the development of rational methods through which specifications can be written regarding: (1) the nature of the side supporting material to be used for a given installation; (2) the method of placing and the minimum degree of initial compaction of the side supporting material for the satisfactory performance of a given installation; and (3) the size of the surrounding supporting mass for a given installation.

The above specifications are necessary because it is realized that certain earthen materials, even though compacted to the optimum amount by the available method of compaction, are not capable of mobilizing sufficient reactive lateral pressures because they fail in shear. Accordingly, on account of plastic flow conditions, the above materials will yield by an amount exceeding the maximum allowable lateral deformation of the given conduit. It is also realized that even if a material meets the first specification it still may not develop the required lateral pressures unless it is compacted by the proper method and to a necessary optimum degree of compaction. Furthermore, if the size of the abutting mass does not meet a required minimum, the side supporting material may act as an integral part of a conduit structure (made of thick walls) and push into the adjoining fill mass without developing the required pressures. Such action will still result in the failure of the conduit as if there were no side supporting material on its sides at all.

Such specifications can only result from an abundance of data obtained from various installations, successful or not. The conditions under which this culvert was installed and the methods by which the fill was constructed have already been described. Nevertheless, from the shape and present condition of the pipe, one may conclude that despite this unorthodox installation the nature, size, and compaction of the side supporting material were sufficient for this material to mobilize the necessary lateral pressures for a satisfactory performance of the conduit. Therefore, the data from this installation may be used for an overall compilation of data on successful installations.

The nature and precompaction of this material have already been presented in Tables 1 and 2, and in Figure 51. The approximate size of this mass may be deduced from the

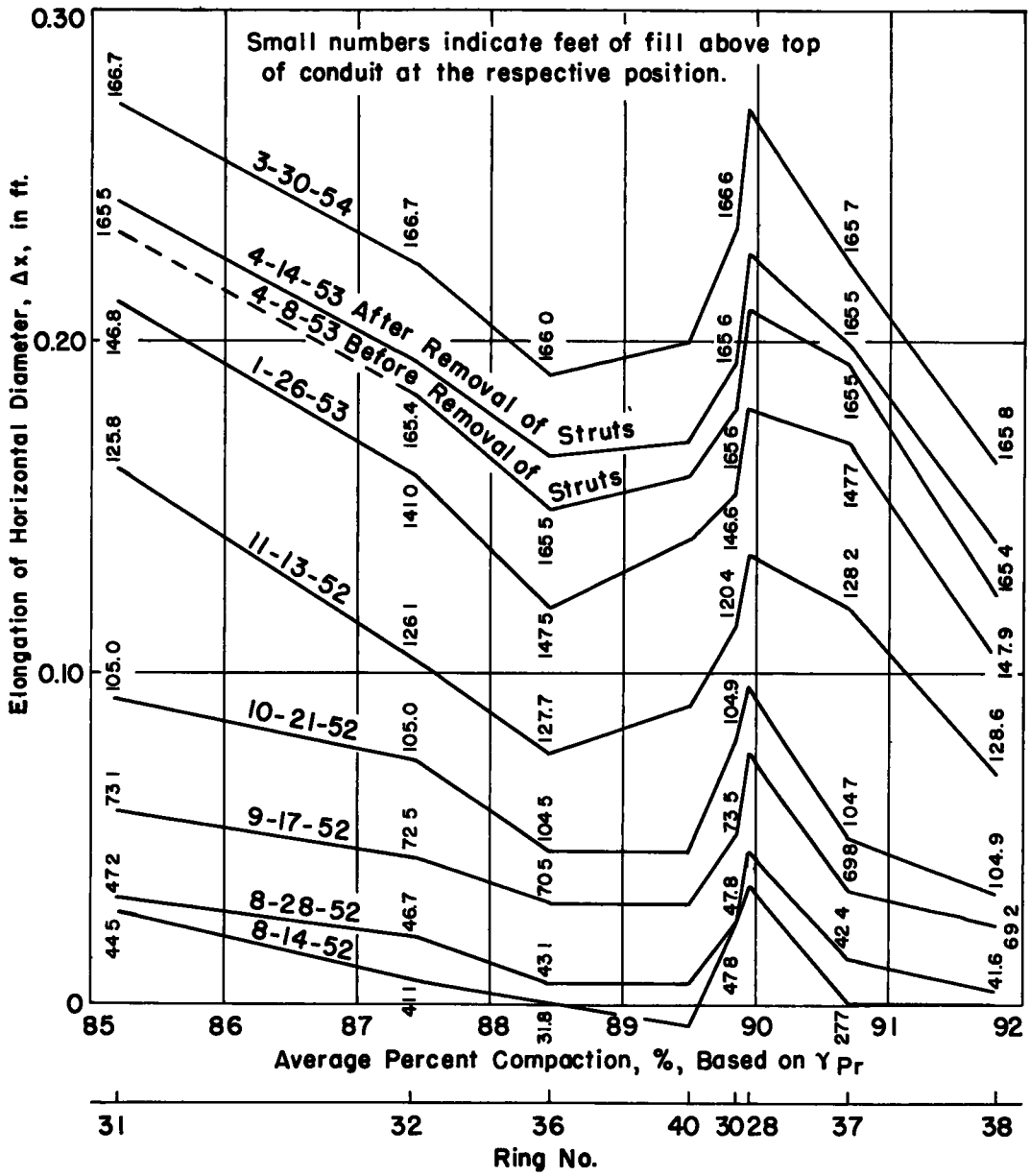

Figure 71. Progressive elongation of horizontal diameter versus percent compaction of side supporting material. Rings 28-40.

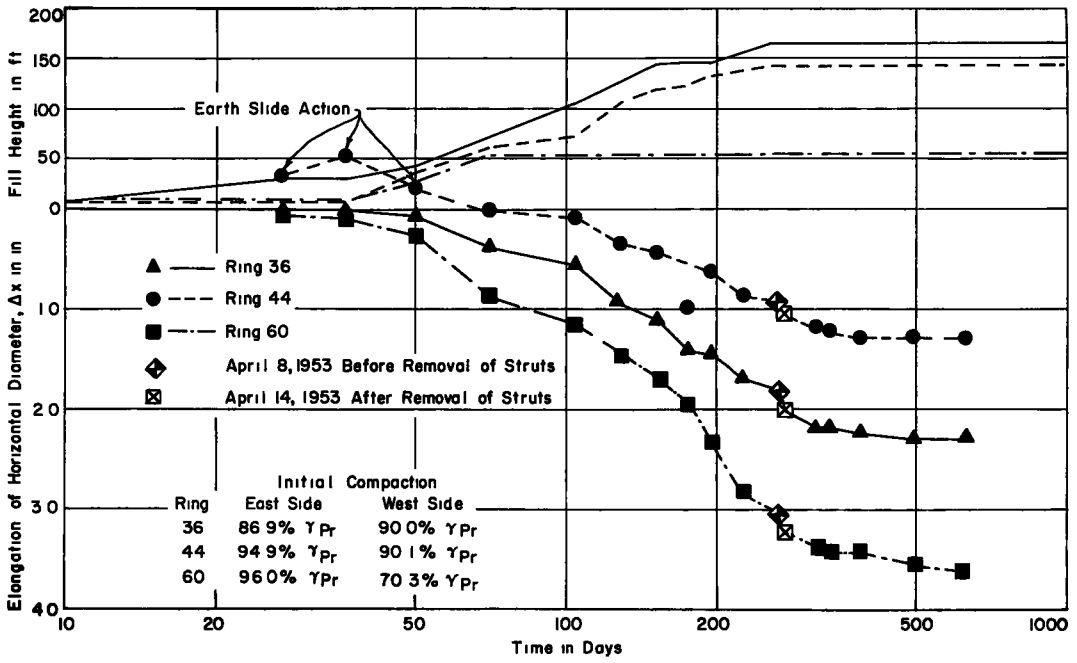

Figure 72. Fill height and elongation of horizontal diameter of pipe versus time.

typical cross-section of the pipe installation on Ring 31 drawn on Figure 46. Furthermore, data from the properties and the compaction condition of the same mass one and one-half years after the completion of the fill are shown in Tables 3 and 4 and in Figures 48 and 51.

The data plotted in Figure 51, indicate that regardless of the varying degree of initial precompaction, the dry density of the side supporting material increased to an average value of 105 pcf. one and one-half years after the completion of the fill. In Figure 48 it will be seen that although sufficient points were not obtained from Rings 44, 45, and 56 to form a good trend, the dry density appeared to decrease with lateral depth at Rings 16, 44, 45, and 64, while it indicated an opposite trend at Rings 8 and 56, and remained more or less constant with an ultimate tendency to decrease with depth at Rings 24 and 34. The water content and the void ratio, as expected, varied in an opposite manner to that of the dry density.

The general tendency of the dry density to decrease with lateral depth may be explained from the fact that the influence of both the lateral deformation of the conduit as well as the arching stresses in consolidating further the side supporting mass is dissipated beyond the immediate vicinity of the conduit. Consequently, for greater lateral depth the soil mass consolidates only as a result of the fill overburden.

To show the influence of the degree of initial compaction of the side supporting material on the lateral deformation of the conduit, a family of curves has been plotted in Figure 71. These curves show progressive elongation of the horizontal diameter of the conduit, versus average percent compaction of the side supporting material regardless of ring position, based on the maximum dry density from standard Proctor compaction tests performed on the same material.

Only data from Rings 28 to 40 have been used in these graphs. Since the fill height, the strut spacing, the gage of structural plate, and the stages of fill construction were the same on these rings, and since for all practical purposes the side supporting material was uniform in nature along these positions, it would appear logical to assume that the only independent variable influencing the lateral bulging of the structure as measured by the elongation of the horizontal diameter is indeed the initial compaction of the side support.

The trend of the above curves indicates that the higher the initial precompaction of the side supporting material, the lower will be the lateral bulging of the conduit. The peak values at Rings 28 and 30 may be due to either: (1) erroneous data on the initial compaction of the side support, (2) a local pocket of dense soil, or (3) the lateral displacement of the culvert, if the structure is considered to deform like a cylindrical beam whose action has been discussed previously and illustrated in Figure 54.

Another set of graphs has been plotted in Figure 72 showing fill construction progress and lateral elongation of the horizontal diameters versus time, on Rings 36, 44, and 60. The initial compaction of the side supporting material at the same locations is indicated also. From these graphs the following comments may be made:

The time-elongation of horizontal diameter curves, which might also be thought of as time-lateral settlement curves, from the side supporting material have the same trend. This fact suggests that the side supporting material is more or less of the same nature at Rings 36, 44, and 60.

For a fill increment there was a corresponding increment in the horizontal diameter of the pipe.

When the fill construction was completed on top of these rings, the structure ceased to deform laterally. The latter action indicates that the side support acted in an elastic manner.

The influence of the slide is indicated clearly on Ring 44 where during the first 70 days of the fill construction the pipe was squeezed in instead of bulging out. However, when sufficient fill overburden had been deposited on top of the culvert, the structure began deforming as originally anticipated.

Further indication of the elastic nature of the side is given by the sudden increase in the horizontal diameter upon removal of the struts.

From the tabulated data on the initial compaction of the side supporting material and since the gage of structural plate as well as the strut spacing were the same at Rings 36 and 44, it appears that lateral bulging of the culvert at those positions may have been influenced by: (1) the fill overburden, (2) the fact that the side supporting material was initially compacted to a greater degree at Ring 44 than at Ring 36, and (3) the initial squeeze-in effect of the slide action.

Although Ring 64 supported considerably less overburden than Rings 36 and 44, the culvert at this point bulged out considerably more than it did at Rings 36 or 44. Although not experimentally proven, this action is attributed to: (1) very low initial compaction of the side supporting material on the west side of Ring 64, (2) thinner gage of the structural plate at Ring 64, (3) less amount of struts per lineal foot of pipe at Ring 60 than at Rings 36 or 44, and (4) load transfer within the soil mass from the middle section of the pipe to the quarter points on account or arching along the longitudinal axis of the conduit.

Discussion of the Data Obtained from Strain Gages, Strut Load Cells, and Compression Pine Caps

By merely looking at the values of vertical and lateral pressures evaluated from the strain gage data and comparing them with the weight of earth column on top of the conduit (Figures 61-63) one can see that these values cannot have any quantitative significance. To make the above statement more comprehensible, the same data have been used to draw the following figures: (1) Figure 73, in which the indicated vertical load, W_V, has been plotted against fill height, H, for Rings 31, 37, and 55. For comparison purposes the overburden pressure or the earth column weight, W, has also been plotted versus fill height on the same figure. (2) Figure 74, in which the ratios of the vertical load, W_V, to the weight of the earth column, W, and to the lateral load, W_L, have been plotted against time.

From the above figures as well as from Tables 6 and 8 it can be seen that:

1. The maximum vertical load as evaluated from strain gages, strut load cells, and pine compression caps was in the vicinity of 300,000 lb. per lin. ft. of pipe for all three rings. The maximum lateral load was about 270,000 lb. per lin. ft. at Ring 31; 250,000 lb. per lin. ft. at Ring 37; and 120,000 lb. per lin. ft. at Ring 55.

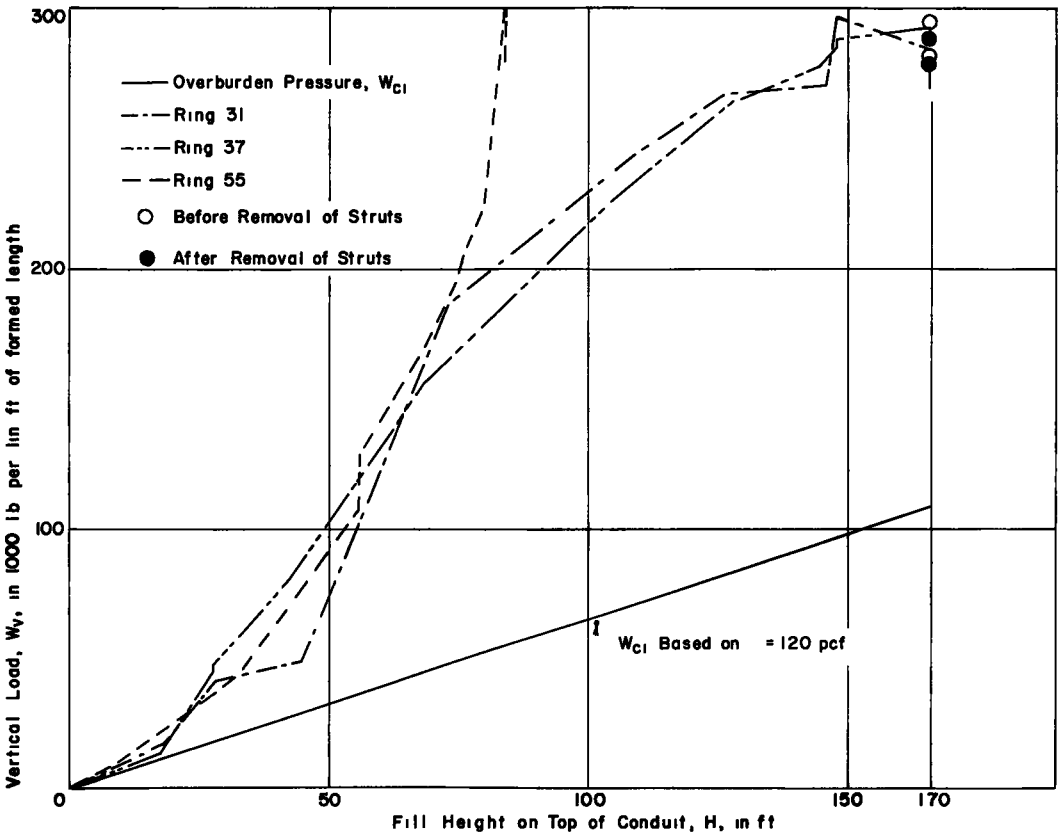

Figure 73. Comparison between vertical conduit earth load, W_v, as evaluated from strain gage, strut load cell, and pine compression cap measurements, and overburden pressure, W_{cl}, due to weight of earth column above the conduit.

TABLE 8

Date	Fill Height on Top of Conduit H - ft			Weight of Earth Column, W_{cl} lb. /ft.			W_v/W_{cl}			W_v/W_L		
	Ring 31	Ring 37	Ring 55	Ring 31	Ring 37	Ring 55	Ring 31	Ring 37	Ring 55	Ring 31	Ring 37	Ring 55
7- 9-1952	9.1	7.4	9.7	6,010	4,880	6,400	2.86	2.43	1.66	1 10	2.42	4.17
8- 5-1952	28.1	27.7	9.1	18,500	18,300	6,010	2.23	2.36	1.35	1.16	1.42	2.77
8-14-1952	44.5	27.7	9.1	29,400	18,300	6,010	1.66	2.42	1.17	1.28	1.21	1.60
8-28-1952	47.2	42.4	32.1	31,100	28,000	21,200	1.97	2.84	2.02	0 90	1.31	3.45
9-16-1952	73.1	69.8	55.6	48,200	46,100	36,700	3.88	3.45	2.92	1.54	1.21	1.91
10-21-1952	105	105	55.9	69,300	69,100	36,900	3.44	3.29	3.47	1.21	1.50	1.99
11-13-1952	126	128	67.3	83,000	84,600	44,400	3.23	3.14	3.73	1.23	-	2.29
12- 8-1952	145	144	74.9	95,900	95,300	49,400	2.83	2.92	3.91	1 21	1.44	2.92
1- 6-1953	146	147	76.1	96,400	97,000	50,200	2.93	2.90	4 18	1 19	1.32	3.22
1-29-1953	147	148	79.2	97,000	97,500	52,300	3.07	2.96	4.24	1.20	1.25	3.46
2-24-1953	165	165	82.2	109,000	109,000	54,300	2.61	2.69	5.10	1 19	1.21	2.27
4- 8-1953 [c]	165	165	82.2	109,000	109,000	54,500	2.56	2.70	5 23	1 07	1.19	2.70
4-14-1953 [d]	165	165	82.2	109,000	109,000	54,500	2.59	2.64	5.13	1.06	1.17	2.60
5-26-1953	165	165	82.2	109,000	109,000	54,500	2.48	2.61	-[b]	1.06	1.23	-[b]
6-16-1953	166	166	83.7	110,000	110,000	55,200	2.54	2.60	-	-[b]	1.24	-
8- 3-1953	166	166	83.7	110,000	110,000	55,200	-[b]	-[b]	-	-	-[b]	-
11-23-1953	166	166	83.7	110,000	110,000	55,200	-	-	-	-	-	-
3-29-1954	167	166	83.7	110,000	110,000	55,200	-	-	-	-	-	-

[a] W_L not obtained.
[b] From this date strain gages became inoperative.
[c] Before removal of struts.
[d] After removal of struts.

2. The vertical load, W_V, increased rapidly during the first 120 days of the fill construction. Then it increased at a decreasing rate and upon the completion of the fill it reached an average value of approximately three times as great as the weight of the earth column above the conduit, assuming that the average unit weight of the fill material was 120 pcf.

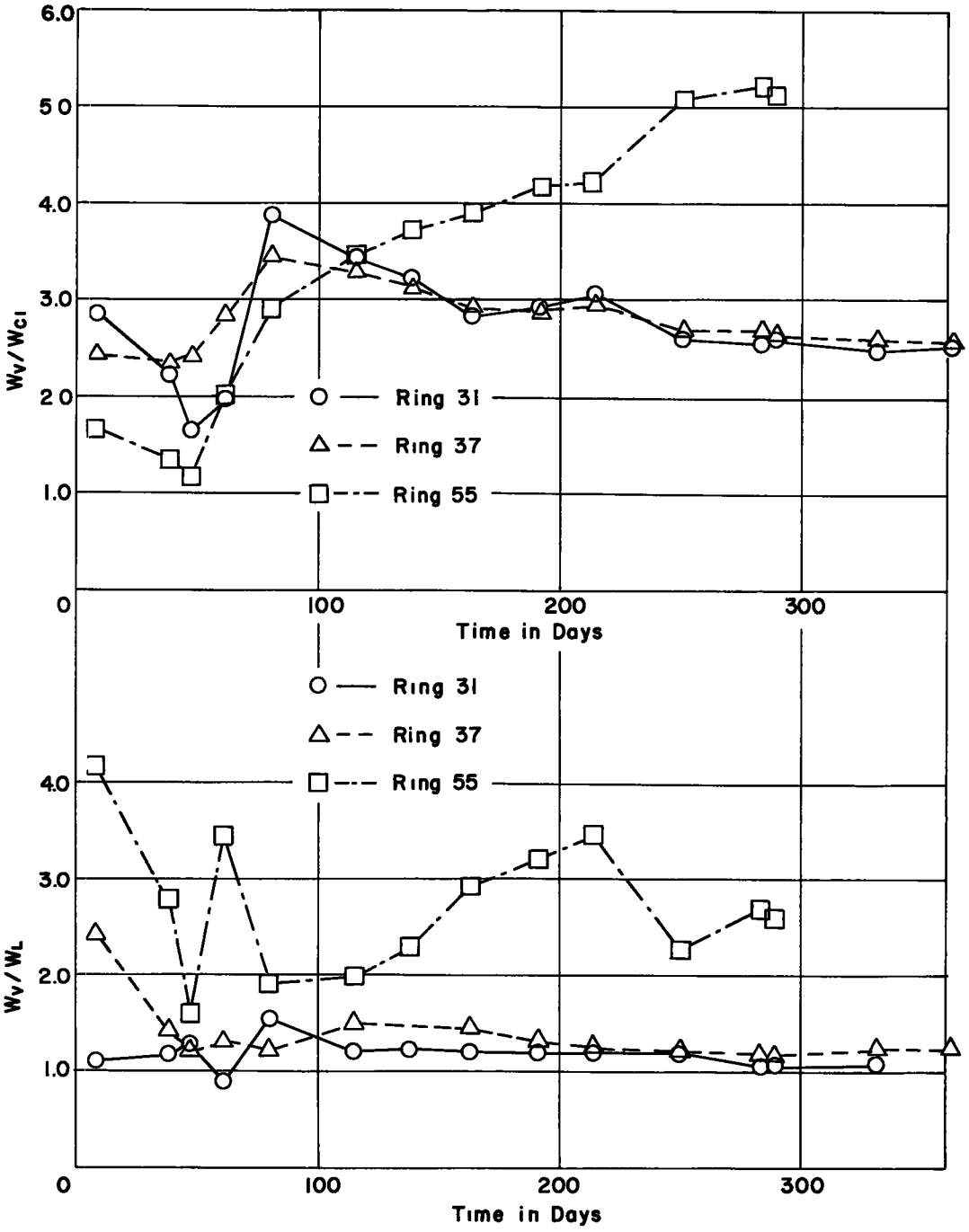

Figure 74. Ratios of vertical earth load to weight of earth column W_v/W_{cl}, and to lateral earth load W_v/W_L acting against the pipe versus time.

3. At Rings 31 and 37 the above recorded vertical load was about 1.3 times the lateral load, W_L, as evaluated from data obtained by the same apparatus. At Ring 55, the ratio of W_V to W_L did not have an approximate constant value but varied with time in a wave-like manner. Maximum values of this ratio were recorded eight days after the beginning of fill construction and at the end of the construction, i.e., 214 days later, these values were 4.2 and 3.5 respectively. The minimum value was 1.3 and it was recorded 46 days after the beginning of fill construction.

From the above numerical results it follows that the evaluated pressure values cannot have any significance because: (1) If the external pressures had attained such great values, the structural connections of the plates would have failed in shear especially in Ring 55 where the bolt spacing and plate gage had been designed for 84 feet of vertical fill height or 46,200 lb. per lin. ft. overburden pressure, the design value of the average unit weight of the fill material having been 100 pcf. Even if a factor of safety of four is applied, the resulting design load will be 184,800 lb. per lin. ft., i.e., about half the value recorded. Not a single sign of bolt shearing has been observed in any ring of the culvert. (2) The inherent rigidity of the flexible culvert would not be able to withstand differential pressures resulting from the uneven distribution of external pressures as mentioned in item 3. Therefore, the culvert would have collapsed by excessive deformation at least at the rings where the above data have been obtained. However, the pipe shape at the same rings, as shown by the protractor data on Figures 55, 56 and 57 and generally in Figure 70, is for all practical purposes circular in shape and does not reveal any signs of excessive deformation at any point.

The experimental error involved in strain gage measurements has not been determined; however, the following factors are considered to have possibly contributed to the above unreasonable results.

1. The bottom strain gages of all three rings although insulated and waterproofed were grounded most of the time due to the flowing water (see Table 6), therefore, erroneous readings must be expected. However, the gages that were installed on the sides and at the top of all three rings were all operative except the No. 1 top gage at Ring 37. Since the results obtained from the latter gages were just as unreasonable as those obtained from the bottom gages, grounding is considered one possibility but not one of the main reasons for obtaining data that are beyond any reasonable expectations.

2. The structural plates due to local stress concentration may have buckled locally, thus indicating excessive strain. Such action is actually accompanied by a partial relief of stresses. However, if one examines the data from each side of each ring, obtained by three gages installed 2 feet apart from each other, he will notice that the readings are of the same order of magnitude. Furthermore, there is a reasonable agreement among the data from the same side of all three rings at the same date. Also data from opposite sides of the same ring are reasonably uniform. Therefore, how local the local buckling is is questionable. With lack of knowledge concerning the experimental error involved, one cannot draw definite conclusions regarding this possibility.

3. The strain at each point of the pipe surface was measured by one strain gage element. This element recorded uniaxial circumferential strain in the metal. The nature of stresses that caused such strains is impossible to determine because a multitude of additional stresses may have been introduced at the point where the gage elements were installed. These stresses could have been of the same direction and sense as the pure axial circumferential thrust that it was desired to measure. As was mentioned before, the pipe was subjected to various other actions in addition to being loaded by the top overburden pressures. Lateral displacements of the pipe-beam structure were observed, tendencies to rotate about the flow line axis were recorded, and a very definite loading action was detected as a result of the continued drive of the slide.

4. The strain gage elements were supposedly installed at the neutral axis of the pipe corrugations. Thus, it was hoped that the recorded strain would be only due to axial thrust. If, however, these elements were installed just a minute amount off the neutral axis of the corrugation, bending stresses would also be introduced on account of the curved beam action of the corrugation. Furthermore, even if these elements were installed exactly on the geometrical neutral axis of each corrugation, the above neutral axis may or may not have coincided with the actual physical neutral axis of the corruga-

tion. The position of the physical neutral axis is a function not only of the shape of the corrugation but also of the homogeneity of the material itself. Any small misplacement of the gage elements from the actual neutral axis would have introduced the same bending stresses as discussed above. On the other hand such stresses, although they may have been undetectable by any other measuring device, would have been recorded by the strain gage indicator whose precision is one millionth of an inch per inch.

5. The strain gage readings as well as the compression measurements from the pine caps indicated that both the steel plates and the pine caps had been stressed beyond their respective elastic ranges. Under such conditions no conversion from strain to stress can be made by means of stress-strain and load-deformation diagrams obtained from laboratory tests on similar specimens. It is known, that when a material is loaded beyond its elastic range, and conditions for plastic flow exist, the rate of load application as well as the total time that each load increment has been allowed to act on the specimens are factors of primary importance. For varying rate of load application the stress-strain or load-deflection curve of the same specimen will have a different configuration on the plastic range. If the total time that a load increment has been allowed to act on the specimens varies, the ultimate deformation that the specimen will undergo on account of this increment will vary also.[15]

6. Even if the conduit material were stressed below its elastic limit it would be absurd to attempt to evaluate the state of stress at a point from a single, unidirectional strain measurement, by applying a simple, directly proportional relationship between stress and strain. Only in the special case of uniaxial stress and along the direction of the stress may such relationship be applied. In every other case, the total strain measured in any direction consists of three separate parts (1) the strain due to temperature change, (2) the strain due to the Poisson effect, and (3) the primary strain that is directly related to Hooke's law if the material is stressed below its elastic limit.

The first part of the above total strain is eliminated by a suitable temperature compensator attached on the strain gage indicator. The second part, however, which is unaccompanied by stress, cannot be determined from a single strain measurement obtained by one gage element oriented in one direction.[16] For plane or two-dimensional stress conditions, strain gage theory shows that the minimum number of strain measurements that must be obtained at a single point in order that the state of strain and, accordingly, the state of stress be defined completely on all planes perpendicular to the plane of stress that pass through the same point, is three measurements, obtained from three different directions passing through the point. In addition to the above measurements the Poisson ratio for the respective material must be known also (Koch and others, 1952; Perry and Lissner, 1955).

From the above discussion and especially from item 6 , it follows that the magnitude of the vertical and lateral external loads cannot be determined from the available strain gage and compression pine cap data. However, since each set of data was obtained at the same time, and since there is a reasonable agreement among the data obtained on the same date, qualitative conclusions may be drawn regarding the build-up of these loads. Specifically:

1. For a fill increment, there was a corresponding load increment both in the plates and the struts.

---

[15] While strut-compression cap specimens were tested in the N. C. State Highway Laboratory in order to obtain the strut load-deflection diagram presented in Appendix, the deformation due to the highest applied load increment was recorded instantaneously, 5 minutes later, and 10 minutes later. It was found that on the average the specimens deformed 4. 7, and 7. 9 percent in excess of the instantaneous reading during the last two time intervals respectively. Furthermore, the load was applied at the rate of 0. 05 inch per minute and can hardly be said to simulate static field conditions.

[16] When a primary strain is produced in the x direction of a structural element by a force in that direction, secondary or Poisson strains are simultaneously produced in the y and z directions normal to the primary strains. These Poisson strains are, however, unaccompanied by stresses in the y and z directions. This point is frequently overlooked in strain measurements.

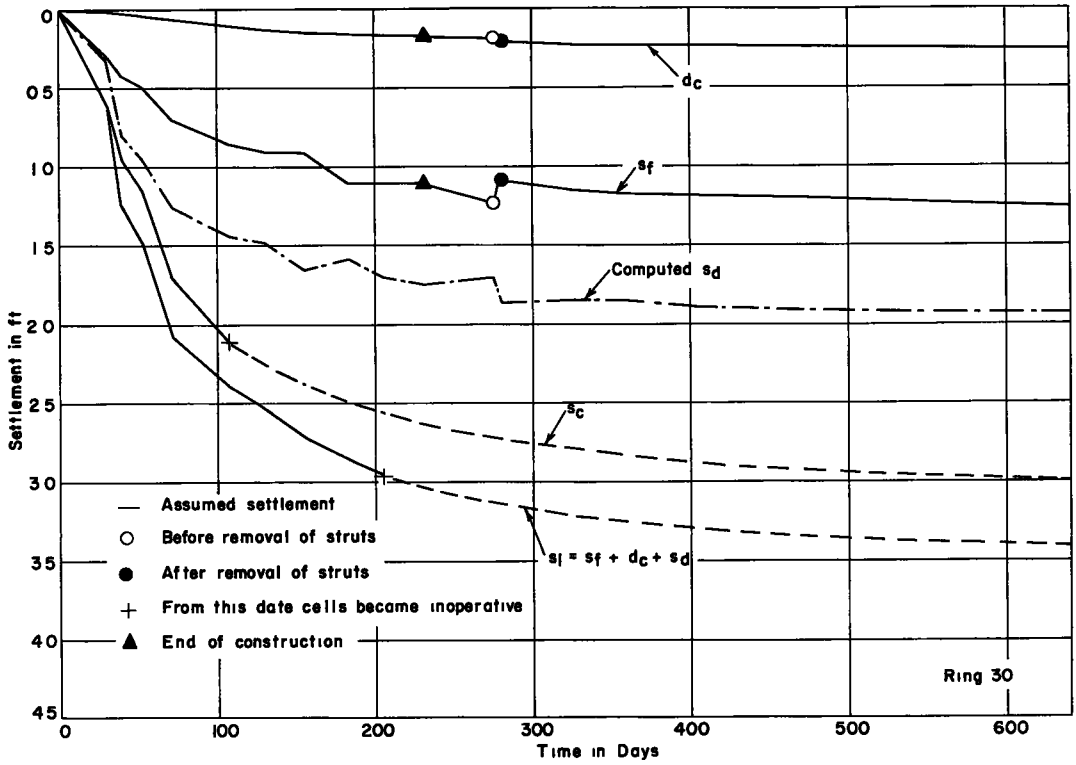

Figure 75. Settlement of various component parts of earth-conduit structure versus time. Ring 30.

2. The load increased at an increasing rate at the earlier stages of the fill construction. Later, however, it increased at a decreasing rate, and, upon the completion of the fill, it remained substantially constant.

3. The removal of the struts affected the load on the plates.

4. The data from the pine compression caps indicate that there was more load concentration at the quarter points than at the middle section of the pipe (Figure 60). The same fact is indicated by the strain gage measurements at Ring 55 (Figure 58). However, as these load values were evaluated from deformations and strains that occurred in the plastic region of these materials, and since the strut spacing, plate gage, and initial compaction of the side supporting material provided less resistance to deformation at the quarter points than at the middle section, one cannot conclude with certainty that such a load distribution came mainly as a result of arching action of the overlying soil mass in a longitudinal way. Instead, it would be more compatible with the actual conditions to conclude that all the above factors, combined together, may have influenced such behavior.

Analysis of Data from Settlement Cells - Evaluation of Settlement Ratio

As mentioned previously, the experimental error from the settlement computations cannot be estimated by means of the available data. However, Table 7 gives a general idea of the magnitude of the discrepancies that may be expected between readings obtained by the settlement cells and readings obtained by level. These discrepancies are not systematic errors, but they result from a multitude of environmental conditions. The most influencial source of error is believed to be the "kinking" of the rubber hose connecting each cell buried in the fill with the manometer board located in the pipe line. Such action was caused by the squeeze-in effect of the earth mass above the conduit and progressed with time until, finally, it rendered the cells inoperative. On account of this, the initial discrepancies are believed to have increased considerably at later dates.

Therefore, the settlement computations that were made by taking the difference between the initial readings and readings obtained at later dates will also be in error. In addition to the above:

1. Due to invert flow line grade, and rotation of pipe about its longitudinal axis, the manometer was not vertical when fitted to the Phillips head screw permanent reference points. Therefore, the recorded vertical distance between the invert elevation and the lower mercury meniscus (distance e - c of Figure 43) was not the true distance.

2. Bulkiness of the manometer board; poor illumination, ineffective valve arrangement on the manometer that resulted several times in losing the mercury while attempting to take a reading; inadequate pumping apparatus that did not secure a slow smooth stroke while pumping water through the cell hose and, therefore, it may have hastened impending hose kinking, rendered each individual reading very questionable from a statistical point of view.

In spite of the above discussion, the plotting of settlement data against time indicate very definite trends that are within a reasonable degree of agreement with the anticipated settlements of the respective soil mass components. Therefore, as a crude method of analysis, the arithmetic mean of a set of readings that were obtained on the same date from the compacted and loose earth masses on top of the same ring, were considered to represent the average settlement conditions for the above masses on that date.

From the points where the cells became inoperative the mean curves were extrapolated in such a manner that their trend was the same as that of data obtained from individual cells of the same group that were still in operation. The extrapolated portions were considered to represent the average settlement conditions for the same masses at later dates (Figures 75-80 and Table 9).

The above data together with the data from the settlement of the flow line and the shortening of vertical diameter at the same points, (Figures 52 and 53) were used to compute the settlement ratio as defined previously (see Apparatus and Experimental

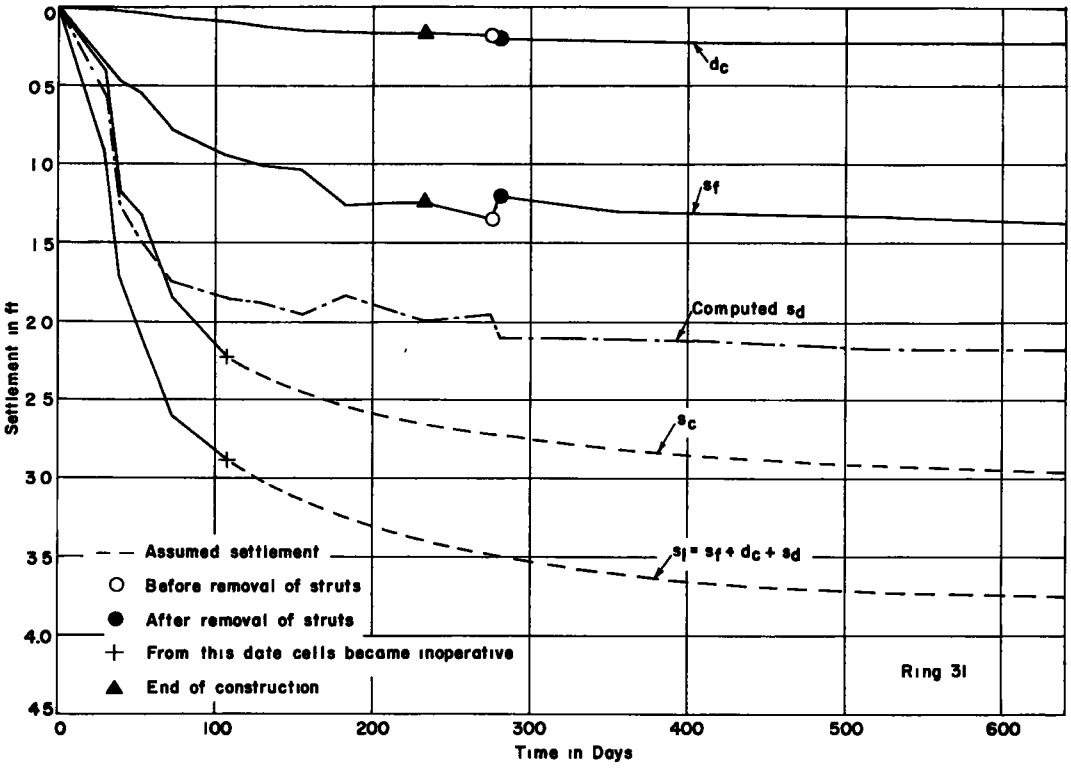

Figure 76. Settlement of various component parts of earth-conduit structure versus time. Ring 31.

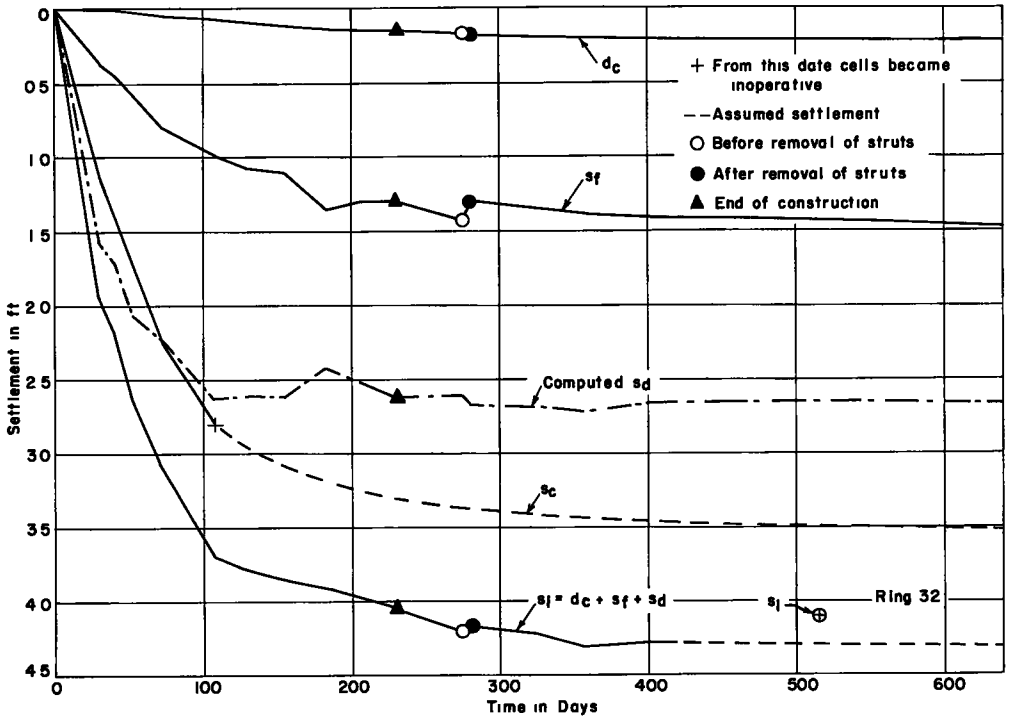

Figure 77. Settlement of various component parts of earth-conduit strucutre versus time. Ring 32.

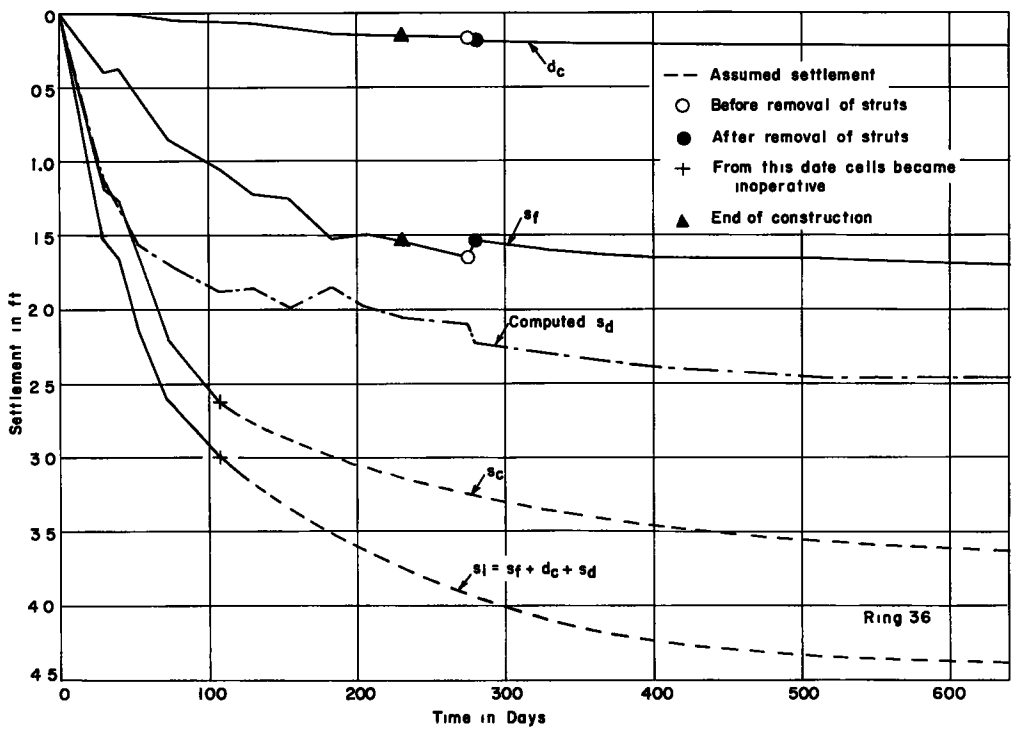

Figure 78. Settlement of various component parts of earth-conduit structure versus time. Ring 36.

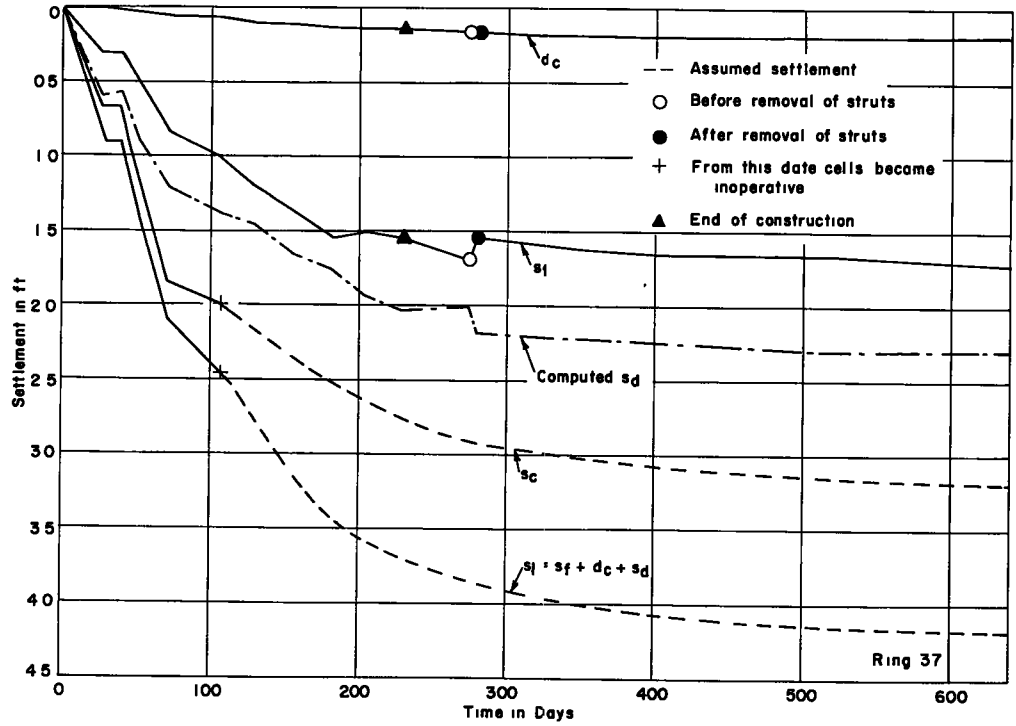

Figure 79. Settlement of various component parts of earth-conduit structure versus time. Ring 37.

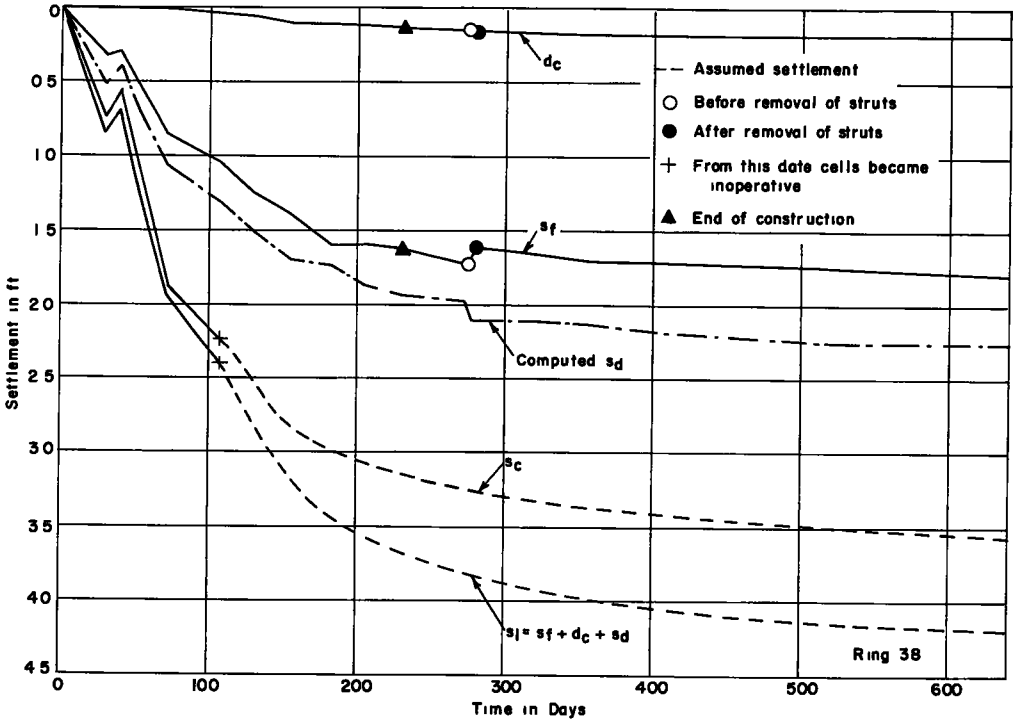

Figure 80. Settlement of various component parts of earth-conduit structure versus time. Ring 38.

Procedure). The results of these computations have been plotted against time in Figures 81 and 82. On the same curves the ratio of the void ratio of the loose mass, e_l, to the void ratio of the compacted mass, e_c, above the respective rings is indicated also.

From the above two figures it can be seen that:

1. During the first 100 days of fill construction the settlement ratio decreased stead-

TABLE 9

EVALUATION OF SETTLEMENT RATIO, r_{sd} - RING 30

Date	Settlement of Compacted Material, s_c ft.				Settlement of Loose Material $s_l = s_f + d_c + s_d$, ft.				s_f ft.	d_c ft	$s_d = s_l - (s_f + d_c)$ ft	$r_{sd} = \frac{s_c - s_l}{s_d}$	$\frac{e_l}{e_c}$
	Cell No. 1	Cell No. 2	Cell No. 5	Cell No. 6	Mean	Cell No. 3	Cell No. 4	Mean					
8- 5-1952	+0.58	+0.74	+0.67	+0.43	+0.61	+0 81	+0.40	+0 61	+0.29	+0.010	+0 31	0	1.30
8-14-1952	+0.84	+1.05	+0 99	+0.96	+0.96	+1.37	+1.13	+1.25	+0 42	+0.030	+0 80	-0 363	
8-28-1952	+1.19	+1 32	+1.15	+0.91	+1.14	+1 55	+1 38	+1 47	+0 49	+0 035	+0 94	-0 351	
9-16-1952	+1.64	+1.72	+1.92	+1 56	+1.71	+1 98	+2 07	+2.03	+0 70	+0.065	+1.26	-0.254	
10-21-1952	+1.96	-[a]	+2.33	+2.00	+2.10	+2.34	+2.42	+2.38	+0.86	+0.100	+1.43	-0.196	
11-13-1952	+2 12	-	-[a]	+2.05	(+2.25)	+2.46	+2.58	+2.52	+0.91	+0 130	+1.48	(-0.182)	
12- 8-1952	-[a]	-	-	-[a]	(+2 38)	+2.68	+2.73	+2 71	+0 91	+0 145	+1.65	(-0.200)	
1- 6-1953	-	-	-		(+2 46)	+2.82	+2 87	+2.85	+1.11	+0 160	+1.58	(-0.234)	
1-29-1953	-	-	-	-	(+2.56)	+2.90	+3 01	+2.96	+1 10	+0 165	+1.69	(-0.237)	
2-24-1953	-	-	-	-	(+2.63)	-[a]	+2.77	(+3.03)	+1 11	+0.175	(+1.74)	(-0.230)	
4- 8-1953[b]	-	-	-	-	(+2.72)	-	+3.15	(+3.12)	+1.23	+0 185	(+1.70)	(-0.235)	
4-14-1953[c]	-	-	-	-	(+2 73)	-	+2.51	(+3.14)	+1.08	+0.205	(+1.86)	(-0.222)	
5-26-1953	-	-	-	-	(+2.78)	-	+3.00	(+3 21)	+1.14	+0 225	(+1.84)	(-0.234)	$\bar{x}$ = -0.2768
6-16-1953	-	-	-	-	(+2.83)	-	+3 09	(+3 25)	+1.17	+0.225	(+1 85)	(-0.227)	
8- 5-1953	-	-	-	-	(+2.88)	-	+3 99	(+3.29)	+1.18	+0.230	(+1 88)	(-0.218)	
11-23-1953	-	-	-	-	(+2.95)	-	+3.36	(+3.37)	+1 20	+0.245	(+1.92)	(-0.219)	
3-29-1954	-	-	-	-	(+3 99)	-	+3 15	(+3 42)	+1 25	+0.250	(+1.92)	(-0.223)	
Mean													
RING 31													
8- 5-1952	+0 69	+0.57	+0.14	+0.14	+0.39	+1 42	+0.41	+0 92	+0.35	+0.010	+0 56	-0 946	1 48
8-14-1952	+1.25	+0 92	+1.34	+1 19	+1.18	+2 11	+1.41	+1 76	+0 47	+0.025	+1 26	-0 460	
8-28-1952	+1 29	+1 29	+1.52	+1.22	+1.33	+2.46	+1 68	+2 07	+0.55	+0.035	+1 48	-0 500	
9-16-1952	+1 64	+1.80	+2.04	+1.88	+1 84	+2.97	+2 23	+2.60	+0.78	+0.070	+1.75	-0 434	
10-21-1952	+2 17	+2.10	+2.43	+2.19	+2.22	+3 22	+2.54	+2.88	+0.94	+0.090	+1 85	-0 357	
11-13-1952	+2 25	+2.38	-[a]	-[a]	(+2 34)	-[a]	+2.83	(+3 02)	+1.01	+0.125	(+1.88)	(-0.362)	
12- 8-1952	+2.50	+2.42	-	-	(+2 46)	-	+2.96	(+3.13)	+1.03	+0 145	(+1 95)	(-0 344)	
1- 6-1953	+2.40	+2.55	-	-	(+2 54)	-	+3.02	(+3.25)	+1.26	+0.155	(+1.83)	(-0.388)	
1-29-1953	+2.46	+2.66	-	-	(+2.60)	-	+3.08	(+3 32)	+1.24	+0.165	(+1 91)	(-0 377)	
2-24-1953	+2.58	+2 79	-	-	(+2.66)	-	+3 10	(+3 40)	+1 24	+0.165	(+1 99)	(-0 372)	
4- 8-1953[b]	+2 39	+2 53	-	-	(+2.72)	-	+3.20	(+3.48)	+1.34	+0 178	(+1.98)	(-0 388)	
4-14-1953[c]	+2.64	+2.53	-	-	(+2 73)	-	+3 21	(+3 51)	+1 21	+0.195	(+1.10)	(-0 371)	
5-26-1953	+2.52	+2.57	-	-	(+2 77)	-	+3.22	(+3.57)	+1.26	+0.210	(+2.10)	(-0.381)	$\bar{x}$ = 0 3753
6-16-1953	+2.61	+2.98	-	-	(+2 82)	-	+3.40	(+3.62)	+1.29	+0 215	(+2.11)	(-0.379)	
8- 5-1953	-[a]	-[a]	-	-	(+2.86)	-	+3 25	(+3 65)	+1 31	+0.220	(+2 12)	(-0.373)	
11-23-1953	-	-	-	-	(+2 92)	-	+3 26	(+3.72)	+1 33	+0.220	(+2.17)	(-0 369)	
3-29-1954	-	-	-	-	(+2.96)	-	+3 30	(+3.76)	+1.37	+0.220	(+2.17)	(-0.369)	
Mean													
RING 32													
8- 5-1952	+0 81	+1.29	+1.16	+1 27	+1.13	+2 57	+1.32	+1.95	+0.37	+0.005	+1.57	-0.522	1 38
8-14-1952	+0 98	+1 52	+1.37	+1.52	+1.35	+2.84	+1.49	+2.17	+0.45	+0.010	+1 71	-0.480	
8-28-1952	+1 40	+1.89	+1.77	+1 75	+1.70	+3 30	+2.00	+2 65	+0 57	+0 020	+2.06	-0.461	
9-16-1952	+1.76	+2 42	+2.32	+2.49	+2.25	+3.70	+2.46	+3 08	+0.80	+0.050	+2.23	-0.372	
10-21-1952	+2.28	+2.98	+2.92	+2 98	+2.79	+4.32	+3.04	+3.68	+0.98	+0.070	+2.63	-0.336	
11-13-1952	-[a]	-[a]	+2.97	+3 04	(+2.97)	+4 33	+3.23	+3.78	+1 07	+0 100	+2 61	(-0.310)	
12- 8-1952	-	-	+2.99	+3 04	(+3.10)	+4 38	+3.29	+3.84	+1 10	+0.120	+2.62	(-0 282)	
1- 6-1953	-	-	-[a]	-[a]	(+3.12)	+4.45	+3.37	+3.91	+1.35	+0.140	+2.42	(-0.326)	
1-29-1953	-	-	-	-	(+3 18)	+4 54	+3.40	+3.97	+1.30	+0.150	+2.52	(-0.313)	
2-24-1953	-	-	-	-	(+3.32)	+4.54	+3.59	+4.07	+1.30	+0.150	+2.62	(-0.286)	
4- 8-1953	-	-	-	-	(+3.36)	+4.79	+3 59	+4 19	+1 43	+0.170	+2.59	(-0 320)	
4-14-1953	-	-	-	-	(+3 37)	+4 79	+3.50	+4.15	+1.30	+0 180	+2 67	(-0 292)	
5-26-1953	-	-	-	-	(+3 41)	+4 65	+3.77	+4 21	+1 34	+0.190	+2.68	(-0.299)	$\bar{x}$ = -0.3029
6-16-1953	-	-	-	-	(+3 43)	+4.85	+3.74	+4 30	+1.38	+0.200	+2 72	(-0.320)	
8- 5-1953	-	-	-	-	(+3 46)	+4 70	+3 83	+4.27	+1.40	+0.205	+2.66	(-0.304)	
11-23-1953	-	-	-	-	(+3.50)	+4.50	+3.69	(+4.29)	+1.42	+0 215	(+2.65)	(-0.298)	
3-30-1954	-	-	-	-	(+3.52)	+4 94	-[a]	(+4 32)	+1 47	+0.220	(+2.63)	(-0.304)	
Mean													
RING 36													
8- 5-1952	+1 05	+1 43	+1.10	-[a]	+1 19	+1.58	+1 45	+1.52	+0.39	0.000	+1.13	-0.292	1.61
8-14-1952	+1 14	+1.42	+1 24	-	+1.27	+1 56	+1 75	+1.66	+0 37	0 000	+1 29	-0.302	
8-28-1952	+1.57	+1.89	+1 56	-	+1 67	+2 13	+2.15	+2.14	+0 56	+0.010	+1 57	-0 299	
9-16-1952	+2 05	+2.38	+2.19	+2 14	+2 19	+2 68	+2.53	+2 61	+0.87	+0.035	+1.70	-0 247	
10-21-1952	+2.44	-[a]	+2.73	+2.68	+2 62	+3 01	+2 97	+2 99	+1.06	+0.055	+1.88	-0.197	
11-13-1952	-[a]	-	-[a]	+2.80	(+2.77)	+2 67[a]	+3.04	(+3 17)	+1.22	+0 085	(+1.86)	(-0.210)	
12- 8-1952	-	-	-	-[a]	(+2.88)	+2 81	+3 32	(+3.35)	+1 26	+0.110	(+1.98)	(-0 237)	
1- 6-1953	-	-	-	+3 67	(+2 99)	-	-	(+3.51)	+1 52	+0.135	(+1.85)	(-0.281)	
1-29-1953	-	-	-	+3.81	(+3 07)	-	-	(+3.62)	+1.49	+0.145	(+1.98)	(-0.278)	
2-24-1953	-	-	-	-	(+3.13)	-	-	(+3.74)	+1.54	+0 150	(+2.05)	(-0.298)	
4- 8-1953	-	-	-	-	(+3 25)	-	-	(+3.92)	+1 65	+0.170	(+2 10)	(-0 319)	
4-14-1953	-	-	-	-	(+3.26)	-	-	(+3.94)	+1 53	+0.185	(+2 22)	(-0 306)	
5-26-1953	-	-	-	-	(+3 34)	-	-	(+4 07)	+1.58	+0 200	(+2.29)	(-0.318)	
6-16-1953	-	-	-	-	(+3.39)	-	-	(+4 16)	+1.62	+0 210	(+2.33)	(-0.330)	$\bar{x}$ = -0.3143
8- 5-1953	-	-	-	-	(+3.46)	-	-	(+4 23)	+1.64	+0 210	(+2 36)	(-0.324)	
11-23-1953	-	-	-	-	(+3 57)	-	-	(+4.34)	+1.66	+0.215	(+2.46)	(-0.313)	
3-30-1954	-	-	-	-	(+3.63)	-	-	(+4.38)	+1 71	+0.220	(+2.45)	(-0.306)	
Mean													

[a] From this date cell became inoperative.
[b] Before removal of struts.
[c] After removal of struts.
Values in parentheses have been obtained by extrapolating mean curves.
Note: All data are in reference to the initial set of readings obtained July 9, 1952.

\+ Sign denotes downward subsidence
s_f = Settlement of flow line.
d_c = Shortening of vertical diameter
s_d = Compression of loose material within ditch
e_c = Initial void ratio of compacted material.
e_l = Initial void ratio of loose material.

TABLE 9 (Continued)

EVALUATION OF SETTLEMENT RATIO, r_{sd} - RING 37

Date	Settlement of Compacted Material, s_c ft.					Settlement of Loose Material ft			s_f ft.	d_c ft.	$s_d = s_1 - (s_f + d_c)$ ft	$r_{sd} = \frac{s_c - s_1}{s_d}$	$\frac{e_1}{e_c}$	
	Cell No. 1	Cell No 2	Cell No 5	Cell No 6	Mean	Cell No. 3	Cell No. 4	Mean						
8- 5-1952	+0 34	+0.52	+0.92	+0.90	+0.67	+0 75	+1.06	+0.91	+0.31	+0 005	+0.59	-0 407	3.44	
8-14-1952	+0.35	+0.55	+0 89	+0 88	+0 67	+0.74	+1.05	+0.90	+0.31	+0 020	+0.57	-0 404		
8-28-1952	+0. 87	+1.06	+1.40	+1.36	+1 17	+1.28	+1.59	+1.44	+0.51	+0.030	+0.90	-0.300		
9-16-1952	+1.48	+1.71	+2.16	+2.04	+1 85	+1.90	+2 29	+2.10	+0.83	+0 055	+1.21	-0.207		
10-21-1952	+1.72	+2.00	-[a]	+2.26	+1 99	+2.18	+2.73	+2.46	+1 01	+0 065	+1 38	-0.341		
11-13-1952	-[a]	-[a]	-	-[a]	(+2.16)	+2.47	-[a]	(+2.76)	+1 19	+0.105	(+1 46)	(-0.411)		
12- 8-1952	-	-	-	-	(+2.34)	+2 71	-	(+3 12)	+1.36	+0.110	(+1.65)	(-0.473)		
1- 6-1953	-	-	-	-	(+2.52)	+3 14	-	(+3.43)	+1.54	+0 130	(+1.76)	(-0.517)		
1.29-1953	-	-	-	-	(+2.64)	+3.33	-	(+3.58)	+1.51	+0.135	(+1 93)	(-0 487)		
2-24-1953	-	-	-	-	(+2.76)	-[a]	-	(+3 71)	+1.54	+0.135	(+2.03)	(-0 468)		
4- 8-1953	-	-	-	-	(+2.91)	-	-	(+3.85)	+1.68	+0.160	(+2.01)	(-0.468)		
4-14-1953	-	-	-	-	(+2.92)	-	-	(+3.87)	+1 53	+0.160	(+2.18)	(-0.436)		
5-26-1953	-	-	-	-	(+2.99)	-	-	(+3.97)	+1 56	+0.175	(+2.21)	(-0.443)		$\bar{x}$ = -0 4469
6-16-1953	-	-	-	-	(+3.03)	-	-	(+4.02)	+1.62	+0.175	(+2 22)	(-0.446)		
8- 5-1953	-	-	-	-	(+3.06)	-	-	(+4 07)	+1.65	+0.180	(+2 24)	(-0.442)		
11-23-1953	-	-	-	-	(+3.15)	-	-	(+4.15)	+1 66	+0.180	(+2.31)	(-0.433)		
3-30-1954	-	-	-	-	(+3.18)	-	-	(+4.18)	+1.72	+0.180	(+2.28)	(-0.439)		
Mean														
RING 38														
8- 5-1952	+0.58	+0.83	+0 85	+0 86	+0.73	+0.57	+1.10	+0 84	+0.32	+0.005	+0.51	-0.216	1.52	
8-14-1952	+0 34	+0 44	+0. 84	+0 83	+0.56	+0 51	+0.86	+0.69	+0 29	+0.005	+0 39	-0.333		
8-28-1952	+0 84	+0 84	+1.17	+1.59	+1 11	+1 02	+1 45	+1 24	+0.53	+0.010	+0.70	-0 186		
9-16-1952	+1 57	+1.67	+2 10	+2.14	+1.87	+1 49	+2 41	+1.95	+0 86	+0.015	+1.07	-0 075		
10-21-1952	-[a]	+1 94	+2.47	+2.42	+2.28	+2 11	+2.66	+2.39	+1 04	+0.035	+1.31	-0.094		
11-13-1952	-	-[a]	-[a]	+2.93	(+2.52)	-[a]	-[a]	(+2 81)	+1 24	+0.060	(+1 51)	(-0.192)		
12- 8-1952	-	-	-	+3 18	(+2.83)	-	-	(+3.17)	+1.38	+0.100	(+1 69)	(-0.201)		
1- 6-1953	-	-	-	-[a]	(+2.98)	-	-	(+3.44)	+1.59	+0.110	(+1.74)	(-0 264)		
1-29-1953	-	-	-	-	(+3.08)	-	-	(+3.57)	+1.58	+0.120	(+1.87)	(-0.262)		
2-24-1953	-	-	-	-	(+3 15)	-	-	(+3.68)	+1.62	+0.130	(+1.93)	(-0.275)		
4- 8-1953	-	-	-	-	(+3.26)	-	-	(+3.83)	+1.72	+0.140	(+1.97)	(-0.289)		
4-14-1953	-	-	-	-	(+3.27)	-	-	(+3 84)	+1.60	+0.145	(+2.09)	(-0.273)		
5-26-1953	-	-	-	-	(+3.32)	-	-	(+3.92)	+1.65	+0.165	(+2 10)	(-0.286)		$\bar{x}$ = 0. 2846
6-16-1953	-	-	-	-	(+3 37)	-	-	(+3 98)	+1 69	+0 165	(+2.12)	(-0.288)		
8- 5-1953	-	-	-	-	(+3 40)	-	-	(+4 04)	+1.70	+0.170	(+2.17)	(-0.295)		
11-23-1953	-	-	-	-	(+3 49)	-	-	(+4.14)	+1 73	+0.170	(+2.24)	(-0.290)		
3-29-1954	-	-	-	-	(+3 56)	-	-	(+4.19)	+1.78	+0.170	(+2.24)	(-0 281)		
Mean														

[a] From this date cell became inoperative.
[b] Before removal of struts.
[c] After removal of struts
Values in parentheses have been obtained by extrapolating mean curves
Note: All data are in reference to the initial set of readings obtained July 9, 1952

+ Sign denotes downward subsidence.
s_f = Settlement of flow line.
d_c = Shortening of vertical diameter.
s_d = Compression of loose material within ditch
e_c = Initial void ratio of compacted material.
e_1 = Initial void ratio of loose material

ily. At later dates, however, it increased slightly at Rings 30, 31 and 32 assuming average constant values upon the completion of the fill after small fluctuations. At Rings 36, 37 and 38 the same ratio increased almost at the same rate it had previously decreased and near the completion of the fill it assumed values that remained constant with respect to time.

2. The higher was the ratio e_1/e_c the higher was the settlement ratio.

3. The removal of the struts caused a sudden increase in the settlement ratio at each position.

4. Analytically it has been shown that the vertical earth load on top of the conduit varies directly as the settlement ratio (Costes, 1951). Accordingly, the following speculative comments can be made regarding the vertical earth load above each ring: (1) The top overburden pressure increased during the first 100 days of the fill construction. At later dates it decreased, and finally it came to rest upon the completion of the fill. Such indication together with the previous analysis of the data from the deformations and settlements of the pipe structure, suggests that mechanical equilibrium between the external earth pressures and the internal resistance of the structure was established upon the completion of the fill. (2) The higher the difference between the initial compaction of the loose material in the imperfect ditch and that of the adjacent mass, as expressed by the ratio e_1/e_c, the greater appears to be the settlement ratio, and, therefore, the lower will be the vertical load on top of the conduit.

Analytical Evaluation of the Vertical Earth Load on Top of the Conduit

In an imperfect ditch installation, if the overall settlement of the bedding material, the vertical dimension of the culvert and the loose, compressible material in the imperfect ditch is greater than the overall settlement of the adjacent, relatively stiff, fill masses, the top of the imperfect ditch may be visualized as part of a foundation supporting the overlying fill mass that yields a greater amount than the adjacent, relatively stationary parts. On account of this yielding the overlying mass has the tendency to slip

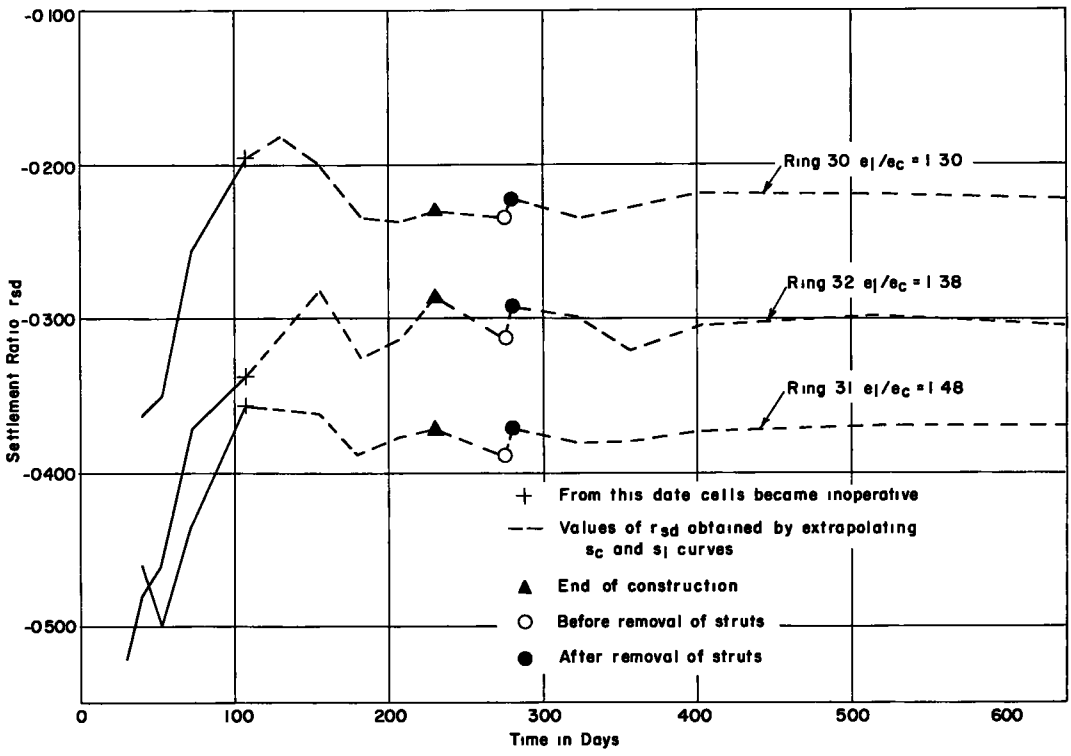

Figure 81. Settlement ratio, r_{sd}, versus time. Rings 30-32.

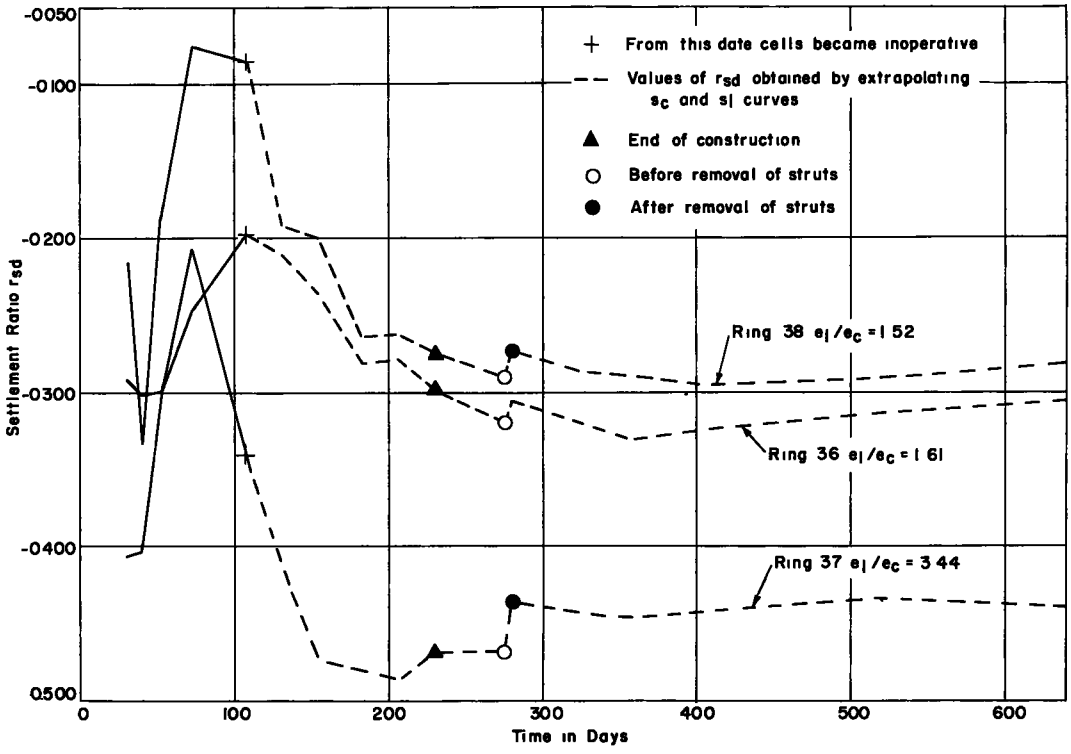

Figure 82. Settlement ratio, r_{sd}, versus time. Rings 36-38.

by the adjacent earth bodies that rest on the relatively stationary supports. Such tendency is opposed by the shearing resistance of the fill material that is mobilized along the potential surfaces of sliding.[17]

As a result of the above shear mobilization, the overlying middle mass braces itself against the adjacent masses, thereby transferring part of its dead weight on these bodies and relieving the top of the conduit by an equal amount of overburden pressure. Such action constitutes the commonly known "arching phenomenon" of soil masses.

The mechanics of the above action have been studied by many authors.[18] The most generally accepted theory in this country has been the so called "Marston Theory on Loads on Underground Conduits," set forth by the late Dean Anson Marston and expanded by Professor M. G. Spangler both of Iowa State College (Marston 1913, 1930; Spangler, 1950a, 1950b).

The above theory deals with the special case of cohesionless earth masses on top of covered-up conduits,[19] for small or medium height fills, and employs the following basic assumptions: (1) The potential sliding surfaces are vertical planes extending from the sides of the imperfect ditch to some horizontal plane through the fill mass called the "plane of equal settlement." (2) Along the vertical sliding planes, the shearing resistance of the fill material has been fully mobilized, and the earth mass behaves as if it were in an active state of plastic equilibrium.

Recently, the junior author of this paper in an effort to ascertain whether the Marston-Spangler expressions are applicable to high fill installations, developed the general case from the fundamental principles of the Marston theory (Costes, 1955). The general expressions include the cohesion as a shearing strength component of a fill mass, and may also be modified to describe the action of earth masses on top of mined-in conduits.[20]

In the above general theory, the special cases of a perfectly cohesionless or an $s = \sigma \tan\phi$ material, and a purely cohesive or an $s = c$ material, appear as limiting conditions of the general expressions. An extensive mathematical analysis is included also in the same paper studying the influence of fill height and various other factors that have been assumed to affect arching.

Although the above treatment is generally based upon the fundamental principles of the Marston theory, it postulates only partial mobilization of the shearing strength of the fill material along the vertical sliding planes. Such postulate is made because it is realized that the Marston assumption that the fill mass is in an active state of plastic equilibrium along the above planes, is incompatible with the deformation characteristics and the size of the same mass.

All the above mentioned theories are sound from a mathematical point of view and have been based on the laws of pure mechanics. However, as is the case with most theories that have been developed with the aid of theoretical soil mechanics, the nature of the various physical constants that are involved in the mathematical expressions is very complicated and very difficult to evaluate. Therefore, unless adequate experimentation indicates that the initial assumptions are valid or at least acceptable, and unless the various physical constants that may be expected from various installations and from actual and not ideal materials, are pinned down within reasonable design limits, the above theories cannot go beyond the realm of pure academic interest and cannot serve any other purpose except to supply the engineer with general qualitative information.

In this project the adverse conditions under which the experimental study was carried out have been mentioned. Furthermore, as no quantitative information can be obtained from the strain gages and the pine compression caps, no means are available to ascertain whether the top load as predicted by the above theories agrees with the actual conditions. To substitute the theoretical load in Spangler's "Iowa Formula" for lateral

---

[17] See References, Costes (1955) pp. 12, 14.

[18] For an extensive analytical treatment as well as a complete bibliography on the subject, see References, Costes (1955).

[19] A "covered-up" conduit is defined here as an underground conduit installed under an artificial earth embankment that is constructed after the conduit has been assembled in place.

[20] A "mined-in" conduit is defined here as an underground conduit installed by a mining process through a natural earth deposit.

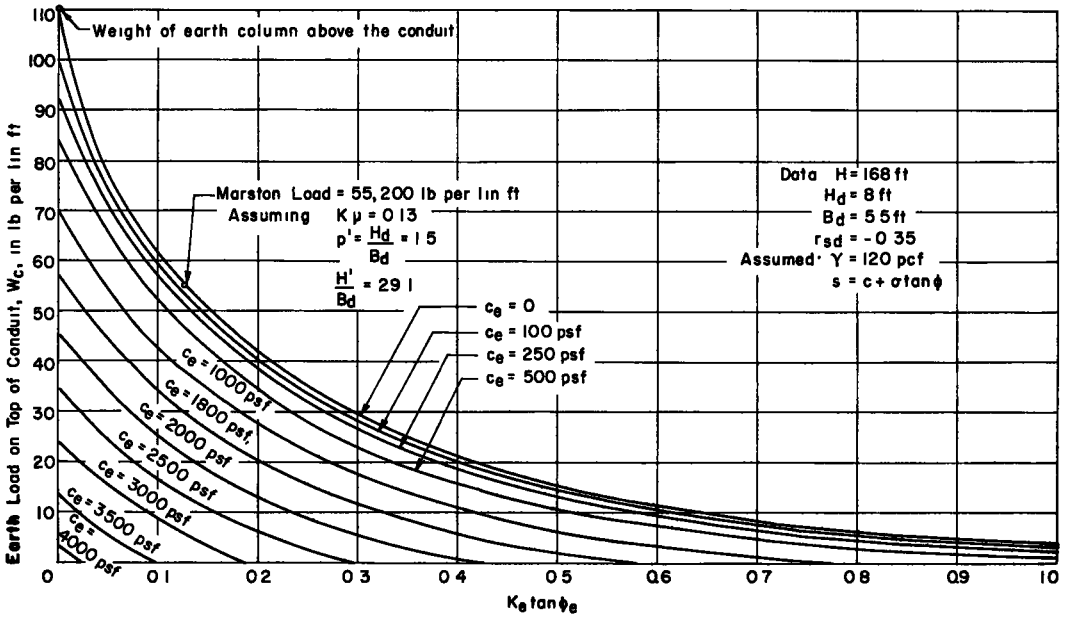

Figure 83. Computed earth load on top of conduit, assuming an s = c + σtanϕ fill material.

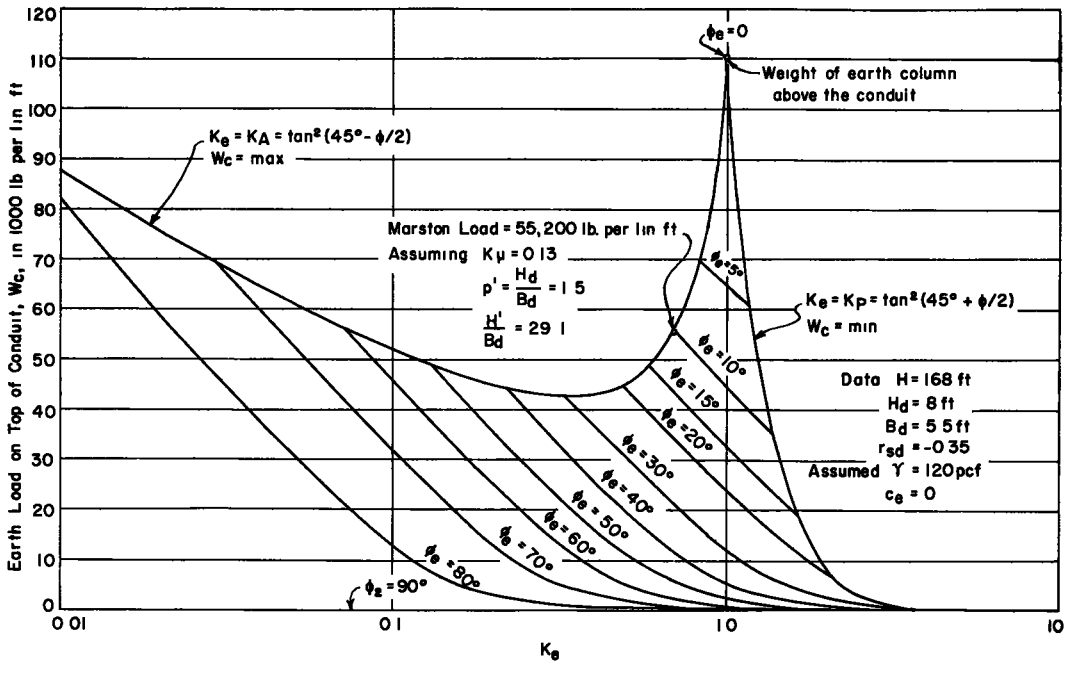

Figure 84. Computed earth load on top of conduit, assuming an s = σtanϕ fill material.

deflection of flexible culverts, and compare the theoretical deflection with the directly measured elongation of the horizontal pipe diameters, would not prove anything, because: (1) the "Iowa Formula" will have to be assumed to be valid for this installation, (2) the modulus of passive resistance of the side supporting material, employed in the "Iowa Formula," is a fictitious physical constant that has not been measured directly but will have to be assumed also, and (3) the modulus of deformation of the struts, if obtained

by the method proposed in the Experimental Procedure, will yield misleading information because of plastic flow conditions that have been discussed in previous sections of this paper.

One, therefore, cannot assume that two out of three interrelated propositions are valid, and then adjust the various physical constants of his mathematical expressions in order to prove the validity of the third proposition. Such analysis would lead to a false sense of satisfaction from a research view point. In this project, in order to obtain some substantial evidence as to whether the above propositions may be accepted as working hypotheses, at least the top, bottom, and lateral earth pressures that act against the conduit must be measured by direct means.

To show how futile it is to attempt to evaluate the earth load on top of a conduit by means of mathematical expressions without having any information regarding the physical properties of the materials involved as well as the environmental conditions of the given installation, the data from this project were substituted in the load equations derived by Costes.[21] Accordingly, families of load curves were obtained for the general

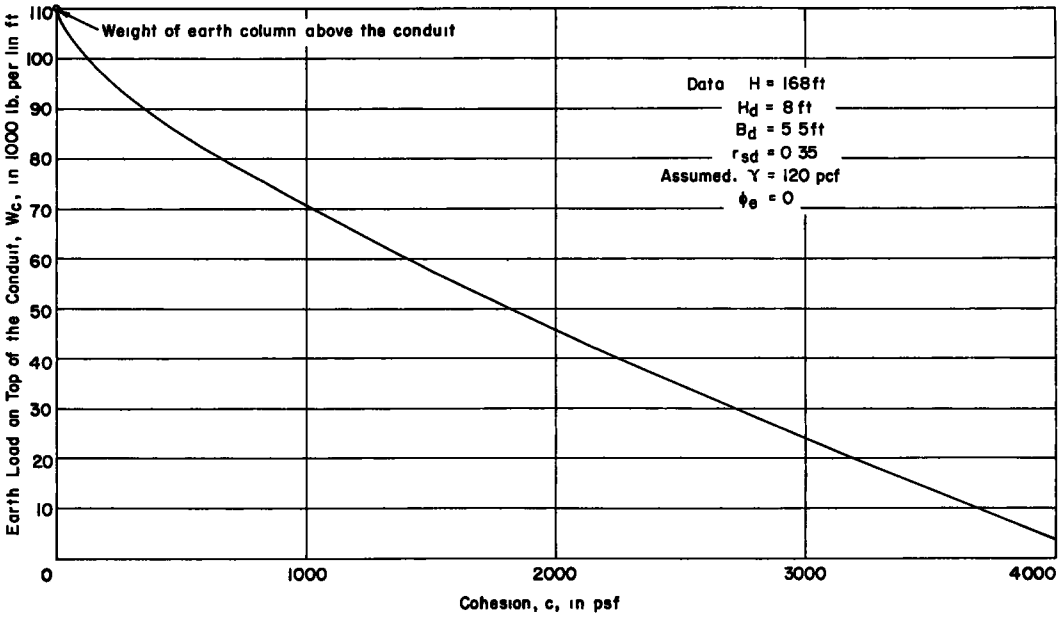

Figure 85. Computed earth load on top of conduit, assuming an s = c fill material.

case of an $s = c + \sigma \tan\phi$ fill material, as well as for the special cases of a perfectly granular or an $s = \sigma \tan\phi$ material, and a purely cohesive or an s = c material. These curves appear in Figures 83, 84 and 85 respectively.

To compute the above curves the following data were employed: Height of fill on top of the conduit, H = 168 feet; height of imperfect ditch, H_d = 8 feet; average width of the conduit, B_c = 5.5 feet; average width of the imperfect ditch, B_d = 5.5 feet; average settlement ratio, r_{sd} = -0.35; average unit weight of fill material, γ = 120 pcf.; ratio of the moduli of deformation of the loose and compacted masses, a = 1.

The top earth load was considered to be a function of the following independently varying physical factors: (1) The effective angle of internal friction of the fill material, ϕ_e, that is assumed to be mobilized along the vertical sliding planes. (2) The effective cohesion of the fill material, c_e, that is assumed to be mobilized along the vertical sliding planes. (3) The equivalent hydrostatic earth pressure ratio, K_e, that is assumed to relate the lateral and vertical earth pressures acting on any element of the earth mass, along the vertical sliding planes.

[21] See Appendix.

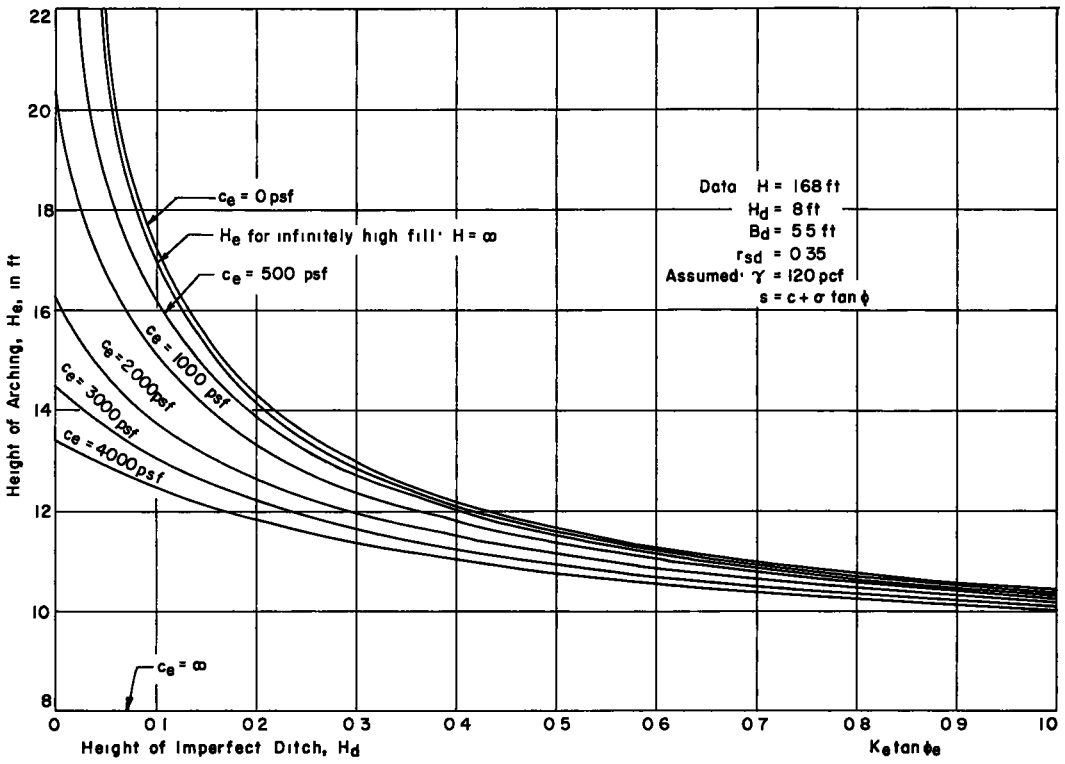

Figure 86. Variation of height of arching, H_e, for the culvert installation under study, with factors c_e and $K_e \tan\phi_e$.

In addition to the load curves, the same data have been employed to compute another family of curves plotted in Figure 86. These curves show the height of arching, or height to the plane of equal settlement, H_e,[22] as a function of the same independent variables, ϕ_e, c_e, and K_e. In the mathematical equations for the load expression, H_e appears as an independent variable, but actually, for a given installation, it is a function of the above physical factors, and, therefore, has to be determined before the load is obtained (See Appendix).

For comparison purposes, H_e has been computed also on the assumption that the fill is infinitely high, and these results have been plotted also in Figure 86. It has been shown that, mathematically, the height of arching for infinitely high fills is independent of the cohesion and the unit weight of the fill material, and that it can be computed by less tedious equations (Costes, 1955, pp. 52 and 64; also see Appendix).

Finally, the same data from this project have been employed to demonstrate the influence of the height of the imperfect ditch, H_d, on the earth load on top of the conduit of this installation. For this purpose, the Marston Load has been assumed to represent 100 percent the present value of the top earth load. Then, by employing the Marston-Spangler assumptions, that c = 0, and $K_A \tan\phi = 0.13$, the earth load has been computed as a function of H_d, and the resulting curve has been plotted in Figure 87.

From Figures 83-87, the following comments can be made regarding the conduit load, the height of arching, and the height of imperfect ditch of this installation as derived from the general mathematical treatment on arching:

---

[22] Height of arching, H_e is defined as the vertical distance between the top of the conduit and the plane of equal settlement. Within this region an effective mobilization of the shearing resistance of the fill material takes place in order that the tendency for relative subsidence of the mass directly above the conduit be opposed. However, above this height, no arching takes place in the earth mass because the fill material settles uniformly (Marston, 1922; Spangler, 1950a, 1950b).

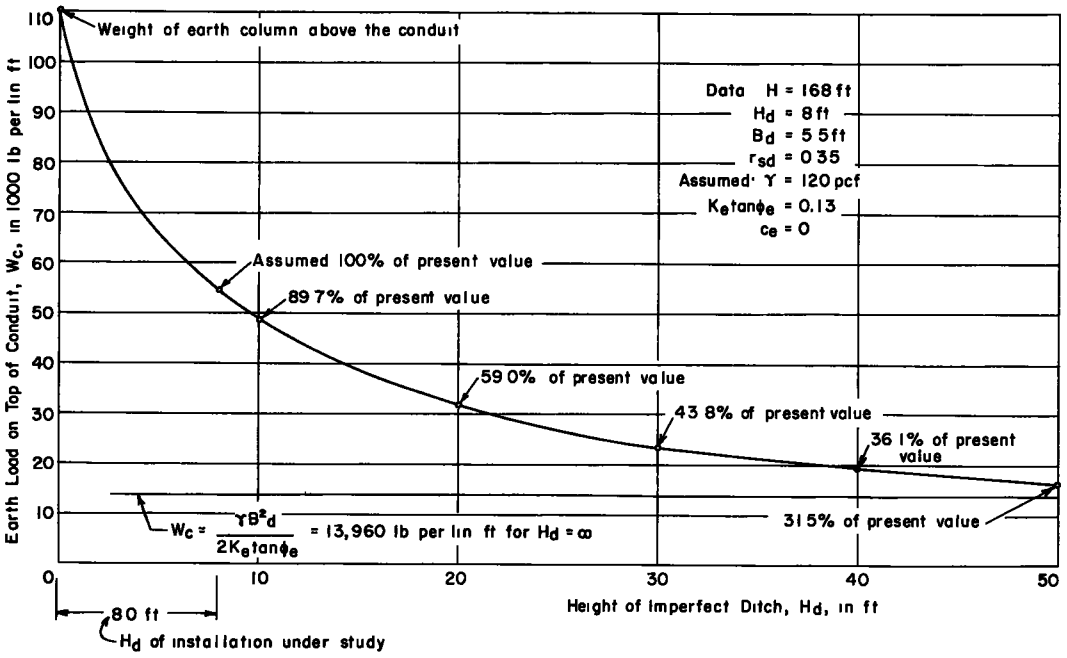

Figure 87. Variation of earth load on top of culvert under study, as a function of the height of imperfect ditch, H_d.

1. For an $s = c + \sigma \tan\phi$ material the combined factor $K \tan\phi$ is very influential on the load. For the range $0 \leqq K\tan\phi \leqq 1.0$, which corresponds to $0 \leqq K \leqq 1$, and $0 \leqq \phi \leqq 45°$, the load, starting from a maximum value, diminishes rapidly for all values of the cohesion c.

2. The cohesion of the fill material up to 250 psf. does not affect the conduit appreciably and, therefore, may be neglected. From the mathematical analysis on the conduit load it has been indicated that if $c_e \leqq \gamma B_d/2$ where:

c_e = Effective amount of cohesion mobilized along vertical sliding planes, psf.
γ = Average unit weight of fill material, pcf.
B_d = Effective width of imperfect ditch, ft.,

the load is primarily a function of the factor $K_e \tan\phi_c$, and it will not vanish for finite values of $K_e\tan\phi_c$ (Costes, 1955).

If, however, the amount of cohesion mobilized along the potential sliding planes is $c_e > \gamma B_d/2$ the conduit load, as indicated by Figure 83, will vanish rapidly for finite values of factor $K_e\tan\phi_e$ that lie within a physically possible range. For this project the critical value of cohesion c_e should be :

$$c_e = \frac{120 \times 5.5}{2} = 330 \text{ psf.}$$

This indicates that in this installation, even for a fairly soft fill material, the cohesion becomes influential on the load.

In the above mentioned analysis (Costes, 1955) it was also pointed out that the actual surfaces of equal pressure above the conduit are not plane as assumed in the mathematical treatment, but they are curved like arches. Therefore, if the conduit has a flat roof, such as a box culvert, the region within the surface of zero pressure and the roof of the conduit will be in a state of tension and, therefore, the material in this region will have the tendency to drop out. For this same reason, Terzaghi, in his treatment on tunnels, suggests that, "in order to prevent such an accident, an unsupported roof in a tunnel through cohesive earth should always be given the shape of an arch."[23]

[23] K. Terzaghi, Theoretical Soil Mechanics (New York - John Wiley and Sons) p. 199.

In the case of a conduit with a curved roof, such as the culvert under study, if the amount of cohesion mobilized by the fill material along the potential sliding surfaces is greater than the value $\gamma B_d/2$, then the possibility of having no load on top of the conduit lies within the realm of physical reality provided the overlying earth mass behaves in an elastic manner. At any rate, even if the load does not vanish completely, it will at least become minimum; thus, a less amount of lateral pressures, mobilized by the side supporting material against the sides of the conduit, will be required to restore mechanical equilibrium in the system.

3. The load curves obtained for a perfectly granular material have been extended mathematically to include values of ϕ that will never be realized in an earthen material. Nevertheless, the purpose of these curves is to show the analytical relationship between the assumed independent variables and the vertical earth load on top of the conduit.

The same graphs have been bounded by limiting curves that have been obtained when the corresponding earth pressure ratio, K, reaches the limiting values $K_A = \tan^2(45^\circ - \phi/2)$, and $K_P = \tan^2(45^\circ + \phi/2)$. Under such conditions K is called respectively, "coefficient of active earth pressure," and "coefficient of passive earth pressure."

The above limiting cases cannot be realized physically unless conditions of incipient shear failure exist in a homogeneous, semi-infinite, cohesionless earth mass that has reached a state of plastic equilibrium by the following two ways respectively: (1) it has been stretched laterally to a very great depth in such a manner that the lateral strain remained constant with depth; (2) it has been compressed laterally to a very great depth in such a manner that the lateral compressive strain remained constant with depth.

4. On the first two sets of load curves (Figures 83 and 84) the "Marston Load" is indicated. One can see that this value is neither the maximum nor the minimum value of either load range. The same value was obtained by employing the following Marston-Spangler assumptions (Spangler, 1950a):

a. $c_e = 0$. Such assumption implies that either the fill material is cohesionless, or that no cohesion has been mobilized along the vertical sliding planes.

b. The equivalent earth pressure ratio, K_e, assumes the limiting value $K_A = \tan^2(45^\circ - \phi/2)$ that was previously designated as "coefficient of active earth pressure."[24]

c. The value $K\mu \equiv K_A \tan\phi \equiv \tan^2(45^\circ - \phi/2)\tan\phi$ is equal to 0.13. Such value corresponds to $\phi \approx 10^\circ$.

The above assumptions are unrealistic because:

a. From experience it is known that even if the least trace of moisture is present in a cohesionless mass, the material will exhibit a property known as "apparent cohesion" and it will behave like a cohesive material.[25]

b. As mentioned before, the assumption of existence of an active state of plastic equilibrium in the fill mass is incompatible with the deformation characteristics and the size of the same mass.

c. An angle of internal friction equal to 10 degrees, as implied by the value $K_A \tan\phi = 0.13$, does not represent average conditions for cohesionless masses. From experience, the angle of internal friction for cohesionless materials range between 15 and 45 degrees.

The above three assumptions can also imply that: "In the 'Marston Load' the influence of cohesion and that of the combined factor $K_e\tan\phi_e$ have been taken into account by assuming a fictitious, semi-infinite, cohesionless mass in an active state of plastic equilibrium that has an equivalent angle of internal friction, $\phi_{equiv.}$, of approximately 10 degrees." Such postulate, however, is entirely arbitrary. Therefore, its validity as a working hypothesis must be proven by adequate experimentation with direct pressure measurements on a wide variety of installations and materials. From an analytical point of view, however, it should be pointed out that, with the exception of only one point, the expression for a fictitious cohesionless mass with an equivalent angle of internal friction, ϕ_e, cannot define the shearing strength characteristics of an $s = c + \sigma\tan\phi$ material (Figure 88).

From the above discussion it is felt that in the conduit design of an installation such

---

[24] The same coefficient is called also Rankine coefficient.

[25] Terzaghi, op. cit., pp. 10, 194.

as this no particular advantage is gained by adopting a load value that: (1) has been derived by assuming fictitious and unrealistic physical conditions; (2) is not necessarily the maximum value of the whole range of possible loads existing on top of the conduit.

Furthermore, it is feared that the blind use of "handbook constants" that are meaningless unless supplied by a special knowledge of the physical properties and the behavior of the earth masses involved, may induce the average engineer, designer or construction man, to make serious blunders either from a safety or from an economy point of view.

5. For a perfectly cohesionless or an $s = \sigma \tan\phi$ material, the assumption that $K \equiv K_A = \tan^2(45° - \phi/2)$ yields maximum load values for any value of the effective angle of internal friction, ϕ_e. Therefore, such assumption is on the safe side for design pur-

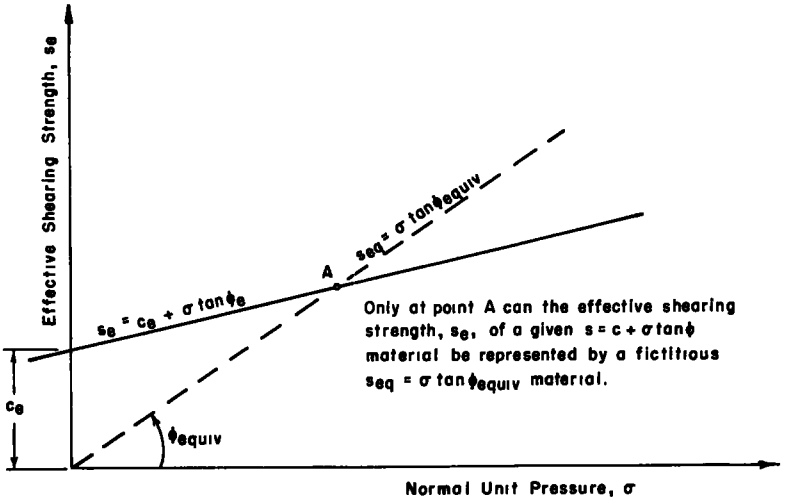

Figure 88.

TABLE 10

ϕ_e	0°	5°	10°	15°	20°	30°	40°	50°
$Wc_{max.}$ if $K_e = K_A$	111,000	69,600	55,900	48,700	44,900	42,700	44,900	49,100
$Wc_{red.}$ if $K_e = 1$	111,000	65,100	45,100	33,200	23,900	12,400	6,170	2,810
% Reduction	0	6.5	19.3	31.9	46.7	70.9	86.3	94.3

poses, although incompatible with the deformation characteristics of the fill mass on top of the conduit. However, in Figure 84 it is also shown that if K is allowed to vary within the range $K_A \leqslant K \leqslant 1$ for a given ϕ_e, the top load decreases from a maximum value Wc_{max}, to a reduced value Wc_{red}, and the percent reduction from the corresponding Wc_{max} value varies directly with ϕ. The results from the above calculations are presented in a tabulated form in Table 10.

The angle of internal friction, ϕ, for a sand, as Terzaghi points out, is at least equal to 30°.[26] Furthermore, experimental investigations conducted by the same author to determine the state of stress in sand located above a yielding strip have shown that the value K increases from unity immediately above the center line of the yielding strip to a maximum of about 1.5 at an elevation above the center line approximately equal to the width of the strip, B_d. At elevations of more than about 2.5 B_d above the center line the lowering of the strip seems to have no effect at all on the state of stress in the sand (Terzaghi, 1936a). Accordingly, if the fill material of this project is assumed to be perfectly cohesionless and if one adopts the values of ϕ and K reported by Terzaghi, the calculated load will be 70.9 percent less than the corresponding maximum value for the same ϕ and for $K \equiv K_A = \tan^2(45° - \phi/2)$. Even if one assumes that only one half of

[26] Terzaghi, op. cit., 196.

the maximum value of ϕ, obtained in the laboratory, is actually mobilized along the vertical sliding planes on account of the deformation characteristics of the fill mass, i. e., that $\phi_e = 15^\circ$, the corresponding reduction from the maximum value will be 31. 9 percent.

From the above discussion it can be seen that the assumption $K \equiv K_A$, although on the safe side from a design view point, may affect economy.

6. From Figures 83, 84 and 85 it can be seen that with a settlement ratio equal to -0. 35 the top vertical conduit load, W_c, is less than the weight of earth column above the culvert, W, for all realistic values of ϕ and c. As has been indicated in the analytical treatment of this subject (Costes, 1955), if the earth mass directly above the conduit subsides more than the adjacent masses, in which case the settlement ratio is a negative quantity, $W_c < W$.[27]

The above figures indicate also that under the same settlement conditions, in order that W_c be equal to the weight of earth column, the following two conditions must exist simultaneously: $\phi = 0$, $c = 0$.

However, such assumption is incompatible with the physical characteristics of earth masses. If the fill material did not have any shearing resistance it would have acted like a liquid. Since a liquid cannot stand on a slope, the earth mass would have sloughed off seeking a horizontal surface throughout the fill site in which case there would not be a fill.

7. From the discussions of items 3 - 5 one can see that in order that a truly rational and economical design may be applied to underground conduits, it is absolutely imperative to develop a technique by means of which c_e, ϕ_e, and K_e can be determined for given installations and materials. The following example from the culvert under study will give a more vivid picture of such need.

If one employs the same data from the installation, and assumes that $\gamma = 120$ pcf., $K_e = 1$, $c = 0$, $\phi = 30^\circ$, and $\phi_e = 15^\circ$, then, from Table 10, the maximum vertical load obtained from the arching theories and assumed to be the actual load, will be W_c = 33,200 lb. per lin. ft. of pipe.

The structural design of the culvert was based on the assumption that the load is equal to the dead weight of the earth column above the conduit. Given, $\gamma = 120$ pcf., B_d = 66 in. = 5. 5 ft., and H = 168 ft., one obtains $W = \gamma B_d H$ = 111,000 lb. per lin. ft. of pipe.

Since it is common practice to employ a factor of safety of 4 in the structural design of flexible culverts, it follows that the design load, W_D was $W_D = 4 \times W$ = 444,000 lb. per lin. ft. of pipe.

If the design load is compared with the actual maximum load developed on top of the conduit, it can be seen that $W_D / W_c = 14.3$. Therefore, if the arching theory is valid, the actual factor of safety employed in the above design was 14. 3 and not 4. Furthermore, it must be pointed out that the above calculations were made on the assumption that the fill material is perfectly cohesionless. However, from quick-consolidated triaxial tests, performed in the state highway laboratory (see Obtained Data and Appendix) as well as from information obtained from other sources (Sowers, 1954), it is estimated that the cohesion mobilized by the highly micaceous sandy silty soils of the region where the pipe is located, may be as high as 1,500 psf. Also, the angle of internal friction of the same material ranges between 28° and 38°. If one assumes that only one third of the laboratory value of cohesion is actually mobilized by the fill mass along the vertical sliding planes, i. e., that $c_e = \frac{1500}{3} = 500$ psf., and also that $\phi_e = 15^\circ$, and $K_e = 1$, then from Figure 83 one obtains W_c = 26,000 lb. per lin. ft. of pipe.

Therefore, if one takes into account the cohesion mobilized by the fill material, the factor of safety employed in the design of the conduit will be:

---

[27] In the same analysis it is shown that if the middle mass settles the same amount as the adjoining masses, which case corresponds to zero settlement ratio, W_c will be equal to W regardless of the magnitude of the shearing components, ϕ, and, c, of the fill material. If the settlement ratio is a positive quantity, in which case the middle mass subsides less than the adjacent bodies, then, mathematically, $W_c > W$ by an amount dependent on the amount of ϕ and c mobilized along the sliding planes.

$$F.S. = W_D/W_C = 444,000/26,000 = 17.1.$$

A structural design based on a factor of safety of either 17.1 or 14.3 is, indeed, very uneconomical and unjustified, even if the relative cost of the structure involved is only a fraction of the overall cost of the project. If, however, the structure itself constitutes the whole project, as is the case of a tunnel, then ultra-conservative "guesswork" due to lack of knowledge of the physical properties and the behavior of the materials involved, may result in a serious financial waste.

8. From Figure 86, one observes the following:

a. For the installation under study, the height of arching, H_e, may be computed on the assumption that the fill is infinitely high. Under such conditions, H_e becomes mathematically independent of the cohesion and the unit weight of the fill material, and

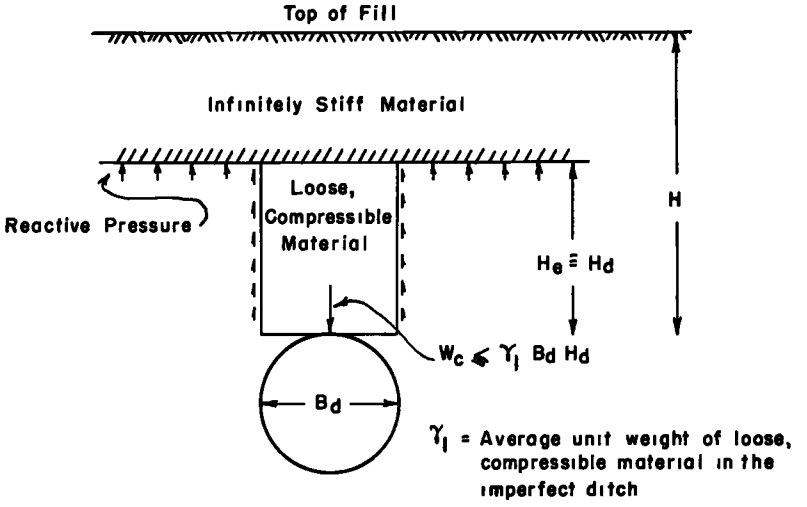

Figure 89.

it can be computed by a much simpler formula. As can be seen from Figure 50, with the previous assumptions that $\phi_e = 15^\circ$, $K_e = 1$, hence, $K_e\tan\phi_e = 0.27$, and $c_e = 500$ psf., one obtains $H_e = 12.50$ feet. For an infinitely high fill and the same $K_e\tan\phi_e$ value, $H_e = 12.58$ feet or 0.6 percent higher than the actual value. The difference is negligible.

b. From the same figure it can be seen that the greater the amount of shearing strength components c_e and ϕ_e, mobilized by the fill material along the vertical sliding planes, the less will be the height of arching. Hence, by observing the load equation,[28] one may arrive at the paradoxical conclusion that the greater in magnitude the quantities c_e, and ϕ_e are, the greater will be the load on top of the conduit. However, it has been shown mathematically that even though H_e varies inversely with c_e and ϕ_e, the greater are the magnitudes of the above shearing strength components, mobilized by the fill material, the lower will be the load on top of the conduit.

c. If the cohesion and the factor $K_e\tan\phi_e$ are allowed to increase without limit, the height of arching will approach the height of the imperfect ditch. This indicates that if the conduit is installed by the imperfect ditch method and the mass inside the ditch is looser and more compressible than the adjoining sides, no matter how stiff the overlying material is, there is always going to be an arching effect within the earth mass above the conduit.

Under the above limiting conditions the overlying material may be visualized as resembling a masonry arch constructed on top of the imperfect ditch and bridging over its sides (Figure 89). Accordingly, although the height of arching will not extend higher than the top of the imperfect ditch, the greatest part of the top vertical pressure will be transmitted on the side masses and the load on top of the conduit will be equal or less

[28] See Appendix.

than the dead weight of the loose material in the imperfect ditch.

From the above discussion it follows that, if the arching theory is valid, in an imperfect ditch installation, the top conduit load must always be less than the weight of earth column above it provided the fill mass behaves in an elastic manner.

9. From Figure 87, it can be seen that for a given installation and material the top conduit load varies directly with the height of imperfect ditch, H_d. It should also be pointed out that the graph plotted in Figure 87 has been computed on the assumption that both the settlement ratio and the factor K tanϕ remains constant as H_d increases. However, in the actual case, the higher the imperfect ditch is, the greater will be the relative settlement of the middle mass; therefore, the greater will be the amount of the shearing component factor K tanϕ mobilized by the fill material in order to oppose such settlement. Hence, since the settlement ratio and K tanϕ will increase with an increase of H_d, the vertical load will decrease by a greater amount than the values shown for each corresponding value of H_d.

From the same figure one notices also that for each installation and material, there is an optimum imperfect ditch height that will yield best results. For values of H_d exceeding the optimum value, the load will not decrease appreciably and, therefore, such imperfect ditch construction will be economically unjustified. In this installation, if the Marston Load is assumed to be the actual load existing at the top of the conduit at the present time, and if the settlement ratio and factor K tanϕ are assumed to remain constant with an increase of H_d, from Figure 87, it is indicated that the optimum height of the imperfect ditch would have been 40 feet. For such height the top load would have been only 36.1 percent of the Marston Load assumed to exist at the present time.

Analytically, it has been shown that if the imperfect ditch is made high enough so that factor $w' = 2K_e\tan\phi_e \frac{H_d}{B_d} \gg 1$, the conduit load can be expressed by the equation

$$W_c = \frac{\gamma B_d^2}{2K_e\tan\phi_e}\left(1 - \frac{2c_e}{\gamma B_d}\right) \quad \text{(Costes, 1955)} \qquad (8)$$

From the above expression it can be seen that under such conditions the load will be independent of the fill height; it will be a function of only the effective width of the imperfect ditch and of the unit weight as well as of the mobilized shearing strength of the fill material.

From the same expression it can be seen also that mathematically: (1) for $c_e \geqslant \gamma B_d/2$ the load vanishes; (2) the greater the factor $K_e\tan\phi$, the lower will be the load; (3) if $c_e = 0$ the load expression becomes:

$$W_c = \frac{\gamma B_d^2}{2K_e\tan\phi_e} \qquad (9)$$

Equation 9 is identical to the expression derived by Terzaghi for the top load on deep tunnels through dry sand. [29]

From the above discussion it is felt that current conduit installation practices fail to exploit fully the advantages that a sufficiently high imperfect ditch may offer to the engineer. At present the general tendency is to construct imperfect ditches that are too low for the corresponding installation. Various recommendations specify arbitrary imperfect ditch heights without realizing what favorable environmental conditions may be created by an optimum H_d, that would justify the extra cost of a higher imperfect ditch construction. [30]

It is hoped that one of the aims of future research efforts on underground conduits will be toward the creation of a rational method by means of which the height of an imperfect ditch for a given installation and material can be designed to yield maximum benefits to the engineer. Such efforts will really do justice to this ingeneous scheme that was initiated and advocated by the late Dean Anson Marston and by Professor M. G. Spangler.

---

[29] K. Terzaghi, Theoretical Soil Mechanics (New York - John Wiley and Sons) p. 196.

[30] See References, Costes (1955) for a proposed method by means of which a high imperfect ditch can be constructed without bracing or sheeting operations.

In the foregoing analysis an attempt was made to apply the arching theories on the culvert under study. Load curves were drawn with the data supplied, and a special effort was made to use physical constants that are as realistic and as compatible with the environmental conditions of this project as such "guesswork" would permit. Qualitative conclusions were, thus, drawn relative to the various features of the installation and comments were made with respect to current conduit design practices. However, it should be emphasized once again that the whole discussion was based on theories that deal with ideal materials and with the geometry and static equilibrium of the culvert installation. The actual properties of the various materials constituting the composite conduit-fill structure have been accounted for by using fictitious equivalent physical constants. Accordingly, it must always be kept in mind that such theories when applied to earth masses, are handicapped by definite limitations.

To construct an earth structure, soil cannot be used in the same sense as a steel bar, or a prefabricated concrete beam, or a wooden block is used respectively to build a steel frame, or a concrete bridge, or a wooden pedestal. The physical properties of each structural component of the latter structures can be determined closely by means of routine laboratory tests and, therefore, one is in a position to predict with a reasonable degree of certainty the overall behavior of the respective integrated structures. An earthen material is far from being a homogeneous engineering material and many of its physical characteristics are developed while the mass is being constructed either by natural or by artificial processes. Consequently, such properties cannot be predicted with a great degree of accuracy from laboratory tests. Only by a "learn as you go" method will the engineer be able to ascertain their true nature and to cope successfully with each circumstance.

The properties and the behavior of a soil mass generally depend not only on the nature, size, and the initial state of the mass, but also on the rate of stress application, on the permeability of the material, and on its strain characteristics. The latter characteristics, except for limiting conditions that may be realized in the laboratory but in an ordinary engineering structure will never be allowed to materialize, are of a highly indeterminate nature. Furthermore, due to seasonal variations, capillary phenomena, and various physical processes such as consolidation, dessication and others, the initial state of a soil mass will not remain constant but will vary with time. Consequently, a great deal more experimentation is required before a reliable mathematical theory is established to predict the behavior of an earth mass on top of an underground conduit under given installation conditions.

As mentioned previously, experimentation on underground conduits must be organized and based on statistical principles and methods and it must consist of as many direct measurements that are not functions of each other as possible. Only under such conditions will one be able to ascertain the validity of the assumptions employed in his theories and to estimate by rational means the proper factor of safety to be used for each design so that optimum results can be achieved from a safety and an economy point of view.

SUMMARY AND CONCLUSIONS

Experimental Data

Installation and Environmental Conditions. The culvert under study was a 66-inch Multi-Plate corrugated metal pipe, 576 feet long, consisting of No. 1, No. 3 and No. 8 gage metal. It was initially elongated three percent vertically by field strutting, the strut spacing varying from 3 foot centers to 6 foot centers. The structural plates were bolted with ¾-inch bolts the spacing of which varied from 6 bolts per foot of longitudinal joint for the No. 1 gage metal, to 4 bolts per foot of longitudinal joint for the other two gages.

The culvert was installed by the imperfect ditch method and it was covered by an earth fill the height of which was approximately 170 feet at the roadway center line. To account for differential settlement, the pipeline was placed with ¼ percent camber.

The fill material ranged from rock fragments of approximately 6 feet in largest dimension to a tannish-gray, highly micaceous, non-plastic, clayey-sandy-silt.

The fill material was not deposited and compacted in layers as it had been repeatedly recommended by key personnel members of the N. C. State Highway and Public Works Commission and by experts on underground conduit installations, but it was end-dumped from either side of the culvert in an unbalanced way. As a result of such construction methods an earth slide occurred on the western mountain slope. On account of the action of the sliding material the pipe was thrown out of alignment, and, although, it was realigned, it continued to deform and be displaced laterally for at least the ensuing 150 days of construction.

To insure a somewhat more balanced distribution of load on the pipe a ramp was constructed across the pipe at a later date. Thenceforth, fill material was end-dumped along the longitudinal axis of the culvert from the ramp instead of being dumped against one of its sides without depositing a counter balancing earth quantity on the other side. However, the construction of the ramp was accomplished by uneven end-dumping also and, consequently, the culvert was displaced laterally, although to a smaller extent.

Table 11 contains in a summarized form the ranges of physical properties, compaction characteristics and soil classification of the side supporting material, the bedding material, and the loose material placed in the imperfect ditch.

TABLE 11

	Liquid Limit LL - %		Plastic. Index P.I. - %		Water Content w - %		Dry Unit Weight γ_d - pcf.		Void Ratio e_m.		Soil Class.
	Range	Avg.	Range	Avg.	Range	Avg.	Range	Avg.	Range	Avg.	
Side Support	26-30	28	NP-NP	NP	10. 1-13. 9	11. 88	77. 8-106	96. 70	0 55-1. 1	0. 699	A-4(4)
Bedding Mat.	39-46	41. 7	12-17	14. 6	15 1-20. 0	17. 63	86. 8-109	100. 5	0. 51-0. 90	0 630	A-7-6(9)
Imp. Ditch Mat.	-[a]	36	-[a]	7	11. 6-13. 3	12. 24	52. 8-79. 9	69. 18	1. 1 -2. 1	1 42	A-4(2)

[a] Only one composite sample was tested.

The side supporting material was more or less uniform throughout the pipe length and it was compacted in 6-inch layers by pneumatic tamping.

The ratio of the void ratio of the loose material in the imperfect ditch, e_l, to the void ratio of the adjacent compacted mass, e_c, at identical positions along the pipe line was as follows:

TABLE 12

Ring No.	e_l/e_c
30	1. 30
31	1. 48
32	1. 38
36	1. 61
37	3. 44
38	1. 52

Settlement and Deformations. By means of a level, an extensometer, a pipe protractor, and a plumb bob, the following measurements were taken from the deforming culvert at various time intervals: (1) settlement of the flow line; (2) shortening of the vertical diameter; (3) elongation of the horizontal diameter; (4) rotation about the longitudinal axis; (5) lateral displacement of the longitudinal axis; and (6) pipe cross-sections showing deformed shape of structure.

From the above measurements the following may be deduced: (1) for every fill increment there was a corresponding increment in the settlement, in the shortening of the vertical diameter, and in the elongation of the horizontal diameter of the pipe structure. (2) Upon the completion of the fill the deformations mentioned in item 1 came substantially to rest. However, small deformations were recorded and, as far as the lateral bulging is concerned, the deflection factor was estimated to 1. 4. (3) The settlement profiles of the flow line were substantially the images of the fill cross section at every stage of the fill construction. (4) Although the actual differential settlement of the flow line exceeded the anticipated one by 0. 15 foot, the amount of camber employed in this installation was considered adequate. (5) The pipe bulged out an amount approximately equal to its vertical shortening for every stage of fill construction. (6) The maximum shortening of the vertical diameter was 5. 82 percent of the nominal circular pipe diameter. Such amount is well below the 20 percent deflection considered to represent failure conditions. (7) The removal of the struts had a definite influence on the deformations and settlement of the culvert as indicated by corresponding sudden jumps in the

time-deformation and time-settlement curves of the structure. This influence, however, was not enough to create any hazardous conditions. (8) The culvert deformed a greater amount at the quarter points than at the middle section. Although not proven experimentally, it is possible that the following factors may have influenced the above action: (a) Load transfer at the quarter points resulting from arching action occurring along the longitudinal axis of the pipe. (b) Low degree of precompaction of the side supporting material that was placed at the quarter points. (c) Less inherent resistance to deformation exhibited by the pipe structure on the quarter points on account of thinner metal gage, larger strut spacing, and less amount of bolts per longitudinal seam of structural plate. (d) A combination of all factors mentioned in items a - c. (9) A strong indication exists that unbalanced forces, generated by the earth slide and by one-sided end-dumping, caused lateral displacements in the pipe line oriented away from the direction of these forces. The pattern of the same displacements indicate that the influence of the above forces continued for at least 150 days after the completion of the culvert installation. In addition to the above, there is a further indication that the conduit was also displaced in an upward direction. Furthermore, during the initial stages of fill construction, the structure was squeezed-in by the sliding material with a subsequent vertical bulging; however, when sufficient overburden was on top of the culvert, the structure began settling and deforming in a manner similar to the other regions where the slide was not influential. (10) The culvert rotated but a minute amount about its longitudinal axis.

Physical Properties and Compaction Characteristics of Side Supporting Material. The material furnishing side support to an underground conduit has been recognized to constitute one of the most important parts of a culvert installation especially under a high fill. This material, if properly chosen and properly compacted, will moblized lateral pressures against the sides of the conduit that will balance the top pressures exerted by the fill overburden. Thus, even if the inherent strength of the conduit is not appreciable, the structure will be able to withstand external pressures of great amount without failing in shear or by excessive deformation.

The side supporting material of this installation was considered to furnish adequate lateral support to the culvert under study. Therefore, for reference purposes, it was considered desirable to ascertain the physical properties and the compaction characteristics of the side supporting material. Such data could be correlated with the directly measured lateral pressures, mobilized by the same material, and at a later date the same information could be compared with identical data from other satisfactory installations.

To obtain the data mentioned above, openings were made on the sides of the pipe structure by means of an electrically driven drill and a power saw. Through these openings a specially designed sampling device was forced into the soil mass by means of a mechanical jack. Thus, soil samples were obtained along lateral depths perpendicular to the longitudinal axis of the pipe line. This operation was performed approximately two years after the culvert was installed and about a year and a half after the completion of the fill construction.

From the various tests made on the above specimens the following are indicated: (1) The side supporting material was mostly an A-4 material with a group index varying between 3 and 5. The only exception was encountered on the eastern side of Ring 24, located near the middle section of the pipe line, where the side support was classified as an A-6(7) material. (2) The dry unit weight, γ_o, the water content, w, and the void ratio, e, ranged as follows: (a) γ_o, from 98 pcf. to 111 pcf. with an average value of 105 pcf. (b) w, from 17 percent to 24 percent with an average value of 19.9 percent. (c) e, from 0.48 to 0.65 with an average value of 0.566. (3) With the exception of erratic variations the dry unit weight increased to the above average value of 105 pcf. regardless of the degree of initial compaction shown on Tables 2 and 11. (4) The dry unit weight has the tendency to decrease with lateral depth. Such tendency may be construed as follows: At the immediate vicinity of the conduit the lateral bulging of the structure, and stresses generated in the soil mass on account of the arching phenomenon tend to consolidate the side supporting material a greater amount than that caused by the fill overburden. However, at greater lateral depths the influence of the above two factors

is dissipated and the soil mass consolidates mainly on account of the fill overburden. (5) The water content and the void ratio of side supporting material, as expected, generally increased with lateral depth. (6) The same material exhibited a greater amount of plasticity than the samples obtained during the installation of the pipe (Tables 1 and 11). The initial data were obtained from six composite samples, whereas the above data were gathered from 32 individual specimens obtained by the sample device from eight different openings, made on the sides of the culvert, and from additional material from the same openings brought to the state laboratories in cloth bags. Therefore, it is felt that the later date more nearly represent the physical characteristics of the side supporting material. (7) Results from "quick-consolidated" triaxial tests, performed on the same specimens, indicate that the angle of internal friction, ϕ, and the cohesion, c, of the side supporting material varied as follows:

		10% Strain Failure	15% Strain Failure	20% Strain Failure
For: $s_s = 2.64$, $\gamma_o = 90.0$ pcf., $e = 0.83$, $w = 11.2\%$	ϕ	26° - 30'	34° - 0'	38° - 30'
	c	649 psf.	432 psf.	274 psf.
For: $s_s = 2.64$, $\gamma_o = 110$ pcf., $e = 0.50$, $w = 17.6\%$	ϕ	22° - 15'	27° - 30'	31° - 30'
	c	1354 psf.	1210 psf.	1066 psf.

For the same fill height, plate gage, strut spacing, and number of bolts per foot of longitudinal joint, the lateral bulging of the conduit structure varied directly with the degree of initial compaction of the side supporting material.

To achieve a more economical conduit design in the future, research efforts must be directed toward the creation of specifications that, for a given conduit type and size, and for a given fill height and fill material, would specify: (1) the nature of side supporting material; (2) the size of the side supporting mass; and (3) the method of placing and the minimum degree of initial compaction that the side supporting material must have for satisfactory performance.

Under the conditions stated in the previous paragraph prestrutting may be rendered an uneconomical and useless operation and, therefore, it may be omitted from future installations.

Data from Strain Gages, Strut Load Cells, and Pine Compression Caps. Stress-strain diagrams and load-deformation curves were employed to evaluate data from; (1) unidirectional strain measurements at various points of Rings 31, 37 and 55 obtained by Baldwin - Southwark SR-4, Type A-1 strain gages (Figure 58); (2) vertical strains at two struts of Ring 31 recorded by strut load cells containing nine permanently installed SR-4, Type AX-5 strain gages (Figure 59); (3) vertical deflection measurements obtained from the pine compression caps along the strutted structure (Figure 60).

The computed loads were excessively large in magnitude and exceeded the structural capacity of the culvert by enormous amounts. Furthermore, from the same computations the ratio of the vertical load to the horizontal load varied from 1.3 at the middle section of the culvert to approximately 4.2 at Ring 55. Such values indicate differential pressures which the flexible culvert under study would never have been able to withstand. Consequently, had these loads existed in reality the pipe would have collapsed long ago, either by excessive deformation, or in shear, or by buckling. Nevertheless, from numerous inspections made of the job the structure appears to maintain an approximately cylindrical shape and not a single sign of shear failure is discernable at the bolted connections.

From a further analysis of the evaluated data it is realized that in addition to being incompatible with the actually observed conditions of the pipe, the above computations do not have any quantitative significance for the following possible reasons:

1. The recorded strains and deformations indicated that shortly after the beginning of fill construction both the structural plates and the pine compression caps had been stressed beyond their respective elastic limits and, therefore, plastic flow conditions

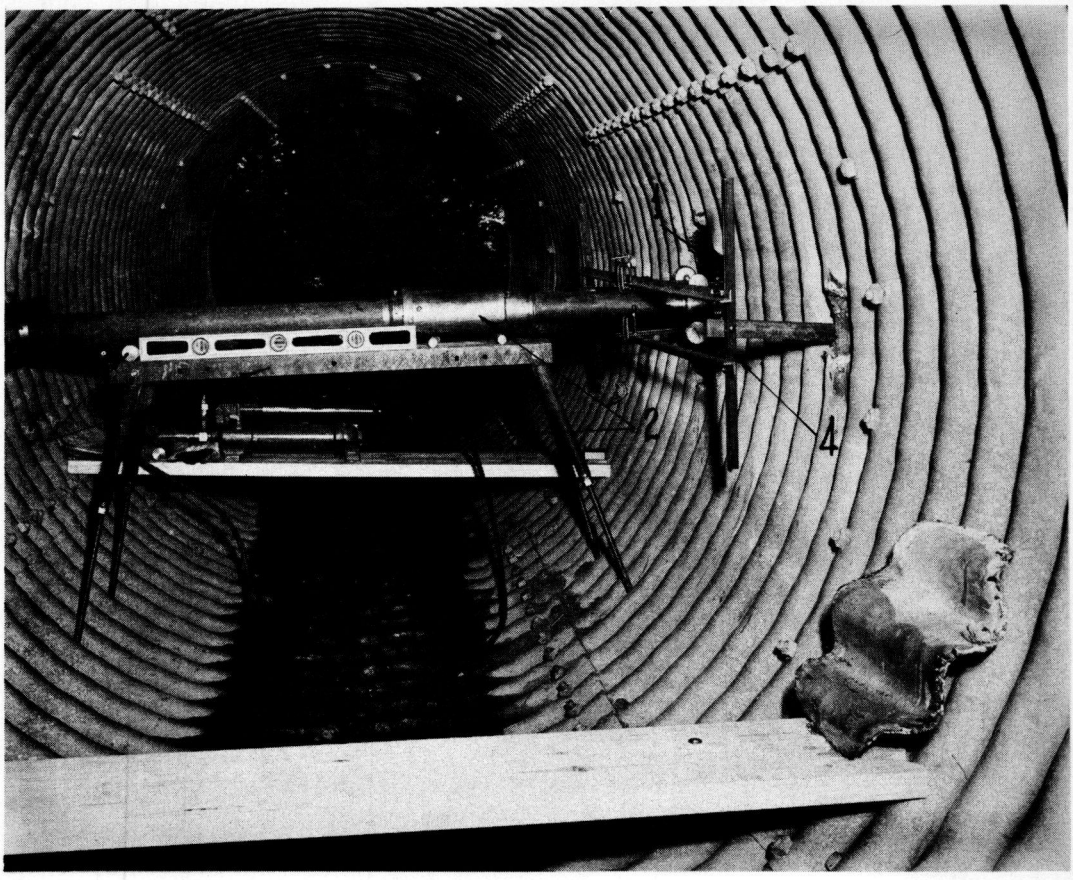

Figure 90. Experimental setup for direct determination of lateral earth pressures against the sides of a flexible conduit. For demonstration purposes circular section cut from the pipe surface by means of a flame torch is shown at right foreground.

had been realized on both materials during the whole test period. Hence, as no records are available from either the actual rate of load application or the total length of time that each load increment was allowed to act on the pipe structure, no intelligent interpretation of the data can be made by using laboratory stress-strain or load-deformation diagrams.

2. Even if the materials were stressed within their respective elastic ranges, the state of strain and, subsequently, the state of stress at a point of the structure cannot be defined by a single strain measurement oriented along one direction. From strain gage theory it follows that, with the exception of uniaxial stress application and along the direction of the stress, one cannot apply a simple, directly proportional relationship between stress and strain to evaluate stresses from strain measurements. In order that such evaluation be possible at a single point, at least three strain measurements must be obtained, each along a different direction through the point. Also, the Poisson ratio for the material being measured must be known.

3. It was endeavored to place each strain gage as close to the geometrical neutral axis of the pipe corrugations as the installation facilities of the Armco laboratories would permit. However, even if such installation was perfect no assurance can be given that the geometrical neutral axis would coincide with the physical neutral axis of each corrugation. On the other hand the sensitivity of the strain gage apparatus is such that it would record even minute bending strains that would be introduced by the curved beam action of the corrugation had not the strain gage element been placed exactly on the actual

neutral axis of the corrugation.

4. Recorded high strains may have resulted from local buckling in the structural plates due to local stress concentration. Such strains instead of being indicative of high stresses, are accompanied actually by a partial stress relief due to yielding.

5. In addition to the vertical loading action of the fill overburden, the culvert may have been subjected to several other actions that cannot be determined within narrow limits. Such actions were due to: (1) arching effect along the longitudinal axis of the conduit; (2) the continued drive of the earth slide; (3) lateral displacements of the pipe structure and local stress concentration due to unbalanced end-dumping; and (4) tendency of the structure to rotate about its longitudinal axis.

Therefore, even if the state of stress at various points of the pipe were completely determined, it would be absurd for one to attempt an external earth pressure evaluation from a combination of stresses of diversified and indeterminate nature.

6. Despite waterproofing most of the bottom strain gages were grounded and, therefore, the validity of the readings is highly questionable.

Although the above readings are of no quantitative significance, the uniformity that was observed among them at identical dates and the pattern of the calculated load curves may yield the following qualitative information: (1) For each fill increment there was a corresponding load increment both in the plates and in the struts. (2) Upon the completion of the fill the load practically ceased to exist. Small increments are attributed to deformation due to plastic conditions rather than to actual load increments. (3) The load increased at an increasing rate during the early stages of fill construction. At later dates, however, its rate of increase decreased until it stopped upon the completion of the fill. (4) The removal of struts affected the load on the plates. (5) A greater amount of load was indicated at Ring 55 than at Rings 31 and 37. However, as this load was evaluated from strains and deformations, and since the rigidity of the pipe varied from Rings 31, and 37 to Ring 55, one cannot ascertain whether these values resulted from actual high earth pressures or from low resistance to deformation exibited by the pipe structure at Ring 55.

Date from Settlement Cells. From settlement cell readings, extensometer measurements, and profiles of the pipe flow line an overall value for the settlement ratio of this installation was estimated to be -0.35.

The above value was obtained by taking the arithmetic mean of the constant portion of the settlement ratio-time curves constructed for all six positions where settlement cells were installed (Figures 81 and 82).

To compute each value of the above curves mean time-settlement curves, constructed from individual settlement cell data, were employed. These curves were extrapolated when the cells became inoperative.

No statistical analysis has been made in connection with the measurements obtained from each individual cell because only one reading was taken each time a new set of readings was obtained. Accordingly, the experimental error associated with those readings has not been determined. Kinking of the rubber hoses connecting each cell with the pipe interior is believed to have been the greatest source of error.

From the above it follows that the validity of the overall value of the settlement ratio mentioned above is very questionable. However, this value has been employed as quasi-factual data to make an analytical evaluation of the vertical load on top of the conduit with the aid of arching theories. Qualitative conclusions from this evaluation appear below.

Although quantitatively the settlement ratio-time curves are very questionable, one may draw the following qualitative conclusions from the general trend of the above curves:

1. During the early stages of fill construction the settlement ratio decreased rapidly in absolute value. At later dates the same ratio had the tendency to increase back to its initial values, however, the patterns of all six curves are of a damped oscillating nature.

2. The above curves stopped fluctuating approximately at the end of fill construction. From then on the settlement ratio of each position remained substantially constant with time, having the slight tendency to decrease in magnitude.

3. From the curves of both ring groups it is indicated that the settlement ratio varied directly with the ratio of the initial void ratios of the loose material in the imperfect ditch to the adjacent compacted masses, e_1/e_c (Table 12). Therefore, since analytic-

ally the vertical load on top of the conduit varies inversely with increasing negative values of the settlement ratio, one may speculate that the greater the difference in compaction between the loose material in the ditch and the adjacent compacted masses, the less will be the top vertical load. Such speculation, however, has to be proved by actual direct measurements of the top earth pressures.

4. The removal of the struts affected the settlement ratio by a small, nevertheless, noticeable amount. From this action as well as from the conclusion of item 2 it is indicated that the various components of the composite conduit-surrounding fill mass structure behaved in a more or less elastic manner.

Evaluation of Top Earth Load by Means of Arching Theories

The data from the geometrical features of the conduit installation were employed to compute the vertical earth load on top of the conduit as a function of the effective values of the cohesion and the angle of internal friction of the fill material, c_e and ϕ_e, and the equivalent hydrostatic earth pressure ratio, K_e (Figures 83-85). The above variables are assumed to act along vertical potential sliding planes, extending from the sides of the imperfect ditch to some horizontal plane through the fill mass called, "the plane of equal settlement." Above this plane no relative settlement occurs within the fill mass. In the same computations the average unit weight of the fill material, γ, was assumed to be equal to 120 pcf., and as an overall value for the settlement ratio of this installation, the previously mentioned quasi-factual value $r_{sd} = -0.35$ was adopted. These curves, supplemented by the general analytical treatment on arching indicate the following:

1. All other factors remaining constant the top load is influenced to a great extent by small variations of all three of the above independent variables c_e, ϕ_e, and K_e that express the strength characteristics of fill materials. Therefore, it is pointed out that the use of mathematical equations to predict the conduit load without ascertaining within narrow limits the physical characteristics of the materials involved is a meaningless and perhaps dangerous operation from a design point of view.

2. For a negative settlement ratio, $r_{sd} = -0.35$ for this installation, the theoretical maximum load value is equal to the weight of the earth column on top of the conduit. However, such value is obtained by assuming that the fill material does not exhibit any shearing strength i. e., that $c_e = 0$ and $\phi_e = 0$ (Figures 83, 84 and 85). As such assumption is incompatible with the physical characteristics of earth masses, it follows that for a negative settlement ratio, the conduit load as evaluated by the arching theories will always be less than the weight of earth columns.

3. For values of c_e up to $\gamma B_d/2 = 330$ psf., where B_d is the effective width of the imperfect ditch[31] and $\gamma = 120$ pcf. is the average unit weight of the fill material, the load value is influenced primarily by the combined factor $K_e\tan\phi_e$ and vanishes only if, mathematically, $K_e\tan\phi_e$ is allowed to approach infinity. However, for c_e greater than $\gamma B_d/2$, the load decreases rapidly and vanishes for finite values of $K_e\tan\phi_e$ that lie within the realistic physical ranges, $0 \leqslant K_e \leqslant 1$ and $0 \leqslant \phi_e \leqslant 45^\circ$ (Figure 83).

4. For each value of ϕ_e greater than zero, the maximum load values are obtained by assuming the $K = K_A = \tan^2(45^\circ - \phi/2)$ (Figure 84). However, if K is allowed to vary between the limits K_A and $K_P = \tan^2(45^\circ + \phi/2)$, the load value decreases, and the percent reduction from the corresponding maximum value varies directly with ϕ_e. Table 10 gives the computed load values for the installation under study and the corresponding percent reductions for values of ϕ_e ranging between zero and 50 degrees and for values of K equal to K_A and unity. The latter value has been reported by Terzaghi from experimental investigations on the state of stress in sand located above a yielding strip.

5. Postulating $c_e = 500$ psf., $\phi_e = 15^\circ$, $K_e = 1$, and $\gamma = 120$ pcf., the top load value for this installation, as computed by the general arching theory is equal to $W_c = 26{,}000$ lb. per lin. ft. (Figure 83). The design load, employed in the structural design of the conduit, is 17.1 times greater than the above load value. This design load has been ob-

[31] In this installation, B_d has been assumed to be equal to the conduit diameter, i. e., $B_d = 5.5$ feet.

tained by assuming that the conduit sustains the full weight of earth column on top of it, and by employing a factor of safety equal to four. Hence, if the above postulates and the arching theory are valid, the actual factor of safety, employed in this conduit design, is 17. 1 instead of 4. 0

6. From the discussion of item 5 it follows that at the present time further research on underground conduits should be aimed toward the development of a technique by means of which the physical characteristics of a given fill material for a given installation may be determined within narrow limits. By such a method the engineer will be able to get away from the mercy of "statistical average field conditions" and he will be able to cope with each situation more intelligently achieving, thus, a truly rational and economical design.

7. The calculated Marston load was found to be neither the maximum nor the minimum possible load value for this installation. Furthermore, it is indicated that the above value has been derived from assumptions that are incompatible with the physical and the deformation characteristics of a fill mass. Therefore, it is feared that the blind use of such value by the average engineer may be conducive to serious blunders from a safety and economy point of view.

The same data as in the previous item were employed to compute the height of arching, H_e, of this installation as a function of the same independent variables, c_e, ϕ_e, and K_e (Figure 86). H_e was also computed on the assumption that the fill is infinitely high. Under the latter limiting conditions it has been shown analytically that H_e becomes independent of the unit weight and the cohesion of the fill material and can be computed by a much simpler equation. From this family of curves the following are indicated:

1. For this installation H_e may be computed on the assumption that the fill is infinitely high. The results from such calculations differ by negligible amounts from similar calculations based on finite fill heights.

2. H_e varies inversely with c_e and ϕ_e. Hence, since the top load in an imperfect ditch installation varies directly with H_e one would arrive at the erroneous and paradoxical conclusion that the greater is the effective shearing resistance of the fill material, mobilized along the vertical sliding planes, the greater will be the load. However, it is also pointed out that the net effect of an increase of c_e and ϕ_e on the load expression, is the decrease in magnitude of the same expression.

3. If factors c_e and $K_e \tan\phi_e$ are allowed to increase without limit the height of arching approaches in magnitude the height of imperfect ditch, H_d. Hence, in the limit one obtains $H_e = H_d$. This indicates that even if the material is infinitely stiff it will arch over the imperfect ditch of such installation in the same manner as a masonry arch supported by the compacted masses adjacent to the imperfect ditch. Such concept may also be applied in the case of a mined-in conduit through hard rock or other very stiff material.

The influence of the height of imperfect ditch, H_d, on the top conduit load was studied by plotting a curve in which the conduit load appears as a function of H_d only (Figure 87). To compute this graph the Marston-Spangler assumptions were employed together with the data from the geometry and the settlement characteristics of the installation. From the above figure it can be seen that:

1. The load decreases rapidly with increasing values of H_d, and approaches asymptotically a finite value. From the general analytical treatment it is indicated that for an $s = c + \sigma \tan\phi$ material, if H_d is large enough so that factor $w' = 2K_e \tan\phi_e \, H_d/B_d$ can become $\gg 1$, and if $c_e \geqq \gamma B_d/2$, the load on top of the conduit will become negligible. If the material is perfectly granular the load will approach the value $W_c = \dfrac{\gamma B_d^2}{2K_e \tan\phi_e}$ obtained by Terzaghi for deep tunnels through dry sand.

2. For each conduit installation and fill material there is an optimum imperfect ditch height for construction economy as well as structural design.

3. An imperfect ditch is considered to be a very important feature of a conduit installation, especially during the early stages of fill construction. During this period the side supporting material is still in a transient condition from a compaction point of view and, therefore, it cannot mobilize the full amount of lateral pressures against the sides of the structure. Therefore, if a sudden increase in the top load due to construc-

tion progress is not checked by arching action induced by the imperfect ditch it will result in excessive lateral bulging of the structure with possible unfortunate consequences.

General Conclusions

From a performance point of view the conduit is functioning very satisfactorily.

The structure has assumed for all practical purposes a cylindrical shape. This indicates that the external earth pressure must be substantially uniform around the culvert otherwise the flexible structure would have been collapsed by excessive deflection.

The top earth load cannot be excessively high. If that were the case the conduit would have bulged out laterally a much greater amount on account of the rubber ball action of the highly micaceous side supporting material that had not been precompacted to optimum amounts.

On account of the unique environmental and construction conditions under which this installation was completed, no generalizations can be made relative to the performance of future high fill installations.

Lack of statistical planning in organizing the research work on the above installation prohibits one from forming a firm opinion relative to the experimental error involved in the various measurements. Consequently, only general conclusions have been drawn from the graphical representation of the data obtained.

Unless the external earth pressures are measured by direct means no conclusive evidence can be gathered relative to the validity of the arching theories as well as the Iowa Formula for deflections in flexible conduits as applied in the installation under study.

RECOMMENDATIONS

In future construction operations it is strongly recommended that in the event end-dumping is considered to be the only feasible method to build an earth fill under which a drainage culvert has been installed, such end-dumping should be carried out in a balanced way so that the resultant force exerted on the conduit structure will be as nearly vertical at all times as possible. End-dumping along the longitudinal axis of the pipe from ramps constructed over symmetrical regions of the conduit appears to be a less hazardous operation than one-sided end-dumping.

In high fill installations, before a conduit structure is installed at a given site, it is imperative that a thorough soil exploration of the site be performed and any unsuitable foundation material be removed. A few extra borings may save a lot of headaches in the future caused by earth slides, differential settlement, slope instability, etc.

To conduct experimental work in future installations of similar nature a statistical outlook is absolutely necessary in planning the various research procedure and apparatus. In order that an intelligent analysis of the data obtained by made, the experimental error involved in each measurement must be ascertained. Accordingly, the number of readings to be obtained at each position and the optimum spacing of positions from which data are to be secured on each date must be predetermined through designed experiment planning.

Unless different installation methods are adopted, earth pressure determination from strain gage measurements is impossible for this type of structure. Even if the materials involved are stressed below their elastic limits, to determine the state of strain and, subsequently, the state of stress at a single point of a pipe structure at least three strain measurements must be obtained along three different directions through the point. Furthermore, the Poisson ratio of the conduit material must be known. Accordingly, it is recommended that in future installation the determination of external earth pressures must be sought by direct means.

If a conduit under a high fill is to be used for experimental studies yielding valuable information for the future, it will be desirable to design the same conduit with a more adequate working space so that the research personnel may accomplish their diversified and precise tasks with a minimum amount of experimental error that are unavoidable under adverse space conditions.

Future research efforts should be directed toward the creation of a rational method

by means of which the following may be accomplished for a given conduit installation:

1. Specifications may be drawn relative to: (1) the type of side supporting material; (2) the minimum size of the side supporting mass; and (3) the minimum degree and the method of compaction of the side supporting material.
2. An optimum imperfect ditch height may be designed, and the loose, compressible material in the ditch may be specified to produce best results.
3. Means by which the amount of effective shearing components c_e and ϕ_e, mobilized by the fill material along the vertical sliding planes during the arching action, may be determined within narrow limits.
4. A procedure by which more substantial information on the equivalent hydrostatic earth pressure, K_e, as well as on the settlement ratio, r_{sd}, may be obtained.

In the event that the features discussed in items 1 - 3, have been given the proper attention, it is felt that prestrutting a culvert, in addition to causing "barn-roof" stress concentration on the structure, is a useless and an uneconomical operation and, therefore, such operation can be omitted.

In the event that no conclusive information exists relative to the physical characteristics of a fill it is recommended that:

1. The side supporting material consists of granular material compacted to the highest possible degree by the available means.
2. The imperfect ditch be made as high as economically feasible.
3. The compressibility of the imperfect ditch material be much higher than that of the adjacent compacted mass. The same material should also be in the loosest possible state when placed in the imperfect ditch.
4. The conduit structure be designed on the assumption that the full weight of earth column is acting against its top, nevertheless, a considerably lower factor of safety could be used than the one employed by current practices. The intuition and experience of the engineer should decide by how much the above factor should be reduced; however, it should be pointed out that from theoretical considerations the assumption of the full earth column weight as a maximum load value represents a limiting condition unlikely to occur in the actual case. Consequently, an inherent factor of safety is incorporated with the above assumption and the use of an ultra-conservative structural design may affect economy appreciably.

To obtain substantial experimental information relative to the discussion of the last three items mentioned, it is imperative that a technique be developed by means of which the earth pressures acting against a conduit structure may be determined by direct means.

The following method has been conceived by the research section of the North Carolina State Highway Division of Materials to determine the lateral pressures mobilized by the side supporting material at various points of the conduit structure.

Apparatus. The main parts of the apparatus, shown in Figure 90, are: (1) conventional circular bearing plate attached with a swivel head connection to a pipe extention; (2) an S 80-50 ton Porto-Power portable hydraulic jack with a pressure gage of 400 graduations, a capacity of 24,000 lb. and a least reading of 50 lb. The jack is connected at one end to the pipe extention of the bearing plate and at the other end to another pipe extention. The latter extention abuts against the flange of an I-beam placed horizontally along the pipe axis and against the inner surface of the structure. (3) The whole setup rests level on rollers that have been placed on top of a metallic table with adjustable legs. (4) A metal frame attached to anchoring angle rods that have been embedded into the side supporting material through openings in the pipe structure by means of a power saw or a flame torch. On this frame four Ames dials are attached by means of two collars, each supporting two dials. The purpose of these dials is to detect any horizontal movement in the bearing plate during the performance of the test. (5) High-early strength cement to fill in the inside valleys of the corrugations abutting the bearing plate so that the bearing plate will be in contact with a flat surface during the performance of the test. (6) A flame torch with an orifice so designed that the flame jet would be of the highest possible burning intensity concentrated in the smallest possible area; (7)a drill and a power saw, electrically driven, to be used to cut openings in the pipe sides to anchor the metal frame discussed in item 4. The flame torch can be used also for the same operation.

Experimental Procedure. On the side of the inner surface of the pipe structure mark off a circular area approximately equal to the area of the flat surface of the bearing plate. Fill up the inside valleys of the corrugations, included in the above circle, with high early strength cement until a smooth vertical plane contact surface is formed.

Install the metal frame where the Ames dials are attached. It is recommended that the anchoring rods of the above frame should be embedded into the side supporting material symmetrically about the circular area, mentioned in the previous paragraph. It is also recommended that the same rods be approximately eight plate diameters apart so that hammering will not disturb the soil conditions at the area where the pressure test is to be performed.

Set up the apparatus as shown in the illustration and apply a small amount of pressure on the jack until a firm contact between the bearing plate and the circular plane surface, described previously, is secured.

Leave the whole apparatus as is for a sufficient period of time, say overnight, to be sure that the high-early cement used to fill-in the corrugation valleys has set.

Immediately prior to the performance of the test, zero all Ames dials in such a manner that any forward or backward movement on the bearing plate can be detected during the performance of the test.

With the flame torch start burning and cutting through the metal surface of the pipe around the circular area of contact between the bearing plate and the plane surface. Be sure to start cuts from symmetrical points around the circular area to prevent any tilting of the bearing plate. The power saw cannot be used for such operation because it generates an objectionable amount of vibrations in the pipe structure that render the dial readings ineffectual.

While cutting around the bearing surface keep all Ames dials at the initial zero reading by increasing the pressure on the hydraulic jack gradually. Record the pressure as it builds up.

As soon as the circular section has been completely severed from the rest of the pipe structure record the corresponding pressure required to keep the plate stationary. Since no movement was allowed in the bearing plate and, accordingly, in the soil mass during the process of cutting, the recorded pressure must be the pressure exerted by the side supporting material against this particular region of the conduit prior to cutting the corresponding circular section.

Divide the recorded pressure by the area of the bearing plate to determine the corresponding stress in psi.

Gradually release the pressure in the jack and record the outward movement of the plate by the Ames dials.

Gradually build-up again the pressure in the jack to the value recorded and note whether the dials indicate the initial zero readings. If not, record the actual deformation.

Gradually build-up the pressure in the jack to higher values than that observed upon the movement of the bearing plate as indicated by the Ames dials.

Release gradually the pressure again and record the corresponding lateral movement.

Remove the whole apparatus and repeat the same experiment at other points of the pipe structure.

Data pertaining to the elastic behavior in situ of the side supporting material can also be obtained. Therefore, if the results from a thorough soil analysis and classification as well as a record of the initial size and compaction of the side supporting material are added to the data obtained by the above tests, a complete picture of the properties of the side supporting material of a given installation will be obtained.

The above described procedure is rather unique in nature as it does not employ any conventional pressure measuring devices such as Goldbeck cells or other gages for which various objections have been raised in the past. The same procedure has the following advantages over other methods: (1) The earth pressure is measured directly under zero strain conditions and, therefore, the readings obtained are not influenced by the deformation characteristics of the abutting earth mass. (2) The contact surface of the apparatus, bearing directly against the soil mass, is the actual corrugated surface of the culvert structure. Therefore, no questions can be raised regarding the

relative stiffness of said apparatus to the soil mass as is the case with Goldbeck cells or other devices. (3) The strain readings are obtained from a reference frame that has been anchored into the soil mass having no contact with the rest of the pipe structure, therefore, its position will always be stationary regardless of any deformations or displacements taking place in the metal structure. (4) Only one movable apparatus is employed in the above procedure and, therefore, it may be more economical to use. (5) As no initial readings are required for the pressure determination, the lateral pressures can be determined at any date during the life of a culvert. Therefore, with the proper improvements made in the design of the apparatus, one can use the same procedure to determine the lateral earth pressures existing against flexible conduits that have been in service for a good many years.

Along with the above discussion, however, it should be emphasized also that the proposed procedure is still in a pioneering and exploratory stage and, therefore, many improvements could be made in the design of the apparatus as well as the experimental procedure itself. At the present time the authors of this paper are concerned mainly with the following improvements: (1) the determination of the best method for cutting the circular section in a symmetrical way so that no hinge action or tilting of the section will result. If a flame torch is used, provisions must be made so that the section is cut off without being heated excessively throughout its surface. Overheating may result in altering the characteristics of both the metal structure and the abutting earth mass. (2) The installation of an automatic device by means of which the pressure in the jack can be increased or decreased in such a manner that the test will be performed in its whole duration under zero strain conditions. It is humanly impossible to avoid lateral earth strains if the pressure in the jack is secured by a manual operation.

It is firmly believed that the above described procedure for the direct determination in situ of lateral earth pressures exerted against a flexible underground conduit can yield a very substantial addition to the fund of information regarding the behavior of these structures as well as that of the surrounding earth masses for given conditions. Accordingly, it is also believed that with the same tests it would be possible for one to ascertain the validity of various theories on the mechanical and physical actions involved in high fill conduit installations, and to gather very valuable information regarding the physical properties of various conduit materials as well as earth masses under given installation conditions.

ACKNOWLEDGMENTS

The authors wish to express their sincere appreciation to all who assisted in making this report possible, even though their names are not included among those given here. H. Dewey Hester, C. R. Penny, James T. Norton, James R. Brandon and J. Prince Pendergrass of the Division of Materials Research Section under the general direction of A. Duke Morgan secured the field data under trying conditions. Division Engineers E. H. Kemper and W. M. Corkill, and Resident Engineer J. E. Terrell for Project 8521 facilitated the coordination of construction and research operations and John H. Graham of W. E. Graham and Sons, contractor for the project, gave every assistance compatible with satisfactory job progress. Thanks go also to The Soils Laboratory under L. D. Hicks, for their analyses of the soil samples and to J. E. Thompson, Jr., in charge of the Physical Testing Laboratory of the Division of Materials where calibration curves were made and strut compression-cap laboratory tests conducted. The excellent photographic work of J. P. (Pete) Bourke, both stills and motion pictures, recorded features which could not have otherwise been so adequately described.

The research project was authorized and plans reviewed by Wm. H. Rogers, Jr., State Highway Engineer, T. B. Gunter, Jr., Bridge Engineer and W. S. Winslow, Hydrographic Engineer.

The invaluable assistance of Professor M. G. Spangler of Iowa State College, H. L. White, Boyd Steed and J. H. Timmers of the ARMCO staff, and Drs. R. E. Fadum and J. W. Cell of North Carolina State College, as consultants in the design, conduct and report of this experiment is gratefully acknowledged and, finally, our appreciation for the painstaking preparation of the manuscript by Mrs. Lucille Crawford.

References

1. Aldous, W. M.; Herner, R. C.; and Price, M. H. 1951. The load transmission test for flexible paving and base courses, part II; triaxial test data on structural properties of granular base materials. Civil Aeronautics Administration, Technical Development and Evaluation Center. Technical Development Report No. 144.

2. American Concrete Pipe Association. 1955. Loads on underground conduits. Concrete Pipe News, 7 No. 1 - 4.

3. American Railway Engineering Association. 1926. Report of the committee on roadbed. 27: 794.

4. American Railway Engineering Association. 1928. Report of the committee on roadbed. 29: 527.

5. Armco Drainage and Metal Products, Inc. 1950. Handbook of culvert and drainage practice. R. R. Donnelly and Sons Co., Chicago, Illinois.

6. Armco Drainage and Metal Products, Inc. 1952. Multi plate 6" x 2" corrugation design data. Middletown, Ohio.

7. Braune, G. M.; Cain, W.; and Janda, H. F. 1929. Earth pressure experiments on culvert pipe. Publ. Rds., Washington, D. C. 10: 153-176.

8. Burington, R. S. and May, D. C. 1953. Handbook of probability and statistics with tables. Handbook Publishers, Inc., Sandusky, Ohio.

9. Cain, W. 1916. Experiments on retaining walls and pressure on tunnels. Trans. Am. Soc. Civ. Engrs. 72: 403-474.

10. Casagrande, A. and Fadum, R. E. 1940. Notes on soil testing for engineering purposes. Harvard University, Graduate School of Engineering. Soil Mechanics Series No. 8.

11. Costes, N. C. 1955. Factors affecting vertical loads on underground ducts due to arching. Research Report. North Carolina State Highway and Public Works Commission, Raleigh, North Carolina.

12. Hoel, P. G. 1951. Introduction to mathematical statistics. John Wiley and Sons, Inc., New York.

13. Hoffman, O. and Sachs, G. 1953. Introduction to the theory of plasticity for engineers. McGraw-Hill Book Company, Inc., New York.

14. Housel, W. S. 1943. Earth pressure on tunnels. Proc. Amer. Soc. Civ. Engrs. 69: 1037-1058.

15. Huber, M. J. and Childs, L. D. 1951. Load deflection tests on corrugated metal sections. Michigan State College, Engr. Exp. Sta. Bull. 109.

16. Koch, J. J.; Boiten, R. G.; Biermasz, A. L.; Roszbach, G. P.; and Van Santen, G. W. 1952. Strain gauges, theory and application. Philips Technical Library. Eindhoven, Holland.

17. Krynine, O. P. 1940. Design of pipe culverts from standpoint of soil mechanics. Proc. Highw. Res. Bd., Washington, D. C. 20: 722-729.

18. Lambe, T. W. 1951. Soil testing for engineers. John Wiley and Sons, Inc., New York.

19. Marston, A. 1930. The theory of external loads on closed conduits in the light of the latest experiments. Proc. Highw. Res. Bd., Washington, D. C. 9: 138-170.

20. Merriman, T. and Wiggin, T. H. 1943. American civil engineer's handbook. John Wiley and Sons, Inc., New York.

21. Peck, O. K. and Peck, R. B. 1948. Earth pressure against underground constructions. Experience with flexible culverts through railroad embankments. Proc. Intern. Conf. on Soil Mechanics, 2: 95-98.

22. Peck, R. B. 1943. Earth-pressure measurements in open cuts, Chicage (Ill.) Subway. Proc. Amer. Soc. Civ. Engrs. 69: 1008-1036.

23. Perry, C. C. and Lissner, H. R. 1955. The strain gage primer. McGraw-Hill Book Company, Inc., New York.

24. Phillips, D. L. 1953. Investigation of the stresses and deflections of a corrugated metal pipe culvert under a high earth fill. Unpublished Thesis. Iowa State College, Ames, Iowa.

25. Schlick, W. J. 1952. Loads on negative projecting conduits. Proc. Highw.

Res. Bd., Washington, D. C. 31: 308-319.

26. Sowers, G. F. 1954. Soil problems in the southern piedmont region. Proc. Amer. Soc. Civ. Engrs. 80: Separate No. 416.

27. Spangler, M. G. 1937. The structural design of flexible pipe culverts. Proc. Highw. Res. Bd., Washington, D. C. 17 part I: 255-237.

28. Spangler, M. G. 1946. Analysis of loads and supporting strengths and principles of design for highway culverts. Proc. Highw. Res. Bd., Washington, D. C. 26: 189-212. Discussion pp. 213-214.

29. Spangler, M. G. and Hennessy, R. L. 1946. A method of computing live loads transmitted to underground conduits. Proc. Highw. Res. Bd., Washington, D. C. 26: 179-184.

30. Spangler, M. G. 1948. Stresses and deflections in flexible pipe culverts. Proc. Highw. Res. Bd., Washington, D. C. 28: 249-257.

31. Spangler, M. G. 1950a. A theory on loads on negative projecting conduits. Proc. Highw. Res. Bd., Washington, D. C. 30: 153-161.

32. Spangler, M. G. 1950b. Field measurements of the settlement ratios of various highway culverts. Iowa State College, Engr. Exp. Sta. Bull. No. 170.

33. Spangler, M. G. 1951. Soil engineering. International Textbook Co., Scranton, Pennsylvania.

34. Spangler, M. G. 1951-1952. Protective casings for pipe lines. Iowa State College, Engr. Exp. Sta. Engineering Report No. 11.

35. Spangler, M. G. 1954. Subsidence under earth embankments. Unpublished discussion presented before the Geology Section of the Iowa Engineering Society, Des Moines, Iowa.

36. Spangler, M. G. and Phillips, D. L. 1955. Deflections of timber-strutted corrugated-metal-pipe culverts under earth fills. Highw. Res. Bd., Bull. No. 102.

37. Taylor, D. W. 1948. Fundamentals of soil mechanics. John Wiley and Sons, Inc., New York.

38. Terzaghi, K. 1936a. Stress distribution in dry and in saturated sand above a yielding trap-door. Proc. Intern. Conf. Soil Mechanics, 1: 307-311.

39. Terzaghi, K. 1936b. A fundamental fallacy in earth pressure computations. Jour. Boston Soc. Civ. Engrs. 23: 71-88.

40. Terzaghi, K. 1942-1943. Shield tunnels of the Chicago subway. Harvard University, Graduate School of Engineering. Soil Mechanics Series No. 19.

41. Terzaghi, K. 1943a. Theoretical soil mechanics. John Wiley and Sons, Inc. New York.

42. Terzaghi, K. 1943b. Liner-plate tunnels on the Chicago (Ill.) subway. Proc. Amer. Soc. Civ. Engrs. 69: part 2: 970-1007.

43. Terzaghi, K. and Peck, R. B. 1948. Soil mechanics in engineering practice. John Wiley and Sons, Inc., New York.

44. Timmers, J. H. 1953. Multi-plate compression measurements at Cullman, Alabama installation. Research Report. Armco Drainage and Metal Products, Inc., Middletown, Ohio.

45. Timoshenko, S. 1936. Theory of elastic stability. McGraw-Hill Book Company, Inc., New York.

46. Tschebotarioff, G. P. 1949. Large scale model earth pressure tests on flexible bulkheads. Trans. Amer. Soc. Civ. Engrs. 114: 415-454.

Appendix

ANALYTICAL EXPRESSIONS RELATING TO VERTICAL EARTH LOADS ON TOP OF IMPERFECT DITCH UNDERGROUND CONDUITS

Referring to Figure 91 let:

H = Height of fill above top of conduit, ft.
H_e = Height of "Plane of Equal Settlement" above top of conduit (height of arching), ft.
H_d = Height of imperfect ditch, ft.
$H' = H - H_d$
$H'_e = H_e - H_d$
z = Vertical distance from Plane of Equal Settlement down to any horizontal plane, ft.

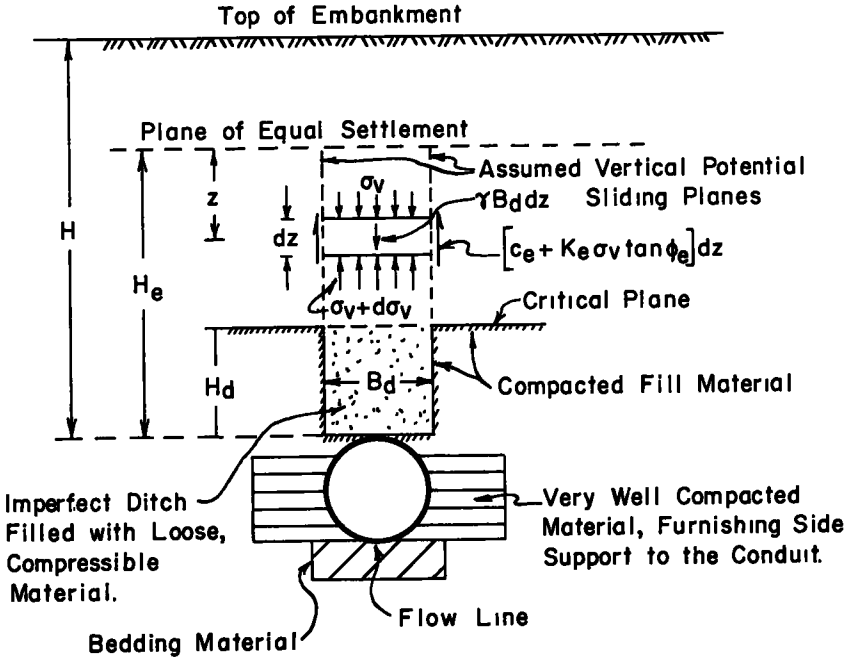

Figure 91. Imperfect ditch installation.

γ = Average unit weight of fill material, pcf.
ϕ_e = Effective angle of internal friction of fill material, mobilized along vertical sliding planes.
c_e = Effective cohesion of fill material, mobilized along vertical sliding planes.
σ_v = Vertical unit stress on a horizontal section at a depth of z below Plane of Equal Settlement, psf.
σ_h = Horizontal unit stress on a vertical section at a depth z below Plane of Equal Settlement, psf.
$K_e = \frac{\sigma_h}{\sigma_v}$ = Equivalent hydrostatic earth pressure ratio, assumed to be constant along vertical sliding planes.
W_c = Vertical earth load on top of conduit, lb. per lin. ft.

Differential Equation Describing Loading Action for an $s = c + \sigma \tan\phi$ Material

$$\frac{dV_z}{dz} + 2K_e \frac{V_z}{B_d} \tan\phi_e + 2c_e - \gamma B_d = 0 \qquad \text{(a)}$$

where $V_z = \sigma_v B_d$.

Limits: $V_z = (H - H_e)\gamma B_d$ for $z = 0$,
$V_z = V_z$ for $z = z$,
$V_z = W_c$ for $z = H_e$.

Load Expressions

For the general case or for an $s = c + \sigma \tan \phi$ material.

$$W_c = \frac{\gamma B_d^2}{2K_e \tan\phi_e} \left\{ e^{-(2K_e \tan\phi_e)\frac{H'_e}{B_d}} \; e^{-(2K_e \tan\phi_e)\frac{H_d}{B_d}} \left[(2K_e \tan\phi_e)\left(\frac{H' - H'_e}{B_d}\right) - \left(1 - \frac{2c_e}{\gamma B_d}\right)\right] - \left(1 - \frac{2c_e}{\gamma B_d}\right)\right\}. \quad (b)$$

Letting:

$$(2K_e \tan\phi_e)\, H'/B_d = v' \quad (c)$$

$$(2K_e \tan\phi_e)\, H'_e/B_d = u' \quad (d)$$

$$(2K_e \tan\phi_e)\, H_d/B_d = w' \quad (e)$$

and substituting in Equation b, one obtains:

$$W_c = \frac{\gamma B_d^2}{2K_e \tan\phi_e} \left\{ e^{-u'} \; e^{-w'} \left[(v' - u') - \left(1 - \frac{2c_e}{\gamma B_d}\right)\right] + \left(1 - \frac{2c_e}{\gamma B_d}\right)\right\}. \quad (f)$$

It can be shown that, mathematically:

$$\lim_{\phi_e \to 90^\circ} W_c = 0, \quad (g)$$

$$\lim_{c_e \to \infty} W_c = -\infty. \quad (h)$$

From Equation b, e, and f it can be seen that if the height of the imperfect ditch, H_d, is made high enough, factor $e^{-(2K_e \tan\phi_e)\frac{H_d}{B_d}} = e^{-w'}$ approaches zero; hence, the first part of the expression inside the bracket in Equations b or f approaches zero also, and the load expression approaches asymptotically the value

$$W_c = \frac{\gamma B_d^2}{2K_e \tan\phi_e} \left(1 - \frac{2c_e}{\gamma B_d}\right), \quad (i)$$

that is independent of the fill height, H, or the height of arching, H_e.

Under the above limiting conditions, if $c_e \geqq \frac{\gamma B_d}{2}$ [32],

$$W_c = 0. \quad (j)$$

Load Expression for a Perfectly Granular or an $s = \sigma \tan \phi$ Material. (k)

$$W_{\substack{c_e = 0}} = \lim_{c_e \to 0} W_c = \frac{\gamma B_d^2}{2K_e \tan\phi_e} \left\{ e^{-(2K_e \tan\phi_e)\frac{H'_e}{B_d}} \; e^{-(2K_e \tan\phi_e)\frac{H_d}{B_d}} \left[(2K_e \tan\phi_e)\left(\frac{H' - H'_e}{B_d}\right) + 1\right\},$$

or,

$$W_{\substack{c_e = 0}} = \frac{\gamma B_d^2}{2K_e \tan\phi_e} \left\{ e^{-u'} \; e^{-w'} \left[v' - u' - 1\right] + 1\right\}. \quad (l)$$

if the proper substitutions from Equations c - e are made.

Equations k or l are identical with the Marston-Spangler load expression (Spangler, 1950a, p. 157), except that $K_A = \tan^2(45^\circ - \phi/2)$ must be substituted for K_e.

Again, if H_d is made high enough, factor $e^{-(2K_e \tan\phi_e)\frac{H_d}{B_d}} = e^{-w'}$ approaches zero and the load expression approaches asymptotically the value

$$W_c = \frac{\gamma B_d^2}{2K_e \tan\phi_e}. \quad (m)$$

Equation m is identical with the one derived by Terzaghi for earth pressure on top of

[32] For this installation, $\frac{\gamma B_d}{2} = 330$ psi.

deep tunnels through dry sand (Terzaghi, 1943a, p. 196).

Load Expression for a Purely Cohesive or an s = c Material.

$$W_c = \lim_{\substack{\phi_e = 0 \\ \phi_e \to 0}} W_c = \gamma B_d^2 \left\{ \left(\frac{H' - H'_e}{B_d}\right) + \left(1 - \frac{2c_e}{\gamma B_d}\right)\left(\frac{H'_e + H_d}{B_d}\right) \right\}. \tag{n}$$

Letting:

$$\frac{H'}{B_d} = v'_o, \tag{o}$$

$$\frac{H'_e}{B_d} = u'_o, \tag{p}$$

$$\frac{H_d}{B_d} = w'_o, \tag{q}$$

and substituting in Equation n one obtains:

$$W_c = \gamma B_d^2 \left\{ (v'_o - u'_o) + \left(1 - \frac{2c_e}{\gamma B_d}\right)(u'_o + w'_o) \right\}. \tag{r}$$

If $c_e \geqslant \frac{\gamma B_d}{2}$,

$$W_c \leqslant \gamma B_d^2 (v'_o - u'_o). \tag{s}$$

Expression to Determine the Magnitude of the Height of Arching, H_e

Let: $r_{sd} = (s_c - s_1)/s_d$ = settlement ratio

where:

s_c = Subsidence of the critical plane (Figure 91) on top of the compacted fill material, ft.

s_1 = Subsidence of the critical plane on top of the loose, compressible material, placed in the imperfect ditch, ft.

s_d = Vertical compression of loose material in the imperfect ditch, ft.

$a' = \frac{E}{E_f} = \frac{\text{Modulus of deformation of loose material}}{\text{Modulus of deformation of compacted fill material}}$

Then, H_e can be determined implicitly from the following expressions in which the substitutions from Equations c - e and o - q have been utilized:

For the general case of for an s = c + σ tanϕ material,

$$v' = \frac{\left(\frac{3}{4}u'^2 - \frac{3c_e}{\gamma B_d}u'\right) - \left(\frac{3}{2} + \frac{r_{sd}w'}{a'}\right)\left(1 - \frac{2c_e}{\gamma B_d}\right) + \left(\frac{3}{2} + \frac{r_{sd}w'}{a'}\right)\left(u' + 1 - \frac{2c_e}{\gamma B_d}\right) e^{-u'}}{\left(\frac{3}{2} + \frac{r_{sd}w'}{a'}\right) e^{-u'} + \frac{3}{2}(u' - 1)}. \tag{t}$$

An inspection of Equations t and c - e will show that if the fill height, H, and hence, factor v' increases without limit, the height of arching H_e is governed by the equation

$$\left(\frac{3}{2} + \frac{r_{sd}w'}{a'}\right) e^{-u'} + \frac{3}{2}(u' - 1) = 0. \tag{u}$$

It follows then, that for infinitely high fills the height of arching is independent of the unit weight, γ, and the effective cohesion, c_e, of the fill material.

For a Perfectly Granular or an s = σ tanϕ Material.

$$v' = \lim_{\substack{c_e = 0 \\ c_e \to 0}} v' = \frac{\frac{3}{4}u'^2 - \left(\frac{3}{2} + \frac{r_{sd}w'}{a'}\right) + \left(\frac{3}{2} + \frac{r_{sd}w'}{a'}\right)(u' + 1) e^{-u'}}{\left(\frac{3}{2} + \frac{r_{sd}w'}{a'}\right) e^{-u'} + \frac{3}{2}(u' - 1)}. \tag{v}$$

Equation v is identical with the expression developed by Spangler for negative projecting conduits (Spangler 1950a, p. 158), except that $K_A = \tan^2(45° - \phi/2)$ should be substituted for K_e.

Again, it can be seen that for infinitely high fills, the height of arching, H_e, is governed by the equation

$$(\frac{3}{2} + \frac{r_{sd}w'}{a'})\, e^{-u'} + \frac{3}{2}(u' - 1) = 0 \qquad (w)$$

which is identical with Equation s for the general case.

Hence, one may conclude that for infinitely high fills the influence of cohesion on the height of arching becomes negligible and the fill material behaves like a granular material.

For a Purely Cohesive or an s = c Material.

From Equations c and o it follows that

$$v'_o = \frac{H'}{B_d} = \frac{v'}{2K_e \tan\phi_e}. \qquad (x)$$

Substituting in Equation x the value of v' from Equation t and taking its limit when ϕ_e is allowed to approach zero, one obtains in terms of the dimensionless factors v'_o, u'_o, and w'_o:

$$\underset{\phi_e = 0}{v'_o} = \lim_{\phi_e \to 0} v'_o = -\frac{2c_e}{\gamma B_d} \frac{\frac{3}{4}u'^2_o - \frac{r_{sd}w'_o}{a'}\, u'_o}{\frac{r_{sd}w'_o}{a'}}. \qquad (y)$$

If the height of imperfect ditch, H_d, increases without limit, $\underset{\phi_e = 0}{v'_o}$ approaches the value $\underset{\phi_e}{v'_o} = \frac{2c_e}{\gamma B_d} u'_o$ as a limiting condition.

Hence, under the above limiting conditions, if $c_e \geqslant \frac{\gamma B_d}{2}$,

$$\underset{\phi_e}{v'_o} \leqslant u'_o. \qquad (z)$$

It follows then from expression s that if the height of imperfect ditch is made large enough and the effective amount of cohesion, c_e, mobilized by the fill material along the vertical sliding planes, is equal at least to $\frac{\gamma B_d}{2}$ (330 psi. for this installation), the top conduit load, as in the general case of an $s = c + \sigma\tan\phi$ material, will approach the value zero, i. e.

$$\underset{\phi_e = 0}{W_c} \simeq 0. \qquad (A)$$

From Equations t, v, and y the following limits can be established.

For an $s = c + \sigma\tan\phi$ material:

$$\lim_{\frac{r_{sd}w'}{a'} \to 0} u' = 0, \qquad (B)$$

$$\lim_{\frac{r_{sd}w'}{a'} \to \infty} u' = \infty. \qquad (C)$$

For an $s = \sigma\tan\phi$ material:

$$\lim_{\frac{r_{sd}w'}{a'} \to 0} u' = 0, \qquad (D)$$

$$\lim_{\frac{r_{sd}w'}{a'} \to \infty} u' = \infty. \qquad (E)$$

For an s = c material:

$$\lim_{\frac{r_{sd}w'}{a'} \to 0} u'_o = 0, \qquad (F)$$

$$\lim_{\frac{r_{sd}w'}{a'} \to \infty} u'_o = \infty . \qquad (G)$$

From the above items, and by inspecting the respective load expressions one may conclude that:

1. If no imperfect ditch is constructed on top of the conduit, in which case $r_{sd} = 0$, $w' = 0$, $w'_o = 0$, and $a' = 1$, regardless of the shearing strength characteristics of the overlying fill material, no arching will occur within the earth mass above the conduit, and the top load will be equal to the weight of the earth column sustained by the conduit structure, i. e.

$$W_c = \gamma B_d H. \qquad (H)$$

2. The higher is the imperfect ditch and the greater is the difference between the overall stiffness of (a) the loose compressible material in the imperfect ditch, the conduit structure and the bedding material, and (b) the stiffness of the adjacent compacted masses, the higher will be the height of arching, H_e,[33] and the load on top of the conduit will approach the values:

$$W_c = \gamma B_d \left(\frac{B_d}{2K_e \tan\phi_e}\right) - 2c_e \left(\frac{B_d}{2K_e \tan\phi_e}\right) \qquad (I)$$

for an $s = c + \sigma \tan\phi$ material,

$$W_c = \gamma B_d \left(\frac{B_d}{2K_e \tan\phi_e}\right) \qquad (J)$$
$$c_e = 0$$

for an $s = \sigma \tan\phi$ material, and

$$W_c = \gamma B_d H - 2c_e H \qquad (K)$$
$$\phi_e = 0$$

for an $s = c$ material.

The above expressions suggest that if the height of arching is large enough, the conduit load will simply be the weight of an equivalent earth column minus the cohesive shearing strength of the fill material that is mobilized along the corresponding equivalent fill height. Accordingly, the equivalent fill height for either an $s = c + \sigma \tan\phi$ or for an $s = \sigma \tan\phi$ material is equal to $H_{equiv.} = \frac{B_d}{2K_e \tan\phi_e}$, whereas for a purely cohesive material the equivalent height is the actual height of the fill above the top of the conduit, i. e. $H_{equiv.} = H$.

DETERMINATION OF LOAD-DEFORMATION CHARACTERISTICS OF MULTI-PLATE CORRUGATED METAL PIPE SECTIONS

Determination of Modulus of Elasticity-Moment of Inertia Product (EI) for a Bolted Multi-Plate Ring, by ARMCO Research Laboratories, Middletown, Ohio

In connection with the tests on the 66-inch Multi-Plate pipe installation near Asheville, N. C., A. D. and M. P. has requested the experimental determination of the modulus elasticity-moment of inertia product (EI) for a bolted Multi-Plate ring. This value can be compared to the calculated value for flexure of hypothetical ring of Multi-Plate without bolted joints.

This determination was carried out on two different test rings, one of which had been annealed, the other as received. The dimensions of these rings as used in the computa-

[33] Physically, the height of arching, H_e, cannot be higher than the height of fill, H. However, if such is the case mathematically, a trough-like depression appears at the top of the fill, and the effective values of the cohesion, c_e, and the angle of internal friction ϕ_e, mobilized by the fill material along the vertical sliding planes, approach the limiting values c and ϕ that the fill material can exhibit. Similarly, K_e approaches the limiting value $K_A = \tan^2(45^\circ - \phi/2)$ at the top of the mass.

tions are as follows:

	Multi-Plate Rings (12 Gage)	
	Not Annealed	Annealed
Metal Thickness	.1095"	.1087"
Actual Plate Width	28.06"	27.84"
Developed Plate Width	32.62"	32.97"
Median Diameter	61.54"	61.33"
Depth of Corrugation	1.67"	1.72"
Tangent Angle	41.5 deg.	44.4 deg.
Pitch	6.17"	6.08"
Moment of Inertia (1)	1.245 in.^{4}	1.328 in.^{4}
Modulus of Elasticity	30 x 10^6 psi.	30 x 10^6 psi.

The rings were loaded on diametrically opposed edges. Horizontal and vertical deflection measurements were read on four corrugations for load increments. Load-deflection curves were plotted and load-deflection values taken from the slope of the straight line portion of the curves (Figures 92 and 93). These values were substituted in formulas for computing deflections in circular rings (2) and the (EI) products were evaluated. The formulas used are as follows:

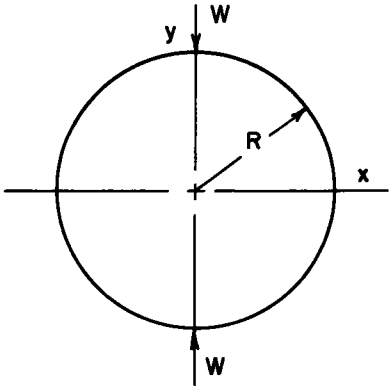

$$(1)\ D_x = +.137\,\frac{WR^3}{EI}$$

$$(2)\ D_y = -.149\,\frac{WR^3}{EI}$$

W = applied load in pounds
R = radius in inches
E = modulus of elasticity (30 x 10^6 psi.)
I = moment of inertia (in.^{4})
D_x = horizontal deflection in inches
D_y = vertical deflection in inches

Solving these equations for EI for the annealed and unannealed rings and comparing with the EI product computed from conventional modulus of elasticity and moment of inertia the following results were obtained:

	EI (psi.) Based on				Ratio of
	Horizontal Deflection	Vertical Deflection	Average Deflection	Conventional Calculations	Average to Conventional
Un-Annealed Ring	20.6 x 10^6	22.2 x 10^6	21.4 x 10^6	37.4 x 10^6	.572
Annealed Ring	23.4 x 10^6	24.0 x 10^6	23.7 x 10^6	39.8 x 10^6	.595

These results show the effective EI product to be approximately 60 percent of the theoretical value for Multi-Plate rings without bolted joints.

A complete summary of these tests will be included in A. I. 76-3-1 entitled Multi-Plate Pipe - Laboratory Study to Develop Thrust and Strain Relations.

Results from Tensile Tests on Structural Steel Specimens

These tests were performed in the ARMCO Laboratories in order to construct stress-strain diagrams by means of which the data from the strain gages could be evaluated.

The tensile tests were made on standard ½ inch wide parallel section by 2 inch gage length sheet tensile samples with a Type A-1 SR-4 strain gage centered in the parallel section (Figure 94).

From the above tests two stress-strain diagrams were plotted that are shown on Figure 95.

To calculate the strain from each strain from the strain indicator readings the follow-

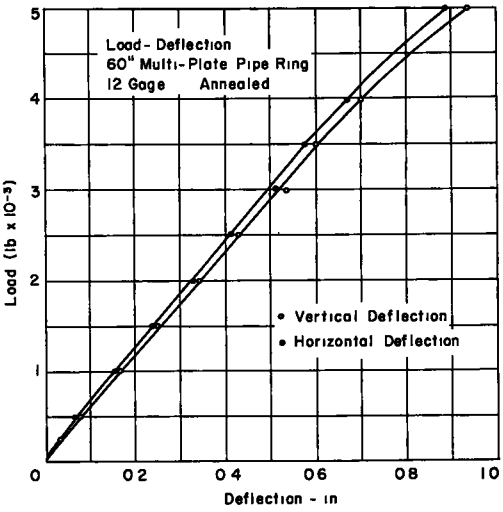

Figure 92.

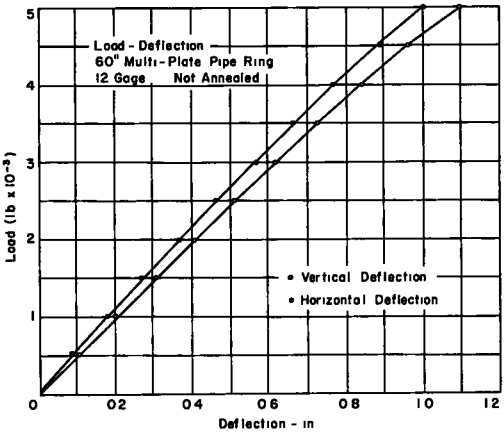

Figure 93.

Results

The results from the above described load cell calibration tests appear on Table 13, and the calibration curves for both cells on Figure 96.

LOAD TESTS ON PINE COMPRESSION CAPS

The purpose of these tests was to construct load-deflection calibration diagrams by means of which one could estimate the load carried by the struts in the pipe from the measured vertical deflection in the pine compression caps (See Apparatus and Experimental Procedure). Nine individual tests were run for this purpose in the N. C. Laboratory and a mean load-deflection curve was constructed (Figure 97).

The experimental setup is shown in

ing formula was used:

$$\epsilon = (T_2 - T_1)\ 1000\ D_2 - D_1$$

where:

ϵ = Strain in micro-incher per inch
T_2 = Final thousands step No.
T_1 = Initial thousands step No.
D_2 = Final Dial Reading
D_1 = Initial Dial Reading

CALIBRATION OF STRUT LOAD CELLS

Calibration Procedure

1. Cells were placed between the compression head of testing machine and were loaded to maximum capacity three times. The large load cell was loaded up to 200,000 lb. The small load cell was loaded up to 120,000 lb. Both cells were subjected to cycle loading.
2. The strain recorder was connected and the initial readings were obtained.
3. Strain readings were recorded at 10,000 lb. load increments for the small cell and at 20,000 lb. load increments for the large cell.
4. For each cell three sets of data were obtained.
5. For each cell the results were averaged after determining total amount of micro-inches per inch for each load increment.
6. The applied load in 1,000 lb. was plotted versus average strain for each cell.

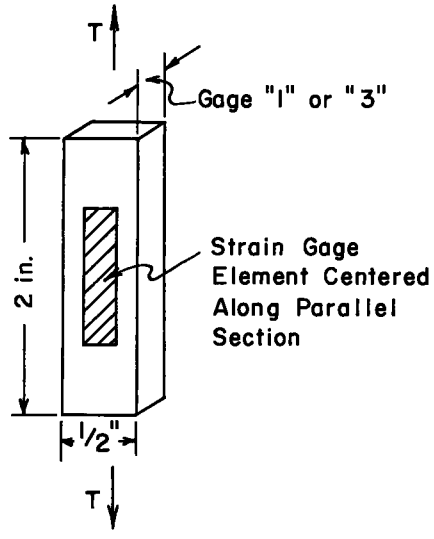

Figure 94. Schematic diagram of tensile samples.

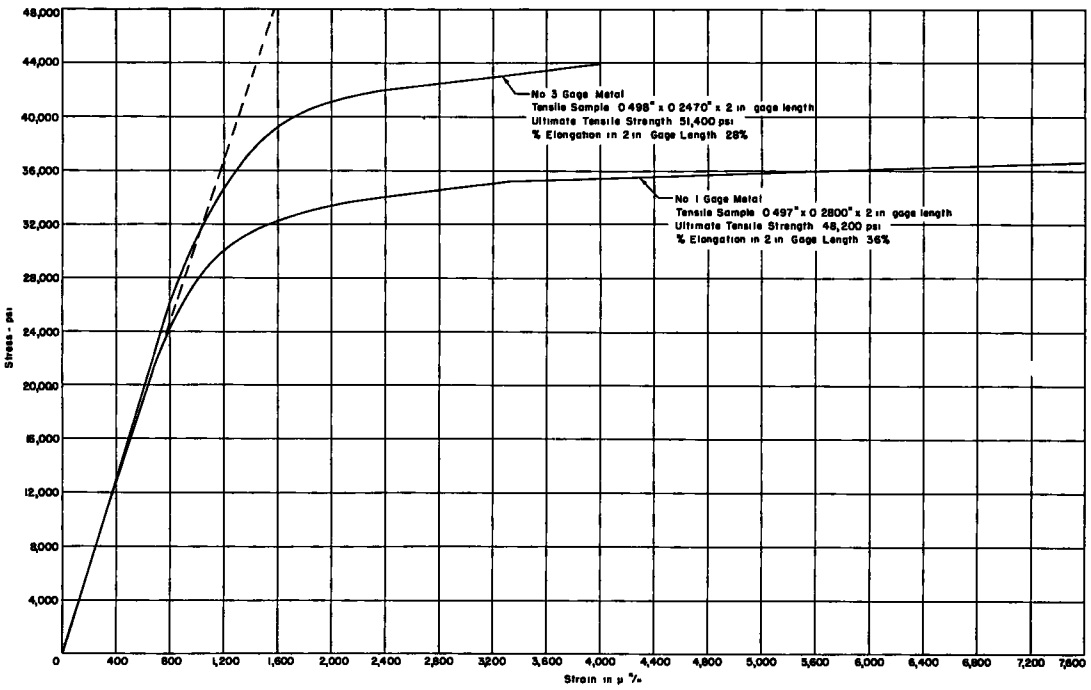

Figure 95. Tensile-stress strain curves determined using SR-4 Type A-1 strain gages.

Figures 98 and 99. The load was applied with a strain controlled Baldwin compression apparatus; the operator recorded the deflection corresponding to 2,000 lb. load increments. Care was exercised to simulate the field conditions as close as possible. Thusly, samples from the same timber area were tested and the strut-compression cap-sill systems had the same cross-sectional areas and the same compression cap length as in the field. Also, to obtain compression measurements, the same method was adopted. However, the rate of load application as well as the total time that each load increment was allowed to act on the systems were far from bearing any similarity to the actual field conditions. Therefore, it is felt that only qualitative conclusions may be drawn from the analysis of this data (See Analysis of Data).

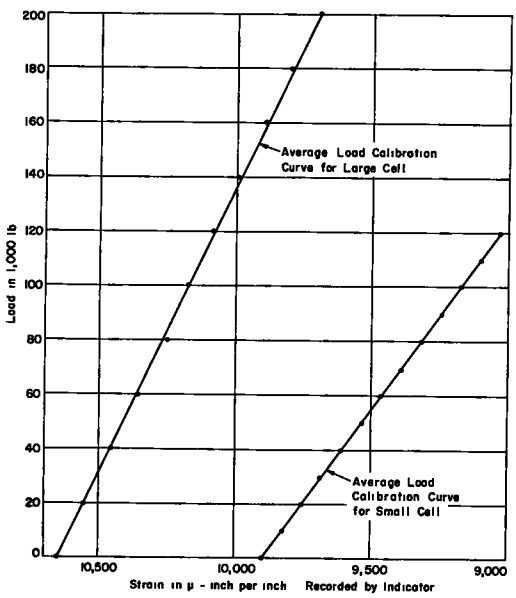

Figure 96. Load calibration curves for strut load cells.

The results from these tests appear on Table 14, and the average load deflection calibration curve on Figure 97. The results from the individual tests show reasonably close agreement with each other. Assuming that each system had identical life history and that it had been exposed to the same physical conditions, a statistical analysis was also carried out in which the standard deviation, s, the coefficient of variation, v, and the confidence limits, C. L., with confidence coefficient $\beta = 0.95$ were computed for each deflection corresponding to each load increment.

TABLE 13

CALIBRATION CHART FOR STRUT LOAD CELLS

Large Load Cell

Load (lb.)	Total Strain (micro-in./in.) Test No. 1	Test No. 2	Test No. 3	Avg. Strain (Micro-in./in.)
0	0	0	0	0
20,000	95	95	95	95
40,000	190	195	190	192
60,000	285	300	285	290
80,000	380	385	425	397
100,000	470	475	470	472
120,000	560	565	560	562
140,000	645	665	655	655
160,000	750	760	755	755
180,000	850	855	845	850
200,000	965	955	945	955

Small Load Cell

Load (lb.)	Total Strain (micro-in./in.) Test No. 1	Test No. 2	Test No. 3	Avg. Strain (Micro-in./in.)
0	0	0	0	0
10,000	70	70	70	70
20,000	145	145	140	143
30,000	220	215	215	217
40,000	300	285	285	290
50,000	360	360	355	358
60,000	435	435	430	433
70,000	505	505	505	505
80,000	580	580	575	578
90,000	650	655	650	652
100,000	720	720	720	720
110,000	790	795	795	793
120,000	860	865	865	863

Recorder-Property of NCSH and PWC.
Data Obtained by J. R. Brandon, NCSH and PWC.
Note: It should be noted that two different recorders were used in calibration of the cells, one the property of ARMCO Research Laboratories, the other the property of the NCSH and PWC Laboratory. The latter was used to obtain all field data. It is obvious by comparison of the calibration data with the field data that the small load cell is inoperative. The data have been plotted on Figure 96.

QUICK-CONSOLIDATED TRIAXIAL COMPRESSION TESTS ON SOIL SAMPLES FROM THE SIDE SUPPORTING MATERIAL

The purpose of these tests was to obtain some idea of the ranges of cohesion, c, and the angle of internal friction, ϕ, exhibited by the fill material under laboratory testing conditions. With such information in hand reasonable deductions could be made relative to the actual magnitudes of c and ϕ, mobilized by the same fill material under field conditions.

The test specimens were made out of soil samples obtained from the side supporting material of the culvert, approximately two years after the pipe installation (See Apparatus and Experimental Procedure). All specimens consisted of material passing the No. 4 sieve.

The above soil samples were thoroughly mixed and were tested under two compaction conditions:

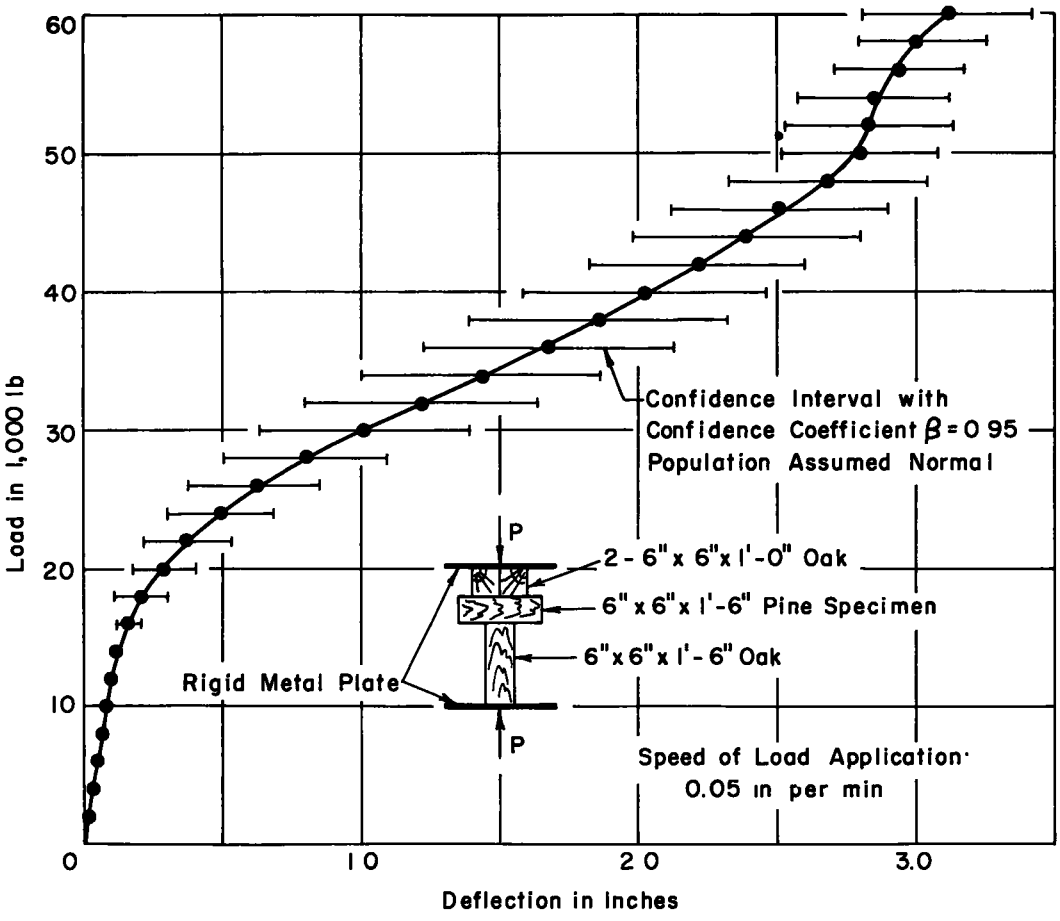

Figure 97. Mean load-deflection calibration curve for pine compression caps.

Condition A:		Condition B:	
γ =	110 pcf.	γ =	90 pcf.
w =	18%	w =	11%
e =	0. 50	e =	0. 80
s_s =	2. 64	s_s =	2. 64

From in situ density tests and soil analyses performed in the laboratory (See Obtained Data), Condition A was considered to represent high state of compaction in the fill material two years after the pipe installation. Similarly, condition B was considered to represent low state of compaction of the same material during the installation of the culvert. Accordingly, from the test results it was expected to obtain some feeling regarding the variation of c and ϕ under the above compaction limits. The erroneous but, nevertheless, safe assumption was made that the interlock between soil particles larger in size than those passing the No. 4 sieve has no effect on the shearing strength characteristics of the fill mass.

All test specimens were cylindrical in shape, 6 inches by 2. 8 inches in diameter (Figure 100). Given the total volume of the soil specimen, V, and the water content of the respective soil mixture, w, and having determined the specific gravity of the solids, s_s, from previous tests, it was possible to determine the wet weight, W, of each specimen in order that the compaction requirements for conditions A or B be satisfied respectively. Accordingly, the proper amount of moist soil was placed in a cylindrical mold whose inside diameter was 2. 8 inches.

The soil was compacted in three, approximately equal layers by means of a steel rod.

Figure 98. Pine compression cap calibration tests. Experimental setup.

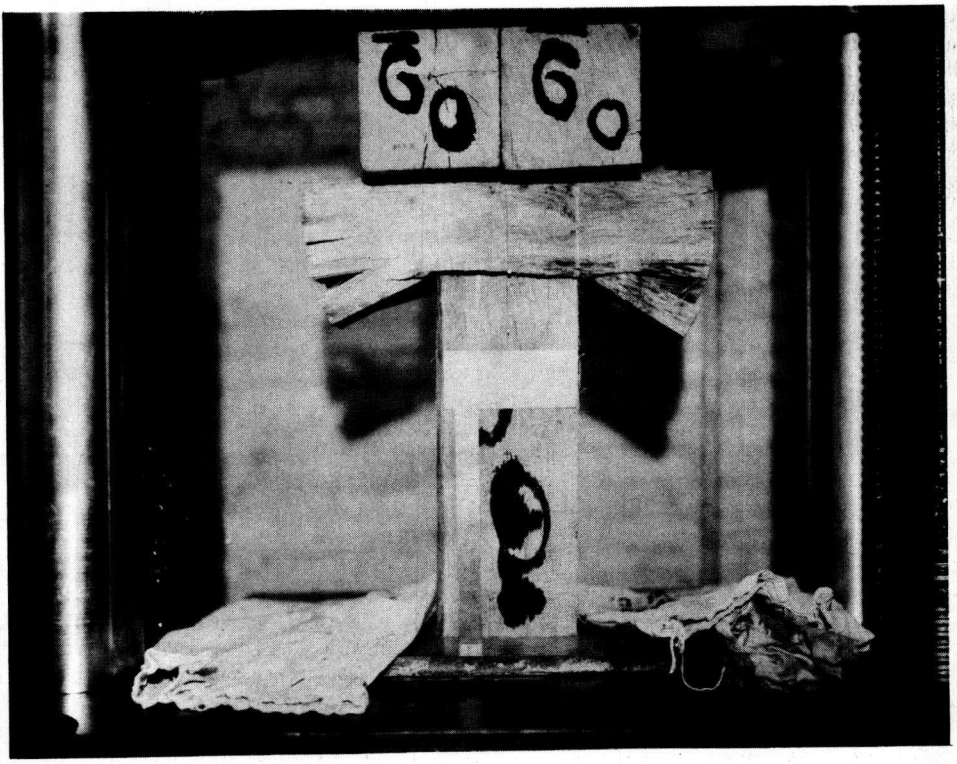

Figure 99. Pine compression cap specimen at failure.

TABLE 14

RESULTS FROM LOAD-DEFLECTION TESTS ON PINE COMPRESSION CAP SPECIMENS

Test No.	Deflections - inches (Load in 1,000 lb.) 2	4	6	8	10	12	14	16	18	20	22	24	26	28	30
1	0.0234	0.0313	0.0625	0.0625	0.0703	0.0781	0.0938	0.1016	0.1250	0.1484	0.2031	0.2969	0.4219	0.6094	0.8438
2	0.0078	0.0234	0.0391	0.0547	0.0703	0.0859	0.1172	0.1953	0.3047	0.4141	0.5469	0.7031	0.8984	1.0938	1.3203
3	0.0234	0.0391	0.0469	0.0703	0.0781	0.1016	0.1641	0.2500	0.3750	0.5391	0.6875	0.8359	0.9688	1.0938	1.3359
4	0.0156	0.0313	0.0391	0.0703	0.0859	0.1093	0.1328	0.2266	0.3125	0.4453	0.5938	0.7031	0.8516	1.0469	1.2422
5	0.0156	0.0313	0.0469	0.0547	0.0703	0.0859	0.0981	0.1016	0.1172	0.1406	0.1484	0.1953	0.2422	0.2969	0.4063
6	0.0234	0.0391	0.0469	0.0625	0.0781	0.0938	0.1094	0.1250	0.1641	0.2109	0.2969	0.5547	0.8438	1.2656	1.7969
7	0.0234	0.0391	0.0703	0.0859	0.0938	0.1016	0.1172	0.1406	0.1641	0.1875	0.2109	0.2578	0.3047	0.3750	0.4453
8	0.0000	0.0156	0.0391	0.0547	0.0859	0.0938	0.1172	0.1328	0.1641	0.2031	0.2500	0.3125	0.3906	0.4844	0.6563
9	0.0313	0.469	0.547	0.0781	0.1016	0.1172	0.1406	0.1797	0.2500	0.3281	0.4297	0.5703	0.6953	0.9297	1.0703
$\bar{x}$	0.0182	0.0330	0.0495	0.0660	0.0816	0.0964	0.1212	0.1615	0.2071	0.2908	0.3741	0.4922	0.6241	0.7995	1.0130
s	0.00958	0.00943	0.01103	0.01099	0.01109	0.01217	0.02172	0.05393	0.12129	0.14563	0.19613	0.23188	0.28343	0.36001	0.46308
$v = \frac{s}{\bar{x}}$	0.526	0.286	0.223	0.167	0.136	0.126	0.179	0.334	0.586	0.501	0.524	0.471	0.454	0.450	0.457
C. L.	±0.00781	±0.00769	±0.00896	±0.00896	±0.00904	±0.00992	±0.01771	±0.04397	±0.09889	±0.11873	±0.15990	±0.189052	±0.23108	±0.29352	±0.37755

Test No.	Deflections - inches (Load in 1,000 lb.) 32	34	36	38	40	42	44	46	48	50	52	54	56	58	60
1	1.1953	1.5938	1.9766	2.2500	2.4219	2.4922	2.6563	2.7188	2.7734	2.8672	2.9063	2.9844	3.0625	3.1172	3.4531
2	1.5313	1.7344	1.9141	2.1094	2.2266	2.4375	2.5625	2.7031	2.7969	2.9063	2.9531	3.0078	3.0625	3.1172	3.1797
3	1.4844	1.6094	1.7422	1.8359	1.9531	2.0703	2.2031	2.3438	2.4688	2.5781	2.6484	2.7266	2.8203	2.8906	2.9609
4	1.4297	1.6172	1.8125	1.9688	2.1328	2.4375	2.5703	2.6719	2.7656	2.8672	2.9063	2.9766	3.0469	3.0938	3.1328
5	0.5469	0.7969	1.1172	1.3438	1.5781	1.6406	1.7656	1.9141	-[a]	-	-	-	-	-	-
6	2.1250	2.3438	2.5625	2.6719	2.7813	2.8594	2.9219	3.0000	3.0469	3.0938	3.1484	-	-	-	-
7	0.5547	0.6953	0.8281	0.9766	1.2344	1.8359	-[a]	-	-	-	-	-	-	-	-
8	0.8125	0.9531	1.0938	1.2188	1.3438	1.4922	1.6875	1.8359	1.9922	2.2734	2.4141	2.5625	2.7031	2.7969	2.8750
9	1.2578	1.5547	1.9766	2.3125	2.5156	2.6484	2.7422	2.8594	2.9531	3.0000	-[a]	-	-	-	-
$\bar{x}$	1.2153	1.4332	1.6693	1.8542	2.0208	2.2127	2.3887	2.5059	2.6853	2.7980	2.8294	2.8516	2.9391	3.0031	3.1203
s	0.51153	0.52499	0.54953	0.56438	0.53818	0.47372	0.45638	0.43190	0.35493	0.28082	0.25872	0.19785	0.16681	0.15003	0.22362
$v = \frac{s}{\bar{x}}$	0.421	0.366	0.304	0.304	0.266	0.214	0.191	0.172	0.132	0.100	0.091	0.069	0.057	0.050	0.072
C. L.	±0.41705	±0.42802	±0.44803	±0.46014	±0.43878	±0.38622	±0.40794	±0.38606	±0.35457	±0.28053	±0.29747	±0.27462	±0.23153	±0.20824	±0.31038

[a] Specimen reached ultimate failure.

$\bar{x}$ = sample mean
s = sample standard deviation
v = coefficient of variation
C. L. = confidence limits with coefficient of confidence $\beta = 0.95$

Two floating plungers, applied on both ends of the mold, were used to compress each specimen to the prespecified length. These plungers were applied very slowly so that their compressive action would not subject the specimen to dynamic loading conditions. To avoid shearing of the specimens during the removal of the mold, the mold was thoroughly greased on the inside surface and it was removed carefully from the enclosed cylindrical sample.

Upon removal of the mold, each specimen was weighed and its mean diameter and height were obtained. Thereupon, it was placed in a moisture container and was allowed to "cure" in a moisture room for at least four days before testing. This period was considered sufficient to cause a relief in any internal stresses that might have been set up in the specimen structure by the above described compaction method.

The experimental setup is shown in Figure 101. The triaxial apparatus is a Soiltest, Type 114, electrically driven, strain controlled apparatus. During the performance of all tests a two-way vertical drainage was allowed in the specimens through two porous stones placed at the top and the bottom of the specimens with the corresponding top and bottom drainage valves open.

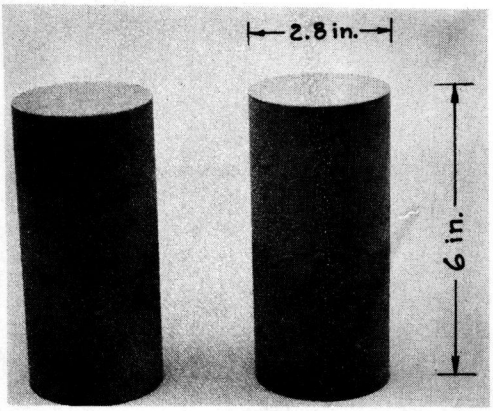

Figure 100. Soil specimens, compacted to prespecified densities, before testing.

Each of the above mentioned two compaction conditions A and B was divided into three groups, each group consisting of four specimens. These groups were tested respectively under confining unit pressures of 5 psi., 15 psi., and 20 psi.

All tests were performed as follows: (1) The soil specimen was placed in the triaxial apparatus and the prespecified confining unit pressure, σ_{III}, was applied gradually by letting compressed air in the lucite chamber (Figure 101). (2) The specimen was permitted to consolidate under the applied chamber pressure until the vertical deflection dial came practically to rest. This process took approximately 20 min. on the average. (3) The deviator

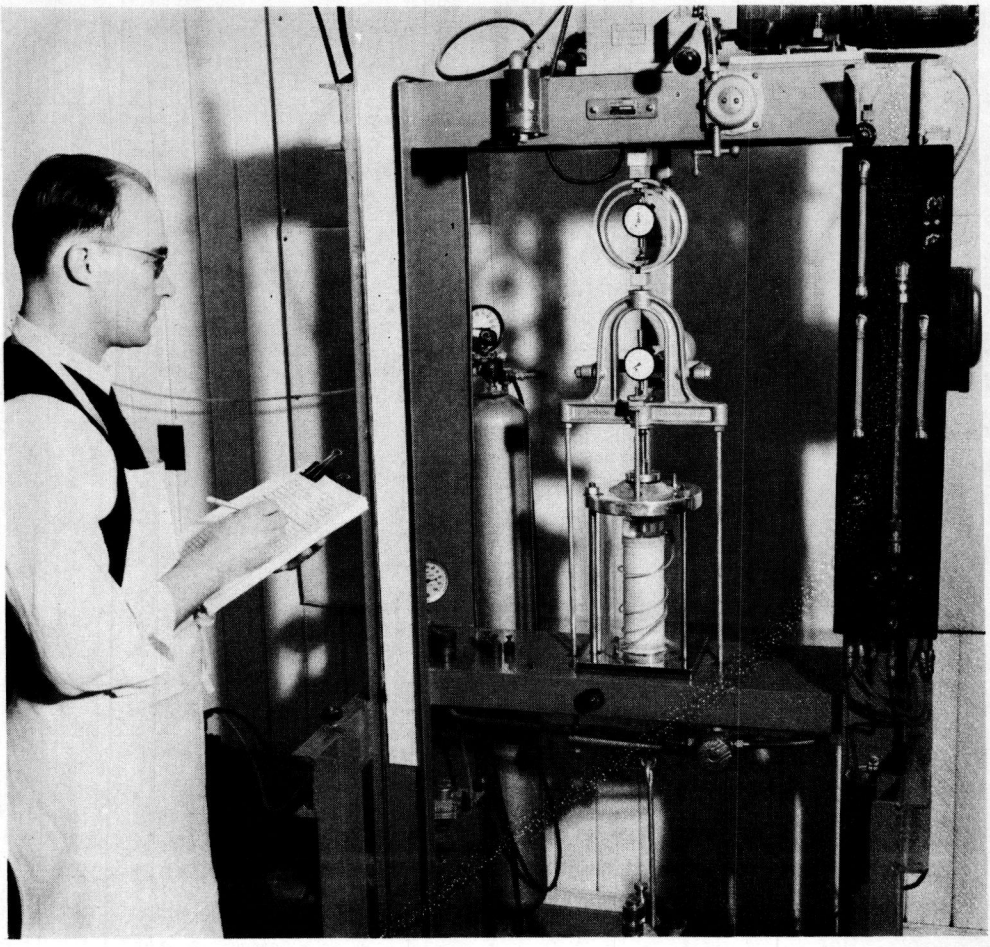

Figure 101. Quick-consolidated triaxial compression tests on samples from side supporting material of culvert. Experimental setup.

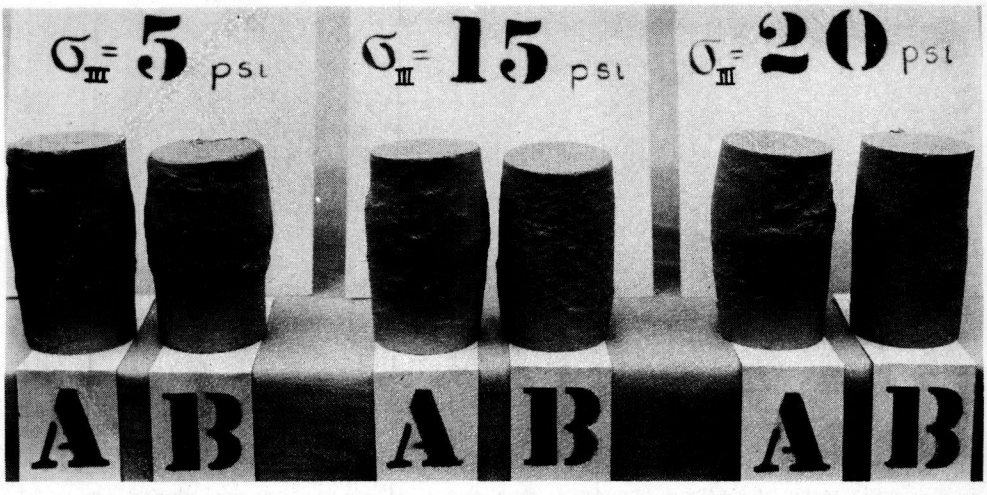

Figure 102. Soil specimens from both compaction conditions, A and B, after testing.

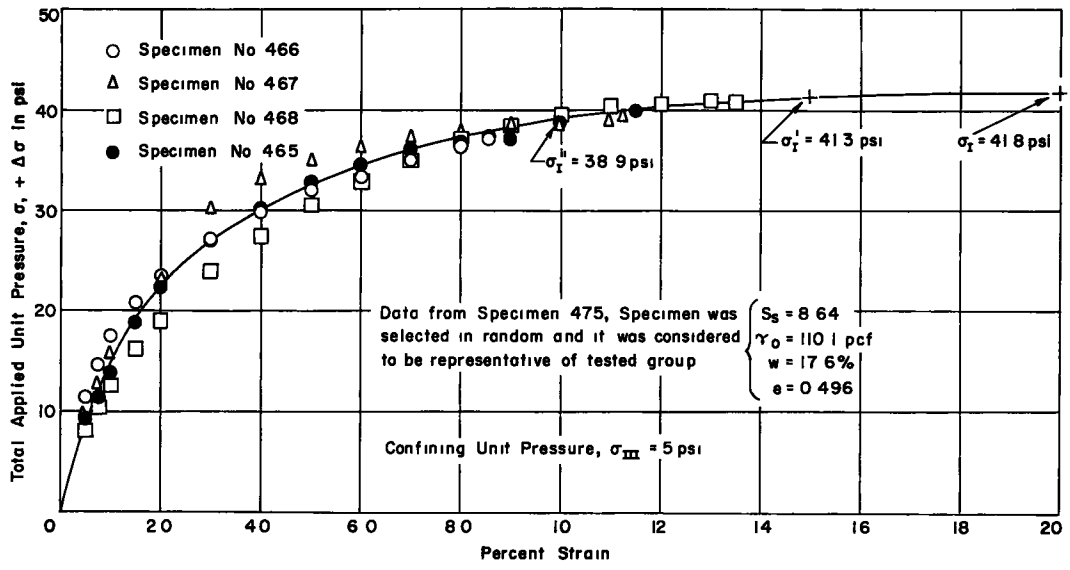

Figure 103. Mean stress-strain curve from quick-consolidated triaxial compression tests. Condition A.

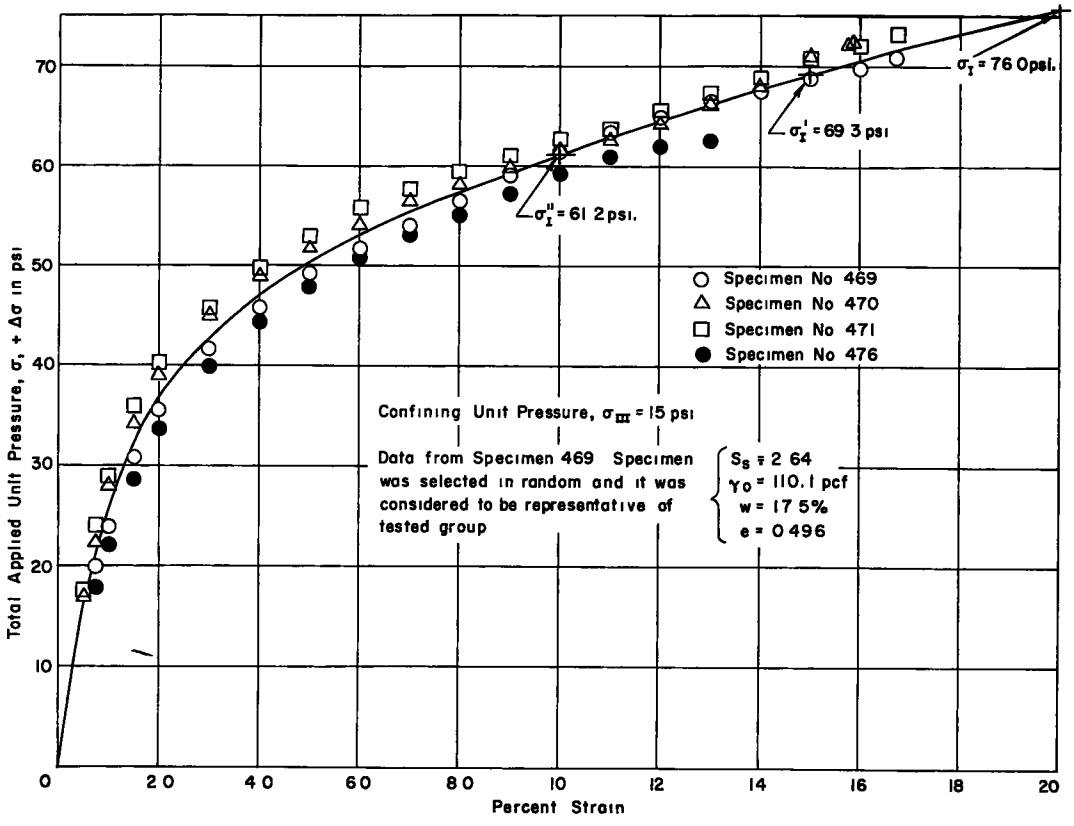

Figure 104. Mean stress-strain curve from quick-consolidated triaxial compression tests. Condition A.

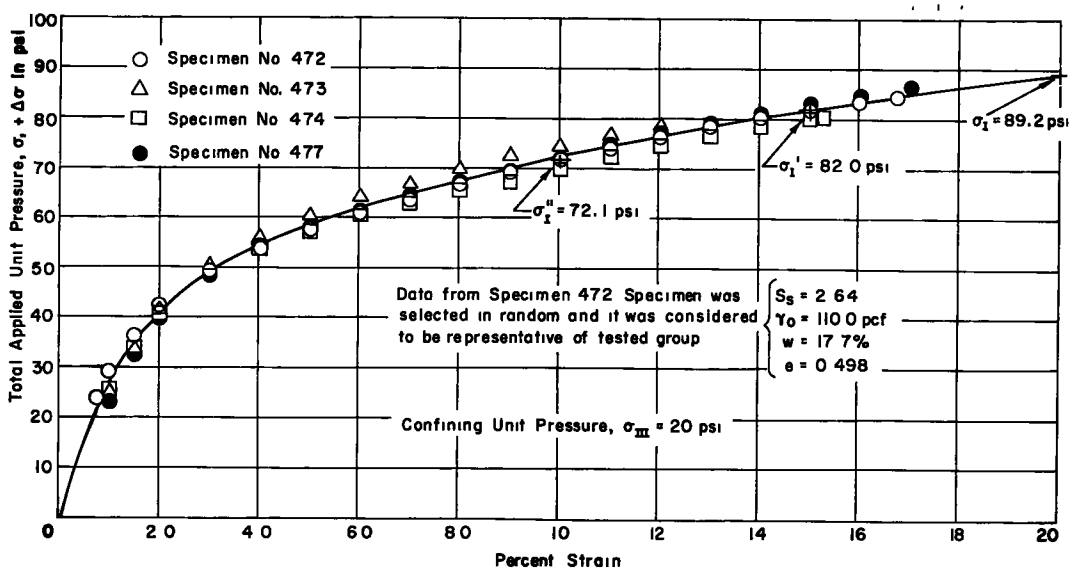

Figure 105. Mean stress-strain curve from quick-consolidated triaxial compression tests. Condition A.

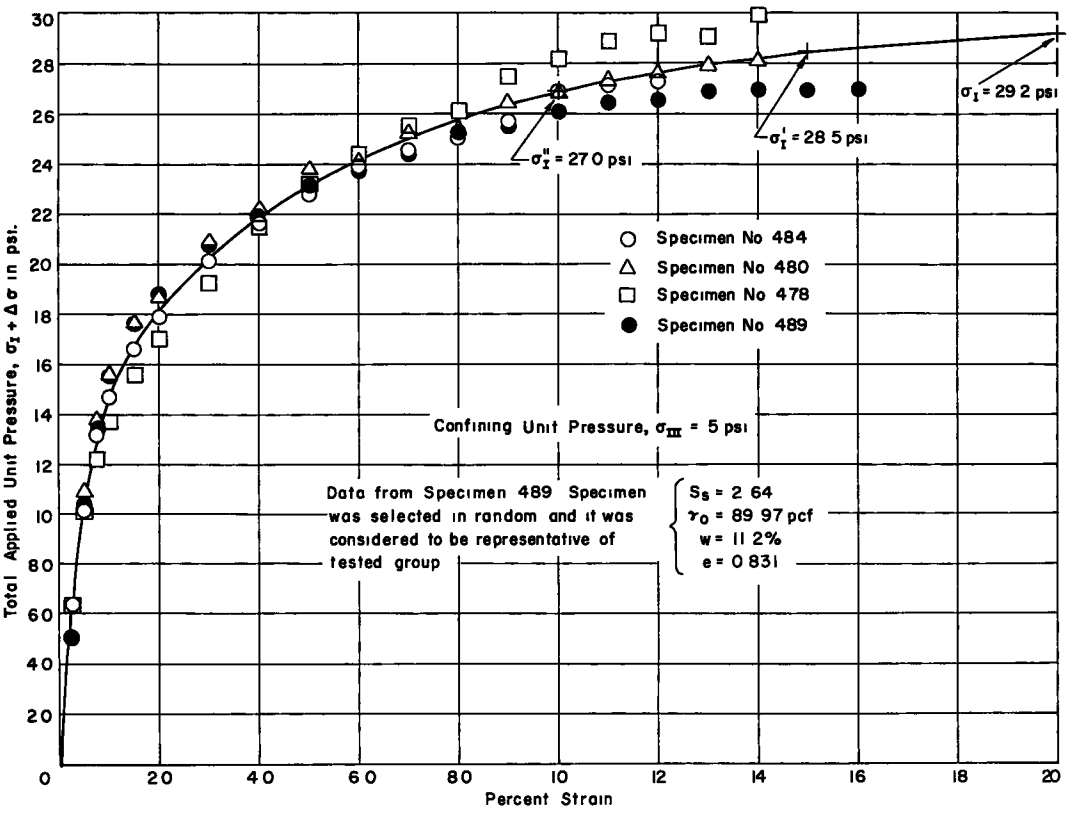

Figure 106. Mean stress-strain curve from quick-consolidated triaxial compression tests. Condition B.

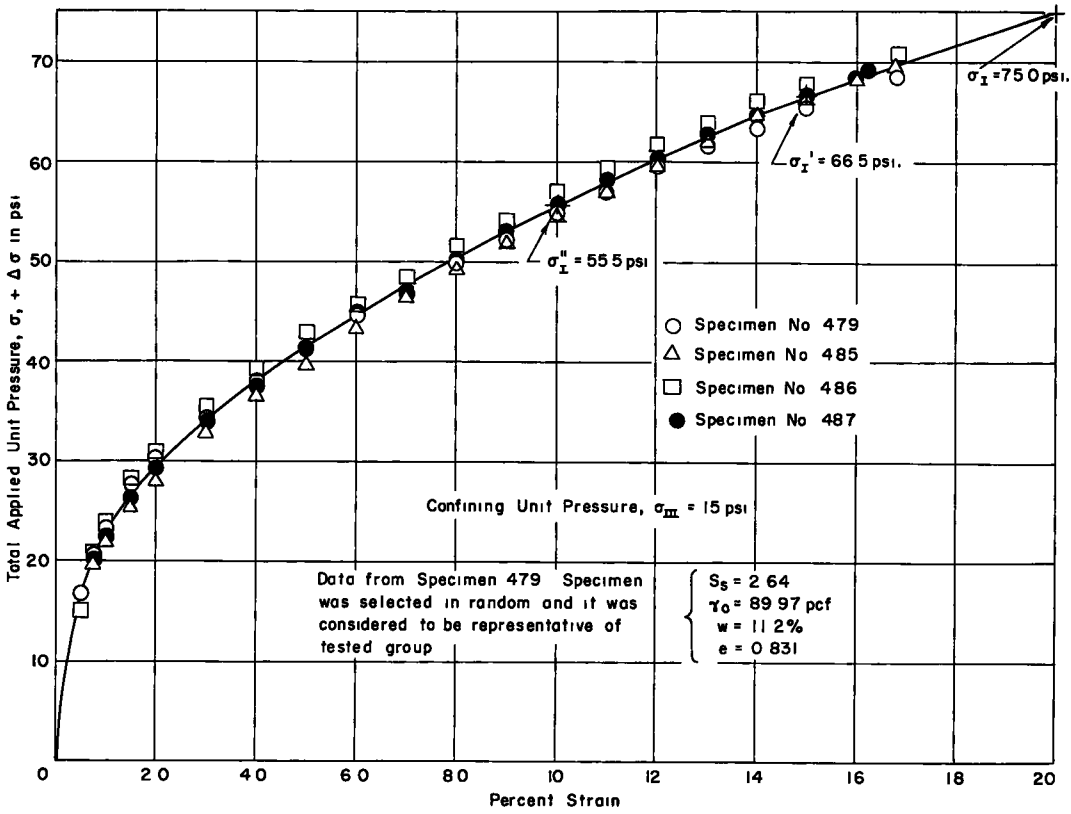

Figure 107. Mean stress-strain curve from quick-consolidated triaxial compression tests. Condition B.

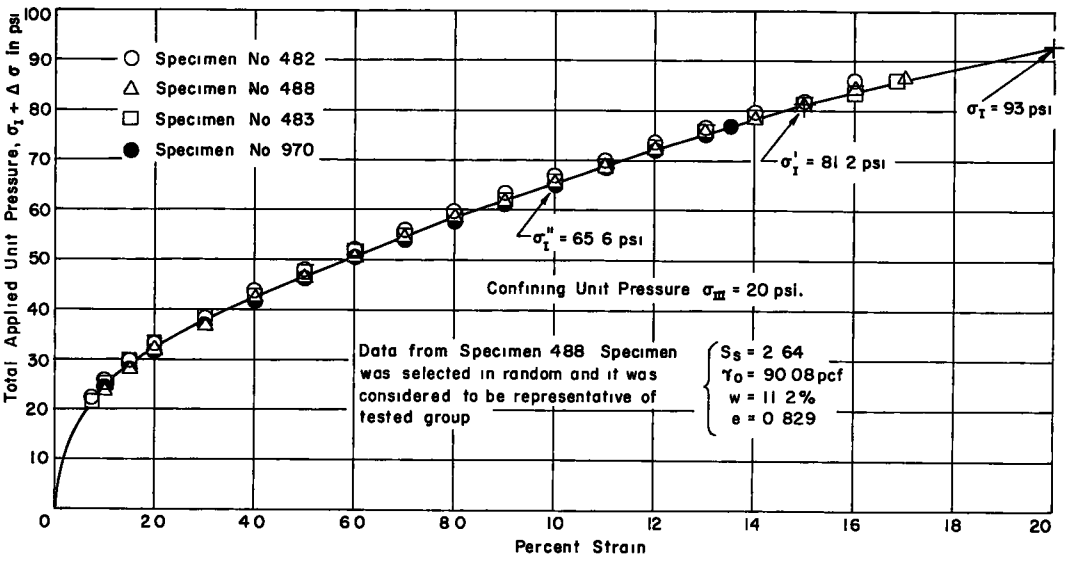

Figure 108. Mean stress-strain curve from quick-consolidated triaxial compression tests. Condition B.

vertical unit load, $\Delta\sigma$, was applied then on the specimen at an average speed of 0. 00260 inch per minute by means of the electric motor of the apparatus. Throughout the test care was taken to hold the confining chamber pressure, σ_{III}, constant.

Load dial readings were recorded every 0.003 inch. These short interval readings were obtained with the intention to use only short portions of the resulting stress-strain curves for other highway problems at later dates. Inasmuch as no definite peak points appeared on the stress-strain curves of the specimens tested, the deviator unit load was increased at the same constant rate until the whole stem of the deflection dial was used (at about 15-17 percent strain). Figure 102 shows specimens after testing from each compaction condition and each confining pressure.

Upon removal from the apparatus, the specimens were all weighed again and from each of the above mentioned four-specimen groups one specimen was oven dried for water content determination. The three remaining specimens were kept for Atteberg limit determination and other routine soil testing. From the obtained moisture content values it was indicated that no moisture was lost during the "curing" period and a very little amount was lost during testing. This fact leads one to believe that the specimens were consolidated under the influence of the applied confining pressure and the deviator load, mainly by squeezing air out of the voids.

The obtained data were plotted in the form of total applied unit pressure, $\sigma_I = \sigma_{III} + \Delta\sigma$, versus percent strain for all tests. Mean stress-strain curves were drawn for each of the above mentioned four-specimen groups (Figures 103-108). From each curve the σ_I values corresponding to 10, 15, and 20 percent strain were used to construct Mohr diagrams for the two compaction conditions, corresponding to 10, 15, and 20 percent strain respectively (Figures 49 and 50). Thus, the shearing strength characteristics c and ϕ of the side supporting material under the above two limiting compaction conditions and for the above considered three strain failure conditions were obtained.

As a check for the values of cohesion and of the angle of internal friction, obtained by the above mentioned Mohr diagrams, the same values were obtained by applying the Price method (Aldous and others, 1951) of leveling the test data by the method of least squares and obtaining c and ϕ by the following equations respectively:

$$c = \frac{a}{2\sqrt{b}}$$

$$\sin\phi = \frac{b - 1}{b + 1},$$

where

a = distance between the origin and the intercept of the σ_I versus σ_{III} straight line plot, leveled by the method of least squares, with the axis of σ_I.

b = the slope of the above straight line

The results from the above calculations appear below on Table 15.

TABLE 15

		10% Strain	15% Strain	20% Strain
Condition A	c	4.50 psi. = 648 psf.	3.01 psi. = 433 psf.	1.94 psi. = 279 psf.
	ϕ	26° - 31'	34° - 07'	38° - 38'
Condition B	c	9.36 psi. = 1348 psf.	8.44 psi. = 1215 psf.	7.38 psi. = 1063 psf.
	ϕ	22° - 12'	27° - 35'	31° - 34'

From the above table it can be seen that for both compaction conditions the cohesion varied inversely with percent strain, whereas the angle of internal friction varied directly with percent strain. Such behavior is expected because for greater strains a greater portion of the stresses in the soil specimens are transmitted directly from grain to grain (effective stresses) and the behavior of the material approximates closer that of a perfectly granular cohesionless mass.

Influence of Compression and Shearing Strains In Soil Foundations on Structures Under Earth Embankments

M. G. SPANGLER, Research Professor of Civil Engineering
Iowa State College, Ames, Iowa

When an earth embankment is constructed on a soil foundation, the weight of the embankment produces compression and shearing stresses in the foundation. The strains induced by these stresses cause settlement of the natural ground surface and an outward movement of the foundation soil from the region of the centerline of the embankment toward the toes of slope.

These settlements and outward movements have important implications in connection with the design and performance of the embankment and of structures under the embankment, such as culverts and sluiceways. Vertical settlements effect the shrinkage allowance in embankment design and influence the choice of an appropriate amount of camber in the flow line of a culvert. The outward movements due to horizontal shearing strains must be taken into account in the design of transverse joints in the barrel of culvert.

The amount of settlement and lengthening of 46 culverts and sluiceways are recorded in the paper.

●IT is axiomatic that engineering materials undergo strain when they are subjected to stress, and the soil, which is the most widely encountered of all engineering materials, is no exception to this general rule. Therefore, when a highway or railway embankment or an earth dam or levee is constructed on an earth foundation, we may expect the foundation soil to compress under the influence of the weight of the embankment. This compression strain manifests itself as settlement of the natural ground surface. Thus in Figure 1(a), if an embankment ABCD is constructed on a soil foundation, the original ground surface AED will settle to a new elevation such as AFD.

In addition to compressive stresses and strains which account for settlement of the natural ground surface, the foundation soil is subjected to certain horizontal shearing stresses and the strains resulting from these stresses cause an outward movement of the undersoil from the region of the centerline toward the toes of the embankment.

These shearing stresses are illustrated in Figure 1(b). The shear on a horizontal plane in the undersoil is essentially zero under the center of the embankment. It increases in magnitude to a maximum value at points approximately under the mid-points of the side slopes and then gradually decreases to zero at points some distance beyond the toes of the slopes.

A typical shearing stress-strain diagram for soil is shown in Figure 2. It is characteristically a curved line beginning at the origin. As the stress is increased the strain increases at an increasing rate. Finally, the strain increases an unlimited amount without further increase in stress. This stress which produces unlimited strain, i. e. shear failure, is the shearing strength of the soil.

It will be noted that a substantial amount of shear strain may develop in the soil even though the shearing stress is at a value considerably less than the shearing strength. It is these shearing strains which primarily account for outward movement of the foundation soil under an embankment even though the shearing stresses may be well below the strength of the soil. Of course, if the shearing stresses become large enough to equal or exceed the strength, the soil will flow outward from beneath the embankment and form mounds parallel to each side and beyond the toes of slope. This action will continue until the mounds are high enough and heavy enough to produce sufficient "back pressure" to stabilize the undersoil. Such failure conditions are not unheard of in engineering practice by any means, but they are not the subject of this discussion.

Movements in embankment foundation soils due to stresses which do not cause failure — compression strains and shear strains — may have important implications in

connection with the design of the embankment and particularly in connection with the design and performance of structures under the embankment, such as culverts and sluiceways.

With reference to the design of the embankment, it is widespread practice in earthwork to apply a shrinkage factor to the excavation quantities. Experience indicates that in practically all cases it takes more than 100 cu. yd. of cut to make 100 cu. yd. of fill. Therefore a designer must estimate a shrinkage factor by which the calculated fill quantities are increased when grades are being laid and balance points established. The shrinkage between cut and fill quantities is attributable to at least three different sources. First, and probably of least importance, there may be an actual loss of material from hauling equipment as the soil is transported from cut or borrow to fill areas. Second, the soil is usually compacted in the fill to a greater density than its natural density before being excavated. A unit volume of soil consists of both solid particles and void spaces or pores and the relationship between the volumes of these two phases

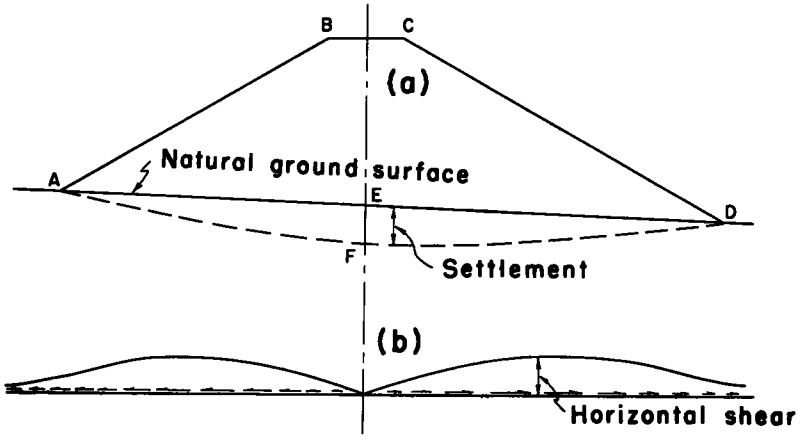

Figure 1.

influences the density of the soil. When a cubic yard is excavated and transported to a fill, the volume of the solid phase remains constant, but the volume of the voids is usually decreased in the fill, either by rolling, by traffic, by the weight of additional fill, by climatic influences or by any or all of these causes combined. Therefore, a greater volume of excavation is required to produce a given volume of fill.

A third source of shrinkage is the settlement of the natural ground surface as a fill is constructed and its weight causes the foundation soil to compress. Referring again to Figure 1(a), the calculated volume of fill is based upon the cross sectional area ABCDE. But the actual volume of soil required to construct the fill is a function of the area ABCDF. In some cases where settlement is considerable, this excess of the actual volume of fill over the calculated volume represents a substantial part of the shrinkage allowance.

When a culvert or sluiceway is constructed on or near the natural ground surface and covered by an embankment, the structure will settle downward and conform to the new contour of the surface, as indicated in Figure 3. In addition, because of the shearing strains in the foundation soil directed outward toward the toes of slopes, the structure has a tendency to lengthen. Also, the structure may

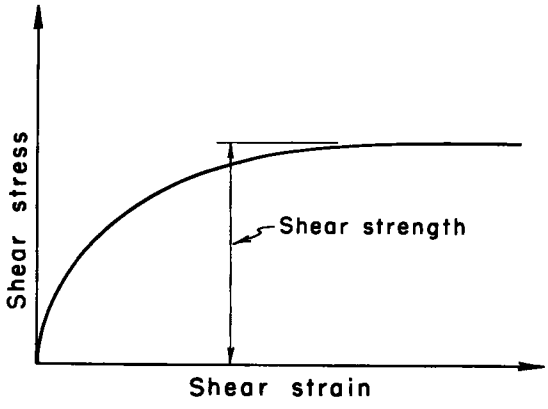

Figure 2. Typical shear stress-strain diagram for soil.

lengthen somewhat simply because the distance around the curve AFD is greater than the chord distance AED, but this source of increase in length is thought to be much less influential in most cases than that due to the outward shearing strains.

As a result of this tendency to settle and to lengthen, it is necessary to design the conduit structure to accommodate these movements without damage to the structure and without impairment of its function as a waterway. The settlement of the flow line of the conduit can be provided for by building the structure on a camber of sufficient amount that there will not be a sag in the flow line after the embankment is completed and settlements have developed. If sufficient camber is not provided and sag develops, water and silt will collect in the conduit. This prevents adequate inspection of the structure, restricts the waterway, and may hasten the deterioration of the conduit material. It may also provide a breeding ground for mosquitoes and be generally unsatisfactory from a number of viewpoints.

In order to accommodate the tendency to lengthen, it is rather common practice to construct monolithic concrete structures, such as box or arch culverts, in independent sections about 20 to 40 feet long. The construction joints between sections are designed to permit them to open up several inches as the sections pull apart due to the

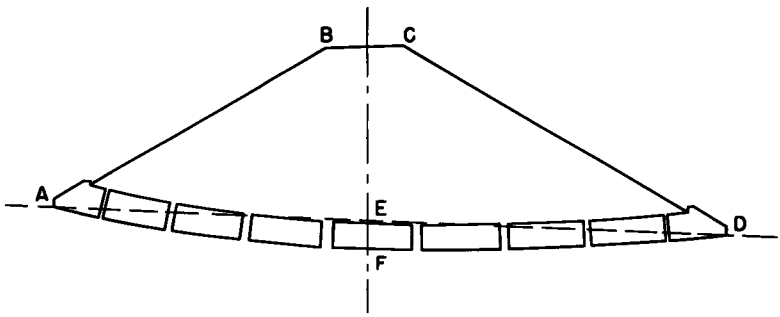

Figure 3. Culverts tend to lengthen as they settle.

outward shearing strains in the foundation soil. One type of design which has been successfully used is to construct a bell on the upstream end of each independent section into which the downstream end of the adjacent section extends in much the same fashion as bell and spigot sewer pipe are laid. This "bell and spigot" or "ship lap" design permits the sections to pull apart at the joints without vertical or horizontal faulting and prevents the intrusion of soil at the opened joint. In the case of a sluiceway through an earth dam, where water-tightness is a prime requisite, it may be advisable to install an accordion-type copper seal to prevent leakage.

Pre-cast concrete pipe with bell and spigot or tongue and groove joints may open up at the joints as the outward strains develop, but the amount of opening at each joint is usually small because of the relatively short length of sections and large number of joints. In most cases, satisfactory results are obtained by simply grouting the opened joints on the inside of the pipe after the embankment is completed and the shearing strains have developed.

Corrugated metal pipe culverts, because of their accordion-like fabrication are able to accommodate themselves to the lengthening tendency without special treatment. The author has heard infrequent rumors to the effect that even corrugated metal pipes have been pulled in two under severe conditions, but he has never actually seen such a case or received a factual report of one. Apparently this phenomenon, if it occurs at all, is very rare.

The first question which confronts a designer in his consideration of an appropriate amount of camber and the design of joints is "how much will the culvert settle and how much will it lengthen?" Presumably it would be possible to estimate these quantities in advance of construction by modern methods in soil mechanics. However, such a procedure would require extensive analysis of the compression and shearing stresses and their distribution in the soil foundation. Also, extensive soundings to establish the geological profile of the undersoil would have to be made. Many undisturbed samples

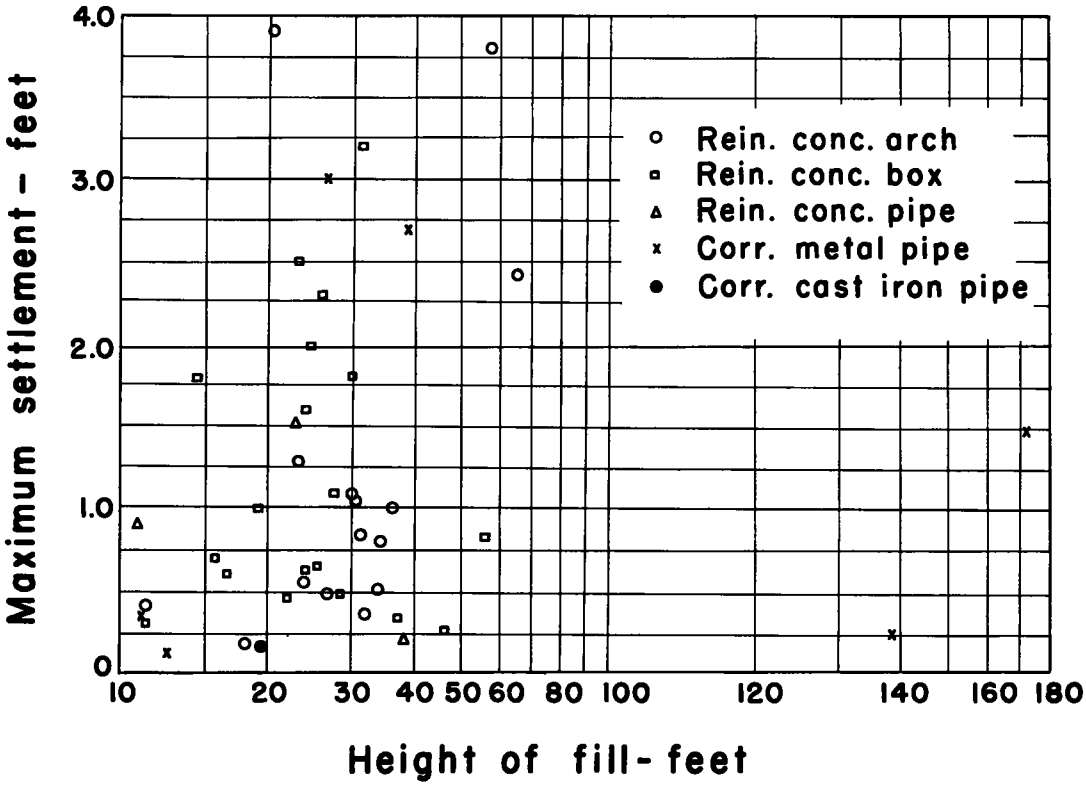

Figure 4.

of the undersoil would have to be taken and the samples tested in the laboratory to determine their stress-strain characteristics. Altogether, this would be a very expensive and time-consuming process. Since culverts under embankments are relatively small structures it is extremely doubtful whether a scientific procedure of this kind would ever be economically justified. Rather it appears that an empirical approach to the problem is the more feasible. A study of the actual settlements and joint opening of culverts and sluiceways of various kinds, under various heights of fill and in various localities, will, it is believed, yield sufficient information for a disigner to make an adequate estimate of the probable settlement and lengthening of a proposed structure of this kind.

The author has been collecting such information for a number of years, both by personal observation and from other sources. He is indebted to the Iowa Highway Commission, the North Carolina Highway Commission, the Rock Island Railroad, the Armco Steel Corporation, the Stanley Engineering Company and the Brown Engineering Company for supplying valuable information concerning the actual settlement and lengthening behavior of culverts and sluiceways.

Information relative to 46 culverts and sluiceways is given in Table 1 including maximum fill height, maximum settlement, and where available, the amount which the structure lengthened and the maximum joint opening.

The maximum settlement versus height of fill for the 46 structures is shown graphically in Figure 4. The magnitude of settlement varied over a very wide range; from 3 inches under 137 feet of fill in the case of an 84 inch corrugated pipe culvert in Cullman County, Alabama to 3.9 feet under 20.2 feet of fill in the case of a 9-by11-foot arch culvert in Woodbury County, Iowa. In connection with this diagram it is pointed out that plotted heights of fill are the design distance from the top of the structure to the top of the embankment. The final distance between the top of the structure and the top of the embankment is essentially equal to the sum of the plotted height of fill plus the amount of settlement. Also, the height of embankment above the natural

TABLE 1

SETTLEMENTS AND LENGTHENING OF CULVERTS

Item No.	Location County	Size and Kind	Max Fill Height ft.	Max Settlement ft	Total Length ft	Increase in Length ft	No of Joints	Max Joint Opening ft	Remarks
1	Tama	3'-8 x 5'-6 RC Arch	35 7	1.00	166	0 64	5	0 30	
2	Tama	4'-9 x 6'-1 RC Arch	30 8	0 83	161	0 31	6	0 13	
3	Tama	6'-3 x 9'-3 RC Arch	29 8	1.05	152	0 38	7	0 15	
4	Tama	10'-0 x 12'-6 RC Arch	11 1	0 39	67	0.07	3	0 03	
5	Tama	5'-6 x 8'-0 RC Arch	18.0	0 18	92	0.01	4	0 30	
6	Tama	4'-9 x 6'-1 RC Arch	26 6	0 46	110	0.51	4	0 30	
7	Tama	3' x 4' RC Box	23 5	0 64	116	0 38	5	0 15	
8	Tama	4'-9 x 6'-1 RC Arch	29 7	1.08	138	1 04	6	0 36	0 2' vert fault at one joint
9	Tama	10'-0 x 12'-6 RC Arch	21 0	1 00	104	0 25	4	0 12	
10	Tama	12'-0 x 12'-6 RC Arch	22 9	1 30	105	0 65	4	0 34	0 1 to 0 2 vert fault at three joints
11	Tama	3'-8 x 5'-6 RC Arch	33 6	0 52	144	0.47	5	0 19	
12	Tama	3'-8 x 5'-6 RC Arch	33 6	0.80	151	0 28	5	0 15	0 1 vert. fault at one joint
13	Pottawattamie	96" Corr Metal	35 8	2 70	170	-	-	-	Outlet raised 1'. 3' silt deposit at center
14	Pottawattamie	90" Corr. Metal	27.2	3.00	144	-	-	-	Inlet raised 0 4', outlet settled 0 6' 3' silt deposit at center
15	Harrison	5'-6 x 8'-0 RC Arch	57 0	3 80	274	1 28	7	0 45	Inlet settled 0 5' Outlet settled 0 2'
16	Cullman (Alabama)	84" Corr Metal	137 3	0.25		-	-	-	2' sand bedding on ledge rock
17	Buncombe (No Carolina)	66" Corr Metal	172 0	1 46		-	-	-	
18	Fremont	3'-8 x 5'-6 RC Arch	64 0	2 53	267	-	8	0 33	Tongue and groove joints broken Some horizontal faulting
19	Des Moines	4' x 5' RC Box	55 0	0 83	420		14	0 19	Outlet raised 0 35'
20	Union	3' x 5' RC Box	29 0	1 81			6	0 69	
21	Jasper	3' x 5' RC Box	27 0	1 11	481	-	none	-	Several transverse cracks up to 1" + in barrel
22	Ringgold	4'-9 x 6'-1 RC Arch	31.3	0.36	207	-	-	-	
23	Olmsted (Minnesota)	48" RC pipe	37 5	0 22	170	-	-	-	Shallow depth to ledge rock
24	Harrison	3' x 3' RC Box	21.8	0 47	121	-	-	-	
25	Pottawattamie	3' x 4' RC Box	15 4	0 70	111	-	-	-	
26	Pottawattamie	3' x 3' RC Box	11 2	0 30	70	-	-	-	
27	Mills	3' x 4' RC Box	24 8	0 65	121	-	-	-	
28	Mills	8' x 8' RC Box	16.2	0 61	94	-	-	-	
29	Marion	3' x 4' RC Box	45 2	0 25	202	-	-	-	
30	Johnson	3' x 4' RC Box	36 4	0.35	158	-	-	-	
31	Johnson	2' x 3' RC Box	26.8	0 48	138	-	-	-	
32	Linn	60" Corr Metal	8 0	0 27	62	-	-	-	
33	Monroe	36" Corr. Metal	12 3	0 12	74	-	-	-	
34	Monroe	36" Corr Metal	11 0	0.28	64	-	-	-	
35	Woodbury	4' x 4' RC Box	30 5	3 20	223	0 79	5	0 29	Inlet settled 0 5'. Outlet settled 0 7'
36	Woodbury	9' x 11' RC Arch	20 2	3 90	157	1 34	4	0 52	Inlet settled 1 6' Outlet settled 1 5'
37	Woodbury	8' x 8' RC Box	22 9	2.50	177	0 71	4	0 37	Inlet settled 0 6' Outlet settled 0 6'
38	Woodbury	48" RC Pipe	22 1	1 50	186	-	15	-	Inlet settled 0 1' Outlet settled 0 7'
39	Woodbury	6' x 6' RC Box	14 0	1 80	126	0.29	4	0 19	Inlet settled 0 6' Outlet settled 0 4'
40	Woodbury	3' x 4' RC Box	23.4	1 60	191	0 50	5	0 18	Inlet settled 0 3' Outlet settled 0 4'
41	Woodbury	4' x 5' RC Box	25 2	2 30	196	0 23	5	0 17	Inlet settled 0 5' Outlet settled 0 1'
42	Woodbury	4' x 4' RC Box	24 0	2 00	181	0.52	4	0 31	Inlet settled 0 3' Outlet settled 0 2'
43	Woodbury	42" RC pipe	10 6	0 90	132	-	10	-	Inlet settled 0 3' Outlet settled 0 3'
44	Woodbury	4' x 4' RC Box	18.7	1 00	154	0 18	4	0 12	Inlet settled 0 3' Outlet settled 0 3'
45	Clayton	36" Corr Cast Iron	19 3	0 16	99	-	32	-	Shallow earth bedding on ledge
46	Clayton	36" Corr Cast Iron	23.7	0 58	117	-	38	-	Shallow earth bedding on ledge

ground surface adjacent to the structures was probably somewhat greater than the plotted height, since many of them were probably installed as projecting conduits. However, factual data in this regard is not available except in a very few cases. Furthermore in some cases the settlement of the ground surface adjacent to the structure may be somewhat different than that of the structure itself, but in general, the structure settles just about the same amount as the settlement of the original ground surface.

The shotgun distribution of the plotted points clearly indicates that the settlement is not a function of height of fill alone, but other factors must be taken into consideration in making an estimate of probable settlement. The most important of these factors are the depth of the foundation soil to ledge rock and the compressibility characteristics of the soil stratum. The influence of this first factor is clearly shown in the case of the 84-inch corrugated pipe in Alabama (Item 16, Table 1). Here the depth to ledge

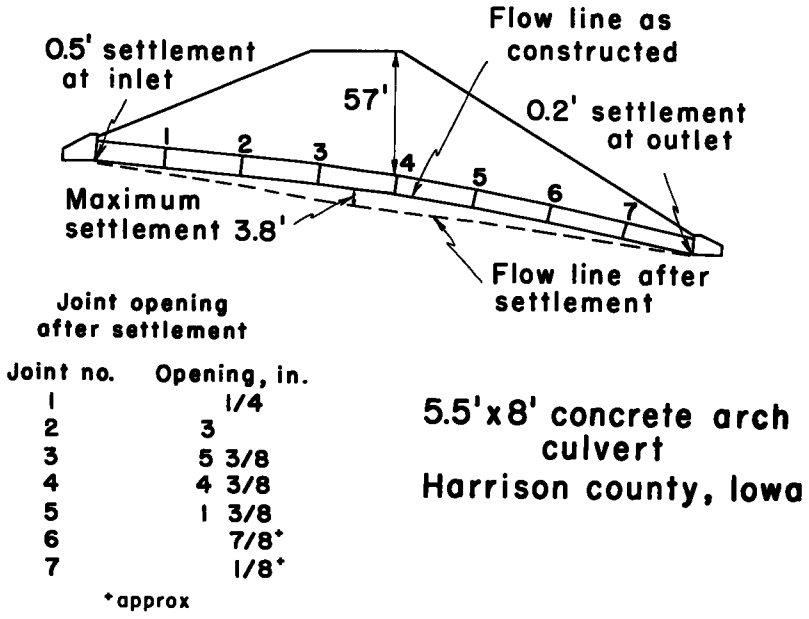

Figure 5.

rock was very shallow. In fact ledge was removed to a depth of 2 feet below the pipe and replaced by a selected sand bedding on which the pipe was laid. The settlement of this pipe was only 3 inches under 137 feet of fill. The 48-inch concrete pipe culvert in Olmsted County, Minnesota (Item 23, Table 1) also illustrates this point. The actual depth to ledge on this job is not known, but the rocky character of the soil in the stream bed and adjacent limestone outcrops indicate that it is very shallow. The settlement in this case was $2\frac{1}{2}$ inches under 37.5 feet of fill.

In contrast to these cases of minor settlement, culverts constructed in the loess region of western Iowa (Woodbury, Harrison, Pottawattamie and Fremont Counties) have experienced large settlements, frequently in the range from 2 to 4 feet. Although specific information relative to the depth of soil foundation is not available in these instances, it is generally recognized that the soil mantle in this region is very thick; in the order of magnitude of 300 to 500 feet.

As a general rule, the settlement of a culvert is roughly proportional to the height of fill over it throughout its length. That is, the settlement is greatest under the roadway portion of the embankment, where the fill height is greatest, and diminishes toward zero at both the inlet and outlet. This observation is illustrated in Figures 5, 6 and 7. Figure 5 shows the initial flow line profile of a monolithic, $5\frac{1}{2}$-by-8-foot concrete arch culvert and the final profile after construction of the 57-foot embankment. This culvert is located in Harrison County, in the Peorian Loess region of western Iowa. The

maximum settlement of the flow line is 3. 80 feet and it occurred between Joints 3 and 4, which are near the centerline of the embankment.

The amount which the various construction joints in this culvert opened up as the structure lengthened under the influence of shearing strains in the foundation soil is shown. There has been no vertical or lateral faulting at the joints and no noticeable infiltration of soil, although the loess in this area is highly erosive in character. Figure 8 is a photograph showing the bell-and-spigot joint construction employed in this design. The bells overlapped the adjacent upstream sections about eighteen inches.

Figure 6 illustrates the settlement of a 96-inch corrugated metal pipe culvert under a 36-foot railroad embankment in Pottawattamie County which is also in the Peorian

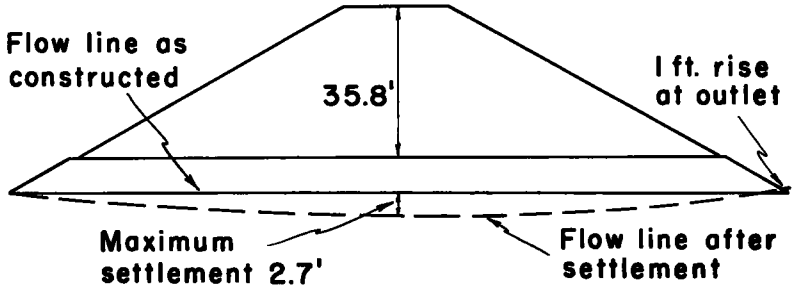

Figure 6. A 96-inch corrugated-metal-pipe culvert, Pottawattamie County, Iowa.

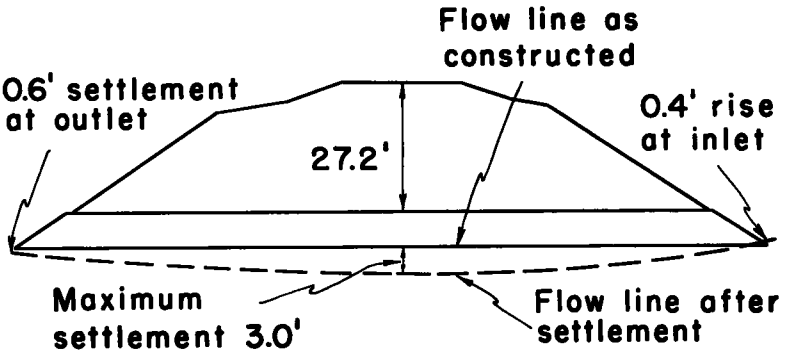

Figure 7. A 90-inch corrugated-metal-pipe culvert, Pottawattamie County, Iowa.

Loess region of western Iowa. The maximum settlement of the flow line of this culvert was approximately 2. 7 feet near the centerline of the embankment. The elevation of the inlet was not affected by the construction of the fill, but the outlet raised about a foot.

The settlement of the flow line of a 90-inch corrugated pipe culvert in the same vicinity is illustrated in Figure 7. The maximum settlement of this culvert, under 27 feet of fill was approximately 3 feet near the centerline of the embankment. The inlet raised about 0. 4 foot and the outlet settled about 0. 6 foot.

Both of these corrugated pipes were constructed on a relatively flat, uniform grade from inlet to outlet. As a result there is an accumulation of silt in the culverts up to 3 feet deep. There is no evidence of the bolted joints pulling apart, although it is probable that rather large outward shearing strains were developed in the soil foundation.

Another matter of considerable interest which is indicated by this study is the fact that the amount which the structure lengthens is roughly proportional to the amount of settlement. No quantitative statement of this relationship can be made, but it seems clear that the greater the settlement, the greater the amount of lengthening of the structure. Also the joint opening is greatest near the center of the embankment and

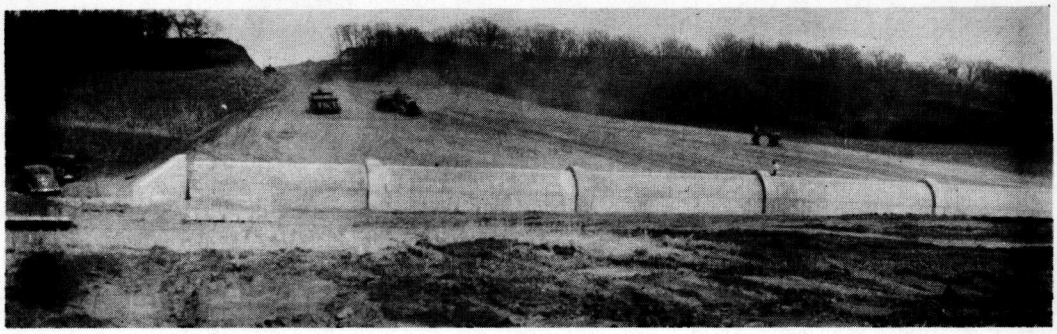

Figure 8. A 5.5' x 8' concrete arch culvert in Harrison County, Iowa, showing bell and spigot type construction joints.

decreases to an insignificant amount toward the ends of the structure, as shown in Figure 5.

Still another matter of interest is the time relationship between construction of the fill and the development of settlement. Although, very little detailed data are available, the indications are that most of the settlements developed during and shortly after construction of the fill. Three culverts in Woodbury County, (Items 35, 36, and 37, Table 1) were built and covered during the 1952 construction season. The settlements of these structures was first measured in February 1953. A re-check of the settlements in January 1954 indicated that no further settlement developed during this intervening period.

In the case of a concrete arch culvert in Fremont County (Item 18, Table 1) the maximum settlement of the flow line was 2.14 feet immediately upon completion of the fill on September 4, 1930. The settlement increased to a maximum of 2.53 feet after a lapse of nearly 9 years, according to the following schedule of observations.

Day of Observation date	Time after Completion of Fill months	Maximum Settlement feet
9-49-1930	0	2.14
10-16-1930	1.5	2.19
5-20-1931	9.5	2.25
6-13-1933	33.5	2.32
4-3-1936	67.0	2.43
6-16-1939	105.5	2.53

In summary, observations show that settlement of the natural ground surface under an earth embankment varies widely depending upon the height of the embankment, the depth of foundation soil to ledge rock and the compression stress-strain characteristics of the foundation soil. Also, it is indicated that there is an outward movement of the foundation from the region of the centerline of the embankment toward the toes of slopes, caused by shearing strains within the undersoil.

These vertical and horizontal movements have important implications in connection with the design of an embankment and of culverts or sluiceways beneath the embankment. It is believed that a study of the settlement and lengthening of a large number of culverts or sluiceways in relation to environmental conditions, such as height of fill and depth and compressibility of the foundation soil layer, will provide a practical means for estimating the probable vertical and horizontal movements of a proposed conduit.

THE NATIONAL ACADEMY OF SCIENCES—NATIONAL RESEARCH COUNCIL is a private, nonprofit organization of scientists, dedicated to the furtherance of science and to its use for the general welfare. The ACADEMY itself was established in 1863 under a congressional charter signed by President Lincoln. Empowered to provide for all activities appropriate to academies of science, it was also required by its charter to act as an adviser to the federal government in scientific matters. This provision accounts for the close ties that have always existed between the ACADEMY and the government, although the ACADEMY is not a governmental agency.

The NATIONAL RESEARCH COUNCIL was established by the ACADEMY in 1916, at the request of President Wilson, to enable scientists generally to associate their efforts with those of the limited membership of the ACADEMY in service to the nation, to society, and to science at home and abroad. Members of the NATIONAL RESEARCH COUNCIL receive their appointments from the president of the ACADEMY. They include representatives nominated by the major scientific and technical societies, representatives of the federal government designated by the President of the United States, and a number of members at large. In addition, several thousand scientists and engineers take part in the activities of the research council through membership on its various boards and committees.

Receiving funds from both public and private sources, by contribution, grant, or contract, the ACADEMY and its RESEARCH COUNCIL thus work to stimulate research and its applications, to survey the broad possibilities of science, to promote effective utilization of the scientific and technical resources of the country, to serve the government, and to further the general interests of science.

The HIGHWAY RESEARCH BOARD was organized November 11, 1920, as an agency of the Division of Engineering and Industrial Research, one of the eight functional divisions of the NATIONAL RESEARCH COUNCIL. The BOARD is a cooperative organization of the highway technologists of America operating under the auspices of the ACADEMY–COUNCIL and with the support of the several highway departments, the Bureau of Public Roads, and many other organizations interested in the development of highway transportation. The purposes of the BOARD are to encourage research and to provide a national clearinghouse and correlation service for research activities and information on highway administration and technology.